Development of an amyloid protein-based composite biomaterial for coating applications

Craig Allan

Submitted to Swansea University in fulfilment of the requirements for the Degree of Doctor of Philosophy

Swansea University

Swansea University Medical School

Supervised by:

Dr G. Van Keulen

Dr D. Penney

2023

DECLARATION OF ORIGINALITY

This work has not previously been accepted in substance for any degree and is not being concurrently submitted in candidature for any degree.

Signed .....*Craig Allan*.....

Date .....12/04/2023.....

This thesis is the result of my own investigations, except where otherwise stated. Other sources are acknowledged by footnotes giving explicit references.

Signed .....*Craig Allan*.....

Date .....12/04/2023.....

I hereby give consent for my thesis, if accepted, to be available for photocopying and for inter-library loan, and for the title and summary to be made available to outside organisations.

Signed .....*Craig Allan*.....

Date .....12/04/2023.....

The university's ethical procedures have been followed and, where appropriate, that ethical approval has been granted

Signed .....*Craig Allan*.....

Date .....12/04/2023.....

Abstract

Streptomyces bacteria are highly versatile micro-organisms, which have been recognised as potent biochemical, soil and biomaterials engineers. In particular, functional non-pathogenic amyloid proteins can be formed from the expression of β-sheet proteins. These β-sheet proteins known as chaplins, which aggregate to form a fibrillar morphology, has been shown to protect against desiccation in hydrophobic environments. These robust Chaplin proteins have served here as a source of inspiration for materials development, based on the chaplins' ability to modulate the properties of its own surface and that of its natural environment.

This study has developed more economical and environmentally friendlier methods for chaplin protein production by replacing the existing TES buffer for a potassium bicarbonate buffer and by modifying the downstream processing to assist in the removal of trifluoroacetic acid. Combinations of different media and buffers were tested for alternative fermentations that support Streptomyces morphological differentiation in liquid media, in which a potassium bicarbonate buffer system proved as efficient as well as more economical when compared to conventional fermentations with expensive organic buffer systems that support differentiation. Downstream processing of amyloid proteins was furthermore improved by adopting synthetic peptide procedures resulting in an environmentally friendlier amyloid purification method. This modified medium was also demonstrated within a bioreactor at 1.7 L scale which further enhances the economic benefit which could be implemented for production of other secondary metabolites.

The resulting chaplin proteins were then applied with β-glucans to form a biocomposite for different industrial applications. Material properties and anti-corrosion were determined by goniometry and high-resolution imaging, and by qualitative and quantitative electrochemistry. Our protein-based corrosion resistant nano-coating has great potential for the manufacturing, defence and other industries, including healthcare and biomaterials manufacturing.

Acknowledgements

Firstly, I would like to extend the greatest of gratitude to my supervisory team and technical partners at the Dstl. Dr Geertje van Keulen and Dr David Penney, there continuous support both experimentally and personally throughout this project has been invaluable and I will forever be in their debt. Phil Duke and Christopher Hawkins, who gave me the opportunity to develop this project and supported me through the difficult times.

This journey has been a mixed bag of emotions and I could not have reached this point without the love and support of my family and friends. Severina Peneva for supporting me every step of the way, dealing with my stressful moments and enabling my love for gin and board games, Michael Allan for tolerating my antics throughout lockdown (still haven't forgiven you for the guitar playing at 6am) and Kulwinder Chima for being the guy that has always had my back when times were tough even from 500 miles away.

A special acknowledgement to the 5th floor lab members in the institute of life sciences building who, from day 1, made me feel at home after relocating to Swansea. Be it the early days of JC's in a suit to terrible karaoke on Wind street. Lydia (not Linda), thank you for everything you have done to make me feel welcome in the group and for the opportunity to rack tips/chit chat/walks on the Gower.

Finally, I would like to dedicate this work, and the years I spent getting to this point in my academic career, to my late grandmother, Margaret, who sadly passed during my PhD. You were always my biggest supporter, taught me to never give up, and to always tie my shoes before running down a hill.

Contents

Table of Figures

Abbreviations

BSA – Bovine serum albumin

Chaplins/chp - Coelicolor hydrophobic aerial proteins

Cys - cysteine

HDG – Hot dipped galvanisation

PTFE – Polytetrafluoroethylene

S. coelicolor – *Streptomyces coelicolor*

SDS – Sodium dodecyl sulphate

SDS-PAGE - sodium dodecyl sulfate polyacrylamide gel electrophoresis

SFM – Soy flour mannitol

TFA – Trifluoroacetic acid

WCA – water contact angle

S. griseus – *Streptomyces griseus*

DMSO - dimethyl sulfoxide

HPC – Hydroxypropyl cellulose

EC – Ethyl cellulose

SKP – Scanning Kelvin Probe

MYM – Maltose-Yeast Extract-Malt Extract

Chapter 1

Introduction

1. Introduction

The drive for new emerging technologies has always been pivotal in the development of new approaches to real world problems. Existing technologies have their advantages and disadvantages but by seeking alternative strategies, advantages can be enhanced and disadvantages can be minimised whilst trying to operate at a reasonable cost [1]. Inspiration for new technologies or technological advances of existing strategies is constantly ongoing and with a drive for more carbon neutral approaches, inspiration from nature may provide key advances. By investigating biological structures and processes, bioinspired approaches can be researched for applications. Mechanisms in nature have been developed over millions of years to adapt to changing external stimuli such as the environment, pathogens and predators. The development of organic nanostructured materials is a lucrative area as it would have improved environmental safety and energy requirements [2]. These mechanisms can be the expression of different compounds, antimicrobials, or structural modifications to aid in their survival. The lotus leaf is a key example of how the microstructure and expression of wax on the surface of their leaves allows them to create a hydrophobic surface [3]. Inspiration has also been taken from the animal kingdom, where the nano structure of the foot seta of a Gecko was investigated for its adhesion properties [4]. The importance of hydrophobicity and adhesion in nature will be discussed and how these mechanisms can be exploited for surface modifications of materials.

1.1. The role of hydrophobicity and adhesion in nature

Etymologically, hydrophobicity means water(hydro) fearing(phobic). When a surface or compound is described as hydrophobic, it means that when water is applied, the surface or compound does not adsorb and leads to poor wetting which appears as beads on the surface (Figure 1). Inversely, if a surface is hydrophilic, the water adsorbs and causes the water to spread across the surface.

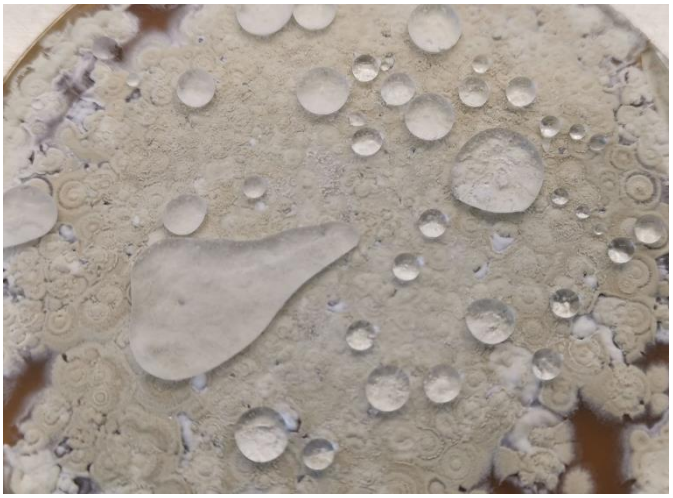

Figure 1: Water droplets on a lawn of *Streptomyces* displaying the hydrophobic effect of the surface (Allan, 2021)

For a surface to be classified as hydrophobic, an advancing water contact angle of greater than 90° would be expected, values less than 90° would be deemed hydrophilic [5]. Surfaces can also be classified as superhydrophobic, which is when water contact angles of 150° or greater are observed [6]. The lotus leaf uses the fine microstructures and water repellent wax to create a superhydrophobic coating [3]. The hydrophobicity of a substrate can be quantified by goniometry. This is achieved by use of a goniometer which can measure the contact angle between the substrate and the solvent. The wetting of a substrate can be defined into two different states, Wenzel state [7] and the Cassie-Baxter state [8]. The difference between these two states is the degree of substrate wetting of the same material. At lower surface roughness, droplets will conform to a Wenzel state but with nano and microscale roughening of the substrate, it causes air to be trapped underneath the droplet, which increases the water contact angle. This phenomenon is known as the Cassie-Baxter state. By achieving a superhydrophobic coating, it limits interaction with the substrate, reducing adhesion and allows for self-cleaning due to the water rolling and carrying any contaminants off the surface[9]. Superhydrophobic surfaces not only characteristically repel water, but it also can provide a surface with adhesive properties. This adhesive property is understood to be due to the increased van der Waals forces between the superhydrophobic surface and an object in direct contact. In nature, different creatures have developed ways to adhere to surfaces. The Gecko has several aligned hairs on its feet known as setae. These hairs are micro in size which also separate at the end forming hundreds of nanospatulae, it is the organisation of both micro and nano structures that provide the high surface area which gives the gecko its ability to adhere and be superhydrophobic [10]. The tree frog has soft pads which under wet conditions allows for adhesion due to micro and nano channels on its toes. This is supported with mucus which is secreted from glands in its toe [11].

Superhydrophobic coatings require low surface energy and surface roughness so that it is functional however, the durability at micro and nano scale is poor [12]. Durability is less of an issue for the lotus leaf, Gecko and tree frog as they have the inherent ability to regenerate. Coatings without the ability to regenerate have a very short lifespan as the functionality diminishes over time which would then require further treatment to maintain performance. Conversion of surfaces to be water repellent may be able provide self-cleaning and antibiofouling benefits to a variety of industries.

1.2. Inspiration from bacteria

Although inspiration can be taken from the animal kingdom for the development of new materials, bacteria and fungi have also evolved mechanisms to protect itself and ensure longevity. The ability for organisms to adapt to changing environmental conditions is crucial for its survival. A feature that has been observed in both bacteria and fungi is the formation of hydrophobic filaments which allows them

to lower the surface tension of the surrounding environment and breach into a hydrophobic environment (air) to allow it to release spores or fruiting bodies for recolonisation. The hydrophobic filaments are crucial for differentiation as desiccation would likely lead to death of the fungi or bacteria. One important soil dwelling bacterium that is commonly researched is *Streptomyces Coelicolor*. To gain a full appreciation of this bacteria, the life cycle and morphological differentiation needs to be understood.

1.3. Streptomyces coelicolor Life Cycle

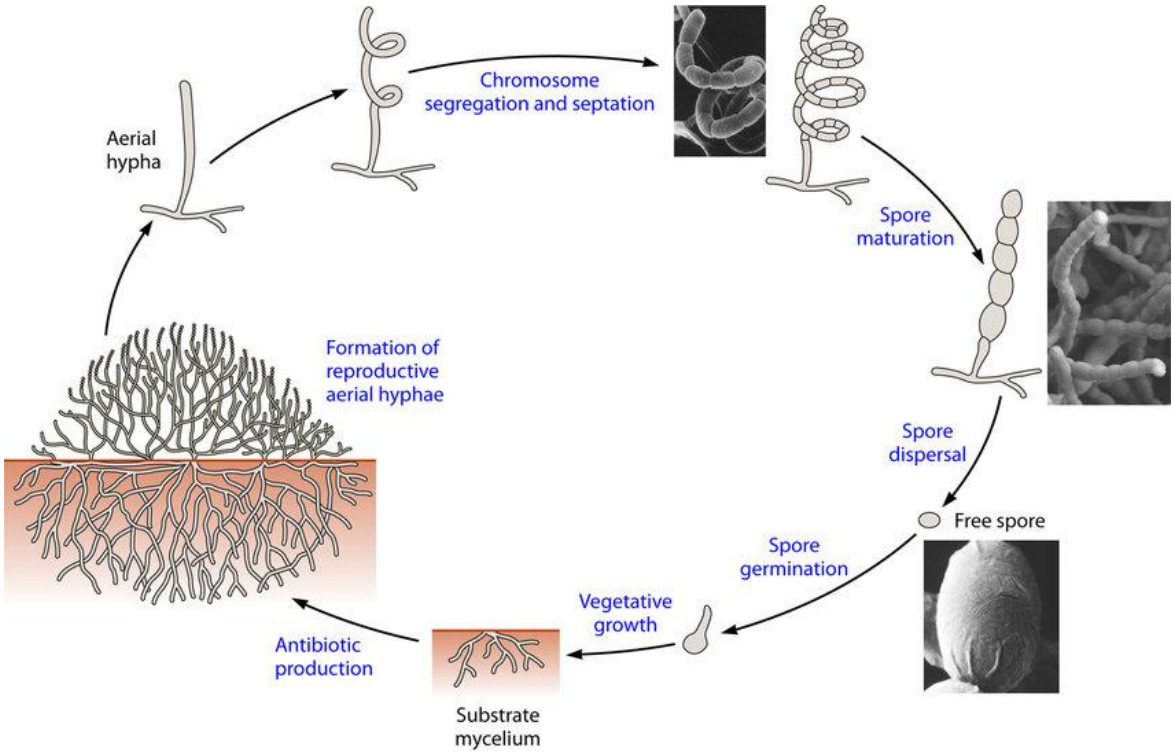

Figure 2: *Representation of the morphological changes of* Actinomycetes *throughout its life cycle* [13].

Figure 2 gives a representation of the life cycle from a single spore to sporulation. From a single spore, it darkens, swells and then the emergence of a germ tube [14]. This continues to grow within the solid medium and as it does this, forms branching filamentous hyphae[15]. Upon nutrient limitations, aerial hyphae begin to form. It is these hyphae that must be hydrophobic to allow for penetration into the hydrophobic environment. This hydrophobic sheath is formed by two sets of proteins known as chaplins and rodlins [16, 17]. The rodlin layer, which is encoded by *RdlA* and *RdlB* [18], has been shown by the use of Rdl mutant strains that the rodlin layer does not contribute to the hydrophobicity of the sheath[19] After the elongation of the aerial hyphae, the aerial hyphae are divided to produce immature spores which is driven by *FtsZ* [20]. These immature spores are matured by the spore-wall synthesizing complex, which surround the spore and drive spore wall development [21, 22]. Once

fully matured, spore dispersal occurs in search for fresh nutrients so spore germination and the life cycle can be repeated.

1.4. Chaplin proteins and their roles

The sporulation of the bacterium is important for its survival and has been shown that with the deletion of chaplin genes, sporulation can be significantly delayed [23] which emphasises the biological importance [24, 25]. In total, there are 8 genes which encode for chaplin proteins (*Chp*A-H). *Chp*A, B & C are what are known as the long chaplins and contain between 210-230 amino acid residues unlike *Chp*D,E,F,G & H which are smaller and contain between 50 and 63 residues. These long chaplins contain two N-terminal hydrophobic regions and a C-terminal sorting signal that is used for sortase-mediated attachment to the cell wall. Whereas the short chaplins contain 1 hydrophobic region following an N-terminal secretion signal peptide, with the exception of *Chp*H which contains 2 hydrophobic regions [16, 23]. These hydrophobic regions are known as the chaplin domains which contain between 60-65% hydrophobic amino acids [23]. The percentage of hydrophobic reisdues varies between the different chaplins.

Different chaplin genes are expressed at different stages of growth. For example, *Chp*E and *Chp*H are expressed highly during both vegetative and aerial hyphae growth [26] whereas the remainder are exclusively expressed during aerial hyphae growth [27]. This expression of *Chp*E and *Chp*H into the surrounding environment, as vegetative growth is prevalent, is to facilitate extension of vegetative growth by reducing the surface tension in the surrounding environment [16]. The surfactant based properties chaplin proteins exert has been shown to reduce the surface tension of water from 72 $mJ.m^{-2}$ to 26 $mJ.m^{-2}$ [16]. The surface tension during the emergence of aerial hyphae into a hydrophobic environment is facilitated by the chaplins in the surrounding environment rather than from the hydrophobic sheath [18, 23]. Claessen et al, depicted the formation of the chaplins onto the surface shown here in Figure 3.

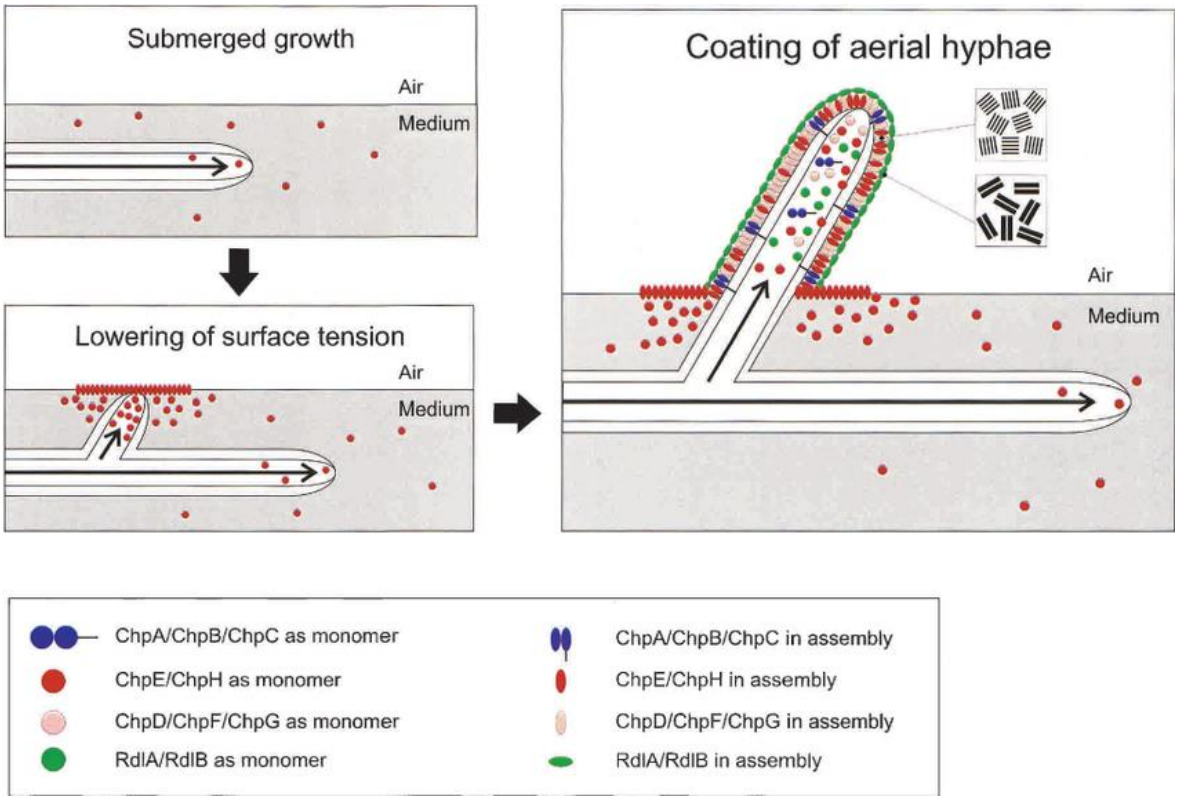

Figure 3: Chaplin protein membrane formation on aerial hyphae of *Streptomyces coelicolor* as it enters a hydrophobic environment [16].

The organisation of the chaplin proteins was shown that they are anchored to the cell surface by cellulose[28]. This is achieved by the covalent attachment of the long chaplins (*Chp*A, B & C) and the interaction with the β(1-4) glycan, which in turn leads to the formation of amyloid fibril structures composed of chaplin proteins. Due to the complexity of how *Streptomycetes* differentiate, their ability to utilise glycans for remodelling is important and has been shown that glucanase (CslZ) and lytic polysaccharide monooxygenase (LpmP) are crucial for the degradation and remodelling of the peptidoglycan, which is proposed to facilitate the movement of glycan at the apical tip [29]. In the attachment of the long chaplins to the cell wall surface, the cellulose synthase-like protein CslA produces the required glycan to mediate anchoring [28, 30]. This ordering of the chaplin proteins along cellulose fibrils is depicted in Figure 4 as a means of attachment to surfaces.

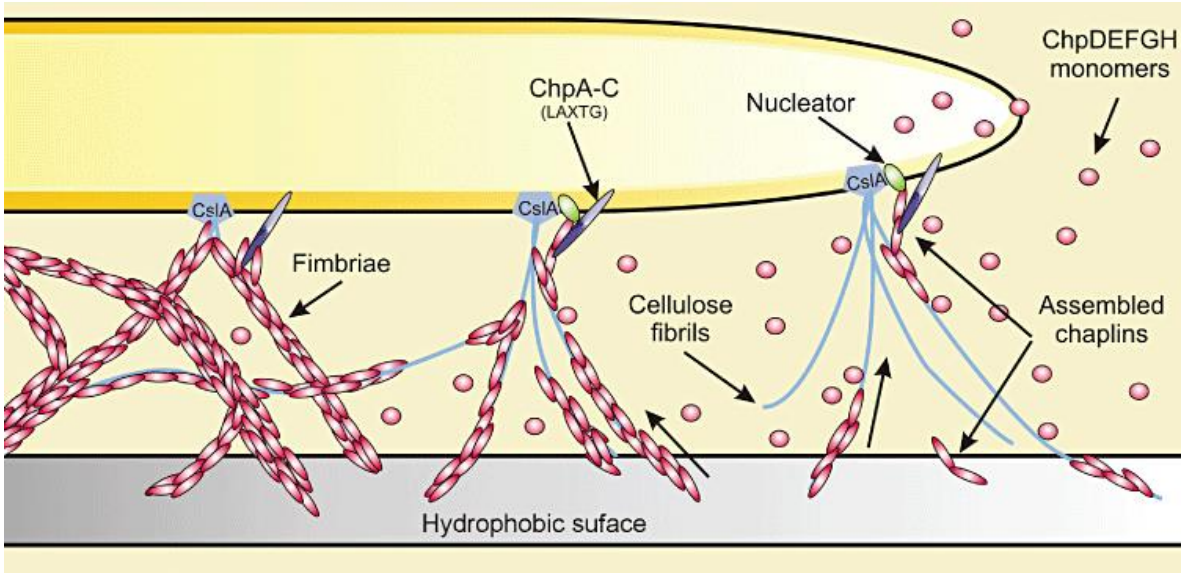

Figure 4: Interaction of chaplin based amyloid fibrils with cellulose fibres as a method of attachment to hydrophobic surfaces. Taken from de Jong et al [28].

The interaction between chaplin proteins and glycans has been shown to promote adhesion to substrates but *Streptomyces* is not the only bacterium which produces cellulose and amyloidogenic proteins [28]. *Salmonella enterica* produces an extracellular matrix which is composed of curli fibrils, cellulose and other polysaccharides[31]. The cellulose within this matrix was shown to be associated with the curli fibrils but was not required for the formation of the fibrils.

Chaplins are bacterial based proteins however, they have a high degree of similarity to hydrophobins[16] produced by filamentous fungi. These hydrophobins carry out similar roles to chaplin protein by being able to interact with surfaces, coat surfaces and lower surface tension. They can be distinguished by their size and properties into two different classes. Class I hydrophobins comprise of between 100 and 125 residues and are resilient against strong detergents such as sodium dodecyl sulphate. Whereas class II hydrophobins have between 50 and 100 residues [32] and can be dissolved in ethanol or SDS [33]. Chaplins have similar properties to class I hydrophobins as they are insoluble to SDS and can be solubilised using trifluoroacetic acid [34]. The transition from a soluble state to the assembled state for class I hydrophobins involves an intermediate step where proteins are rich in an α-helix structure. This intermediate stage is uncommon in chaplins as they have a low propensity to form this α-helical structure [27]. This low propensity of α-helix leads to the ordered self-assembly of the β-sheets.

Both chaplin proteins and hydrophobins can form amphipathic membranes when exposed to a hydrophobic-hydrophilic interface such as air-water interface. The membrane causes the nature of the surface to be changed which has potential to be exploited for medical and technical applications where less stable hydrophobins have been unsuccessful.

1.5. Functional amyloids

Amyloid proteins are not novel and are usually formed when proteins aggregate forming long fibrils. These fibrils are resilient to degradation and have been shown to be associated with diseases such as Alzheimer's [35]. In nature however, amyloids play pivotal roles which can include biofilm formation or surface monolayers. Chaplin proteins are the monomers which form the amyloid fibril, which is then used to assist aerial hyphae development.

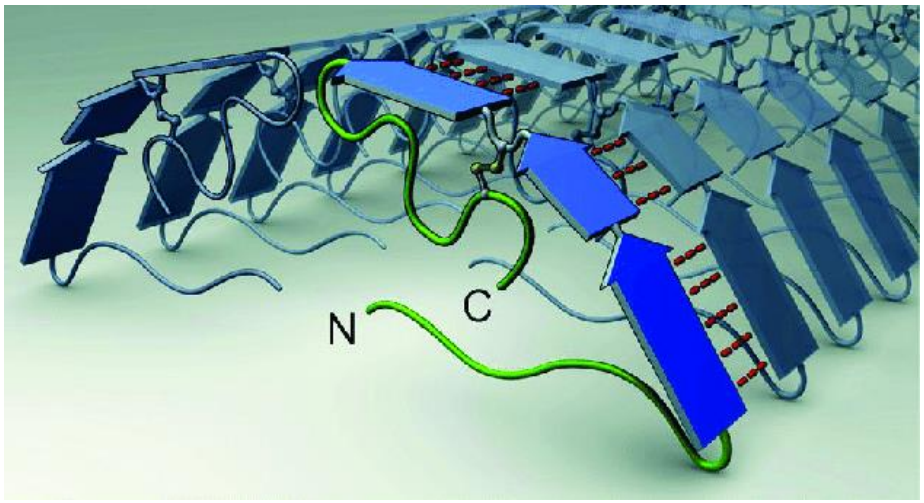

Figure 5: Chaplin protein structure with the Chaplin domain (Blue) facing outwards and the -C and -N termini (Green) at the core. Adjacent chaplin proteins hypothesised to be stabilised by hydrogen bonding (Red) [36].

The chaplin proteins are hypothesised to align side by side by hydrogen bonding with the -C and -N termini at the core of the fibril. All chaplin proteins except chaplin E have cysteine residues in the hydrophilic domains which leads to disulphide bridges. These bonds are not crucial for formation of the chaplin amyloid fibrils.

1.6. Streptomyces biotechnological importance

Streptomycetes have been employed for biotechnology processes due to their ability to bio-convert different substrates using a range of enzymes which they produce [37]. During the life cycle, primary and secondary metabolism occurs. During primary metabolism vegetative biomass is prevalent as well as enzyme production, whereas during secondary metabolism, aerial hyphae have developed, and the production of antimicrobials and pigment formation is observed. The range of enzymes produced have the capabilities for, but not limited to, oxidation, hydroxylation and dehydrogenation. The use of biological based approaches has the ability to provide significant benefits over synthetic chemical processes as enzymatic reactions can occur under milder and safer conditions[38]. With the development of synthetic biology techniques, the ability for genome engineering approaches can provide enhanced expression or function in both primary and secondary metabolism. During

secondary metabolism, *Streptomyces* produce a wide variety of antimicrobial molecules which vary in chemical composition that have advantages to its survival in the environment [39]. During the 1940s, Selman Waksman developed a research method for antimicrobial activity of soil bacteria, which led to the discovery of antibiotics and antifungals such as actinomycin[40] and streptomycin[41]. These compounds are still used today. The discovery of new antimicrobial compounds has drastically decreased over the past 50 years but *Streptomyces* still produce approximately two thirds of all antibiotics[42].

1.7. Bioprocess design

To allow for sufficient extraction and use of antimicrobials within medicine, production at a large scale must be achieved. The scale up of bioprocesses is not strictly limited to antimicrobials as proteins[43], organic acids[44] and enzymes can also be extracted for industrial applications. The use of fermentation technologies over chemical reaction processes has gathered considerable interest as the reactions are carried out in a more sustainable manner by using natural resources and lower temperatures[45]. The progression from shake flasks to litre size fermenters can cause lower yields due to many factors such as shear stress and physiological responses to the extracellular environment. Lab based fermentations(~200ml) using conical flasks normally require the use of a shaking incubator to maintain temperature and mixing. This mixing is generally carried out in a rotational pattern at a set rotations per minute. The medium and parameters required would vary depending on the bacteria or fungi being investigated. The incorporation of shear stress from the impeller can cause mechanical lysis of the bacteria or fungi. Another key difference between shake flask cultures and bioreactor fermentations is the method of aeration. Shake flasks are oxygenated by the mixing process and the ability to have an unsealed fermentation vessel unlike a bioreactor. A bioreactor relies on the pumping of air into the vessel via a sparger, which forces air through small holes at the bottom on the fermentation vessel. The flow of air can be controlled which does provide a benefit over the shake flasks. The design and operating parameters of a fermentation are important on the overall growth[45] and the ability to monitor, in real time, provides further advantages over shake flasks. Dissolved oxygen, pH, anti-foam and temperature are common parameters which can be monitored throughout the course of the fermentation. As the readings are recorded in real time, reagents or changes to the operating parameters can be changed automatically to maintain the same set value. For example, if the pH of a fermentation fluctuates above or below a set value, the addition of acid or base can be used to alter the pH without compromising the sterility of the culture.

Although the optimisation of fermentation parameters are important for efficient growth, a full techno-economic evaluation of the process is important to ensure or improve the commercial

competitiveness. One aspect which can be optimised is the medium used during the fermentation, but it can affect the morphological differentiation and/or the ability to produce secondary metabolites in *Streptomyces* species.

1.8. Glycan-protein interactions

Glycans comprise one of the four building blocks of life, nucleic acids, amino acids, lipids and glycans[46]. These glycans usually consist of O-glycosidic linkages of monosaccharide monomeric units. Two examples of glycans which are common in nature are cellulose and chitin. Cellulose is composed of β-1,4-linked D-glucose (Figure 6) whereas chitin is composed of β-1,4-linked N-acetyl-D-glucosamine. Cellulose is the most abundant polymer on earth [47] and is the main constituent of plant cell walls. Some bacterial species can secrete cellulose and aid in the formation of biofilms [48].

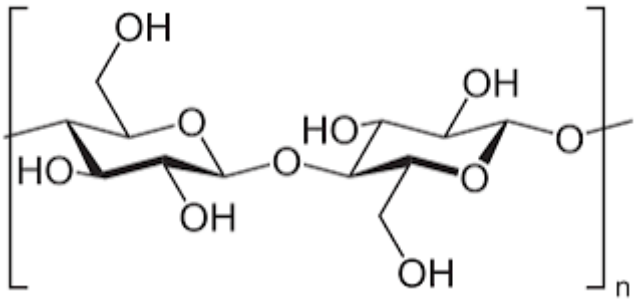

Figure 6:The β-1,4-linked D-glucose molecular structure of cellulose [49].

Cellulose has a number of hydroxyl groups present that can be reacted with specific reagents to modify its structure to form cellulose ethers and cellulose esters. The modification of a hydroxyl group to a new side chain can significantly change the properties. Unmodified cellulose is insoluble in water but when reacted with propylene oxide, hydroxypropyl cellulose is formed which is soluble in both water and ethanol. This particular type of cellulose is film-forming and has been shown to be an effective corrosion inhibitor in acidic environments [50].

1.9. Corrosion

Corrosion is the electrochemical conversion of a refined metal into a more chemically stable form such as an oxide. As this occurs, the metal can be aesthetically displeasing before further degradation of the metal leads to mechanical property failure which ultimately requires repair or replacement. Corrosion is a global issue with a cost of 3.4% GDP ($2.5 trillion) linked with corrosion but there are strategies being employed for the prevention of corrosion. Corrosion rates can vary dependent on the type of metal and the environment in which they are situated [51]. Specifically, the temperature, moisture and environmental availability of electrolytes such as chlorides have a significant effect on the corrosive degradation [52]. Within the marine environment, the chlorides are dissolved within the

moisture which then attacks the metallic substrate by increasing the conductivity on the surface, due to the increasing conductivity, the rate of corrosion within marine environments is a function of the chloride ion concentration [53]. Corrosion is not limited to the marine environment; terrestrial environments also support corrosive degradation. Furthermore, microbes in any environment can influence the rate of corrosion in a process known as Microbially Induced Corrosion (MIC). Within anaerobic conditions, sulphate-reducing bacteria produce hydrogen sulphide which leads to cathodic cracking. The electrochemical reaction for iron is composed of the dissolution of the metal and the consumption of electrons which are given in Equation 1 and Equation 2, respectively.

Equation 1: Anodic reaction for iron

$$\mathrm{Fe} \leftrightarrow \mathrm{Fe}^{2+} + 2\mathrm{e}^{-} \ (\mathrm{Anode})$$

Equation 2: Cathodic reaction for iron

$$\frac{1}{2}\mathrm{O}_2 + \mathrm{H}_2\mathrm{O} + 2\mathrm{e}^{-} \leftrightarrow 2\mathrm{OH}^{-} \ (\mathrm{Aerobic}) \text{ or } 2\mathrm{H}^{+} + 2\mathrm{e}^{-} \leftrightarrow 2\mathrm{H} \leftrightarrow \mathrm{H}_2 \ (\mathrm{Anaerobic})$$

Under aerobic conditions, oxygen is freely available at the cathode and is reduced. This reaction typically happens in most solutions and is known as the cathodic reaction whereas the anode reaction occurs at the metal/environment interface and results in the oxidation of the metal [54]. With both the anode and cathodic reactions present, the flow of electrons through the substrate and the ionic flow through the electrolyte occurs, resulting in the formation of the circuitry, an electron transport chain, which forms the corrosion cell.

The formation of the corrosion cell is ultimately unavoidable as current methodologies for corrosion prevention have a certain life span depending on the type (organic or inorganic) and the environment in which it is subjected to. Metallic substrates will remain protected until a defect occurs such as a scratch or indentation. The defect would cause exposure of the unprotected substrate and unless quenched, the underlying substrate, albeit protected on the exterior, would corrode. Specific coatings have been developed to be self-healing and to limit the extent of corrosion once a defect become present. One technology developed by Siva et al, was the use of poly(o—phenylenediamine) nanotubes within an epoxy resin. When a crack or scratch forms, the nanotubes causes the passivation of the substrate [55] and limits the degradation of the substrate.

The design considerations for corrosion coatings can be extensive as the properties of the coating may have to extend beyond corrosion resistance. Ultimately, electrolyte and an electrical connection between the cathode and anode must be present for corrosion to occur. By creating a coating which interferes with either of these would reduce/stop corrosion of the substrate. Coating systems must

be able to withstand environmental conditions as well as mechanical forces. The coating can provide an effective barrier, but a soft or brittle coating would be easily damaged allowing electrolyte to connect the anode and cathode. The application of the coating is also an important parameter to be considered during design as different methods rely on different coating characteristics such as low viscosity.

1.10. History of chaplin-based biomaterials developments

Chaplin and rodlin proteins have been investigated since the early 2000's, where their association with *Streptomyces* differentiation was identified [16, 17, 23]. Their structural and functional similarities to fungal hydrophobins have been identified. One such similarity is the ability for interactions with glycans to aid in the adhesion to substrates [28]. Although like hydrophobins, chaplin proteins are more resilient to enzymatic degradation whilst facilitating the morphological differentiation of *Streptomycetes***.**

The review of chaplin proteins and their similarities to hydrophobins was described in Chapter 1.4. These fundamental scientific observations have been exploited in a series of applied studies at Swansea University for the development of chaplin protein-based biomaterials, notably anti-corrosive coatings and transparent adhesives. In an award-winning industrial collaboration with TATA Steel™, Alex Harold investigated the use of the chaplin proteins as a hydrophobic barrier coating on hot dip galvanised steel (HDG). This EngDoc study was able to show that corrosion resistance of HDG was improved by increasing the number of coating deposits of chaplin proteins by limiting the interaction between the electrolyte and the substrate [56].

The corrosion-based testing was qualitative by visually inspecting coated and uncoated metallic coupons before and after the exposure to enhanced weather tests. The study was also able to make progress with respect to improving the yield of chaplin proteins from *Streptomyces* cultures by changing extraction from labour- and resource intensive agar-grown cultures of *S. coelicolor* to extraction of chaplins from submerged sporulated biomasses from *S. griseus* grown in small shake flasks. Other liquid sporulating strains such as *S. venezuelae* were also trialled, but protein extracts of these strains resulted in coatings on glass with lower water contact angles, which were deemed suboptimal for development of barrier-based biocoatings.

Corrosion resistance of chaplin-based coatings on defence-relevant metals HDG steel and the magnesium alloy AZ31 was investigated further in a project funded by the Centre of Defence Enterprise (CDE), which operates under the Defence Science and Technology Laboratory (Dstl) of the UK government.

The CDE project, investigated the barrier properties and corrosion resistance of single and multiple chaplin deposits quantitively with the use of goniometry, electrochemical and evolution of hydrogen assays followed by some limited explorations of the coatings by Scanning Kelvin Probe (SKP) and Scanning Vibrating Electrode Technique (SVET) methodologies [57].The project determined that by increasing the number of chaplin layers, the water contact angle can be increased on AZ31 magnesium alloy to 94°. The corrosion resistance of HDG was improved >20 times, while AZ31's corrosion resistance was improved >2-fold, upon 6 applications of chaplin proteins. Within this project, the investigation into the expression of chaplin proteins using universal synthetic biology elements such as different promotors and ribosome binding sites to determine if the (over)expression in *S. coelicolor* M1146 could be achieved. It was concluded that chaplin proteins could be expressed but the submerged pellet morphology was significantly altered due to the constitutive expression of the proteins. The protein-only coating performed well as a barrier coating offering improved corrosion resistance, but the mechanical and bonding strength properties associated with the still only nanometres thin protein-only barrier coatings were suboptimal allowing quick occurrence of mechanical defects which would undermine the coating's performance.

Characterising and optimising the bonding strength of chaplin-glycan biocomposite materials was subsequently investigated in two-phased projects funded by the Defence and Security Accelerator [57]. The promising results from the chaplin-only anticorrosion coatings were combined with the advances made in the fundamental understanding of molecular interactions driving chaplin- β-glucans interactions for development of biological nanostructures in solution enabling the adhesion of Streptomyces to solid substrates (Figure 4). The project focussed on optimising chaplin β-glucans composite materials as a novel transparent adhesive material for glass and polycarbonate laminations as a possible replacement for poly vinyl butyral (PVB) adhesive in armoured glass [58, 59]. A screening of organic acids and solvents was carried out to determine their efficiency on monomerising chaplin proteins from extracts. Hexafluoroisopropanol was very efficient at the extraction of high concentrations of protein however, the functionality of the resulting peptides was lost with respect to adhesive strength. Trifluoroacetic acid, as used extensively in literature, was able to monomerise the peptides and maintain their functionality, while other organic acids such as formic, acetic and propionic acids also allowed monomerization though to different yields and processing times. The latter limitation was mostly due to poor volatilities of the acids tested and not necessarily due to poor monomerisation. The biocomposite containing chaplin proteins and a β-glucan was able to bond glass together within minutes and at a fraction of the thickness of the PVB control. The tensile strength of the biocomposite was tested by pulling apart the bonded glass and measuring the force required to disbond them. The biocomposite did not outperform the PVB, however, the biocomposite was

estimated to be less than 100 nm thin in comparison to the PVB which was between 3-4 mm. The adhesion strength shown within the 1st phase of the DASA study was used inspiration for the development of a novel biocomposite coating material for corrosion resistance. The material characteristics and barrier properties to be determined in this PhD study.

The second phase of the DASA project investigated optimisations for scaling up for the growth and extraction of chaplin proteins from liquid cultures in collaboration with the BEACON Biorefining Centre of Excellence at Aberystwyth University. *Streptomyces bikiniensis* was the main liquid-sporulating strain being analysed due to its great potential for protection of Intellectual Property, while *S. griseus* remained a work horse. The collaborative project led to the successful scale up from 200 ml to 2 L in bioreactors using R2YE medium (a medium known to support submerged sporulation of many strains of *Streptomyces*) in which fermentation parameters were optimised using 16 small-scale parallel reactors. In parallel, maltose-yeast extract-malt extract (MYM) medium was investigated to determine if *S. bikiniensis* and *S. griseus* would sporulate in this medium like *S. venezuelae*. The MYM medium on its own alas did not facilitate the sporulation of *S. bikiniensis* in submerged liquid, but with the addition of a buffering agent (TES) and trace elements, the sporulation of the strain was facilitated. Although the submerged sporulation of the strain was successful and the culturing using MYM resolved the issues with R2YE complexity and contamination, the use of TES as the buffer did not resolve the economic issue. A techno-economic evaluation was not conducted within the time frame of the project and as such no investigation into alternative buffers were researched. The development of a further modified sporulation medium for *S. bikiniensis* provided a modified basis for this PhD study's investigation into improved corrosion resistant coatings with the scale up using *S. griseus*, within a primary focus on the effects of alternative buffers and calcium on the sporulation.

With biotechnological processes, each bioprocessing step to purified product is critical to ensure the final extracted product is purified to an appropriate standard. A main limitation conclusion of the 2nd phase of the DASA project was that extraction relied on TFA. TFA is used for the monomerization, however after solubilisation of the chaplin proteins prior to application testing, residual TFA was detected and was thought to result in high variances in tensile strength and therefore affecting the performance of the biocomposite adhesive negatively.

1.11. Research Aims

The aims of this PhD thesis were to develop a novel anti-corrosion barrier coating with improved bonding and mechanical properties consisting of a chaplin-glycan biocomposite material. The strategy to improve corrosion resistance draws on multiple fundamental and applied advances of the knowledge surrounding chaplin protein based biocomposites as a potential replacement for the very effective anticorrosion but highly carcinogenic compound, hexavalent chromium. As steel production is millions of tonnes per year, the requirement for a sustainable corrosion-resistant coating, that can be produced on a large scale is high. The main aims were addressed through specific objectives to increase the technical knowledge of this biotechnology. The main aims, optimization of biomaterial production, alternative production methodologies and material characterisation were investigated in the following experimental chapters:

Chapter 3 – Media and downstream process optimisation for chaplin protein extraction

- To compare morphological differentiation of *S. griseus* submerged cultures using alternative buffering agents in R2YE and MYM medium compositions.
- To assess the effects of scaling up of culture volumes from 200 ml to 1700 ml on submerged sporulation and chaplin protein yield
- To determine if protein precipitation can aid in the extraction process of chaplin proteins in order to remove TFA contamination

Chapter 4 – Controlled production of specific chaplin proteins with potential for modification

- To develop an inducible expression system for Chp secretion by a homologous host consisting of a S*treptomyces* chassis strain
- To determine the optimal medium and conditions for expression
- To assess whether chaplin proteins can be secreted into the culture supernatant
- To determine a purification method for chaplin proteins from the culture supernatant

Chapter 5 – Biomaterial characterisation and corrosion resistance of a chaplin protein-based biocomposite coating

- To assess the functionality of (combined) synthetic peptides based on predicted *S. griseus* chaplin proteins as hydrophobic barrier coating on a hydrophilic substrate
- To examine whether different glycans influence water contact angles of coatings on hydrophilic substrates when combined with chaplin protein extracts or synthetic peptides

- To determine the optimal concentration and ratio of glycan to chaplin protein extract from *S. griseus*
- To examine the topography of protein-only and biocomposite deposits on glass and steel using high-resolution imaging
- To assess the mechanical properties of protein-only and biocomposite coatings on glass and steel
- To ascertain the efficacy of biocomposite coatings for improved corrosion resistance on steel

1.12. Research Approaches

The objectives of each chapter of research were addressed using the following approaches:

Chapter 3 –

Firstly, *S. griseus* flask cultures were grown using two different media (R2YE and modified MYM) with a different buffering agent (TES, $KHCO_3$ or MOPS). The biomass settling, spore counting and Thioflavin T response to amyloidogenic proteins (chaplins) were analysed for each culture (Section 3.3.1). Next, cultures with a high spore count and high Thioflavin T response were taken forward for scale up trials. A fermentor with a culture volume of 1700 ml and with real-time monitoring of pH, dissolved oxygen and temperature was used to investigate the likelihood of scale up. The media that facilitated a high degree of sporulation from the previous objective (Section 3.3.1.1) was grown at this increased volume and the parameters were monitored to allow for comparison. The yields of biomass were also compared (Section 3.3.4). Lastly, the investigation into the introduction of a precipitation step using diethyl ether to remove TFA whilst purifying chaplin proteins was carried out. Proteins were extracted from the high sporulating media types determined in section 3.3.5.3 with and without the inclusion of the diethyl ether precipitation step. Extracted chaplin proteins were subjected to the Thioflavin T fluorescence assay, SDS-PAGE, pH measurements and corrosion observations (Chapter 5).

Chapter 4 –

Firstly, the cloning of full-length *S. coelicolor chpE* into a thiostrepton-inducible promotor plasmid (pIJ6902) using restriction enzymes was carried out before conjugating into the *S. coelicolor* superhost M1146. Insertion of the *chpE*-containing plasmid into the chromosome was checked by different sets of polymerase chain reaction (PCR) to distinguish between wild-type and cloned copies. Different media (Nutrient broth, R2YE and the modified MYM from Chapter 3) were assessed for the expression and secretion of chaplinE protein in both the cellular biomass and the culture supernatant using the amyloid-specific fluorescence dye, Thioflavin T. Finally, the purification of chaplinE from the supernatant was investigated using ammonium sulphate and acetone precipitation before assaying

with Thioflavin T, SDS-PAGE, modified western blot with amyloid-specific antibody and Matrix Assisted Laser Desorption Ionisation Time of Flight (MALDI-TOF) mass spectrometry to detect ChpE and other chaplin proteins.

Chapter 5 –

Initial experiments were carried out to determine the composition requirements of synthetic chaplin proteins as a protein-only coating by dropcasting deposit and carrying out goniometry to determine Water Contact Angles (WCAs). The synthetic peptide-based biocomposite containing different concentrations of hydroxypropyl cellulose was tested to determine if increases in water contact angle could be achieved. Chaplin proteins extracted from *S. griseus* were combined with ethyl cellulose (EC) or hydroxypropyl cellulose at different concentrations to determine the effects of different β-glucans on the water contact angle. The protein-only and biocomposite formulations with synthetic peptide or chaplin protein extract coated onto glass and steel were imaged using Scanning Electron Microscopy and Atomic Force Microscopy (AFM) to investigate the surface topography of the deposits. As the mechanical properties of the biocomposite was unknown, AFM was also used to analyse the elastic modulus of the coatings to determine if improvements in desired mechanical properties could be gained. Finally, chaplin protein extract-based biocomposite was analysed for cathodic disbondment using a Scanning Kelvin Probe and exposing coated low carbon steel coupons to HCl fumes to ascertain the corrosion resistance of the coatings.

1.13. Covid-19 Impact Statement

The training, progression and research outcomes of this project have fluctuated due to the pandemic and the lasting effects experienced in the middle of this PhD project. Mitigations and amendments to approaches eased the pressures of delivering this research slightly, however the ability to carry out an interdisciplinary project with restrictions to laboratory equipment and training remained problematic until the end phase. The lockdown and subsequent conditions for working in a shared laboratory significantly hampered obtaining data which had a knock-on effect for the latter stages of the project, specifically material characterisation studies.

Initial results were obtained for biocomposite and protein-only deposits using extracted chaplin proteins, but the results did not conform to expectations, so a full repeat of the experiment was required. This occurred on the eve of the laboratory shutdown, so this resulted in an alternative approach by the designing and ordering of synthetic peptides to reduce the requirement for specific lab equipment located in other buildings under the control of other departments where access was heavily restricted post-lockdown. Designed peptides were expected to be soluble in ethanol (the solvent of choice for chaplin solutions for metal coatings), however, this was not the case, so the use of ethyl cellulose was restricted to biocomposite development with extracted chaplin proteins.

The government legislated self-isolation for contracting and proximal contact of Covid-19 also limited research time somewhat. However, contracting Covid-19 and the subsequent knock-on symptoms were a factor in the development of this research: ‘Brain fog’, lack of focus and insomnia were hindrances to both my personal and research development.

The loss of training opportunities, research time and equipment access led to some aspects of the material characterisation and corrosion tests to be conducted under a lower than desired number of replicates (n=1) with no opportunity for further repeats.

2. General materials and methods

2.1. Growth

The *Streptomyces* strain used in this study was *S. griseus*. Growth of this strain was monitored in two media recipes, R2YE and Malt extract – Yeast extract – Maltose (MYM). Strains were cultured in flasks containing steel springs which were placed in a shaking incubator at 30°C at 200 rpm in either R2YE broth (103 g Sucrose, 10 g Glucose, 0.25 g K_2SO_4, 10.12 g $MgCl_2$, 0.1 g casaminoacid, 5 g yeast extract, 10 ml 0.5% KH_2PO_4, 80 ml 3.68% $CaCl_2$, 15 ml 20% Proline, 100 ml 5.73% TES Buffer [pH 7.2], 2 ml Trace Elements and 2 ml Antifoam) in 1 L of distilled water or MYM (4 g Maltose, 4 g yeast extract, 10 g Malt extract, 80 ml 3.68% $CaCl_2$, 100 ml 2.5% $KHCO_3$ [pH7.2], 2 ml Tract elements, 2 ml Antifoam) in 1 L of distilled water.

Each component was made up according to literature [60] and autoclaved separately before adding into the culture flask. Flasks were autoclaved and contained steel springs to increase aeration and reduce aggregation of mycelia. Culture volumes were carried out at 30-40% of the total volume to allow sufficient aeration. After addition of all components, flasks were inoculated with spores to a final concentration of $5x10^6$ spores per ml and grown for 6 days.

2.2. SDS-PAGE for visualization of proteins in supernatants and precipitates

Sodium dodecyl sulphate has a strong denaturing effect on protein folding and bind to the backbone of the peptide chain in a constant molar ratio. This binding onto the backbone leads to a net negative charge proportional to the length of the peptide. The separation of the peptides occurs as an electrical current is passed through a polyacrylamide gel which is subsequently stained to visualise the peptides in relation to a series of standards, at known molecular weights.

Pre-cast 20-10% tricine electrophoresis gels were purchased from Invitrogen. For each protein extraction, 20µg of protein, 5 µl of X5 loading buffer and 1 µl of DTT was combined. Samples were neutralised with 12.5% ammonia if required. Distilled water to a total volume of 25 µl was added before samples were incubated at 95°C for 5 minutes. In Tris-tricine running buffer, gels were run for 90 minutes at 110 volts.

2.3. Matrix assisted laser desorption ionisation time of flight mass spectrometry

Using the synthetic chaplin peptides, the protocol for detection with the matrix composition of 1-part sinapinic acid to 1 part 0.1% Trifluoroacetic acid in acetonitrile was used. Using the Bruker UltraflexTOF, the reflector acquisition mode, 13000 shots were applied to the sample and matrix. Synthetic peptide or extracted chaplin proteins were provided at a concentration of 1 mg/ml to NMSF for sample preparation and analysis.

2.4. Statistical Testing

Data sets were tested for check the normality of the distribution. Non-parametric t-test known as the Mann-Whitney U test was carried out to determine the significance on data sets. Confidence level for the significance was set at 95% ($P<0.05$). p-values higher than 0.05 were deemed to be insignificant.

2.5. Protein Quantification and detection

Extracted protein was quantified using the Pierce™ BCA total protein assay. The working reagent was prepared with 50 parts of reagent A to 1 part of reagent B as per the manufacturer's instructions (Thermofisher). A dilution series of bovine serum albumin was used as standards for determining the protein concentration of the unknown extract's samples. 50 µl of each standard and unknown was added to 1 ml of the working reagent before incubating at 37°C for 30 mins. All samples were cooled before measuring the absorbance at 562 nm. For detection of amyloid proteins, Thioflavin T fluorescence assay was used.

2.6. Detection of Amyloid Proteins

Following the extraction protocol, monomerised protein was resuspended in water or ethanol for 24 hours. The total protein concentration was determined using a Pierce BCA total protein assay. Part A and Part B were mixed at a ratio of 1:50 (20 µl in 1000 µl) to create the working reagent. 10 µl of the unknown samples were added to each tube and incubated for 30 minutes and 37°C. The absorbance at 562 nm was then recorded and compared to the BSA standard curve to determine the total protein concentration. The Thioflavin T assay was used to specifically detect and quantify amyloid proteins.

Thioflavin T was dissolved in PBS to a stock concentration of 0.8 mg/ml, aliquoted and stored at -20°C with tubes wrapped in foil to protect from light. For the detection of amyloid proteins, the 0.8 mg/ml Thioflavin T stock solution was diluted 1 in 50 Phosphate Buffered Saline (PBS) and 25 µl was aliquoted into each well of a flat bottom, black, 96-well plate. A serial dilution of the protein samples were created and 20 µl was added to each well. The wells were then made up to 100 µl with PBS. Each concentration was analysed in triplicate. As a positive and negative control, chaplin E synthetic peptide (GeneCust) and water are used respectively. The plate was then covered and incubated at 37°C for 1 hour. Using a fluorescence plate reader (BMG PolarStar), the fluorescence intensity was recorded using a 448-10 nm excitation and 482-10 nm Emission filter set, with a gain of 1500.

3. Media and downstream process optimisations for liquid grown cultures of *Streptomyces griseus*

3.1. Introduction

Streptomyces is very commonly used within the biotechnology sector to produce antibiotics and hydrolytic enzymes for laundry detergents. Approximately, two thirds of all antibiotics produced are from *Streptomyces* [61]. *Streptomyces* are gram-positive bacteria which develop through three key stages of differentiation, vegetative growth, aerial hyphal growth and sporulation. These stages occur depending on various factors such as environmental, specific strains and medium. Medium selection is important as it must facilitate growth and production of the desired product. Most streptomyces strains sporulate on solid media. *Streptomyces coelicolor* is a well-researched strain that sporulates on solid media. During the process of sporulation, amphiphilic proteins, known as chaplins, cover the aerial hyphae and spores to protect against desiccation. To extract these proteins from solid media, cellophane disks are placed on top of the plate and after the grey coloured spores become evident, the hyphae and spores are collected by scraping. This process however is not scalable as the number of agar plates required is significant and requires time consuming extraction from the plates. The use of liquid sporulating strains eliminates the need for cellophane disks and removes the need for manual scraping of the plates. A specialised media, R2YE, was developed to facilitate sporulation of streptomyces within liquid cultures. There are very few strains that sporulate in submerged cultures, strains such as *S. venezuelae* [62], *S. chrysomallus* [63], *S. antibioticus* ETH 27451 [64], *S. albidoflavus* [65] and *S. brasiliensis* [66]. However, R2YE is a complex and expensive medium which requires numerous post autoclave additions that can easily lead to contamination if aseptic technique is not stringently carried out. *S. coelicolor* is a well-researched strain in regards to its regulation of sporulation [19, 67]and chaplin proteins play a significant role for this to occur. Within *S. coelicolor*, there are three long chaplins (ChpA-C) and five short (ChpD-H). Manipulation of the *S. coelicolor* chromosome to remove the chaplin proteins has been shown to eliminate and/or delay the formation of aerial hyphae and subsequently sporulation. For the successful production of chaplin proteins, sporulation gives a strong indication of their presence. *S. griseus* was identified by Alex Harold as the strain that sporulates in liquid cultures and gave a high yield of chaplin proteins but is not as well researched [56]. This highlights the need for novel data on the growth of *Streptomyces griseus* for the sporulation and subsequently the extraction of chaplin proteins. *S. griseus* is commonly used for secondary metabolite production but this does not necessarily mean that the culture sporulates.

The main component that adds to the expensive nature of the media is the buffer that is used, 2-([1,3-Dihydroxy-2-(hydroxymethyl)propan-2-yl]amino)ethane-1-sulfonic acid (TES). This particular buffer is effective at maintaining a pH between 6.8 and 8.2, which is similar to the optimal range for *Streptomycete* growth of between 6.5 and 8.0 [68, 69]. The use of phosphates by *Streptomycetes* as a

regulatory signal causes the onset of differentiation meaning that phosphate buffers cannot be used as it does not lead to sporulation [70].

Ease of downstream processing of cultures is equally as important as the growth itself. The optimisation of downstream processes are crucial to ensure purity and performance are achieved. The development and optimisations can vary depending on the product of interest. The processing of small-scale cultures can be achieved by manipulating the protein properties and removing all other components, i.e., medium and biomass. When scaling up growth, it often requires the optimisation of downstream processing to improve yield. Within the biotechnology sector, there are various methods for the purification of products, such as tangential flow filtration which allows for extraction of small metabolites from the supernatant of the culture. This method would be ineffective on chaplin protein purification as the chaplin proteins play a structural role and has an affinity for the cell wall as the growth cycle develops and differentiates. This purification method would also be considered ineffective due to the morphological changes which chaplin proteins undergo.

Proteins are polypeptide structures composed of amino acids which form 3-dimensional structures. Secondary structures such as β-sheet and α-helix are common. β-sheet are formed by β-strands which form laterally. This conformation makes the protein structurally robust and resistant. The chaplin proteins when expressed are β-sheet proteins but is more commonly found to be in an amyloid fibral state, which is the aggregation of these β-sheet proteins into fibrils. This would significantly increase the molecular weight and hence would not be purified through a tangential flow filtration module. Due to the hypothesised inability of purification from the supernatant using the wild-type strain, an extensive extraction process is carried out which requires used of TFA. Trifluoroacetic acid is a strong acid which is used for the monomerization of chaplin proteins during the extraction process. This acid is commonly used in the purification of synthetic proteins as part of the cleavage cocktail. TFA is very corrosive and requires evaporation as part of the extraction process which can be detrimental to aquatic life and the environment. It has been identified that TFA remains residual in solubilised samples which caused issues in its application. Adapted from the synthetic peptide process, the use of diethyl ether may provide an alternative for the removal of TFA, which, if effective, could improve the application performance.

The aims of these experiments were to determine if sporulation of *S. griseus* can be achieved within the Maltose-Yeast extract-Malt Extract (MYM) medium and to investigate the potential use of different buffers to reduce the overall cost of the recipe and improve the economic viability for the production of chaplin proteins. Monitoring the growth by microscopy and assaying for amyloid proteins after extraction gives an indication of chaplin proteins.

Thioflavin T is a widely used stain for the detection of amyloid fibrils. As chaplin proteins form amyloids, this stain gives an indication of their presence, however it is only semi-quantitative due to the degree of fibrillation can vary.

3.2. Material and Methods

3.2.1. Media Preparation

Each medium was made as described in section 2.1. An additional medium was prepared by autoclaving all components together to determine if post autoclave additions could be removed. The buffer used and the change in the medium preparation is summarised in Table 1.

Table 1: Media composition and preparation method used for each medium

	TES	MOPS	$KHCO_3$	Pre autoclaved components?
R2YE + TES (Control)	+			+
R2YE + MOPS		+		+
R2YE + $KHCO_3$			+	+
MYM + TES	+			+
MYM + MOPS		+		+
MYM + $KHCO_3$			+	+
MYMc + $KHCO_3$			+	

3.2.2. Bioreactor Set up

The scale up trial was achieved by increasing culture size from 200 ml to 1.7 L using a LabFors MiniFors bioreactor. The bioreactor contains numerous ports for the insertion of different probes to monitor and control growth parameters. The main probes used in this study were temperature, pH and dO_2. The dissolved oxygen probe can be autoclaved whereas the pH probe's performance diminishes with increased number of autoclave cycles, so sterilisation of the pH probe was achieved by submersion in 70% ethanol. For autoclaving, a two times strength medium was added, in this case 850ml. This allowed for sterilisation of the medium whilst also sterilising the bioreactor. The ports which were submerged into the medium (Sampling port and sparger) were clamped off to ensure that the medium was not ejected from the vessel when under pressure and a port which was not submerged was left loose so the vessel did not pressurise. The equipment containing the medium was autoclaved for 30 mins at 121^{o}C and then allowed to cool before adding the relevant post autoclave additions and water until the final volume was 1.7 L. During autoclaving, around 10% of the volume is lost by evaporation and was accounted for by post additions of water. gives an illustration of the set up and components required from small scale fermentations.

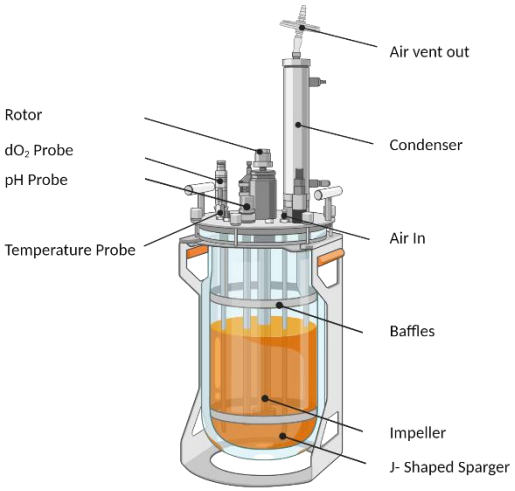

Figure 7: Typical fermentation apparatus and set-up for the controlled growth and real-time monitoring of bacterial cultures. Created using Biorender.

The vessel was hooked onto the main unit which had the relevant probe cables attached as well as the motor for rotating the impeller. The air in port was connected to the equipment which was set at 1.5 VvM (vessel volume/minute). This connection to the air had a sterile air filter added to ensure the culture remained contamination free. The air was expelled via the condenser unit. This unit was connected to a water cooler set at 10^{o}C; this condenses vapour as the air leaves the vessel. This also kept the attached filter dry and avoided clogging. Once all probes, air pump and water were connected, the fermentation system was started, and recordings were made using the IRIS software. The impeller speed was set at 350 RPM and 1.5 VvM. The vessel was run for 24 hours without inoculum added to ensure that the medium and equipment were sterile.

3.2.2.1. Bioreactor Inoculum

For inoculating the bioreactor, a seed culture was made. A dense culture of spores was grown for 24 hours in the same medium as the bioreactor before adding the total volume of the seed culture to the bioreactor. The density of the seed culture was determined by the total volume of the bioreactor as if it were inoculated with $5x10^6$ spores per ml.

3.2.2.2. Bioreactor Monitoring

The bioreactor gave real time data obtained during the growth cycle of the strain within the bioreactor. Samples were taken via the sampling port with a syringe attached to a sterile filter to draw up sample into the collection bottle. These samples were visualised by light microscopy every 24 hours. The microscopy images in conjunction with the pH and dissolved oxygen data was used to determine the end point of the fermentation.

3.2.2.3. Biomass Collection from Bioreactor Culture

To collect the biomass from the bioreactor, the impeller and the air flow was stopped, and the condenser unit was removed. The open port left by the condenser was closed to seal the vessel. The sampling tube was pushed to bottom of the vessel and the opposite end was placed into a 2 x 1 L Duran bottle. The air flow was then restarted which caused a positive pressure within the vessel and ejected the culture via the sampling tube. The biomass was then separated by centrifugation at 10,000 x g for 15 minutes.

3.2.3. Extraction and Monomerisation

After the growth of the bacteria, samples were transferred to 50 mL tubes and spun down at 15,000 x g and the supernatant was discarded. Each tube was resuspended in 20 mL of dH2O and sonicated for 30 seconds at 50% amplitude, three times to lyse spores. Following the sonication, 20 ml for 4% SDS was added to each sample to give a final concentration of 2% SDS before being boiled for 15 minutes. Once boiled, samples were transferred to centrifuge tubes and spun down at 15,000 x g then the supernatant was removed. 2% SDS was then used to resuspend the sample and then boiled again for 15 minutes. Centrifugation of the sample and boiling was completed once more before a series of washing and spinning to remove residual SDS. The remaining pellet was placed in a -80^{o}C freezer for 15 minutes, before being lyophilized overnight. This process has been summarised in . Samples were kept as freeze-dried pellets within a desiccator until required for quality assurance and application testing.

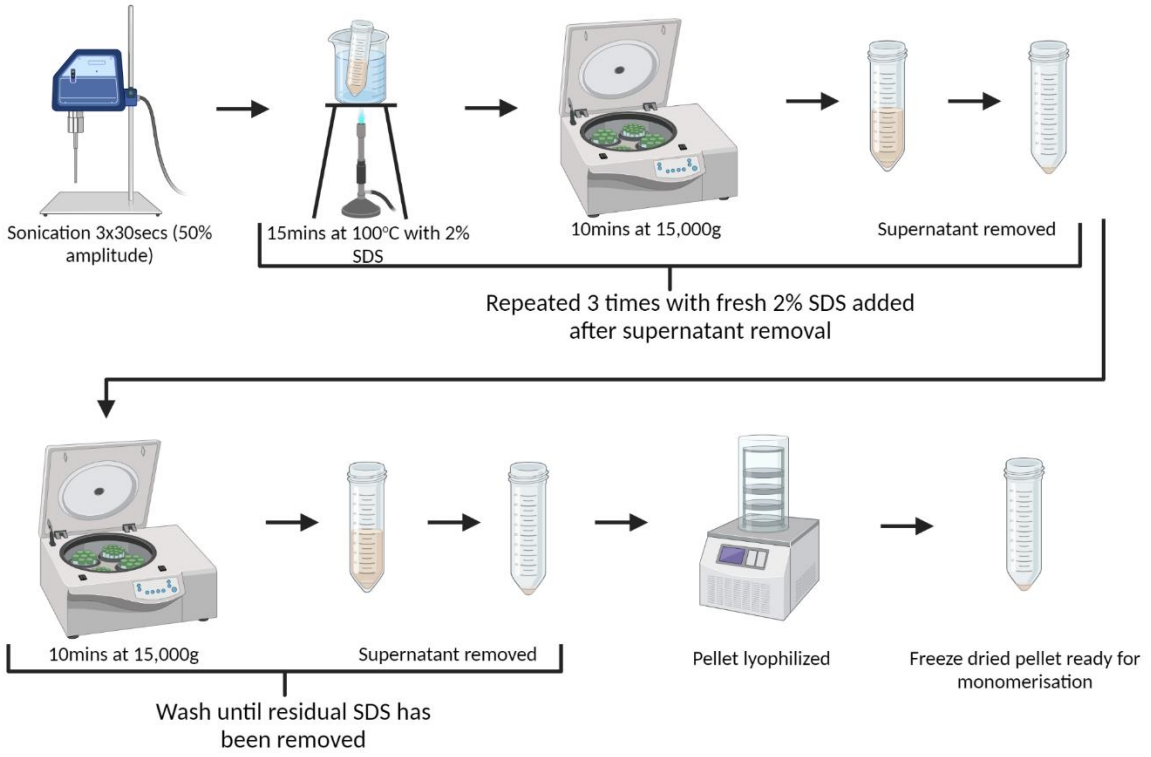

Figure 8: Flow diagram showing the sonication, SDS boiling, washing and freeze-drying process for the extraction of chaplin proteins.

To prepare samples for quality assurance and application testing, Trifluoroacetic acid (TFA) was added to the ground up freeze-dried pellets and left for 24 hours before aliquoting the supernatant into 1.5 mL tubes. The TFA in aliquoted samples was then evaporated in a fume hood under a steady stream of nitrogen or air. Once evaporated, sample tubes were closed and stored at room temperature ready for solubilisation in water or ethanol. This process if graphically represented in .

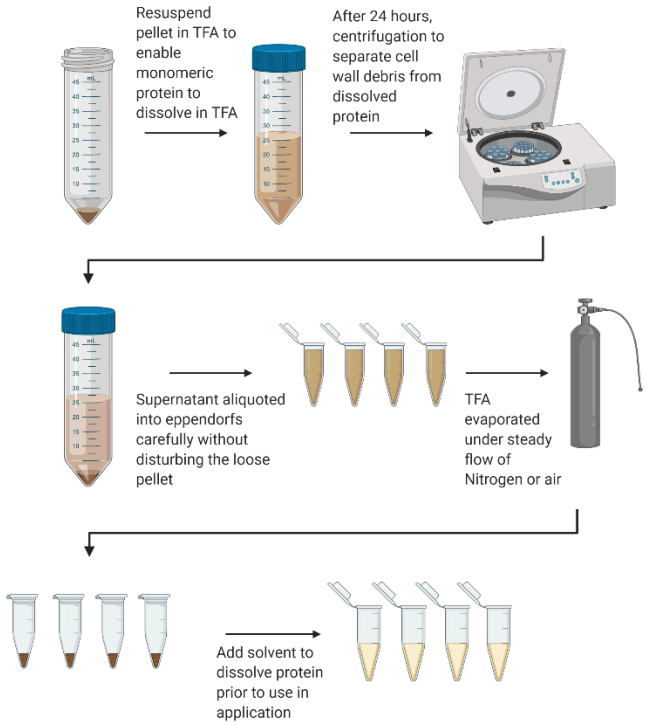

Figure 9: Flow diagram of the monomerisation of chaplin proteins from freeze-dried pellets using trifluoroacetic acid (TFA).

For the repeat extraction process, the same pellet was used to determine the concentration of residual chaplin proteins remain after each extraction. summarises the repeated extraction process.

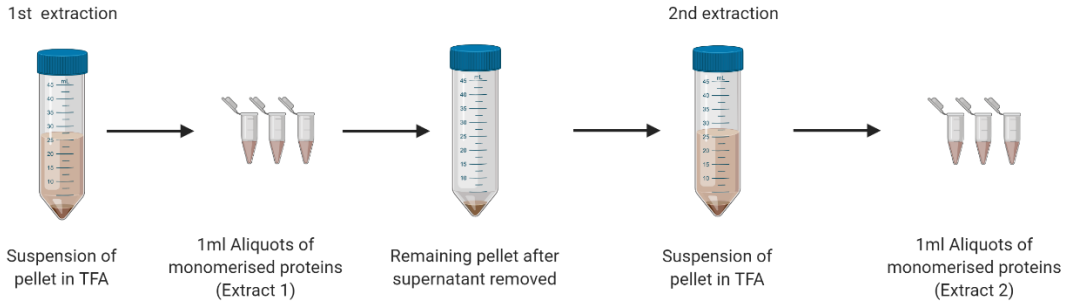

Figure 10: Schematic of repeat extractions from the same pellet. This was repeated up to 5 time to determine the total amount of protein that could be extracted

3.2.4. Diethyl Ether Precipitation

After following the standard extraction process, TFA was added to the freeze dried chaplin pellet and left overnight to allow for monomerisation of the chaplin proteins. The tube containing the TFA dissolved protein was then spun lightly to pellet any residual cell wall fragments that have been carried over from the extraction process. The supernatant was added dropwise to cold diethyl ether and was then incubated on ice for 30 minutes. Protein was thus precipitated and centrifuged at 10000 x g.

Diethyl ether was removed and the pellet was washed once more with diethyl ether. The supernatant was again removed, and the remaining pellet was allowed to air dry for evaporation of any residual diethyl ether. Caution was taken to not over dry the pellet. Samples tubes were closed and stored at room temperature. The dried chaplin pellet was solubilised in ethanol or water and assayed for total protein, Thioflavin T quantifiable protein content and pH.

3.2.5. Quantification of Sporulation

The number of spores were counted using a Helber bacterial counting chamber. The average count of spores was taken from three sectors of the counting chamber and was used to determine the number of spores per ml.

Equation 3: Concentration of spores calculation

$$Area\ of\ counting\ chamber\ sector = 0.2\ mm\ x\ 0.2\ mm\ x\ 0.02\ mm$$

$$= 0.0008\ mm^3$$

$$= 0.0008\ ul$$

$$Spores\ per\ ml = \frac{ul\ to\ ml\ conversion\ factor}{Area\ of\ counting\ chambre\ sector}\ x\ Average\ number\ of\ spores\ from\ 3\ sectors$$

$$= Spores\ per\ ml\ x\ dilution\ factor$$

3.3. Results

3.3.1. Growth

3.3.1.1. Biomass and Sporulation

S. griseus was grown in two rich media, R2YE and MYM which were buffered at pH 7.2 with either TES, MOPS or Potassium Bicarbonate ($KHCO_3$). *S. griseus* was cultured under shaking conditions for 6 days at 30°C in shake flasks. The morphology of the cultures were examined by microscopy which identified that the cultures containing MOPS buffer did not lead to completion of the full life cycle over the same time as the other cultures. Cultures were transferred into 50ml tubes to observe the settling of the biomass (Figure 11). A larger pellet observed indicates that the hyphae did not septate and during settling the pellet would be loose with more space between hyphae. In contrast, cultures that did septate into spores led to a smaller pellet as the space between spores would be less than that of a non-sporulated culture.

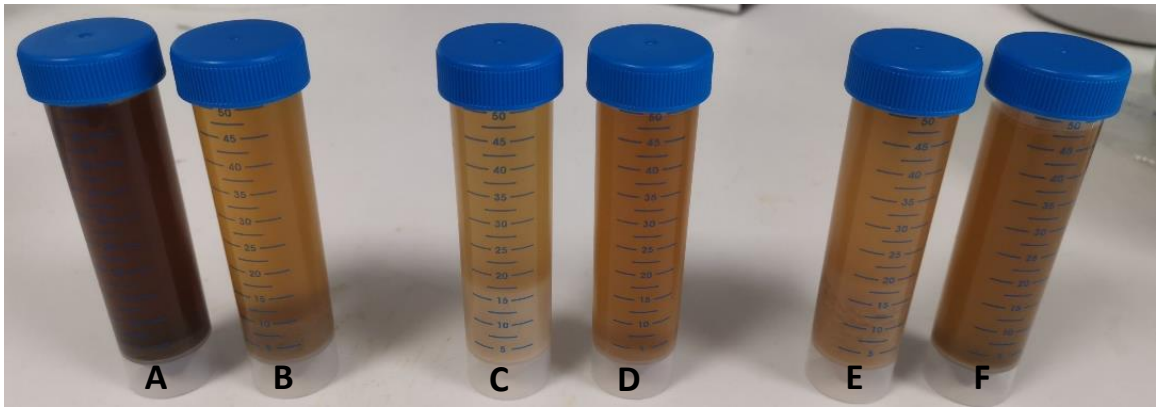

Figure 11: Settling of culture biomass for each medium. R2YE + TES (**A**) MYM + TES (**B**) R2YE +MOPS (**C**) MYM + MOPS (**D**) R2YE + $KHCO_3$ (**E**) MYM + $KHCO_3$ (**F**). Low biomass is normally indicative of sporulation as observed in cultures A, D and F.

R2YE + TES (Figure 11A) had a distinctive pigmentation and was abundant in spores. By changing the buffer to MOPS (Figure 11C) the pigmentation was not present, and a high abundance of hyphal growth was observed, however some spores were identified. The morphology observed here suggested that the differentiation of the strain was slower than the other samples or septation of spores was not occurring and the identified spores were ungerminated. The settling of the R2YE with $KHCO_3$ (Figure 11E) gave a larger pellet than the control but an abundance of spores were identified. MYM + TES (B) had a slightly larger settled pellet and lacked a change in pigmentation, but spores were present. Comparing this to MYM + MOPS (Figure 11D), hyphae were short which suggested slow growth and hence the observed small, settled pellet. MYM with $KHCO_3$ had a high abundance of spores and slight change in the pigmentation. The fragmentation of this medium composition appeared to be more efficient as clumps were smaller than that of the R2YE + TES (A) control. From the six media

iterations, the two containing the MOPS buffer did not sporulate within the same time frame (Figure 11C & D).

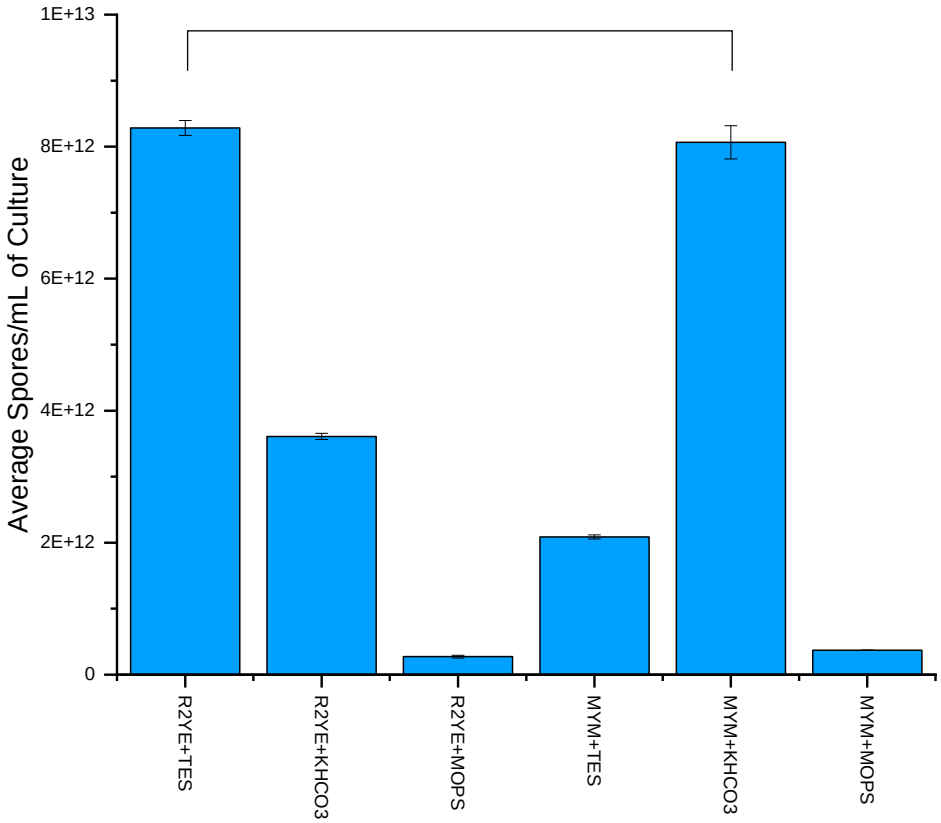

Figure 12: Quantification of spores using a Helber counting chamber for each medium using the different buffers (n=3). Mann-Whitney U Test P>0.05 indicating no significant differences between R2YE + TES and MYM + $KHCO_3$.

R2YE + TES was used here as a positive control for the sporulation of *S. griseus*, a high spore count of $8.28x10^{12}$ was quantified (Figure 12 R2YE + TES). When the buffer was changed to MOPS, a clear difference in morphology was observed with a dramatic reduction in the number of spores counted at a density of $2.9x10^{11}$ (Figure 12 R2YE + MOPS). When the $KHCO_3$ was used as the buffer, this led to an intermediate spore density of $3.61x10^{12}$ (Figure 12 R2YE + $KHCO_3$). The alternative and much easier and cheaper rich media, MYM, showed different results. Media MYM with TES buffer saw a reduction in the number of spores quantified in comparison to the control, with a spore density of $2.12x10^{12}$, while MYM with $KHCO_3$ resulted in a similar number of spores to the control with a spore density of $8.3x10^{12}$. MYM medium with MOPS was far less productive, which mirrored the R2YE medium supplemented with MOPS (Figure 12, MYM + $KHCO_3$ & R2YE + MOPS). Media containing MOPS was not analysed further due to the low spore count. A Mann-Whitney *U* test showed that there was no significant difference (*P*=0.275) between the two high sporulating culture (R2YE+TES and MYM+$KHCO_3$)

3.3.1.2. Chaplin Protein Detection from Sporulating Cultures

Although spores indicate that *Streptomyces griseus* can complete its lifecycle within these different media compositions, the biomass was processed for the extraction of the chaplin proteins from the sporulating cultures and then assayed using Thioflavin T. Cultures that did not sporulate were not processed. Figure 13 shows the absolute fluorescence intensities of ThT-bound amyloid proteins using BMG PolarStar plate reader.

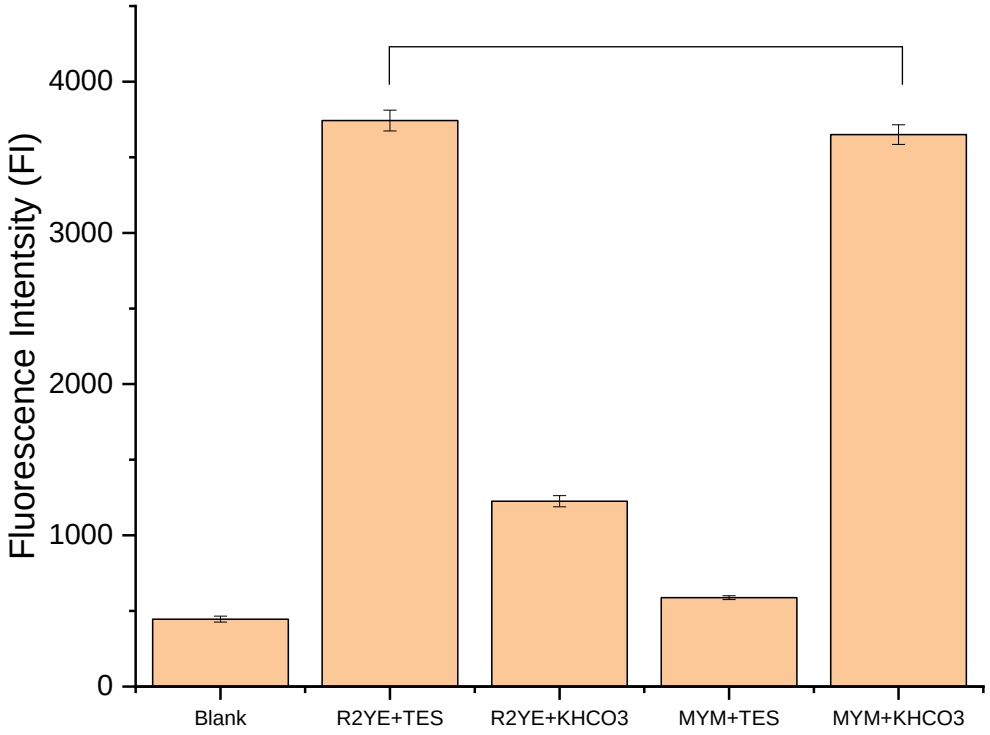

Figure 13: Thioflavin T fluorescence assay for the detection of amyloid proteins from cultures with a high spore count as identified from the spore quantification displayed in Figure 16. Statistical testing shows that there was no significant difference between the two samples. Mann-Whitney U Test P>0.05.From the spore count and the ThT assay, sporulation had occurred, and the extracted material gave a strong response for chaplin proteins. Upon statistical comparison of the R2YE+TES and MYM+$KHCO_3$, no significant difference was determined by the Mann-Whitney U Test (p=0.05).

3.3.2. EDTA Treatment of MYMc Precipitate

The media making process for both the R2YE and MYM required multiple post autoclave additions. In order to simplify the media preparation process and to reduce the chance of contamination, all components for the MYM medium, including the $KHCO_3$ buffer, were autoclaved together (MYMc). The medium formed a precipitate during the autoclave process which resulted in a turbid appearance (Figure 14A MYMc). As it is believed that the precipitate is related to the calcium and phosphates, the metal chelator EDTA was added to test for improved solubility and reduced turbidity.

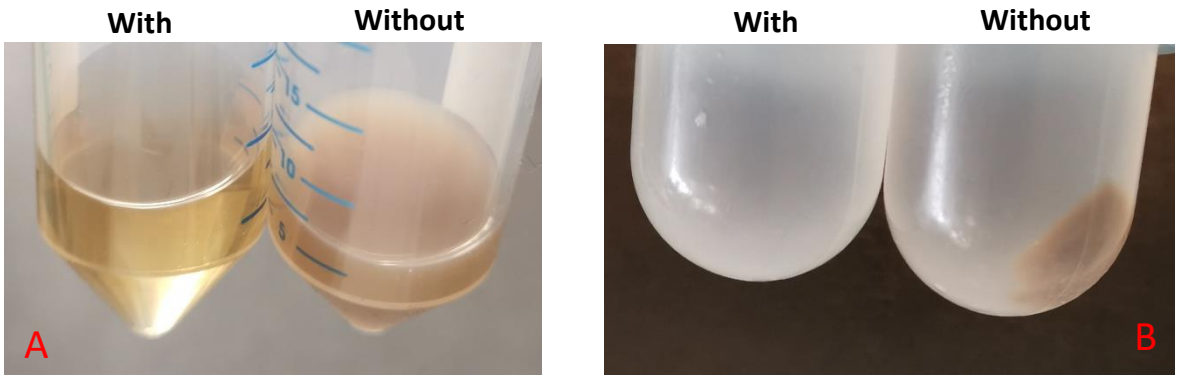

Figure 14: Comparison of MYMc medium with and without the addition of EDTA before (**A**) and after (**B**) the SDS washing step of the extraction protocol. The chelation of the precipitate appears to have allowed for easy removal of the precipitate formed during the autoclave process.

From Figure 14A, the turbidity of the sample is evident. After the addition of EDTA, the turbidity was reduced to an opaquer solution. The sample was then subjected to sonication and boiling SDS to determine if the precipitate would be removed and to investigate if the EDTA treated medium would remain precipitate free. After the SDS boiling and washing, a distinctive pellet was observed upon centrifugation for the non-EDTA treated sample. The sample with the EDTA treatment had no observable pellet. Next, *S. griseus* was grown in MYMc to determine if the presence of the precipitate and/or EDTA affected sporulation and the downstream processing.

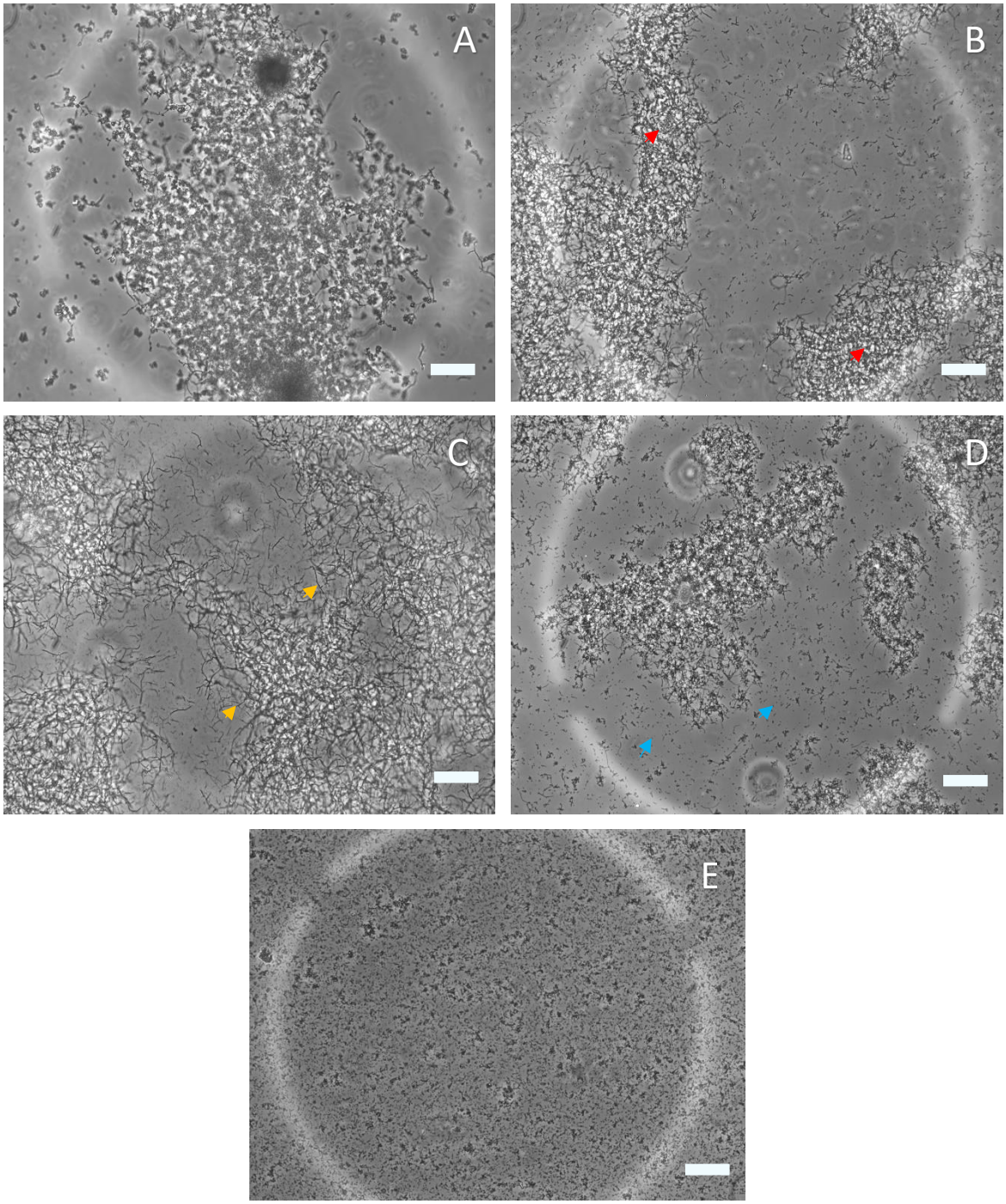

Figure 15: Microscopy images showing the life cycle of *S. griseus* from a liquid culture. Vegetative hyphal formation which forms vast networks and become entangled (Red), Aerial Hyphae growth from the vegetative hyphae which are generally narrower and protrude from the vegetative hyphae (Yellow) and spore formation as the aerial hyphae septate into spores (Blue). Scale bar = 20 µm

The growth of the strain was monitored by microscopy and shows that sporulation can still occur when all components are autoclaved together. Figure 15A shows the culture after 24 hours of growth and that the precipitate formed during the autoclave process was visible. By 48 hours (Figure 15B), the precipitate was not as evident as the vegetative hyphae were observed. After 72 hours (Figure 15C), aerial hyphae became prevalent. The septation and spore formation was observed after 96 hours of growth (Figure 15D) before a large abundance of spores observed after 120 hours (Figure 15E). The

sporulated cultures were extracted with and without the presence of EDTA. The resulting chaplin protein extracts were examined by the Thioflavin T assay (Figure 16) and SDS-PAGE (Figure 17).

This analysis was carried out on 25 µl of the solubilised material with the relevant dilutions made (1 in 2 and 1 in 4). As expected, the neat R2YE + TES (Figure 16) provided a very high response and the fluorescence intensity decreased as the sample were further diluted. MYM+TES (Figure 16) did respond to the assay but for the neat sample, an average value of 3304 was obtained. Only a slight response was recorded for the R2YE+$KHCO_3$ (Figure 16). The MYM+$KHCO_3$ (Figure 16) had a high response with an average value of 10212. The fluorescence intensity recorded for the combined medium (Figure 16 MYMc) was like that of the negative control sample (dH_2O). With the inclusion of an EDTA treatment step before sonication, the response to the assay was negligible in comparison to the negative control.

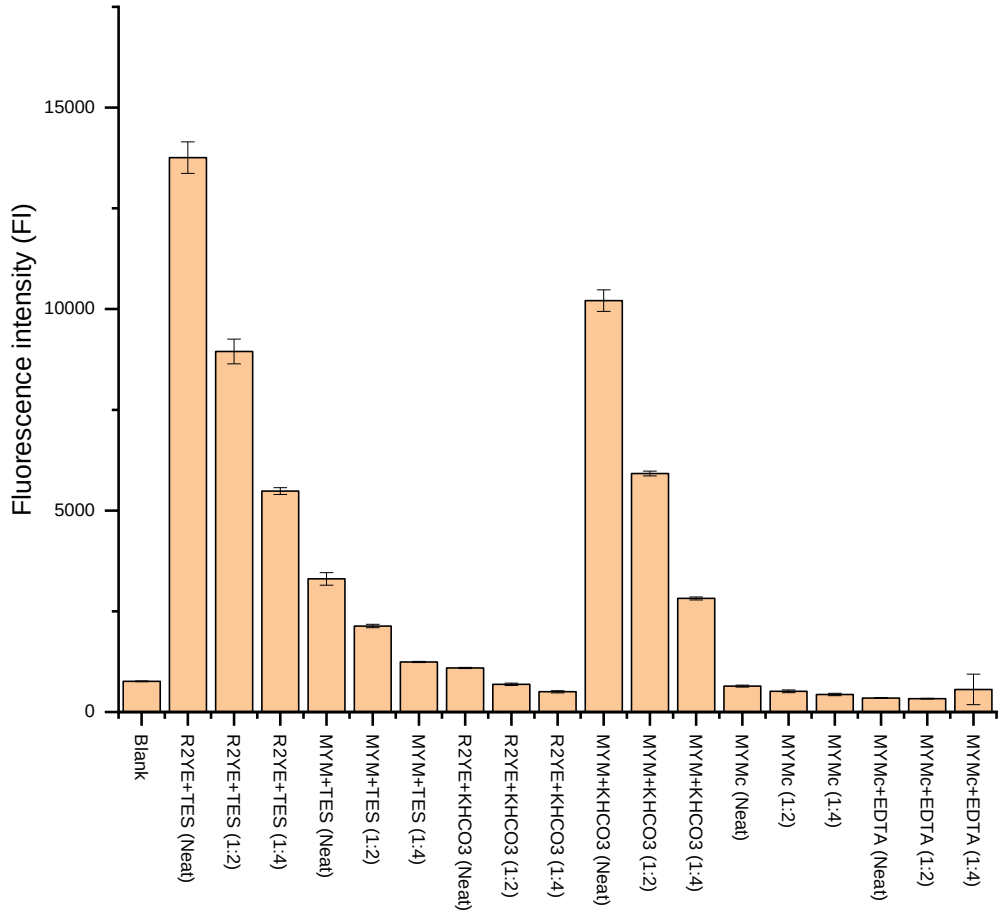

Figure 16: Amyloid protein response to the thioflavin T fluorescence assay for each protein extract from the different media compositions. Strong fluorescence for both R2YE + TES and MYM + $KHCO_3$ indicating high abundance of amyloid proteins.

Given the responses recorded from the Thioflavin T assay for each of these samples (Figure 16), SDS-PAGE was used to determine the purity of the samples (Figure 17).

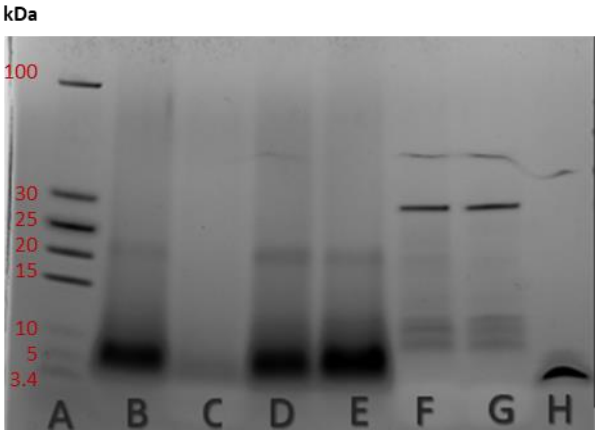

Figure 17: SDS-PAGE of extracted materials from the different media. PageRuler Low range ladder #26632 (Thermo Scientific) (**A**).R2YE+TES (**B**), R2YE+$KHCO_3$ (**C**), MYM+TES (**D**), MYM+$KHCO_3$ (**E**), MYMc (**F**), MYMc+EDTA (**G**) and Synthetic ChpE (**H**).

The bands observed for the media and buffers are shown in Figure 17. The synthetic *S. griseus* chpE peptide was used as a control and gave the expected band size (Figure 17 Lane H). When comparing this control to the different media compositions (Figure 17, Lanes B-E), a solid band was observed. The bands were more prominent in samples R2YE+TES (Lane B), MYM+TES (Lane D) and MYM+$KHCO_3$ (Figure 17 Lane E). A band was present in Lane C, but less abundant in comparison to the other extracts. Lanes F and G were extract samples from autoclaving all components (MYMc) with and without the additional extraction step using EDTA. Bands were observed but not at the appropriate molecular weight.

3.3.2.1. Scale up of Growth using MYM with $KHCO_3$

The growth of *S. griseus* in the newly developed medium, MYM+$KHCO_3$ successfully led to sporulation in small-scale flasks (200 ml). In order to analyse how the culture is performing throughout the growth cycle at large-scale, the use of a fermenter was carried out. This not only allowed for monitoring of the pH and dissolved oxygen over the course of the growth cycle, but it also investigated any effects of scale up. The scale up of the growth was achieved using a Minifors fermenter (), which allowed for a 1.7 L culture as well as pH and dissolved oxygen monitoring. As a control, *S. griseus* was grown under the same monitored conditions in R2YE + TES to allow for comparison.

Over the time course of the growth, the dissolved oxygen for both the MYM and the R2YE followed a similar pattern (Figure 18). After inoculation, there was a sharp decrease in the dissolved oxygen by 24 hours. After 24 hours, the dissolved oxygen remained low until 72 hours, except for fluctuations at 36 hours within R2YE and 42 hours within the MYM. At 66 hours, there was a sharp increase to 75% in the dissolved oxygen for MYM. This sharp increase transitions to a slow steady increase over the

final hours of the fermentation. The sharp increase observed with the R2YE fermentation occurred 7 hours after the MYM fermentation, but the pattern observed was similar to the MYM.

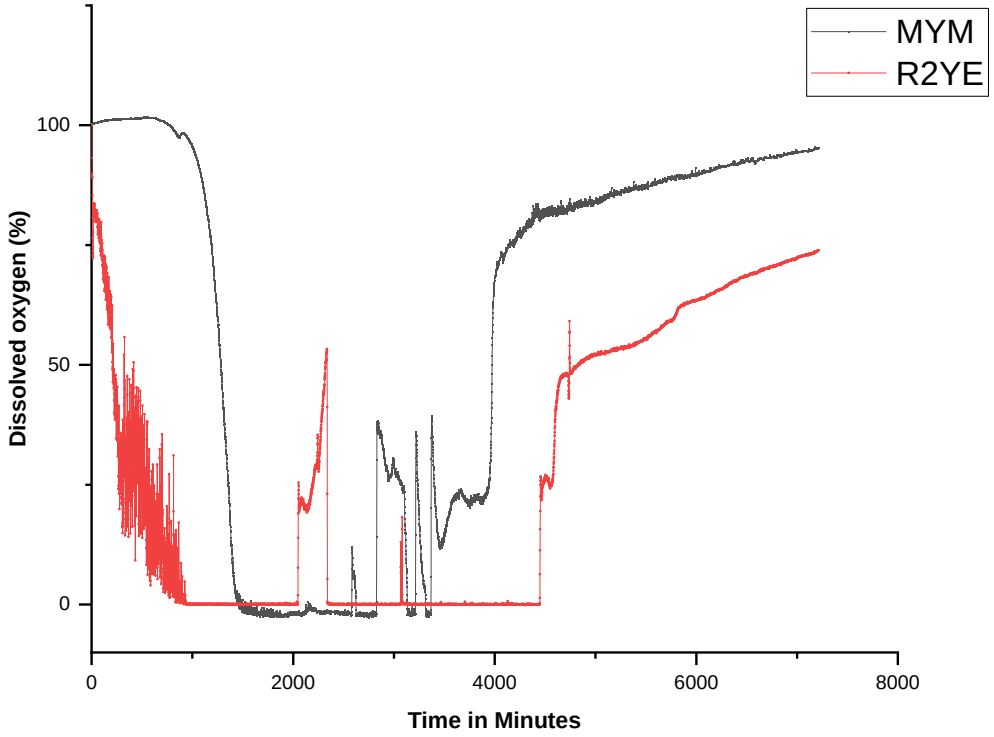

Figure 18: Real-time oxygen consumption of *S. griseus* fermentations in MYM + $KHCO_3$ (Black) and R2YE + TES (Red) showing similar trends over the course of the growth suggesting life cycle completion to sporulation.

The pH of the fermentation was also monitored in real time and both MYM and R2YE followed a similar pattern. The MYM+$KHCO_3$ had a higher starting pH but decreased to 7.6 by 24 hours (Figure 19). Between 24 and 66 hours, the pH fluctuated between 7.6 and 7 before slowly increasing until the end of the fermentation. The R2YE+TES had a starting pH of 7.6 and remained relatively steady until 36 hours before decreasing from 7.7 to 7.2 over the course of 6 hours. The pH remained steady at 7.2 for 24 hours before sharply increasing to 7.4 which then steadily increased to 8.2 until the end of the fermentation.

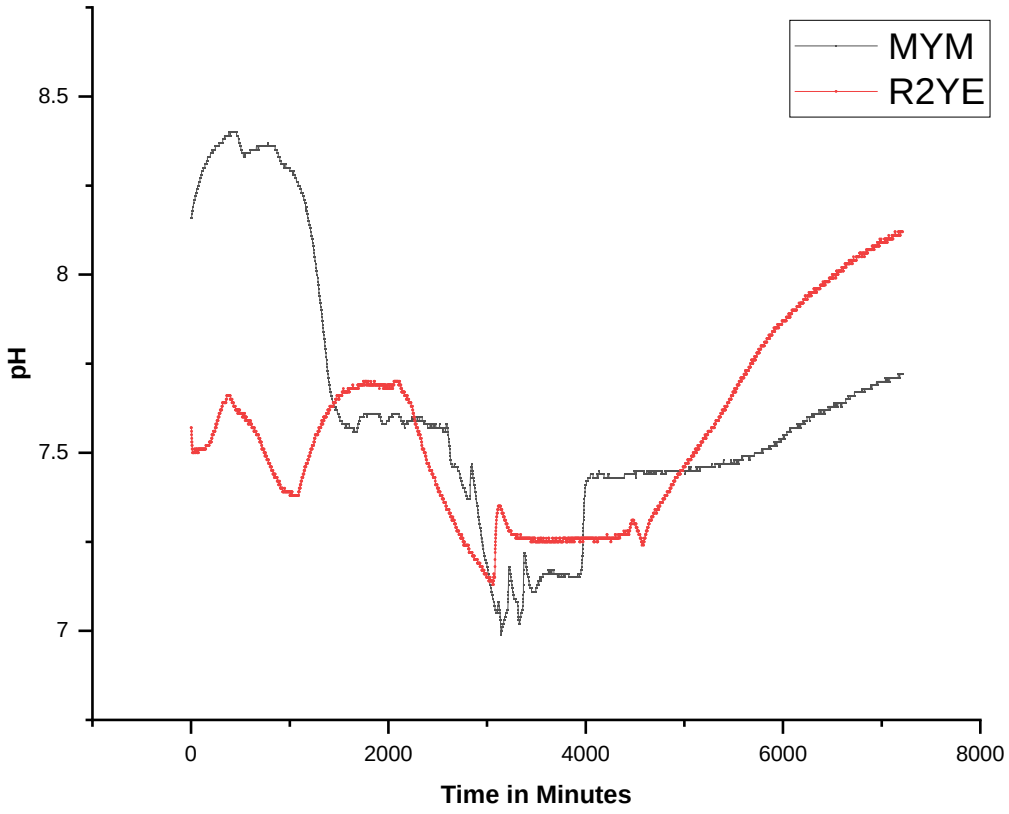

Figure 19: Real-time pH measurements of *S. griseus* fermentations in MYM + $KHCO_3$ (Black) and R2YE + TES (Red) showing similar trends over the course of the growth suggesting life cycle completion to sporulation.

3.2.2. Downstream Processing

Following the successful sporulation of *S. griseus* in MYM+$KHCO_3$, a comparison of biomass was made between the small scale and large scale. After extraction, Table 2 gives an overview of the concentrations of total protein extracted from the different volumes of cultures.

Table 2: Comparison of media at small- and large-scale fermentation

	200 ml Culture			**1.7 L Culture**		
	Before extraction	**Post extraction, freeze dried weight**	**freeze dried weight per ml of culture**	**Before extraction**	**Post extraction, freeze dried weight**	**freeze dried weight per ml of culture**
R2YE+TES	5.54 g	0.15 g	0.75 mg	34.62 g	4.06 g	2.39 mg
MYM+$KHCO_3$	6.02 g	0.17 g	0.85 mg	38.89 g	4.54 g	2.67 mg

3.2.2.1. Repeat TFA Extraction of Chaplin Proteins

TFA is used as part of the extraction process to monomerise the proteins after freeze drying. During this process, chaplin proteins would become solubilised within the TFA, however it was not clear if all proteins present within the pellet would be monomerised and solubilised. To test this, repeat extractions were carried out on the same pellet to determine the efficiency of protein monomerisation.

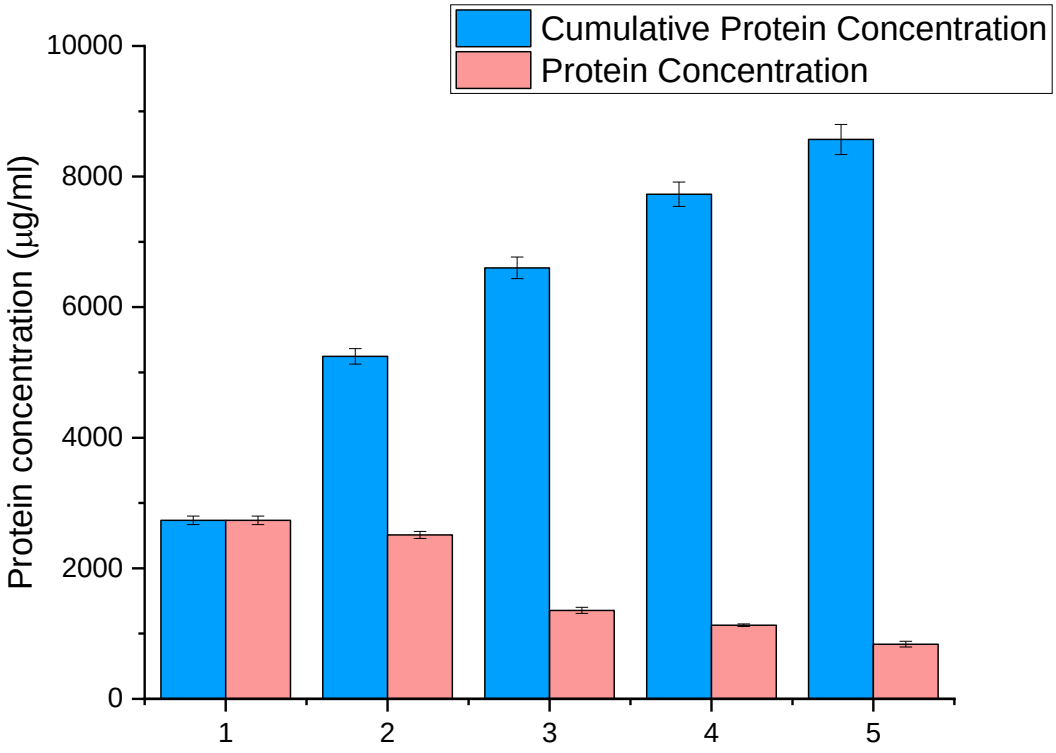

Figure 20: Repeat monomerisation using TFA and the total protein concentrations after each monomerisation. Protein extract concentration after each monomerization (Red) and the cumulative total protein extracted after each extraction (Blue).

Shown in pink in Figure 20, the total protein concentration obtained after each TFA extraction. The highest concentration was obtained after the first extraction with a concentration of 2734 µg/ml. After the second extraction, a similar amount was extracted (2511 µg/ml). By the third extraction, a 50.5% reduction in the total protein extracted in comparison to the first extraction. At extractions four and five, concentrations of 1128 µg/ml and 838 µg/ml were obtained, respectively. Cumulatively, by the 5th extraction a total protein concentration of 8566µg/ml was obtained. It is evident that as the number of extractions increase, there is a reduction in the protein concentration. This assay was

followed by SDS-PAGE to visualise the proteins present and by the fifth extraction no proteins could be observed at 5 kDa as highlighted in Figure 21.

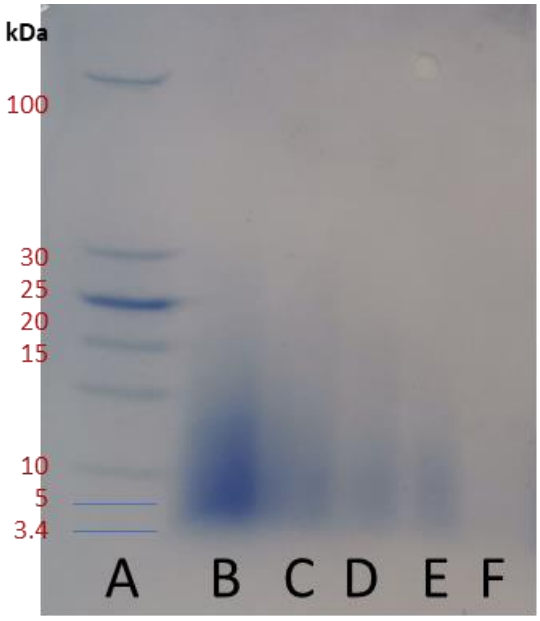

Figure 21: SDS-PAGE stained with Coomassie blue showing the 5kDa bands indicative of chaplin proteins. The letters correspond to the PageRuler #26632 (Thermo Fisher) (**A**), First extraction (**B**), Second Extraction (**C**), Third Extraction (**D**), Fourth Extraction (**E**) and Fifth Extraction (**F**).

Bands are blurred due to the presence of coextracted proteins, but this blurred appearance is stereotypical for chaplin protein extraction using the standard TFA protocol.

3.2.2.2. Diethyl Ether Precipitation of Chaplin Proteins

As TFA is very corrosive, the application of chaplin protein solutions with residual TFA from the extraction process onto steel coupons can result in corrosion. The evaporation process under nitrogen gas, still results in residual TFA and low pH of solutions. This low pH can be neutralised with the addition of ammonia to water-based solutions. In summary, TFA is used to monomerise the chaplin proteins from their fibral conformation and then require evaporation of the TFA prior to solubilisation. TFA is a fluorinated compound and is virtually non-degradable which raises environmental concerns when using. Alternative compounds have been attempted as a replacement to TFA, such as, acetic acid, humic acid and Hexafluoro-2-propanol (HFIP). Although a certain degree of success has been achieved with some of these compounds, issues with material application remains unresolved so an alternative strategy was adopted. As part of the cleavage cocktail used in the preparation of synthetic peptides, TFA is present and the extraction of peptide without the peptide cocktail is achieved by the precipitation of the peptides in diethyl ether. Adapted from how synthetic chaplins are produced[71], precipitating the chaplin proteins in diethyl ether may be an effective process addition to the

downstream processing to eliminate/reduce the residual TFA as well as reducing TFA release into the atmosphere. Following the TFA monomerization step but prior to the TFA evaporation, the monomerised peptides in TFA was added to ice cold diethyl ether. A washing step of the pellet was also included to remove any residual TFA still present. To test the change in the extraction protocol, the same volume was added to either a 2ml tube (for evaporation) or to diethyl ether (for precipitation). Samples were solubilised in either water or ethanol and then assayed for total protein and amyloid response using the thioflavin T assay. Table 3 shows the protein concentrations and amyloid response of the extracts that have been precipitated compared to the conventional evaporation method.

Table 3: Total protein concentration and ThT fluorescence data from 25 µl of sample

	Blank		**TFA Evaporation**		**Diethyl Ether Precipitation**	
	H_2O	**EtOH**	**H_2O**	**EtOH**	**H_2O**	**EtOH**
Total Protein Concentration (µg/µl)	0.00	0.00	1.16	1.06	2.14	1.63
ThT Fluorescence intensity (25 µl of sample) with standard deviation	899.67 ±87.08	514.67 ±48.05	2165.67 ±30.43	2704.67 ±278.02	3218.33 ±531.70	2785 ±215

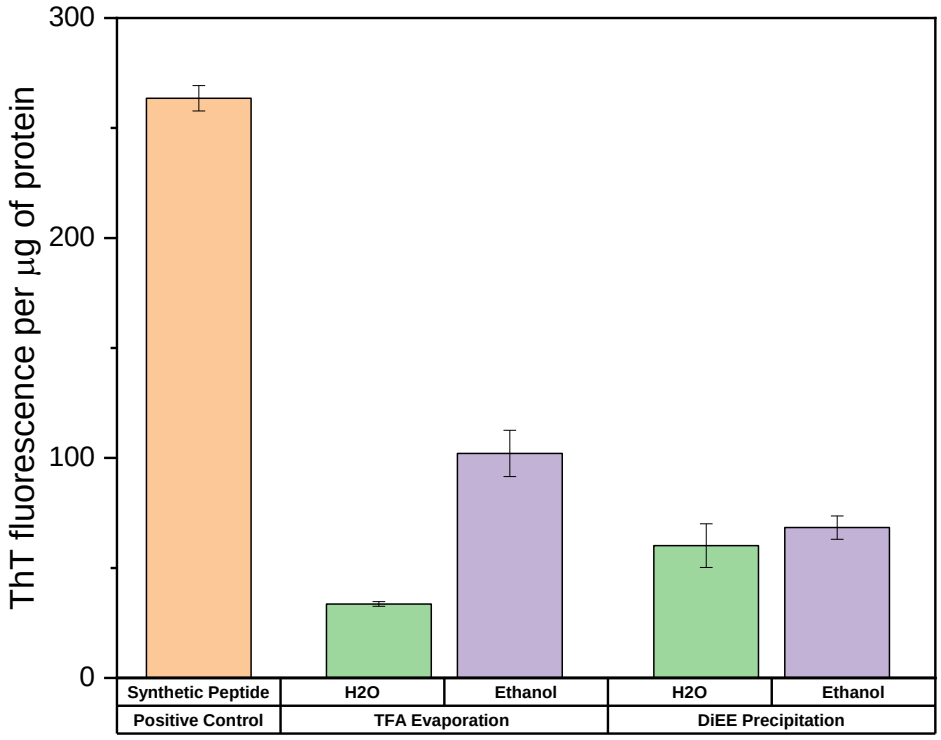

Figure 22: Normalised fluorescence intensity per microgram of protein present between TFA extracted proteins and after the treatment of diethyl ether (n=3).

From Figure 22, the fluorescence intensity was normalised for total protein and a response was detected across both the evaporation and precipitation methods as well as across both solvents, water and ethanol. Per microgram of protein present, the TFA evaporated pellet solubilised in ethanol gave the highest response. Diethyl ether precipitated pellets solubilised in water and ethanol gave similar results to each other and with an improvement over the TFA evaporated pellet solubilised in water. To determine the purity of the samples, SDS-PAGE was used (Figure 23). For each well, the same amount of protein was added, and the bands were compared. From the SDS-page gel, bands were evident across all samples with slight reductions in both ethanol samples (Figure 23C & E) when compared to the water based samples (Figure 23B & D). A 30 kDa band was observed in the TFA evaporated sample solubilised in water. The other samples did not have this band present.

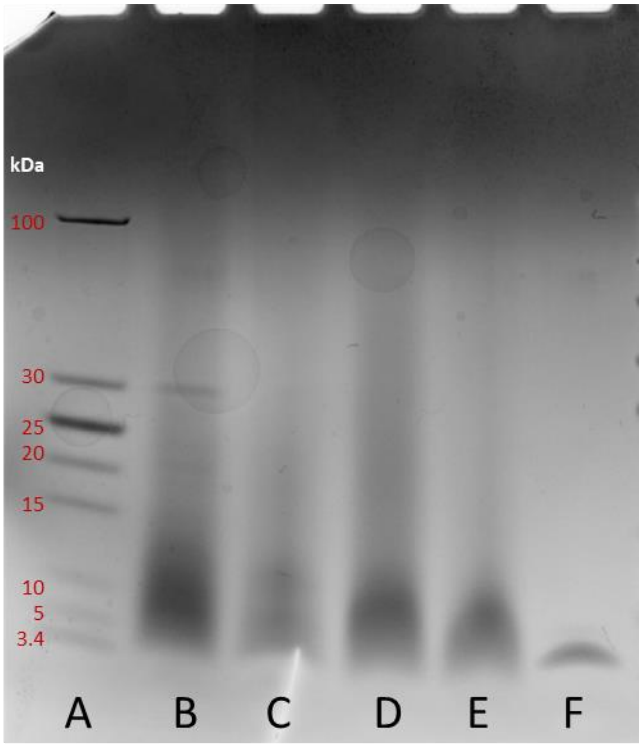

Figure 23: Silver stained SDS-PAGE gel comparing TFA evaporated proteins against diethyl ether precipitated. PageRuler26632 (Thermo Fisher) (**A**), TFA Evaporation in H_2O (**B**), TFA Evaporation in EtOH (**C**), Diethyl Ether precipitation in H_2O (**D**), Diethyl Ether precipitation in EtOH (**E**) and Synthetic peptide positive control (**F**).

To check whether the TFA has been successfully removed, the pH of the extracted material was tested using pH indicator paper. TFA is a strong acid, and a pink colour change would be indicative of remnants still present. No colour change would indicate the pH is neutral.

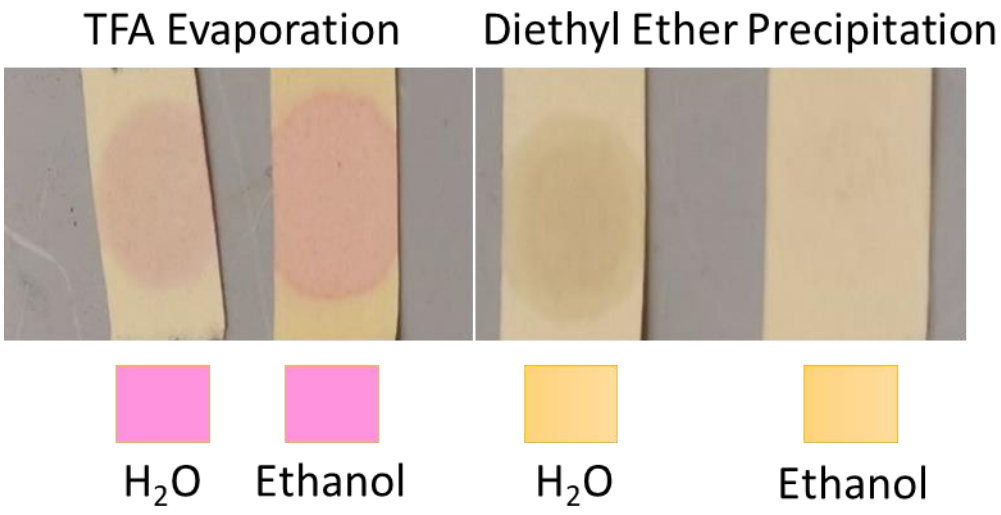

Figure 24: pH comparison of TFA evaporation against the Diethyl ether precipitation for chaplin proteins solubilised in water and ethanol respectively.

Using pH indicator paper, a solution at low pH changes the colour to pink, whereas at high pH the colour changes to green. Figure 24 shows that the TFA evaporated samples give a strong response by quickly changing from yellow to pink which indicates a low pH which can be assumed to be residual TFA. A more intense change in colour was observed for extracts dissolved in water in comparison to ethanol. In comparison to the TFA evaporated samples, the results obtained from the pH paper using the diethyl ether precipitated samples, did not change colour, indicating the pH of the solubilised proteins in both solvents were neutral.

To demonstrate the effects of the residual TFA, the TFA evaporated extract and the diethyl ether precipitation extract were dissolved in water and deposited onto bare polished steel to determine if the removal of the TFA has a decrease in the observable corrosion.

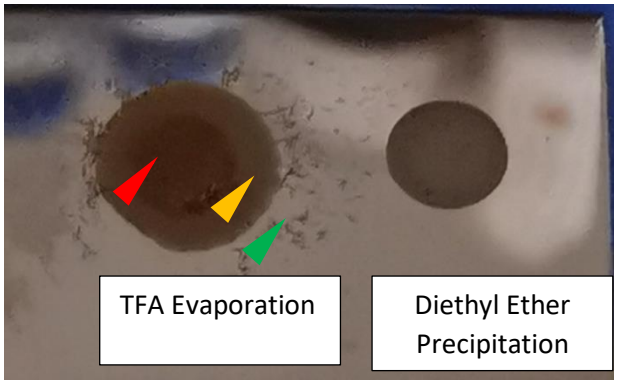

Figure 25: Effects of chaplin protein preparation when deposited onto polished steel. Residual TFA within the TFA evaporation prepared sample has clear evidence of corrosion whereas diethyl ether prepared does not appear to cause obvious signs of corrosion. Protein deposit (Red), area of corrosion surrounding the deposit (Yellow) and pitted areas of corrosion (Green).

In Figure 25, the TFA evaporation protein extract had a darker centre where the deposit and corrosion was present (Figure 25 Red). Immediately out with the centre was a zone of corrosion where no material was deposited (Figure 25 Yellow). Highlighted by the green arrow (Figure 25 green) were pitted areas which were not directly adjoined to the zone of corrosion. The deposit of the diethyl ether precipitated extract had a clear area of material with no visual appearance of any corrosion.

3.2.2.3. Mass Spectrometry analysis of Extracts

Following the Thioflavin T fluorescence and SDS-Page, MALDI/TOF was carried out in order to detect the chaplin proteins being extracted from both the R2YE+TES and modified MYM+$KHCO_3$. The detection of the synthetic *S. griseus* chaplin protein was achieved (Figure 26).

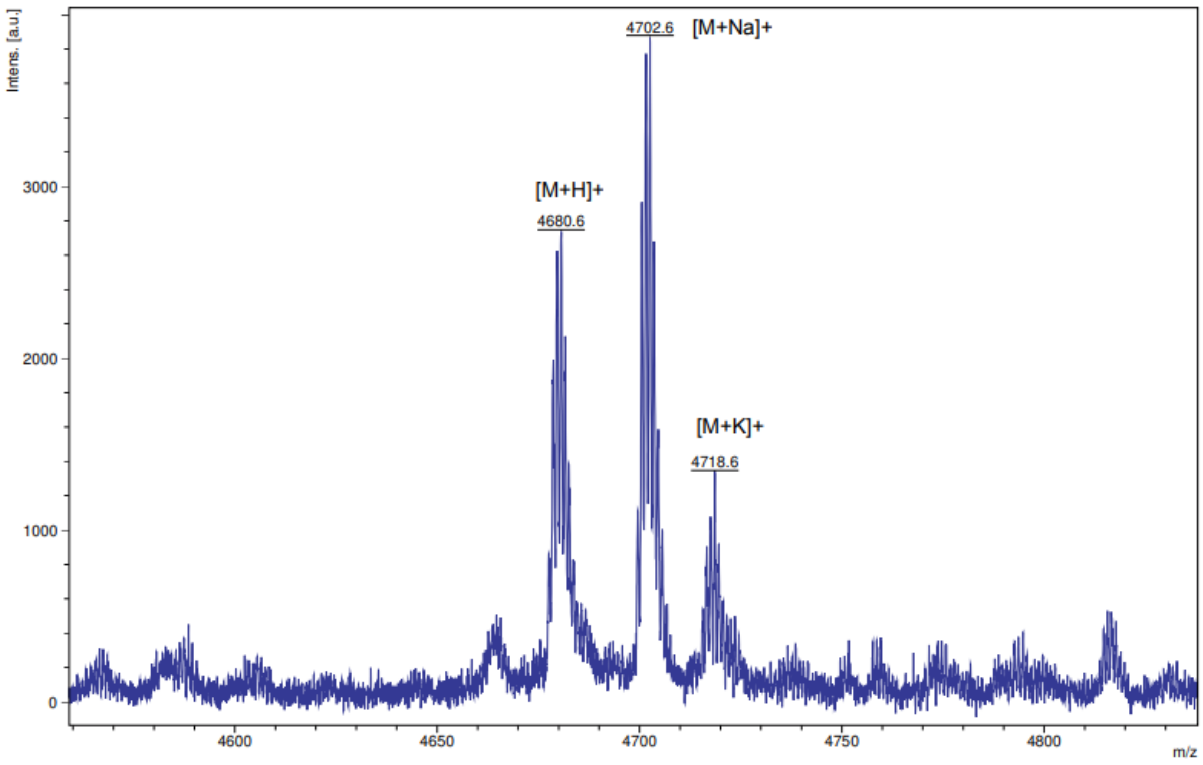

Figure 26: MALDI/TOF spectrum of synthetic *S. griseus* chaplin E peptide in water as a control. Peaks identified for three chemical species, hydrogen, sodium and potassium.

Three ChpE-short chemical species were identified for synthetic Sgris-ChpE-short (m/z =4679.25), hydrogen (m/z +1), sodium (m/z +22) and potassium ions (m/z +39) (Figure 26). This corresponded well with the supplier's information. The synthetic chaplin G (m/z =6397.95) and chaplin H (m/z 4969.61) were also identifiable at their respective m/z (Figure 27 and Figure 28).

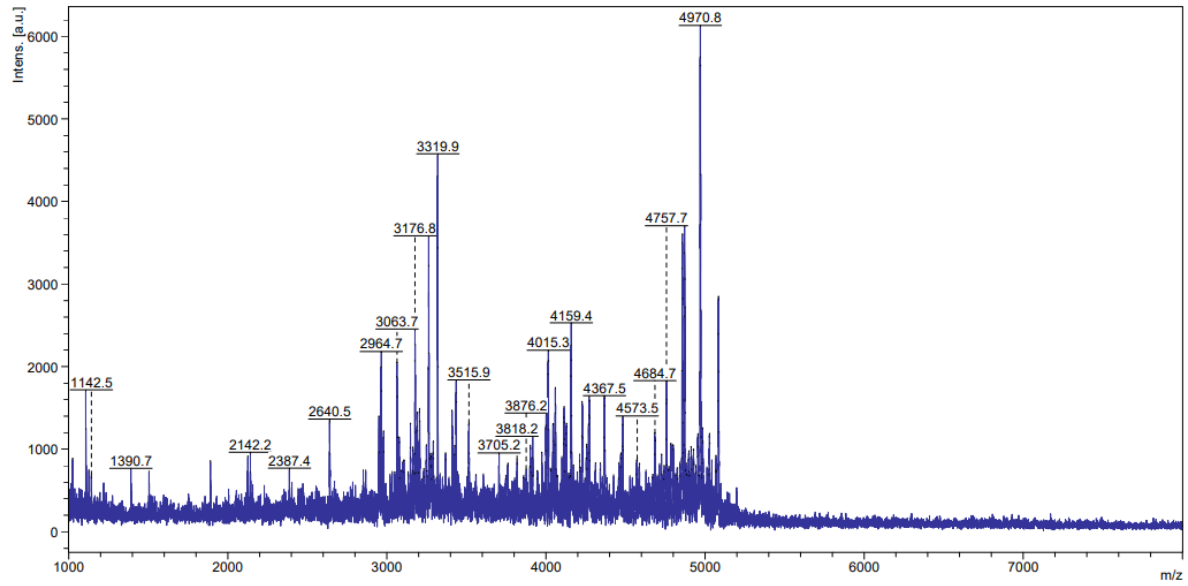

Figure 27: MALDI/TOF spectrum of *S. griseus* chaplin G in water

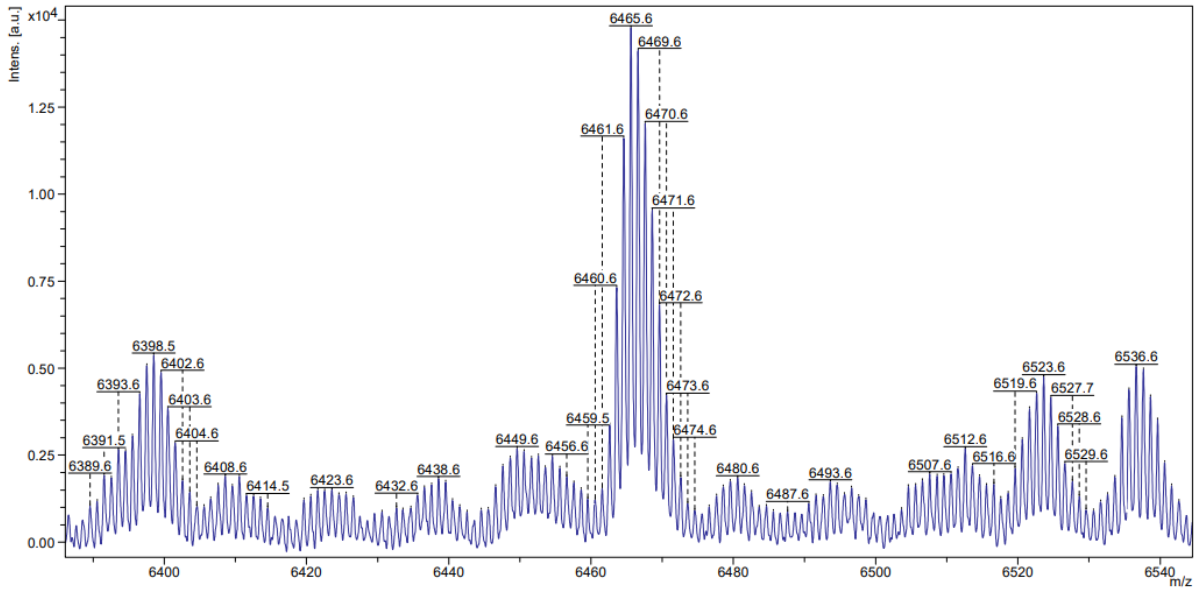

Figure 28: MALDI/TOF spectrum of synthetic *S. griseus* chaplin H in water

The detection of the synthetic *S. griseus* chaplins by MALDI/TOF indicates that the sinapinac matrix and ionisation of the chaplins can be achieved. Chaplin extracts for the different media types were then processed for the detection of chaplin proteins E, G and H.

S. griseus extracts from the R2YE+TES and modified MYM+$KHCO_3$ did not yield distinctive m/z peaks for any of the chaplin proteins (Figure 29 and Figure 30).

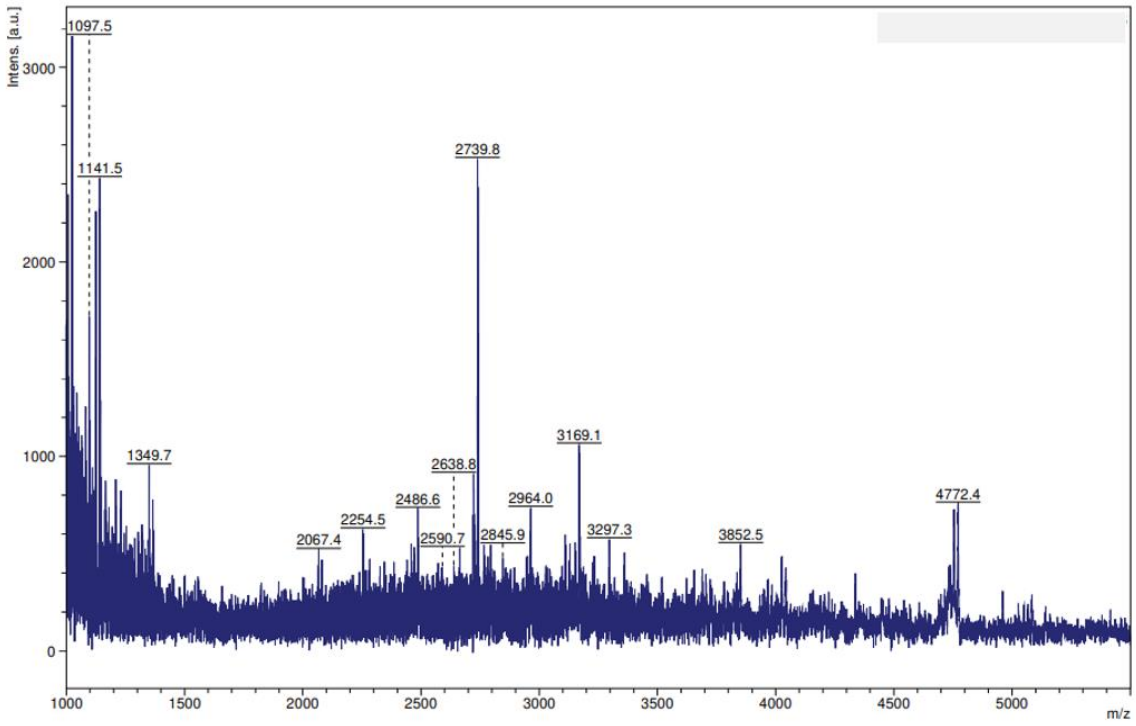

Figure 29: MALDI/TOF spectrum of R2YE+TES chaplin protein extract

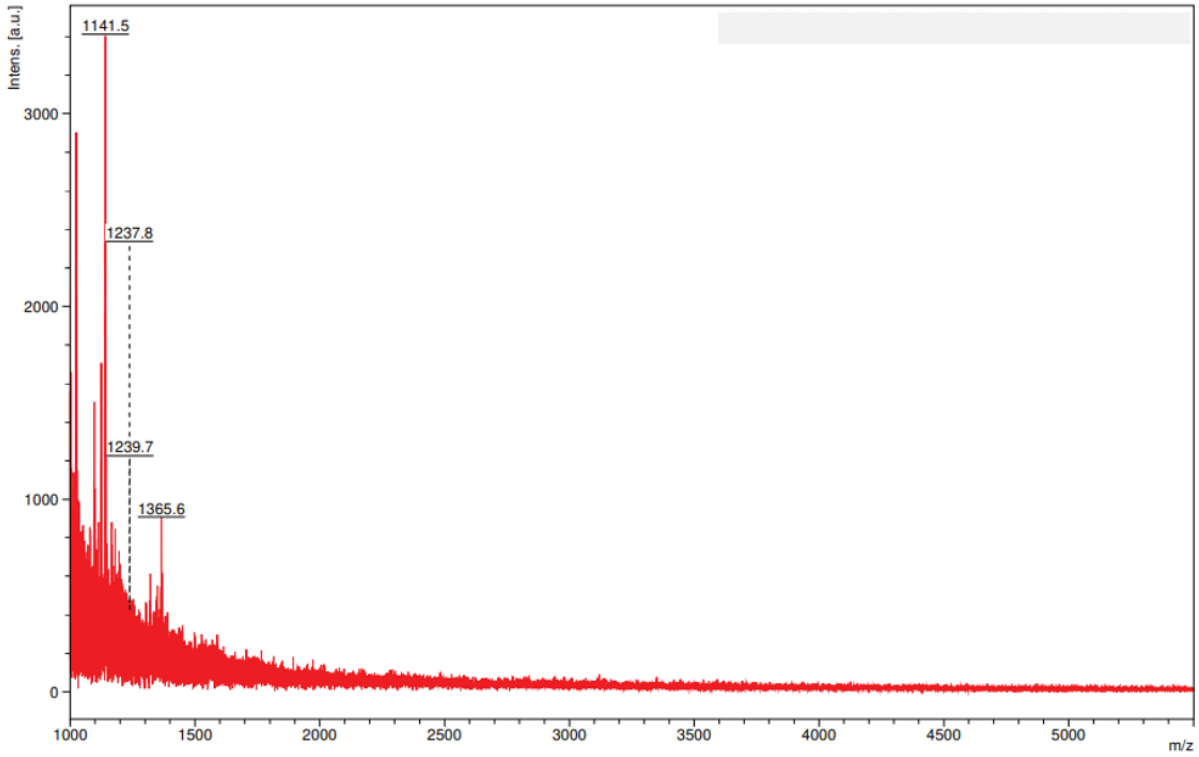

Figure 30: MALDI/TOF spectrum of MYM+$KHCO_3$ chaplin protein extract

3.3. Discussion

3.3.1. Growth

3.3.1.1. Biomass and Sporulation

R2YE is a commonly used medium for the sporulation of streptomyces strains however this particular medium is complex, expensive and cumbersome to prepare so required review. This review was important as the R2YE required several components which must be autoclaved separately and added aseptically post autoclave which posed a significant risk in contamination during its preparation. One particular component which contributes a large proportion of the cost of this medium is the TES buffering system. This medium is not the only medium which facilitates the sporulation of *Streptomycetes* in liquid cultures as *S. venezuelae* can also sporulate in a medium composing of maltose-malt extract and yeast extract (MYM). This medium type is attractive as the components are compatible to be autoclaved together and no buffer required for the sporulation of *S. venezuelae*. Given the sporulation of *S. venezuelae* in MYM, experimentation was carried out to determine if MYM would be viable for the sporulation of *S. griseus*.

Initial results showed that MYM did not lead to the sporulation of *S. griseus* so additional components were considered that may aid in the sporulation of this strain. Upon review of the R2YE medium

composition and the ability to facilitate the sporulation of *S. griseus*, Calcium chloride, the buffer and trace elements were considered as post autoclave additives to the MYM medium [72]. The importance of calcium for sporulation within the medium composition for *S. griseus* was highlighted by Daza et al and this was also demonstrated using the MYM medium [70].

In total, 8 components are required for R2YE with the TES buffer used within this medium contributing a significant proportion of the cost so alternatives have been investigated to determine if alternative buffers can be used for the sporulation of *S. griseus*. In addition to the complex nature of the R2YE media, it requires a high number of post autoclave additions which can be a source of contamination. Firstly, the sporulation of the *S. griseus* strain was investigated using different buffers within both R2YE and modified MYM medium recipes. Trialling different buffering systems varied in results with MOPS appearing to have a delayed sporulation in comparison to the R2YE and modified MYM (Figure 11). However, Potassium Bicarbonate did lead to sporulation. This was clear when examined by microscopy and spore counting (Figure 12). The media containing MOPS did have the presence of some spores, the values calculated for these were significantly lower that the control R2YE recipe containing TES but this may be due to a delay in sporulation as MOPS has been shown to lead to sporulation with *S. griseus [70].* Although sporulation was not evident using *S. griseus* with MOPS, it does not suggest that other strains of *streptomyces* would not grow and sporulate under these conditions[73]. Potassium bicarbonate and TES buffers have a similar buffering capacity of 6.5-7.6 and 6.8-8.2, respectively. The ability for the MYM + $KHCO_3$ to facilitate the sporulation of *S. griseus* also provides striking financial savings. A techno-economical comparison shows a reduction of ~75% which has a positive impact on the scalability of the technology.

Literature surrounding growth of *Streptomyces* mainly have a focus on the production of secondary metabolites such as antibiotics and how the medium composition affects production[74]. The secondary metabolites produced either function as part of a cascade of reactions or for protection against fungal and microbial attack. Chaplin proteins form a structural component of the hydrophobic sheath protecting itself from desiccation in hydrophobic environments and there are few reports on the medium composition and requirements for the production of structural proteins. The information gathered here, suggests that the pH buffer used within medium compositions had a significant effect on the ability for *Streptomyces griseus* to sporulate in liquid cultures.

The production and extraction of chaplin proteins for industrial processes is limited by the expensive nature of the medium used and the complexity of the extraction process. The ability to reduce the medium and/or the extraction process may lead to significant improvements in its economic viability. In previous work carried out by Alex Harold, growth was carried out on solid media which is not a

scalable process so the development and improvement for the production of spores is essential [56]. Chaplin proteins are mainly produced towards the end of the life cycle of *Streptomyces* growth [23]. Although, chaplin E in certain strains can be expressed into the medium which lowers the surface tension and assists in the growth of the aerial hyphae into a hydrophobic environment [27].

3.3.2. Chaplin Detection from Sporulating Cultures

For the sporulating cultures, the extraction of the material was carried out using the standard protocol and assayed to determine the presence and yield of the chaplin proteins and the purity of the extract. To investigate the presence of the chaplin proteins, the Thioflavin T assay was used. The binding of the thioflavin T to amyloid fibrils causes a significant increase in fluorescence at 445 nm to 482 nm when excited at between 385 nm and 450 nm. The binding of the stain causes rotational immobilisation, which maintains the excited state of the molecule and results in an increase in fluorescence. After extraction and assayed with Thioflavin T, the MYM medium recipe containing the potassium bicarbonate recorded a similar fluorescence intensity in comparison to the control culture of R2YE containing TES (Figure 13). All other sporulating culture extracts did give a response to the assay but not to the same extent as the control which appears to be due to the presence of residual spores that did not germinate or that the differentiation was slower than that of the other media recipes. It is well established that environmental signals such as the composition of the culture medium has effects on differentiation [75-77]. The extraction process exploits the amyloid protein properties and full conclusions cannot be drawn based on the ThT assay as it cannot distinguish between chaplin proteins and other amyloid proteins.

3.3.3. EDTA Treatment of MYMc Flask Precipitate

After identifying that a precipitate was present within the combined component flask (MYMc), EDTA was used as a potential method for the removal of this precipitate and allow for a more purified chaplin protein product. The medium only experiment did show that the turbidity of the sample could be resolved, indicating that it would be effective at chelating the precipitate. However, it was unknown what effects this EDTA treatment would have on the extraction of the chaplin proteins.

Following the extraction of the chaplin proteins using the standard TFA evaporation method, the combined flask (MYMc) did not lead to the characteristic band when run on SDS-PAGE gel. Due to the visualisation of spores by microscopy and the lack of chaplin proteins detected may suggest that the thick hydrophobic layer which protects the genetic information may be thicker and causing the spores to be more resilient to degradation by mechanical and chemical means [78]. A protein band was visible on the protein gel after Coomassie staining which has appeared on previous extractions from the R2YE

control media, this band has not yet been determined but has the potential to be an oligomer of chaplin proteins.

Although the combined medium experiment was unsuccessful, the MYM flasks with the post autoclave additions did give promising results when detected by the Thioflvain T assay (Figure 16). This was also corroborated with the analysis conducted by the SDS-PAGE gel where significant bands were found that matched both with the control culture (R2YE+TES) and the positive control synthetic chaplin E (Figure 17). The gel also was able to provide insight into the purity of the extractions from each of the modified medias and was able to show that the MYM containing potassium bicarbonate had a similar profile to that of the R2YE containing TES, suggesting that this modified medium may be able to be used as a replacement for chaplin production. As an additional step in the analysis of these sporulating cultures, MALDI-MS was carried out detect any of the *S. griseus* chaplin proteins after extraction.

3.3.4. Scale up of Growth

The ultimate goal is for the advancement of these findings to allow for significant increases in the production of chaplin proteins. By increasing the production from flask cultures of 200 ml to bioreactor growth of 1.7 L, it gives insight into the feasibility for further scale up to allow for larger application trials. To test the viability of scale up, *S. griseus* was grown within a Labfors minifors 2 L bioreactor. This equipment allowed for the control and monitoring of key parameters throughout the lifecycle. The results achieved at small scale for the modified medium with potassium bicarbonate were compared to the control growth medium, R2YE with TES. Over the five days of growth, the pH and dissolved oxygen were monitored. The pH was monitored between the range of 7.2 and 8.2 over the growth period. Changes in the pH appear more apparent at the vegetative hyphae growth and the septation stages before gradually increasing to 7.4 as sporulation was evident. Although pH gives an indication on the growth cycle of the culture, the data recorded for the dissolved oxygen appeared to give a more conclusive depiction [79]. Between 24-48 hours of growth, the dissolved oxygen remained low due to the high amount of biomass, but with this increase in biomass, a striking increase in the viscosity was apparent. This was observed visually but was also observed within the data of the temperature recordings. During the period of hyphal growth and higher viscosity, the fluctuations in the temperature recordings appear to increase which would corroborate findings on heat transfer through viscose liquids[80]. The fluctuations recorded reduce towards the end of growth as expected as the septation and sporulation occur due to the onset of the nutritional downshift. The utilisation of the oxygen within the culture decreased rapidly which suggested the onset of sporulation. The dissolved oxygen after the sharp increase at 72 hours began to slowly increase as the septation of

hyphae and spores were formed. With this gradual increase is dissolved oxygen, the pH of the culture also increased gradually. The 48-hour period in which the dissolved oxygen was low has been observed in other studies, albeit with *Streptomyces coelicolor*, which does not sporulate in liquid culture [79, 81, 82]. When monitored by microscopy, it was clear that the life cycle did complete resulting in a high abundance of spores. The fermentation with R2YE and TES provided a clear representation of the levels expected to be observed for any future fermentations. Under the same growth conditions, modified MYM, containing the potassium bicarbonate buffer, was cultured within the Minifors bioreactor. The pH and dissolved oxygen readings recorded for the MYM growth were like that of the R2YE growth. This was again monitored by microscopy and a high quantification of spores was present after 5 days (Figure 15). The pH recorded was slightly higher than the TES buffer but remained within pH values of 7.4 and 8.4. This difference in pH does not appear to be problematic as *Streptomyces spp* prefer a neutral to alkaline growth medium [73]. The ability for this modified medium, with a more cost-effective buffering system, increases the economic feasibility to produce chaplin proteins. Based on the components of the two media, around 75% of the cost can be reduced by switching to the modified MYM recipe containing potassium bicarbonate. A 1.7 L culture inoculated with $5x10^6$ spores per ml allowed for the extraction of over 38 g of biomass, mainly spores. By increasing the culture volume 8.5-fold, a 22.5-fold increase in freeze dried material was obtained. The parameters for growth can affect the differentiation and production of secondary metabolites, but it is known that bioreactor fermentations can increase the resulting biomass [83, 84].

The use of chaplin proteins has been shown to provide some corrosion resistance however the protein only samples had mechanical property issues [56]. Protein depositions required concentrations of 150 µg/ml for 4 cm^2 steel coupons equating to 30 ng/mm^2. Given this information, the need for scale up is crucial for it to become an alternative strategy for corrosion resistance over existing technologies such as chromium-based coatings. Although the focus of this research is on corrosion resistance and the ability for a barrier coating to be formed, alternative applications for chaplin proteins may become apparent as hydrophobins have been investigated in different applications such as: low friction surfaces, protein attachment prevention and textiles [85-87]. Although modified MYM cultures of *S. griseus* provided an indication that chaplin proteins can be produced at a larger scale at a fraction of the cost, the presence of calcium-phosphate precipitates may become an issue for the extraction and purification of the chaplin proteins.

The molarity of the potassium bicarbonate buffer within the MYM medium was kept at 50 µM, in line with the R2YE recipe. As the buffering agents are generally expensive, there is scope to optimise the medium further to ensure that the concentration of the buffer is at its optimum. An alternative strategy which was considered was the use of acid and base to control the pH. This strategy may

eliminate/reduce the need for a buffering agent to be added to the culture. The difficulty with this strategy is the time in which the culture is growing for and the maintenance of the pH between 7.4 and 8.4 would require a substantial volume. Increasing the concentration of the acid and base would reduce the total volume being added to the culture, but the use of stronger concentrations would cause more dramatic shifts in the pH, so rather than an equilibrated pH, the pH value would fluctuate throughout as the acid and base is added.

Streptomyces is a filamentous bacterium, and the hyphae can become entangled which leads to clumping. Given this, further optimisations could be made to reduce clumping such as increased aeration and/or agitation or a decrease in the initial concentration of spores added to the culture. Another issue with *Streptomyces* growth within a bioreactor is the build-up of foam. The build-up of foam is a common issue when growing *Streptomycetes* [79] and can be very problematic if not controlled. If uncontrolled, the foam can build up into the condenser unit and may lead to the blocking of the air filter present on the condensing unit. This then can lead to a pressure build up within the culture vessel and cause the ejection of the culture through the sample port. This is normally controlled by the addition and real-time monitoring of anti-foam. Within these experiments, automated anti-foam addition was not carried out, so an initial dose of antifoam was added and did not appear to affect the culture. Further experiments would be required to determine if the cumulative addition of anti-foam across the growth cycle would have a detrimental effect on sporulation and/or chaplin production. Other strains have been tested when grown with antifoam and no detrimental effects were observed on the production of secondary metabolites [79].

3.3.5. Downstream Processing

3.3.5.1. Biomass Comparison

The optimisation of the medium gives promise to the potential for future scale up trials, however, the downstream processing involved for the extraction of chaplin proteins may still be problematic. On a small scale, protein extraction can be carried out with relative ease but the ability for these processes to be scaled up will require optimisations. With increased biomass, the processes involved must be as effective as small-scale extractions. Alternative strategies have been attempted previously [57]. The current process for extraction of chaplin proteins relies on the proteins properties to be resistant to detergents, pH and elevated temperatures. To purify the chaplin proteins from the biomass, the biomass is degraded and removed by sonication then SDS boiling [36]. Chaplin proteins remain during these processes and then monomerised in TFA.

It was identified that the R2YE + TES and the MYM + $KHCO_3$ had a more densely packed pellet after allowing the biomass to settle. This tighter packing is due to how close spores can get to one another

unlike vegetative and aerial hyphae. The hyphae are larger in size with space between them causing the appearance of a less dense pellet.

3.3.5.2. TFA extraction and monomerization efficiency

It was assumed that all chaplin proteins were monomerised and remained within solution of the TFA. Additional extractions of the same pellet were carried out to determine if this was true. It was identified that additional chaplin proteins can be extracted after 3 repeat monomerization steps in TFA (Figure 20). After each monomerization, there was a decrease in the amount extracted and was visualised by SDS-PAGE (Figure 21). The presence of chaplin proteins after the first monomerization displays how ineffective the solubilisation process is and optimisations are required for a more efficient extraction of the chaplin proteins. It appears that the TFA has a limit to the amount of chaplin proteins it can solubilise. This finding may assist in improving current hydrophobin class I and chaplin protein yield to facilitate further experimentation. However, alternative strategies in the downstream processing is required due to the environmental impact TFA can have [88].

3.3.5.3. Protein Precipitation as an Alternative to TFA Evaporation

The use of TFA itself, carries its own issues due to its highly corrosive nature. Residual TFA is problematic for application onto metallic substrates. Figure 24 shows the pH of the solubilised chaplin proteins in both ethanol and water. The low pH of the solubilised chaplin proteins prompted investigations into reducing/eliminating residual TFA from solubilised samples. TFA is commonly used in the production of synthetic peptides as part of the cleavage cocktail, in fact, synthetic chaplin peptides have been used successfully without residual TFA and pH problems [71]. Peptide synthesis techniques and processes were examined to determine the feasibility of adopting these for removal of the TFA from monomerised chaplin extracts. The method trialled was the precipitation of peptides in diethyl ether. By using this method as a replacement to the TFA evaporation, the processing time of the samples would be reduced as well as improving the sustainability of the process. The diethyl ether solubilises the TFA whilst precipitating the proteins [89]. The litmus paper turned pink very quickly for TFA evaporated samples in ethanol and water unlike the diethyl ether precipitated proteins which remained yellow (Figure 24). The solubilised proteins were quantified and assayed for chaplin proteins. The SDS-PAGE gel of the extracted material (Figure 23) gave bands that were expected at 5 kDa and resembled the synthetic peptide control. Interestingly, the TFA evaporation process when solubilised in water also gave a distinctive band at 30 kDa. When compared to the diethyl ether precipitated proteins that were solubilised in water, this distinctive band was not present. As this band was larger than the chaplin proteins, it suggests that the diethyl ether process also acts as an additional purification step. The diethyl ether precipitation does appear to be effective however over drying of

the diethyl ether pellet after washing can lead to the pellet becoming insoluble. Diethyl ether has an evaporation rate of 34.6 – Compared to Acetone which has an evaporation rate of 5.6-, it is crucial that the evaporation is closely monitored. Over drying of the pellet causes issues when resolubilising the monomerised protein pellet. If the pellet cannot be resolubilised, a reduction in the concentration of chaplin proteins would occur. With the data obtained on the precipitation using diethyl ether, if it evident that the chaplin proteins can indeed be extracted via this method to a similar level of the TFA evaporated method.

As an additional test of the ability for the diethyl ether precipitation to remove TFA, solubilised protein samples from the diethyl ether precipitation and TFA evaporated process were deposited onto a polished steel coupon (Figure 25). Of the two samples deposited, the TFA evaporated protein deposit produced the distinctive red rust on and surrounding the deposit. The TFA that remained after evaporation explains the accelerated corrosion present around the edges of the deposit. Meanwhile, the diethyl ether precipitated deposit showed less corrosion in comparison which would conform to research by Osarolube *et al* who showed the weight loss of different concentrations of various acids[90]. Although corrosion does not appear to be initiated by the initial deposit, the corrosion resistance of the material requires further analysis to determine if the proteins exert corrosion resistant properties.

3.4. Conclusions

In comparison of the media and buffers tested, the use of modified MYM with $KHCO_3$ can be offered as an alternative medium composition for the growth and sporulation of *streptomyces griseus*. By changing the medium to MYM, it provides a significant cost reduction over the R2YE by around 75% while also reducing the number of post autoclave additions which subsequently reduces the chances of contamination of the culture.

The optimisations achieved here at small scale were also demonstrated at a larger scale which gave insight into key parameters throughout the growth cycle of culture. One of these being the significant change in the viscosity during the hyphal growth phase. This parameter may provide additional evidence for the sporulation of the culture in conjunction with microscopy. The viscosity of the culture was not quantified so further analysis would be required to determine if this parameter would be viable as a sporulation indicator. This development allows for advancement of chaplin protein production technologies, which is crucial for scale up and development of chaplin protein technologies to advance to larger scale applications.

As identified previously, residual TFA within samples has detrimental effects on application properties. The data given within these experiments suggests that replacing the TFA evaporation step with a diethyl ether precipitation method, can effectively remove the TFA present within the samples.

4. Controlled Expression of Chaplin E in the homologous host *Streptomyces coelicolor* via the Thiostrepton-Inducible promotor *pTipA*

4.1. Introduction

In addition to the process optimisation of the traditional growth and extraction method, it is important to investigate alternative strategies for the production of chaplin proteins to increase the feasibility of chaplins being used for real world applications. A potential avenue for expression is by using genetic engineering and other synthetic biology approaches to develop or modify strains that would enable technological advances to be made for the production of wildtype and modified chaplins. A synthetic biology approach to expression of chaplin proteins could provide increased benefits over traditional extraction methods from sporulating cultures which require extensive biomass processing with strong acids and detergents [17, 23, 91, 92]. Culturing *Streptomyces* also requires understanding of regulatory aspects that govern how and when *Streptomyces* changes cell morphology when differentiating when exposed to different stimuli [93, 94]. Changes to culturing conditions can lead to a change in chaplin gene expression [95, 96].

The *S. coelicolor* chromosome encodes eight chaplin proteins (ChpA-H), which are all secreted via the Sec translocation machinery [23]. ChpA-C are 'long' chaplins which are covalently linked to the cell wall and ChpD-H are 'small' chaplins which can be extracted from the cell envelope upon breaking of non-covalent bonds [27]. ChpE is a chaplin of interest: ChpE is the only *S. coelicolor* chaplin that does not contain cysteine residues, meaning that disulphide bridges cannot be formed. In addition, the expression of *chpE* occurs during both the vegetative and aerial hyphae growth stages. During vegetative growth, ChpE is secreted into the surrounding environment to reduce the surface tension [97], while the large increased expression of chaplins during morphological differentiation results in the chaplin spore coat providing a water-repellent and protective surface [19]. The ability of *S. coelicolor* to express ChpE throughout the growth stages makes it an ideal target for over-expression. Overexpression of proteins can typically be easily achieved in heterologous host organisms such as *Escherichia coli* and yeast cells.

4.1.1. Expression in *E. coli*

E. coli has been extensively used as a host for protein expression due to the relatively quick and easy processes involved [98]. An array of plasmid vectors can be used for cloning and expressing genes of interest [98]. The multiple cloning site (*mcs*) area of a plasmid contains numerous restriction sites which can allow for ligation of a gene fragment of interest. Other plasmid loci of relevance are the *ori* which enables replication of the plasmid within the cell, and a selection marker gene, usually an antibiotic resistance gene such as *ampR* and *apraR* that confer resistance to ampicillin and apramycin antibiotics, respectively. Upon successful transformation of a vector into *E. coli*, transformants can then be selectively grown when cells are exposed to the relevant antibiotic while other cells without

the plasmid would not grow. This resistance can be used to check the uptake of the plasmid containing the gene of interest.

To incorporate the gene of interest into an expression plasmid, *in silico* analysis is performed first to determine the optimal restriction enzymes to be used for restriction and ligation into a specific site of the *mcs* of the plasmid. Once ligated the gene can then be transcribed and translated into the protein of interest. The process of transcription is driven by a promotor next to the incorporated gene fragment. The strength and type of promotor can vary. Vectors can contain a constitutive promotor which continues to express the gene until energy sources of the host has depleted. Alternatively, an inducible promotor can be used. This type of promotor is only active in the presence of its corresponding inducing agent such as thiostrepton and isopropyl-β-D-thio-galactoside (IPTG), which induce the *pTipA* and *pLac*-type promoters respectively. The use of an inducible promotor allows for the controlled expression at a desired timepoint.

4.1.2. Expression of Microbial Amyloid Proteins in *E. coli*

Certain strains of both *E. coli* and *Salmonella* spp. have been shown to produce an amyloid fibre known as Curli [99]. These fibres are used for the adhesion to surfaces and biofilm formation [100] and has been predicted to be rich in β-sheets similar to chaplins [101]. The main Curli protein is encoded by the genes *csgA* and *csgB*, which has been overexpressed successfully in *E. coli* using plasmids pET22b, and pPICZAα, containing inducible promoters. Often a polyhistidine tag (His-tag) has been tagged on to the N- or C-terminus of the peptide, enabling purification of protein via nickel-affinity chromatography.

The construction of *chpE*-containing plasmids and ChpE expression using a constitutive promotor has been investigated and found the strain used as a host led to the chaplin proteins being expressed into the periplasm in its immature form (unpublished).

4.1.3. Expression of Chaplins in *Streptomyces* spp.

The introduction of universal synthetic modular regulatory elements for *Streptomyces* to drive *chpE* expression from the integrative plasmid pSET152 in superhost *S. coelicolor* M1146 has been previously investigated [57, 102]. The tested regulatory elements for ChpE expression consisted of four synthetic promoters of increasing strength, a RiboJ insulator and the SR40 Ribosome Binding Site (RBS) cloned in front of the full-length *chpE* sequence. After growing the exconjugants in liquid R2YE media,

the morphology changed significantly as the promotor strength increased. The cause of this was not investigated but may have been due to the chaplin proteins being retained within the biomass, specifically between the vegetative hyphae resulting in a ‘fluffy’ settled pellet which appeared larger

in volume in comparison to other pellets. After centrifugation, the differences in the pellet volumes were observed. ThT assays of crude supernatants showed that chaplin yields were highest in the culture with the strongest promoter. Remarkably, the different constitutive promoter strengths do not appear to affect chp fibre yields in agar-grown cultures. The latter may be due to the intricate and tight regulation of *chp* expression when undergoing aerial development which appears to be absent or at least less stringently controlled in liquid culture. It is hypothesised that the use of an inducible promotor system would allow for a better controlled expression of the chaplin E protein after an initial increase in biomass. The initiation of protein expression after a period of time has the potential to limit its effect on the changing morphology.

The two main pathways for protein translocation of the cell membrane are the general secretory pathway (Sec) and the Twin-arginine translocation pathway (Tat). The Tat pathway transports folded proteins across the cytoplasmic membrane whereas the Sec pathway requires the protein to be folded outside the cell. Each of these pathways recognise specific amino-acid sequence motifs or signal peptides. Full-length proteins destined for Sec translocation are required to contain a signal peptide at the N-terminal end of the full-length protein, which is cleaved during the translocation process, rendering a smaller 'mature' secreted protein. Recognition of predicted signal peptides and the likely cleavage sites can be achieved with bioinformatics, e.g. SignalP. Application of SignalP and follow-on mass spectrometry showed that ChpE was secreted via the Sec pathway with cleavage of the signal peptide between residues 27 and 28 [16, 23] causing the presence of the mature ChpE. If ChpE was expressed and secreted efficiently, then the subcellular localisation would be outside of the cell membrane, possibly secreted into the supernatant. Alternatively, chaplin protein could be retained by the cell envelope and/or within the 'pseudo'-periplasmic space. If ChpE protein was expressed highly, then the Sec translation machinery may get overburdened, including titration of the Signal Recognition Particle, with possible translation and retention of Chp protein in the cytoplasm.

4.1.4. Chaplin Protein Purification

The purification of proteins is a crucial part of many biotechnology processes. For successful purification, the protein of interest's key characteristics such as, molecular weight, charge and solubility are exploited to remove it from a complex mixture [103]. Depending on the properties of the protein of interest, some are engineered to contain tags to accelerate purification, different techniques can be employed. Common techniques employed for the purification process are chromatography based, which works based on the protein being attracted to a ligand in the stationary phase which is generally in the form of a resin within a column. A mobile phase is passed through the column which removes impurities whilst the protein of interest is retained in the stationary phase

[104]. The protein of interest is finally eluted from the stationary phase after washing, or sometimes cleaving dependent on the tag. Modifications to the process can allow for the properties of the protein to be exploited via alternative, methods such as affinity chromatography, size-exclusion chromatography and gel filtration chromatography.

Proteins can also be purified by precipitation. This involves introducing a high osmolarity to the solution with the addition of salt [105]. Ammonium sulphate is a common salt used for this process; however, use of this technique requires further purification to remove the salts after precipitation by dialysis. The salt is added at a known concentration, incubated and then centrifuged to pellet any precipitated protein. The concentration of salt is then increased and centrifuged again. This process is repeated until the solution becomes saturated. Another precipitation-based method involves the use of acetone. Proteins are insoluble in acetone, particularly at low temperatures, whereas other small molecules remain soluble. This difference in solubility allows for the removal of non-protein-based medium components whilst concentrating the total proteins within the mixture. The pellet formed can then be redissolved in a suitable solvent for future analysis. This method however does not purify the protein of interest from the other proteins present and would require additional purification methods to isolate the protein of interest.

Of the expression systems described, *E. coli* has significant advantages over expression in *Streptomyces spp* due to the ease of genetic manipulation and growth rate. However, the long string of (semi) failed chp expression attempts in *E. coli* and the odd observations for constitutively expressed chp in *S. coelicolor* has led to the investigation into the use of an inducible promotor [57, 58]. Therefore, the initial objective of this chapter is to conjugate a plasmid with the Thiostrepton-inducible promotor *pTipA* (pIJ6902, John Innes Centre) with and without *chpE* cloned into the correct location into the *S. coelicolor* M1146 superhost for stable integration into the chromosome to facilitate induction of ChpE expression and determine the levels of expression into the supernatant of R2YE, MYM and Nutrient broth liquid grown cultures. Conjugation is only the process of transformation, it has no effect on direction of where the plasmid ends up, that is an integral part of the actual plasmid.

After conjugation, a self-replicating plasmid would self-replicate if it has the correct loci on the plasmid for it to work in *Streptomyces*. An integrative plasmid would insert into the chromosome via homologous recombination at the specific site present on the plasmid and chromosome (ϕC31). pIJ6902 is an integrative plasmid so after conjugation it would recombine at the specific site in the chromosome. Finally, an amendment to the standard purification protocol of the ChpE protein will be

tested to determine whether acetone or ammonium sulphate precipitation would be an efficient process for purification of ChpE from the supernatant.

Given the previous research on the over expression, this research will investigate the use of an inducible promotor plasmid for expression of the chaplin E gene in the streptomyces superhost, M1146. This research will also look at the purification methods for chaplin proteins for culture supernatants.

4.2. Materials and Methods

4.2.1. Strains, Plasmids and primers

Over the course of this investigation plasmids and strains were created, the following table gives an overview of the strains, plasmids and primers used.

Table 4: Full list of strains and plasmids which were used for the development of the inducible M1146 strain

Plasmids

pSET152+chpE	ΦC31, Apra, LacZa	[57]
pIJ6902	ΦC31, Apra, PtipA, tsr	John Innes Centre
pIJ1800	pIJ6902+*chpE*	This Work
pGemT Easy Vector	T-cloning vector for taq-PCR products	[Promega]
*pGemT Easy Vector+*chpE		This Work

Streptomyces coelicolor A3(2)

M1146	Δact Δred Δcpk Δcda	[106]
M1146-pIJ6902		This work
M1146-pIJ1800	pIJ6902+chpE	This work

E. coli

DH5α		[Promega]
ET12567/pUZ8002	*dam-13::Tn9 dcm-6 hsdM Cmr*	[60]

Table 5: Primer sequences with restriction sites highlighted in red:

Primer Name	**Sequence**
ChpE-F	5'-ATTCCATATGAAGAACCTGAAGAAGGCAGC-3'
ChpE-R	5'-AAGATCTTCAGTGGTTGACGCCCAGGTTG-3'
TipA-F	5'-TTGCACCTCACGTCACGTG-3'

4.2.2. Purity Analysis of Chaplin Extracts

To determine the purity of the extracted samples, SDS-PAGE was carried out. The extracts were prepared and run on a 10-20% Tricine gel with a PageRuler Low range protein marker (Thermo Scientific, #26632) as a reference. Synthetic peptide for chaplin E was used as a positive control. The gel was run at 110 V for 60 minutes with a tricine running buffer. The gel was run until the dye front

was 75% of the way down the gel. The gel was removed from the plastic case and subjected to a fixative solution of Ethanol and acetic acid for 15 minutes to ensure smaller molecular weight bands remained within the gel during the staining process. Once complete, the gel was placed in 0.25% Coomassie blue stain for a minimum of 4 hours before being destained using 30% ethanol. Destain solution was changed every hour until bands became evident.

4.2.3. Plasmid Selection

pIJ6902 (supplied by John Innes Centre) was selected the plasmid for integration after inclusion of the *chpE* gene. NdeI and BglII are found at the ends of the multiple cloning site directly adjacent to the promotor, p*tipA.* NdeI was selected as a restriction site due to the presence of the start codon, ATG.

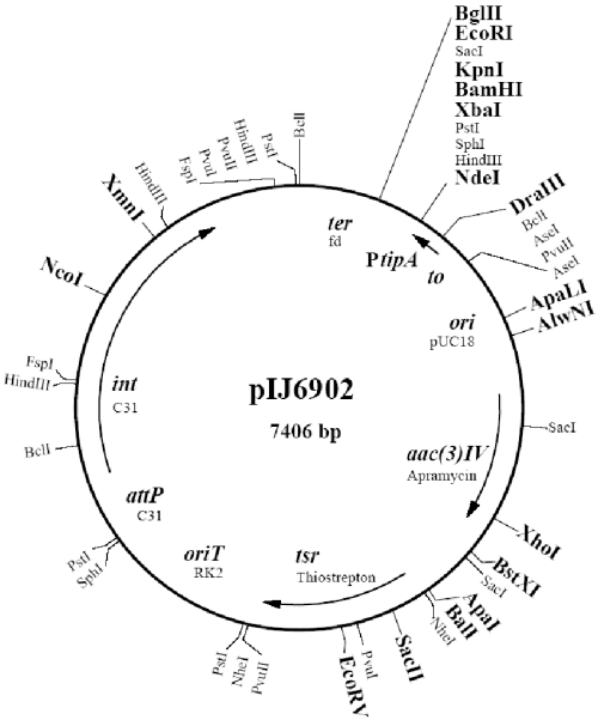

Figure 31:Plasmid map of pIJ6902 with restrictions sites. Ori for Ecoli replication, oriT for conjugation, attP for chromosome insertion and tsr and aac(3)IV (or apraR) as selection/resistance markers

4.2.4. Primer Design

For amplification of the *chpE* gene, a forward (F) and reverse ® primer were designed with the inclusion of NdeI and BglII restriction sites for specific site integration into the multiple cloning site of plasmid pIJ6902. The design of the primers was checked *in silico* to ensure that the amplification was as expected. This was achieved by using Serial Cloner© and Snapgene© software.

4.2.5. Fragment Amplification and Cloning

Using the designed primers, *chpE* amplification was achieved by polymerase chain reaction(PCR) using an existing plasmid with the presence of the *S. coelicolor* wild type *chpE* gene as the template [57]. The flanking regions- that contains restriction sites- on the primers do not bind to the template but during PCR they are replicated so that the fragment can be restricted [107]. The PCR reaction was set up in a PTC-200 Peltier Thermal cycler with 30 cycles each with different annealing temperatures ranging from 54°C to 60°C to determine the optimum. A high-fidelity, proofreading polymerase was used within the reaction mix to ensure accurate amplification (MyFi™ Polymerase, Bioline). The amplification process causes overhangs which allows for T-A ligation into a vector for Blue-white selection. Using the pGemT® Easy vector system (Promega), reactions were set up with 3µl of the purified PCR product, 1 µl of the pGemT® easy vector, 5 µl of 2x rapid ligation buffer (Promega) and 1 µl of T4 DNA ligase (Promega) before being incubated overnight at 4°C. The ligation mixture was transformed into $CaCl_2$-competent *E. coli* DH5α cells via heat shock which were then spread onto LB agar plates containing IPTG at a final concentration of 0.1 mM ampicillin at a final concentration of 100 µg/ml and Xgal at a final concentration of 40 µg/ml. White colonies indicated successful ligation of *chpE* amplified product due to the fragment interrupting the *lacZ* gene. If not interrupted, colonies resulting from *lacZ* expression in the presence of IPTG and X-gal are blue. Single white colonies were picked and grown in LB broth (25 g/L) for 16 hours at 37°C containing Ampicillin. A plasmid mini-prep (Zymo) was used for purification of the plasmid DNA.

4.2.6. PCR and gel extraction

The purification of PCR products or restricted DNA fragments from a gel were purified using the Nucleospin® clean-up kit. Either 100 µl PCR product or 100 mg of excised DNA fragment, was combined with 200 µl of NTI. When dissolved the gel fragment, the tube was incubated at 50°C for 10 minutes. The DNA was then bound to a spin column by centrifuging at 11000 x g for 30 seconds. To wash the silica membrane, 700 µl of NT3 reagent was added to the spin column and centrifuged for 30 seconds, this process was repeated twice as recommended by the supplier. The membrane was dried by centrifugation for 1 minute before adding 20 µl of distilled water, incubating for 1 minute at room temperature then centrifuging for 1 minute at 11,000 x g. DNA was quantified using a Nanodrop™ spectrophotometer.

4.2.7. Plasmid restriction and DNA electrophoresis

The restriction of the *chpE* fragment from the pGemT™ easy vector and the linearisation of the pIJ6902 was achieved by using NdeI and BglII restriction enzymes. Restrictions were carried out at 37°C for 1 hour before separation by gel electrophoresis on a 0.8% agarose gel for 50 minutes at 90 V containing

ethidium bromide (EtBr). This allowed for the NdeI and BglII restriction products to be cut from the gel, purified and ligated.

4.2.8. Ligation

The ligation of the linearised plasmid and the *chpE* fragment was carried out at 4°C overnight in the presence of T4 ligase.

4.2.9. Transformation into DH5α

After the ligation period, $CaCl_2$ competent *E. coli* DH5α were used for the transformation. Competent cells, which were stored at -80°C were thawed on ice for 15 minutes before 5 µl of ligation mix was added to the competent cells and subjected to a 50°C water bath for 45 seconds then immediately placed on ice for 30 minutes. Nutrient broth was then added and placed into a shaking incubator at 37°C for 2 hours as a recovery period before being spread onto LB agar plates containing apramycin. Plates were then incubated at 37°C overnight to allow for growth of successful transformants which would be apramycin resistant.

4.2.10. Quality assurance of transformants

Colony PCR was carried out to determine whether the *chpE* fragment was successfully inserted and if it was in the correct orientation in the plasmid. This was achieved by using two primer sets. One set, the ChpE-F/R set used previously for amplification, and a primer designed for the thiostrepton inducible promotor (*pTipA*-F) along with the reverse primer ChpE-R. The reactions were set up with 30 cycles using the individual colonies as the template were smeared into the PCR reaction mix.

4.2.11. Transformation into *E. coli* ET12567(pUZ8002)

The conjugation of the developed pIJ1800 was first transformed into an *E. coli* methylation-defective strain (*dam-13::Tn9 dcm-6 hsdM Cm*^{r}) ET12567(pUZ8002) and was used as the conjugal donor to the *Streptomyces* strain. The transformation into this strain before conjugation is important due to the methyl-specific restriction mechanism present within *S. coelicolor* M1146. This was achieved by heat shocking the plasmid and competent cells at 50°C for 45 seconds before plating on LB agar containing Apramycin(50µg/ml).

4.2.12. Conjugation of pIJ6902 into *Streptomyces coelicolor* M1146

$1x10^8$ spores for the *S. coelicolor* superhost M1146 were pregerminated at 60°C for 30 mins in 500 µl of LB broth (25 g/L) before cooling. An overnight culture of *E. coli* ET12567 containing the pIJ1800 plasmid was grown in LB broth (25 g/L) containing Apramycin (50 µg/ml). 10ml from the overnight culture was centrifuged at 13,000 x g to pellet and the supernatant was removed. The pellet was washed twice in LB broth to remove any residual antibiotic. The washed pellet was then resuspended

in 1 ml of LB broth (25 g/L). 500 µl of pregerminated spores was combined in equal volumes with the washed *E. coli* culture. The mixture was then centrifuged, the majority of the supernatant was removed with the pellet resuspended in the residual liquid. The mixture was incubated at room temperature for 1 hour.

A ten times dilution of the conjugation mix was plated on Soya flour-mannitol agar (SFM) supplemented with 10 mM $MgCl_2$. After 18 hours incubation at 30°C, a 1ml overlay of antibiotics containing Nalidixic acid (0.5 mg/ml) and apramycin (1 mg/ml) was gently placed and spread on each dilution plate. The plates were incubated for a further 4 days to allow for colonies to grow before selecting exconjugant colonies and streaking onto SFM plates containing both antibiotics. Samples were placed at 4°C for 4 months before removing and incubating at 30°C for 5 days due to lockdown 1 and lab closure.

4.2.13. Colony PCR

After the second passage, exconjugants were picked and grown on SFM agar containing Apramycin and from the same colony, spores were crushed in 50% DMSO and heated at 60°C for 1 hour to extract the genomic DNA. A PCR was carried out to determine the presence of chromosome-integrated plasmid pIJ1800. This was achieved by amplifying the *chpE* gene using two sets of primers as described earlier in. As positive and negative controls, the pIJ6902 and the *S. coelicolor* M1146 mutant were used.

4.2.14. Extraction of spores from sporulating solid grown cultures

Spores were spread Soya flour Mannitol Agar and incubated for 5 days before harvesting by scraping the spores in the presence of 2ml of sterile distilled water from the plate and stored in 25% glycerol at -80°C.

4.2.15. Cultivation and extraction/purification conditions for the homologous expression and purification of ChpE

Media were prepared as mentioned in section 2.1. Final concentration of $5x10^6$ spores per ml for each strain (M1146, M1146-pIJ6902 and M1146-pIJ1800) were added and grown at 30°C for 2 days in the presence of Apramycin at a final concentration of 100 µg/ml. After 2 days, Thiostrepton was added at a final concentration of 50 µg/ml to induce the plasmid. The solid and liquid fractions were separated by centrifugation at 7,500 x g.

4.2.16. Acetone precipitation

Acetone was incubated at -20°C for 1 hour before vortexing 3 parts cold acetone to 1 part supernatant. The mixture was then incubated at -20°C for 1 hour. Precipitated proteins were collected by

centrifugation at 10,000 x g and the supernatant was removed before allowing the pellet to air dry. The pellet was resuspended in 500 µl of distilled water.

4.2.17. Antibody detection of amyloid peptides

As the chaplin proteins form amyloid proteins, they can be detected by using specific antibodies [108]. This was carried out using a rabbit polyclonal to β-amyloid as a primary (ab2539, Abcam) and a goat anti-rabbit IgG isotype with a conjugation to horseradish peroxidase (ab205718, Abcam). Using these two antibodies, a dot blot was carried out to detect chaplin proteins. A nitrocellulose membrane (Amersham™ Protran™, GE Healthcare Life science) was cut to size and sectioned using pencil to allow for sufficient separation of the samples and to avoid merging of samples during the blotting phase. 2 µl of sample was slowly added and dried to each section of the membrane before blocking the membrane with 5% Bovine serum albumin (BSA, Fisher scientific) in TBS-T (0.05% Tween20, 20 mM Tris-HCl, 150 mM NaCl, pH 7.5) for 1 hour at room temperature. The solution with blocking reagent was removed and then subsequently incubated with the primary antibody at a final concentration of 5 µg/ml in BSA/TBS-T (0.1% BSA in TBS-T) for 30 minutes at room temperature. After the incubation, the antibody was retrieved, and the membrane was then washed three times in TBS-T. The secondary antibody 0.5 µg/ml in BSA/TBS-T) was added to the membrane and incubated for 30 minutes at room temperature before washing with TBS-T three times (15 minutes, 2 x 5 minutes) then TBS (20 mM Tris-HCl, 150 mM NaCl, pH 7.5) once for 5 minutes. Using Clarity Western ECL substrate (BioRad), the membrane was incubated for 1 minute before imaging on a GelDoc Go (Biorad) to capture chemiluminescence.

4.3. Results

4.3.1. Amplification of *chpE*

Primers were designed based on a previous construct (pSET+ChpE) to allow for amplification and subsequent ligation into the thiostrepton inducible promotor plasmid. *In silico* PCR analysis was carried out and a 263 base pairs (bp) amplicon was predicted (Figure 32).

Figure 32: *In silico* analysis of fragment amplification using ChpE-F and ChpE-R primers producing a 263 bp fragment with A-base overhangs.

PCR amplification of *chpE* was then attempted with template pSET+*chpE* and primers chpE-F and chpE-R at different annealing temperatures, after which the reaction products were subjected to DNA electrophoresis and imaged. Figure 33 shows the fluorescence of DNA fragments resulting from amplification at different annealing temperatures.

Amplification at 54°C annealing temperature resulted only in a very weak band when compared to DNA fragments resulting from higher temperatures. An increase in the temperature to 55.7°C and 58.5°C, respectively, there was an increase in the fluorescence observed. The fluorescence of the band at 60°C appeared to be slightly reduced in comparison to the 55.7°C and 58.5°C bands. From these annealing temperatures, 58.5°C appeared to be the most efficient temperature -of the temperatures analysed- for these primers. All bands for the different annealing temperatures were at the expected fragment size as indicated by the ladder, specifically between 200 bp and 400 bp.

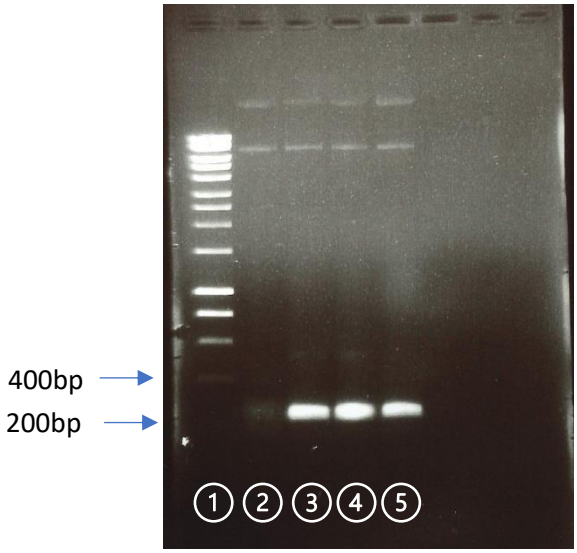

Figure 33: *DNA amplification products following a polymerase chain reaction at different annealing temperatures for the amplification of ChpE using ChpE-F and ChpE-R. 1kb Hyperladder (Lane 1), 54°C (Lane 2), 55.7°C (Lane 3), 58.5°C (Lane 4) and 60°C (Lane 5).*

Ligation of the purified *chpE* fragment into pGemT Easy vector was carried out after which the ligation product was transformed into *E. coli* DH5α which produced both blue and white colonies as expected. Two white colonies were individually collected and grown overnight in LB broth containing ampicillin for plasmid mini prep.

4.3.2. Restriction Digest and Ligation into pIJ6902

To confirm the correct plasmid was being used, pIJ6902 obtained from plasmid preps of four individual cultures was restricted using the HindIII restriction enzyme. The fragments were then separated and visualised. The plasmid map of pIJ6902 suggests that with the use of HindIII, the plasmid would be cut four times giving four fragments of different sizes. This restriction was analysed firstly *in silico* to determine the expected band sizes before restricting the plasmid (Figure 34).

```
Restriction analysis of pIJ6902.gb.xdna [Circular]
Incubated with HindIII

4 fragments generated.

   1:    5,227 bp  -  From HindIII[413]  To  HindIII[5640]

   2:      969 bp  -  From HindIII[5640] To  HindIII[6609]

   3:      723 bp  -  From HindIII[6609] To  HindIII[7332]

   4:      421 bp  -  From HindIII[7332] To  HindIII[413]
```

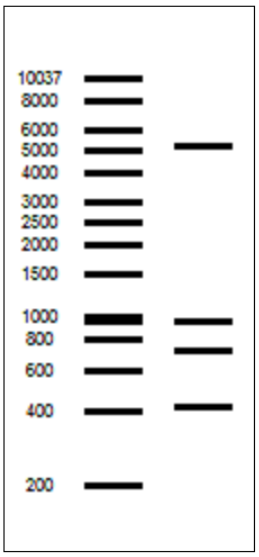

Figure 34: *In silico* restriction digest of pIJ6902 using HindIII giving expected band sizes of 5227 bp, 969 bp, 723 bp and 421 bp.

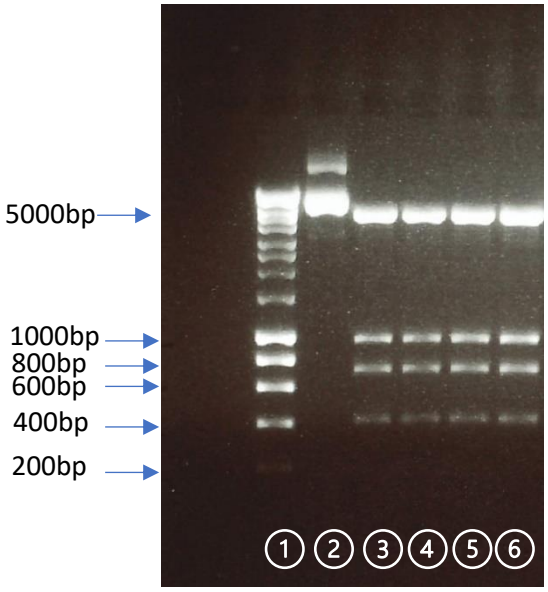

Figure 35: HindIII restriction of pIJ6902 followed by DNA electrophoresis.1kb hyperladder (Lane 1), Unrestricted plasmid(Lane 2), restricted plasmid from four different mini-prepped cultures (lanes 3-6).

The unrestricted plasmid gave the expected bands for the circular, coiled and supercoiled (Figure 35, lane 2) The restricted plasmid also gave the expected band sizes (Fig 4, lanes 3-6) as identified from the *in silico* restriction (Figure 34). These results indicate that the plasmid in the preps was indeed pIJ6902.

The white colonies from the pGemT Easy (Promega) ligation with the *chpE* amplicon (pGemT+*chpE)*, and pIJ6902 in *E. coli* DH5α were grown in LB broth overnight before being mini-preped (zymo) to extract the plasmid DNA. Using NdeI and BglII, fragments were restricted then resolved with DNA electrophoresis. Double-digested pIJ6902 and pGemT+*chpE* were purified from the agarose gel slices and ligated.The ligation mixture and the relevant controls were transformed into E. coli DH5α.

Table 6:Transformation negative control (competent cells and + distilled water), transformation positive control (competent cells + pSET152+chpE, ligation control (Competent cells + ligation of BglII restricted pIJ6902) and pIJ6902 with ChpE fragment ligation (competent cells + pIJ6902+chpE ligation mix)

Sample	**Colonies present**
Transformation Negative control	-
Transformation Positive control	+
Ligation control	+
pIJ6902 + ChpE ligation	+

The negative control for the transformation was achieved using dH_2O and no colonies were present after 18 hours at 37°C as expected. Abundant number of colonies were obtained from transformation of the intact pSET152+*chpE* positive control. Colonies were present for the ligation control using a linearised pIJ6902 restricted with BglII which had been ligated. The pIJ6902+*chpE* ligation also had colonies present suggesting the ligation and transformation were successful. To confirm the presence of plasmid pIJ1800, colony PCR was carried out on four colonies using primers *chpE*-F and *chpE*-R.

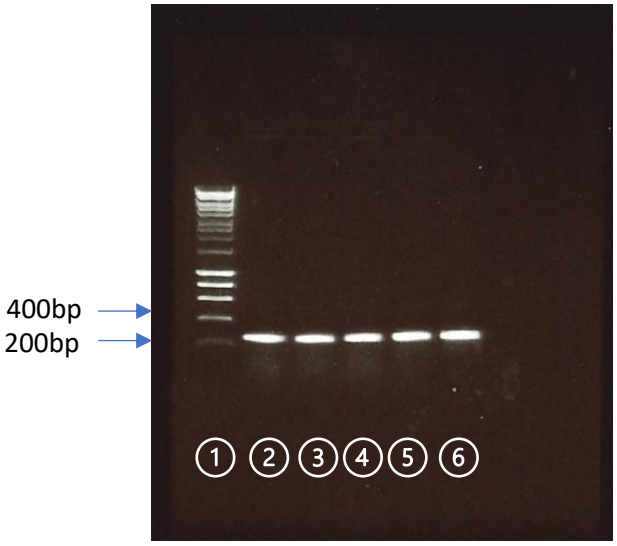

Figure 36: DNA amplification products following colony PCR of pIJ1800 and DNA electrophoresis. 1kb Hyperladder (Lane 1), Colonies 1- 4 (Lanes 2-5) ,pSet152-ChpE positive control (Lane 6) and negative control (Lane 7).

Figure 36 shows DNA fragments of 264 bp size, indicating that all four selected colonies appeared to contain the desired plasmid pIJ1800. The positive control for the colony PCR had a band of similar size to the unknown colonies which indicated successful amplification of the c*hpE* fragment. The negative control containing water as the template and PCR mix, gave no indication of amplification as expected due to no template.

4.3.3. Conjugation to *S. coelicolor* M1146

After a plasmid preparation from a PCR-confirmed pIJ1800, the plasmid was transformed into *E. coli* ET12567/pUZ8002 strain. Colony PCR was carried out to determine the success of the transformation.

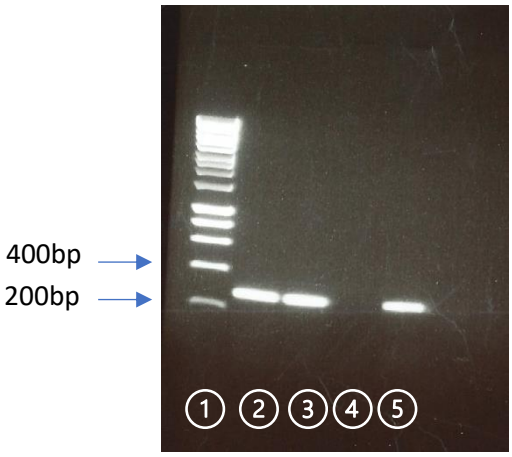

Figure 37: DNA amplification products following colony PCR of pIJ1800 and DNA electrophoresis from *E. coli* ET12567/pUZ8002. 1kb Hyperladder (Lane 1), Colonies 1-3 (Lanes 2-4) and positive control pSET152-ChpE (Lane 5).

From the colony PCR (Figure 37), the positive control gave a clear band at the expected size and two of the three colonies selected gave a similarly sized band to the control. The third colony (Figure 37, lane 4) did not amplify a fragment with the ChpE-F and ChpE-R primers. This culture was subsequently disposed of.

One of the successfully transformed strains of *E. coli* ET12567-pUZ8002-pIJ1800 was then used for conjugation into *S. coelicolor* M1146 (2.8.9). One resultant exconjugant colony was subjected to PCR with primer sets *chpE*-F/*chpE*-R and *pTipA*-F/*chpE*-R to check for successful conjugation and insertion of plasmid pIJ1800 into the chromosome, whilst also discriminating against wild-type *chpE* on the chromosome.

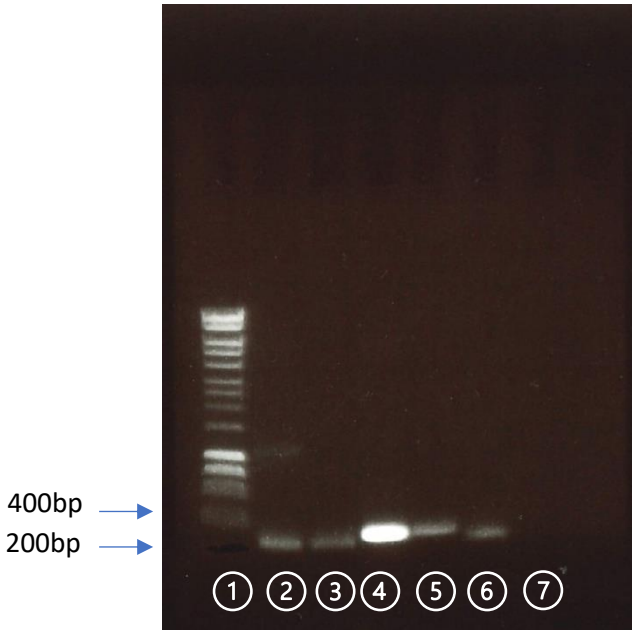

Figure 38: Colony PCR of exconjugants using internal and external primers. Lane 1 – 1Kb Hyperladder (Bioline), Lane 2 – pIJ1800 (plasmid), Lane 3 – M1146 with pIJ1800 (gDNA), Lane 4 – pIJ1800 (plasmid), Lane 5 – M1146 with pIJ1800 (gDNA), Lane 6 – M1146 (gDNA), Lane 7 – M1146 (gDNA). Lanes 2,3 & 6 amplified used ChpE-F and ChpE-R. Lanes 4,5 & 7 amplified using TipA-F and ChpE-R

The positive control for the amplification of *chpE* (Figure 38, lane 2) using the internal primers (*chpE*-F and *chpE*-R) gave the expected band size 263 bp. This was used as a comparison for Figure 38lanes 3 (genomic DNA extracted from exconjugant) and 6 (genomic DNA extracted from wild type M1146). Both of these lanes had a similar band size to Figure 38 lane 2 (pIJ1800 plasmid). Using the p*TipA*-F and *chpE*-R primers, a slightly larger fragment size was expected. The expected band size was observed for PCR amplification of the pIJ1800 using the p*TipA*-F and *chpE*-R primers (Figure 38, lane 4). Given the amplicon presence and size (Figure 38, Lane 5) which gave a similar sized band, suggests that the plasmid had been successfully conjugated and inserted onto the chromosome. The M1146 mutant strain control reaction (Figure 38, Lane 7) with the p*TipA*-F and *chpE*-R primers gave no visible band as expected due to the absence of the *pTipA* promoter. Glycerol stocks of the M1146 strain containing the pIJ1800 plasmid were made and stored at -80°C.

4.3.4. Induced Expression of ChpE in different media

Three different media were trialled for the expression of the chaplin E gene, R2YE, MYM and Nutrient broth. For each media, M1146, M1146 containing the pIJ6902 and M1146 containing the pIJ1800. 200 ml flasks were inoculated with $5x10^6$ spores. M1146 provides a baseline expression of the native *chpE* and the M1146 pIJ6902 is a negative control the addition of Thiostrepton. Induced cultures were grown for 2 days at 30°C before *chpE* expression was induced by the addition of Thiostrepton (50 µg/ml in DMSO). Thiostrepton was not added to uninduced cultures. Uninduced and induced cultures were incubated for a further 48hrs before cell biomass and supernatant were harvested. Culture

supernatant and pellets were analysed separated by centrifugation and were both assayed using thioflavin T fluorescence to determine if chaplin E was (over)expressed. The pellet was resuspended and sonicated prior to assaying. The assay was carried out using media only to establish the baseline fluorescence and to be used as a comparison for uninduced and induced cultures.

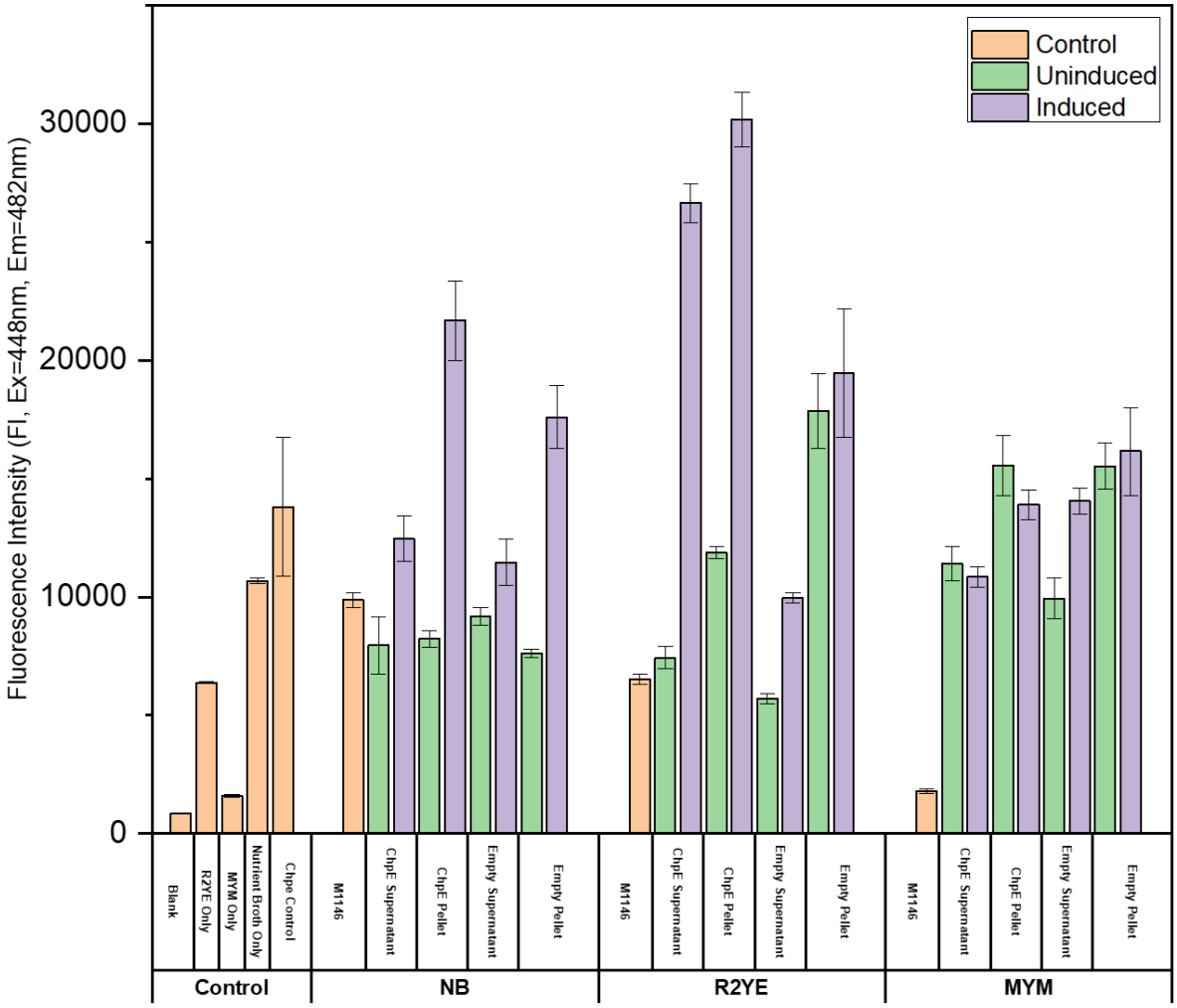

Figure 39: Averaged Thioflavin T fluorescence response for each fractionated biomass from M1146, M1146 with pIJ1800 and M1146 with pIJ6902 in different media (Nutrient broth = NB, R2YE and MYM) (n=3).

Fluorescence intensity readings of the media only, gave a baseline for each culture. When comparing the three un-inoculated media types, nutrient broth had the highest response in the ThT assay and MYM gave the lowest response (Figure 39). The ThT fluorescence for cell pellets and supernatants of all uninduced strains grown in nutrient broth remained similar to the medium only and M1146 control strain. After induction by thiostrepton, the greatest increases in ThT fluorescence for pellets and supernatants were strains cultured in nutrient broth that contained pIJ1800. The pellet of the M1146 pIJ1800 strain had the highest fluorescence intensity of all strains grown in nutrient broth. The pellets of M1146 pIJ6902 had a slight increase over their uninduced counterpart. For growth in R2YE, a 3.58-fold increase in the fluorescence intensity was observed for both the supernatant and the pellet of

the M1146-pIJ1800. The fluorescence recorded for the pellet of the M1146 pIJ6902 was higher than expected but no differences were observed after induction. The modified MYM medium with $KHCO_3$ buffer developed in Chapter 3 was also tested for expression of chaplin E. From the recorded values, there were no discernible differences between the uninduced and induced cultures for both the pellets and the supernatant. Comparatively, the largest fold increase in ThT fluorescence between uninduced vs induced cultures was seen for supernatants of R2YE-grown M1146-pIJ1800, implying expression as well as secretion of ChpE. Due to the detection of chaplin proteins within the supernatant, purification of the chaplin E protein from the supernatant was investigated.

4.3.5. Purification

Section 4.2.4 determined that the expression of *chpE* into the supernatant was being achieved when cultured in R2YE (Figure 39). To negate the long and tedious extraction process associated with chaplin extractions from sporulated cultures, precipitation of chaplin proteins was investigated to determine if chaplin proteins could be concentrated from supernatants following expression. R2YE medium cultures using M1146, M1146-pIJ6902 and M1146-pIJ1800 were grown and induced before precipitating the proteins from the supernatant. Ammonium sulphate precipitation was trialled but due to poor pelleting and residual salts after purification, acetone precipitation was chosen as the preferred method.

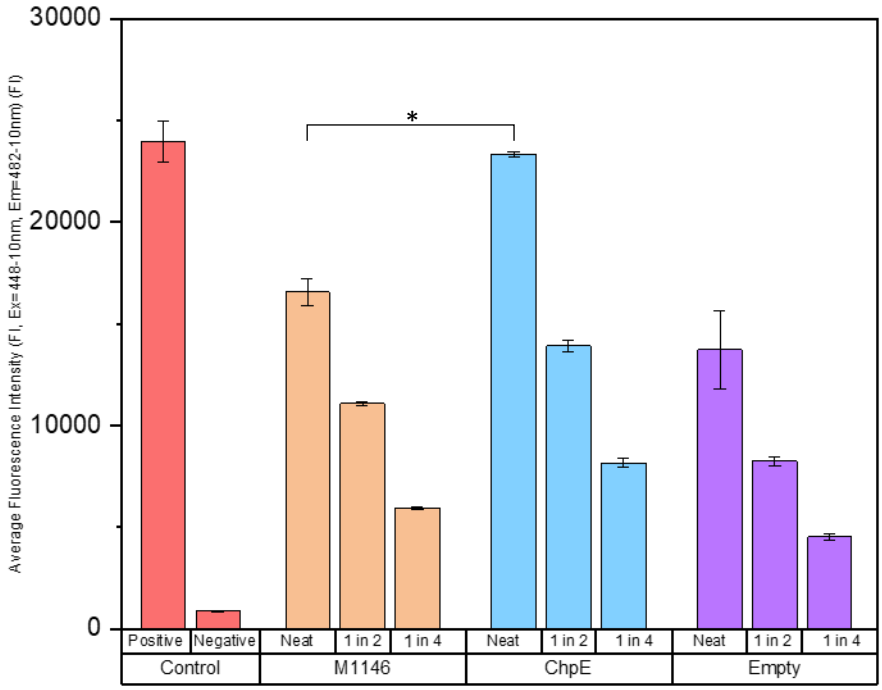

Figure 40: Averaged Thioflavin T fluorescence responses after Acetone precipitation of culture supernatants. M1146 (Orange), M1146 pIJ1800 (Blue) & M1146 pIJ6902-Empty (Purple) n=3. Mann-whitney t-test, *P<0.05.

Supernatants of cultured strains were collected and subjected to acetone precipitation followed by centrifugation. The resuspended pellet in distilled water(neat) was diluted by 50% (1 in 2) and by 75% (1 in 4). The positive control used for amyloid detection in the ThT assay was synthetic chaplinE-short at 2 mg/ml. Distilled water was used as the negative control, to provide the background fluorescence of the ThT fluorescence dye.

As expected, the positive control for amyloid proteins using the synthetic chaplinE gave a strong response with an average ThT fluorescence intensity of 23934 (Figure 40). This can be compared to the negative control, containing no amyloidogenic material which gave a low fluorescence intensity of 867. The detection of amyloid proteins in the M1146 mutant strain supernatant averaged a fluorescence intensity of 16556. The M1146 pIJ6902 supernatant had a lower response but greater variance (13723 ±1902). From the M1146-pIJ1800 strain, the fluorescence intensity of the supernatant was 1.41-fold higher than the M1146 control strain, which was identified as significant (*p=0.045*) using a Mann-Whitney U Test. These results indicate the use of acetone can be used for the precipitation of chaplin proteins from culture supernatants.

4.3.6. Antibody Detection of Amyloid Proteins

The Thioflavin T assay on the precipitated proteins indicated, a response above the negative control across all samples, suggesting the presence of chaplin proteins. To further confirm the presence of amyloid proteins, conformational antibodies were used that recognize a generic amyloid fibril epitope [109]. This particular protocol did not require the running of samples through SDS-PAGE and subsequently did not require the electrophoretic transfer of the peptides from the gel onto nitrocellulose. The gels used for separation of chaplin proteins are high percentage gradient gels which results in the gel being fragile. The process for the transfer of proteins requires the sandwiching of gel and can result in the gel being broken. The detection of amyloid proteins was carried out on dotblots using a synthetic chaplin as a positive control. This allowed for comparison to the untreated supernatants of cultures of M1146, M1146-pIJ1800 (chpE) and M1146-pIJ6902 (empty) strains.

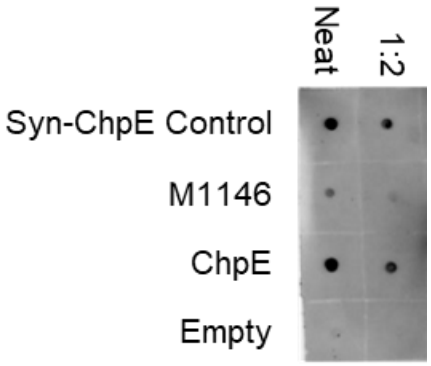

Figure 41: Dot blot detection of amyloid proteins from unprecipitated R2YE supernatants for M1146, M1146-pIJ6902 and M1146-pIJ1800 using a rabbit polyclonal to β-amyloid as a primary antibody (ab2539, Abcam) and a goat anti-rabbit IgG isotype with a conjugation to horseradish peroxidase (ab205718, Abcam) as a secondary antibody. A neat supernatant and half diluted supernatant were blotted for each with a synthetic peptide positive control.

The chemiluminescence of the synthetic chaplin E control was as expected, with a reasonable reduction observed for the diluted synthetic peptide (Figure 41). The neat supernatants for each of the tested strains gave a positive response to the assay with the supernatants of M1146-pIJ6902 giving a lower chemiluminescence in comparison to the M1146-pIJ1800 strain. The 1:2 dilutions of the supernatants also showed reduced chemiluminescence for each sample respectively.

The acetone precipitated samples were then subjected to dotblotting with β-amyloid antibody to determine if the precipitation method was successful for concentrating amyloid proteins.

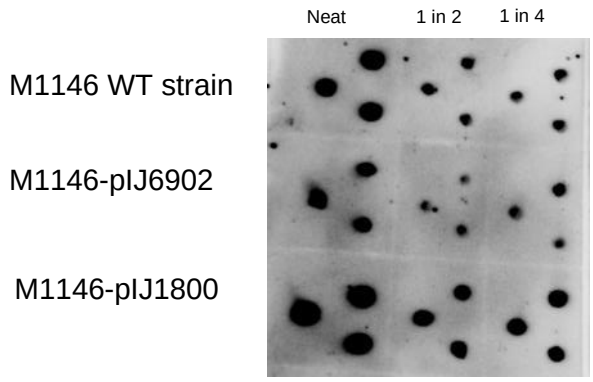

Figure 42: Dot blot detection of amyloid proteins from acetone precipitated R2YE supernatants for M1146, M1146-pIJ6902 and M1146-pIJ1800 using a rabbit polyclonal to β-amyloid as a primary antibody (ab2539, Abcam) and a goat anti-rabbit IgG isotype with a conjugation to horseradish peroxidase (ab205718, Abcam) as a secondary antibody. A neat, 2x diluted and 4x diluted supernatant were blotted for each. n=3

4.3.7. Dotblot Detect of Precipitated Chaplin Proteins

The dot blot of the precipitated samples (Figure 42) suggested that amyloids were present in each of the strains' precipitated supernatants. 2 µl of solubilised peptide in water was used per dot. Figure 42 shows that acetone-precipitated protein in the supernatant of M1146-pIJ1800 resulted in the high

response to the assay across all dilutions. Both the M1146 and M1146-pIJ6902 strain indicated the presence of amyloid proteins.

4.3.8. SDS-PAGE of Acetone Precipitated Supernatants for ChpE Detection

Acetone precipitated supernatants were subjected to SDS-PAGE to visualise the ChpE proteins. M1146, M1146-pIJ6902 and M1146-pIJ1800 were subjected to SDS-PAGE to separate the peptides present within the sample.

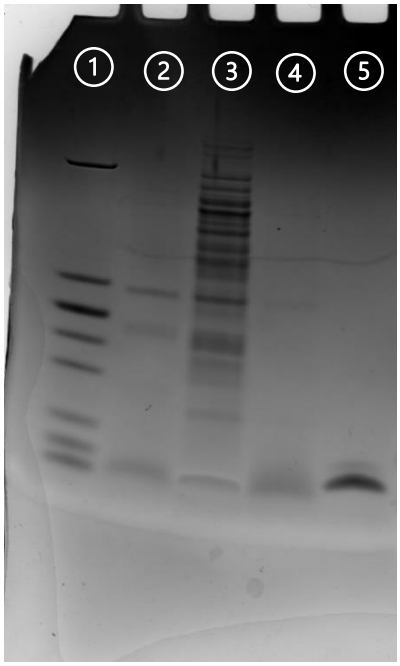

Figure 43: SDS-PAGE of acetone precipitated supernatants from M1146 (lane 2), M1146-pIJ6902 (Lane 3), M1146-pIJ1800 (lane 4) and synthetic peptide S*. coelicolor* ChpE control (lane 5). Page ruler #26632 (Fisher Scientific).

4.3.9. Mass Spectroscopy for Detection of Chaplin Proteins

To ensure the amyloid protein being detected by both the Thioflavin T assay and the antibodies was chaplin E, matrix-assisted laser desorption/ionisation time of flight mass spectrometry (MALDI/TOF-MS) was carried out. Positive control synthetic chaplins were measured first before testing (precipitated) supernatants. The synthetic chaplin E designed from the *S. coelicolor* genome was subjected to MALDI to establish the protocol.

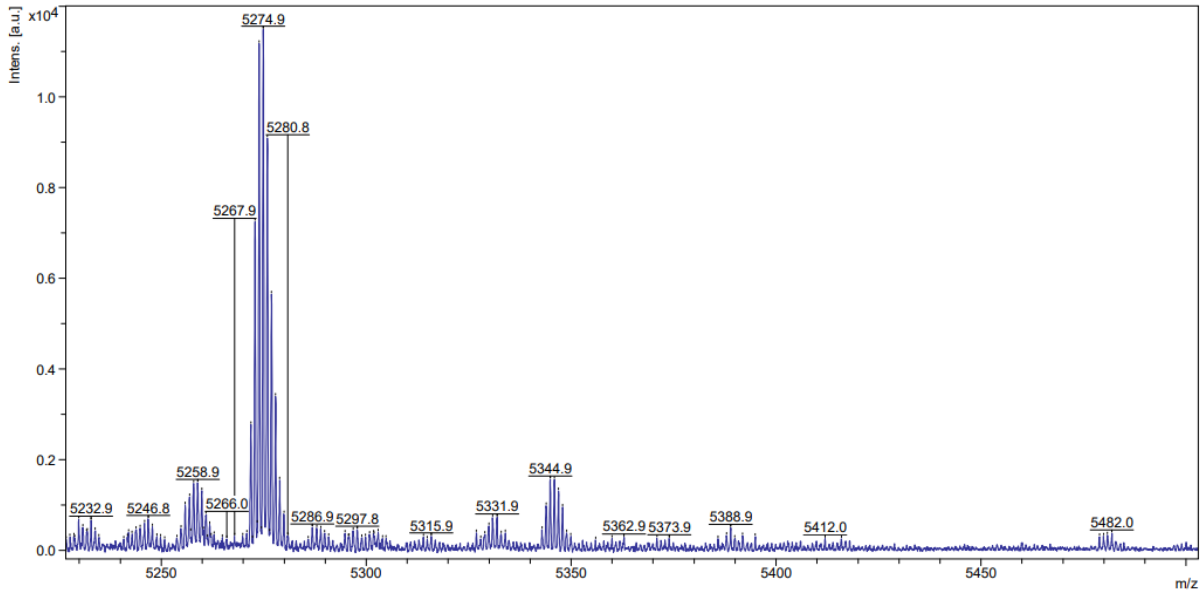

Figure 44: MALDI/TOF-MS spectrum of synthetic chaplin E (S. coelicolor) peptide with an expected m/z of 5273.95.

The expected m/z of the *S. coelicolor* ChpE peptide was 5273.95. From the spectrum, the m/z was +1, which is likely to be due to the presence of a hydrogen adduct.

As chaplin E could be detected positively, this set up was then also used to detect ChpE protein in the (precipitated) supernatants of the newly created expression and control strains (after induction with thiostrepton).

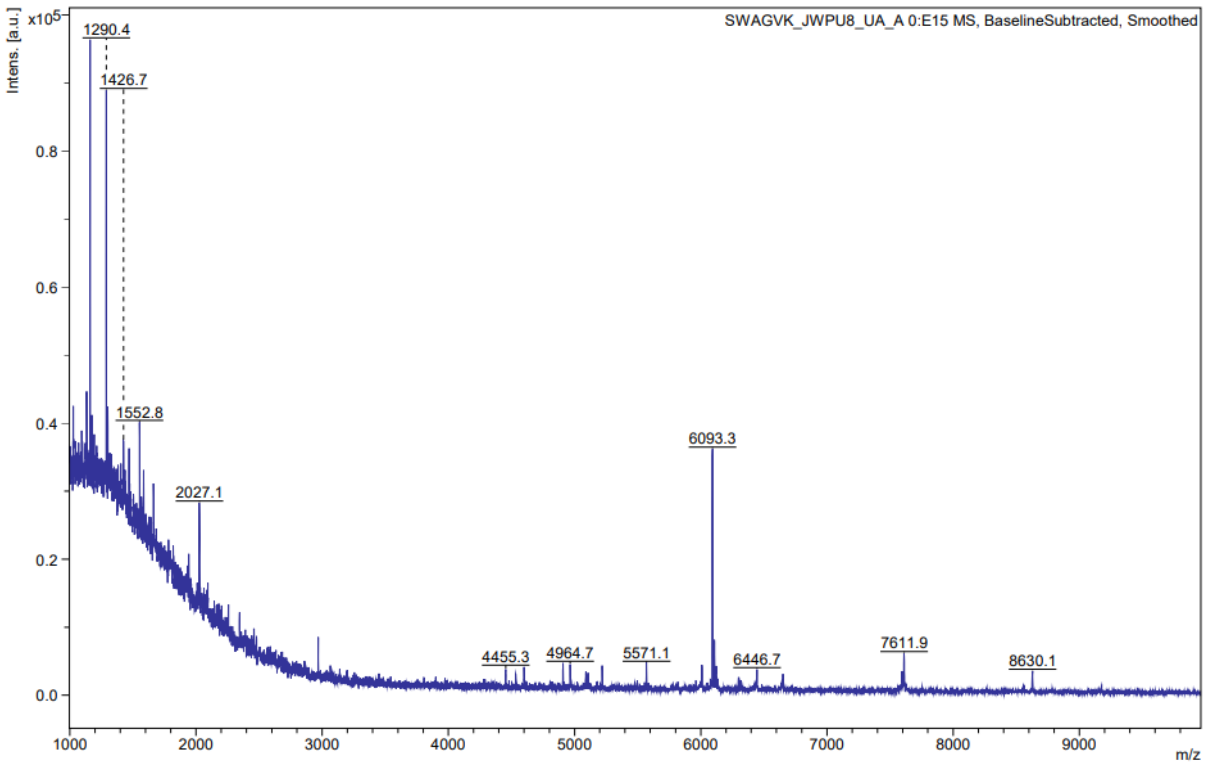

Figure 45: MALDI-TOF spectrum of acetone-precipitated supernatant of parent strain M1146.

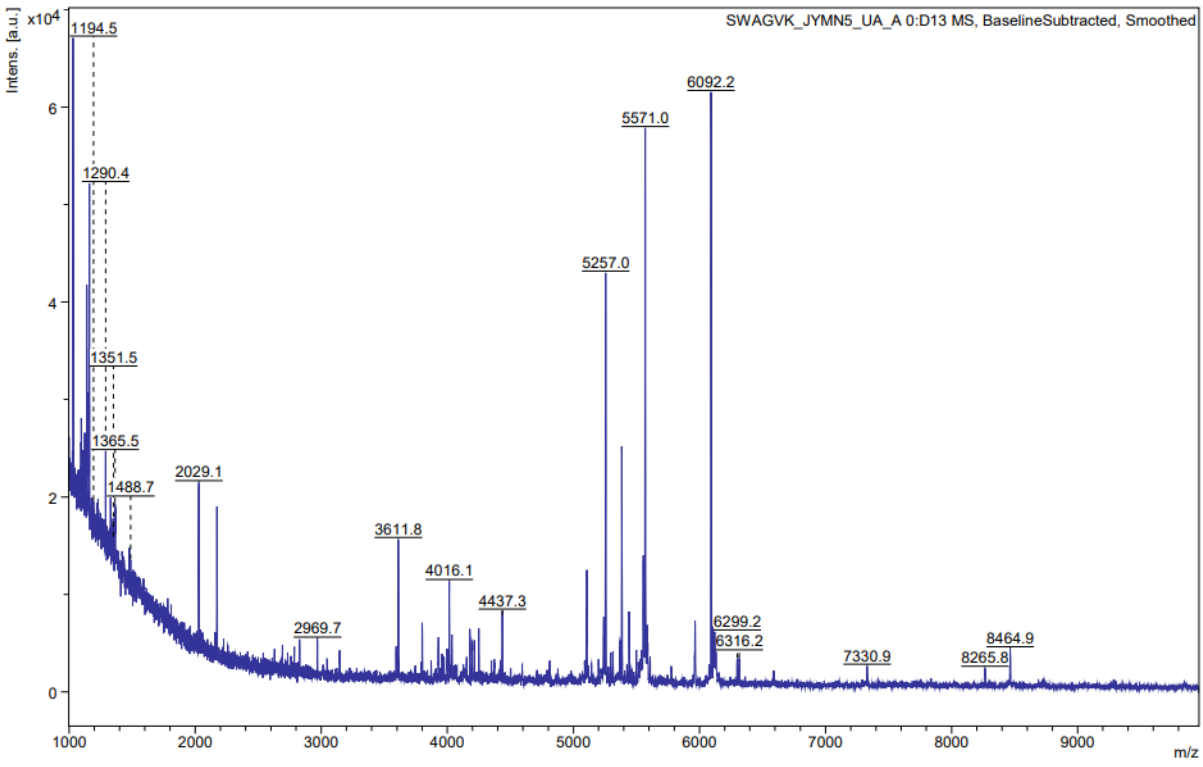

Figure 46: MALDI-TOF spectrum of acetone-precipitated supernatant from the induced strain of M1146-pIJ6902.

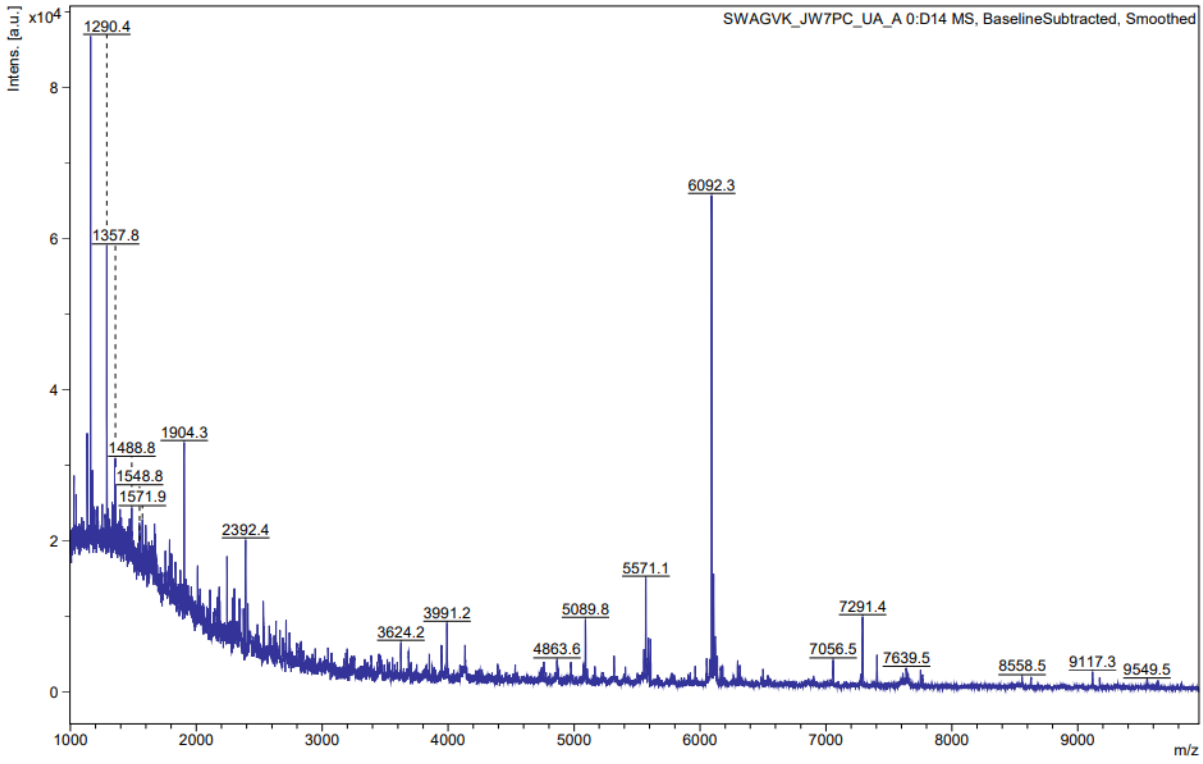

Figure 47: MALDI-TOF spectrum of acetone-precipitated supernatant of induced strain M1146-pIJ1800

Parent strain M1146 contains the full complement of *S. coelicolor* chaplins, of which ChpE and ChpH can be expressed in submerged liquid media[110], and prior to the onset of morphological differentiation when grown on agar [16]. Therefore, all M1146 derived strains with plasmids pIJ6902 and pIJ1800 are also expected to be able to express chaplins E and H. It is hypothesised that the peak intensity for ChpE at the mass to charge ratio of 5270 should be larger for the acetone-precipitated supernatant of strain M1146-pIJ1800 due to (over)expression of *ChpE*. However, no observable chaplin E peak was identified at 5270 across the samples, nor could ChpH be detected at an m/z of 5121 (Figure 45, Figure 46 and Figure 47). Alternatively, if ChpE was expressed upon induction of strain M1146-pIJ1800 but not secreted (efficiently), the protein may be present with its signal peptide which was predicted to yield a peak at m/z of 7628.

4.4. Discussion

4.4.1. Host Strain and Plasmid Selection

Design and in silico analysis was a key part in the development process to enhance the chances of success of (over)expressing ChpE protein. Firstly, the plasmid and host strain were selected. The *S. coelicolor* M1146 strain was selected as the host as it does not sporulate in liquid cultures and as M1146 is derived from M145 it should be able to express ChpE and ChpH proteins in submerged cultures [97]. M1146 is slower growing but the lack of four of its main antibiotic gene clusters would allow for more nutrients to be expended on the production of chaplins once induced plus would not produce pigmented compounds that may co-extract/purify. *E. coli* is typically a very attractive host and is commonly used for expression of proteins due to the large quantities of protein that can be produced quickly and easily. However, the formation of misfolded proteins is commonly observed. The overexpression of chaplin proteins has been attempted in both *E. coli* and *Bacillus subtilis,* both of which have been unsuccessful or given undesirable effects [59].

Plasmid pIJ6902 was selected for its inducible expression options [111]. It was also compatible for integration due to the presence of the *attP* locus for integration at the ϕC31 integration site on the chromosome. It also contains a range of restriction sites next to the inducible promotor *pTipA* for the cloning of the desired fragment of interest. Plasmid pIJ6902 was selected over plasmid pIJ8600 (which also contains a *pTipA* promoter) as it was claimed genes inserted to pIJ8600 were easily lost due to the presence of accidental tandem repeats that flanked the cloning sites enabling loss of the insert by homologous recombination (Actinobase; Dr David Widdick Personal Communication).

4.4.2. Integration of pIJ1800 onto M1146 *S. coelicolor* Chromosome

After successful construction and transformation of pIJ1800 into *E. coli* ET12567 (pUZ8002). The conjugation protocol was carried out (section 2.8.9). Due to lab closures, the conjugation protocol was modified in comparison to the standard protocol. After the flooding of plates with the antibiotic cocktail, plates are normally incubated at 30^{o}C for 3-4 days to facilitate the growth of spores which have successfully integrated the plasmid. However, after the flooding of plates, the storage conditions were modified. The plates were incubated at 4^{o}C for four months to slow the rate of growth and to avoid over growing. This modification may have generated secondary mutations leading to downregulation.

4.4.3. Media Comparison

The purpose of this research was to investigate the effects of an inducible promotor on the expression of *chpE* in a *Streptomyces* strain as constitutive expression gave unexpected culture morphology

phenotypes. After the confirmation of strain M1146-pIJ1800, determining the optimal medium was investigated for the controlled expression of *chpE*. This was achieved by comparing three different media types, R2YE, modified MYM (Chapter 3) and Nutrient broth. These complex, nutrient-rich media were selected as they greatly support growth of *Streptomyces* in submerged cultures yielding high resulting biomass. Each of these media recipes provided benefits but the expression behaviour of the strain for ChpE was unknown. *S. coelicolor* M1146 does not sporulate in liquid cultures [82] but *chpE* is expressed at low levels during hyphal growth [17]. The R2YE medium is a well-defined medium which has been used in natural product studies. The high sucrose content limits the size of the mycelial fragments. This medium also allows some strains of *Streptomyces* to grow and differentiate but this particular medium is expensive due to the presence of the TES buffer. The modified MYM medium developed in chapter 3 was used, but MYM is good at supporting high biomass generation. Nutrient broth is a simple medium recipe and requires no post autoclave additions unlike the R2YE and modified MYM. This particular benefit is less significant as Apramycin is added which would be selective for the strain containing the pIJ6902 plasmid exerting Apramycin resistance. This reduces the chances of contamination which could be introduced with the increased number of post autoclave additions.

The media were compared with and without the addition of thiostrepton to determine if expression differed between media. As the M1146 parent strain does not sporulate in liquid cultures, it was expected that its chaplin protein levels would be low across all three media types. Initial experiments were carried out to determine the optimal medium which would facilitate high expression of chaplin proteins into the supernatant. From the comparison of the uninduced and induced strains (M1146, M1146-pIJ6902 & M1146-pIJ1800) in different media (Figure 16), there was a clear increase in the Thioflavin T response after thiostrepton addition for the nutrient broth and the R2YE, however, this increase in fluorescence was not observed in the MYM. This observation was evident for the supernatants and the pellets. This would suggest that modified MYM medium did not appear to provide the appropriate growth conditions for the (over)expression of chaplin E. By inducing the M1146 pIJ1800 in R2YE, the pellet and the supernatant gave a significant increase in the Thioflavin T fluorescence assay (Figure 16). For the pellets, a crude extraction method was carried out by sonicating the pellet to breakdown the biomass. This would release any peptides trapped within the 'pseudo-periplasm' to then be detected by the amyloid assay. The intensity values recorded (Figure 16) suggest that there may be a large proportion of the chaplin protein still being retained. The chaplin proteins may also be interacting with the cell wall of the hyphae. This particular association is caused by ClsA, a cellulose-like synthase enzyme which produces a bacterial cellulose like beta-glycan which chaplin proteins are known to associate to form a structure that aids in the adhesion to solid

substrates [28]. The possible retention at the cell wall may be limiting the amount of peptide being present within the supernatant of the culture. The different strength constitutive promotor research led to phenotype changes which ultimately resulted in less dense pellets[57]. The increased expression may be resulting in the chaplin proteins being trapped between the hyphae causing this 'fluffy' appearance. This was the focus of this research was to investigate the expression of chaplin proteins into the supernatant, pellet analysis was limited. Future work is be carried out with expression into mutant strains without the presence of *CslA* to determine if this was a major factor in the secretion of chaplin proteins into the culture supernatant. The morphology of the strains within the different media types varied. In R2YE and MYM, typical growth of long vegetative hyphae was observed, however, in nutrient broth, the strains were clustered into a tight spherical morphology. The morphology observed here in the nutrient broth may be a potential explanation to the poor expression after induction. If these cell masses were tightly packed, the expression into the supernatant would be hindered, which would lead to a lower thioflavin T response. In conjunction with the different media types, thiostrepton also has an effect on cell morphology [112] causing the hyphal dispersion to be lower with a densely packed core.

The growth and expression of the chaplin proteins varied across these three media types, with R2YE appearing to give high expression into the supernatant (Figure 16). The expensive and complex nature of this medium does not make it ideal for scale up when expressing chaplin proteins from *S. coelicolor* M1146. Alternative media or further optimisations could be developed by investigating alternative carbon sources as the carbon source is an environmental factor which has a strong effect on the differentiation [113] and the ability for secondary metabolite production. Although the carbon source can be changed, the nitrogen source and composition of amino acids used can also have a significant effect on the secondary metabolism [114].

The development of this expression strain looked to improve upon the current method for production and extraction of chaplin proteins. Currently, chaplin protein are extracted from the surface of spores and aerial hyphae and the presence of co-extracted cell wall and other cell envelope fragments is common unless chromatographic purification methods are carried out. The expression of the chaplin proteins into the media is a strategy being developed here to reduce the overall downstream processing and to improve the culturing conditions. The current process for extraction requires extensive boiling in SDS, sonication and freeze drying [23]. The ability for purification from the supernatant would allow for a more streamlined process and would reduce the processing time of sample for the extraction of chaplin proteins. Knowing that there is a portion of chaplin proteins within the pellet, optimisations could be made to improve the efficiency of expression. Due to the increased

amyloid fluorescence observed in the supernatant of the R2YE, this was selected as the growth medium for the expression strains for the future experiments.

Repeat cultures were carried out using R2YE, and as a corroborative test, a dotblot was carried out using an amyloid-specific antibody (Figure 41). From testing the untreated supernatant samples, a slight detection was observed for both the M1146 and the M1146-pIJ6902 strains. The M1146-pIJ1800 strain and the synthetic peptide control however gave a strong response. Given the strong response to the thioflavin T assay and the dotblot, chaplin E appeared to be expressed into the supernatant at a higher level than the control (M1146). The pellet samples were not tested using dotblot as the objective for this research was to determine if chaplin proteins could be expressed into the supernatant which would reduce the downstream processing. The results from this led to examining effective concentration and purification methods for chaplin proteins from the supernatant.

4.4.4. Purification

The ammonium sulphate precipitation trial did precipitate a small fraction of peptide between the range of 20% to 80% w/v NH_4SO_4, however pelleting was very poor and a significant portion of the sample was difficult to retain. The acetone precipitation was carried out on each of the samples and a pellet was observed unlike the ammonium sulphate and the supernatant acetone mix was easily removed without disturbing the pellet. This improved removal of the supernatant was a key factor in the decision to use the acetone precipitation method as the ammonium sulphate method contained a high proportion of salts. The acetone precipitation of the supernatant from growth in R2YE gave a strong response to the thioflavin T assay for the M1146-pIJ1800 strain (Figure 42). There was still a response from the M1146-pIJ6902 and the M1146 strain but M1146-pIJ1800 showed a 1.4-fold improvement. To provide additional support to the detection by the Thioflavin T assay, the detection of amyloid proteins with the use of antibodies was carried out which is a highly sensitive and specific assay. For each strain (M1146, M1146-pIJ6902 and M1146-pIJ1800) induced with thiostrepton, a dot blot of the culture supernatants after 2 days post induction was carried out and chemiluminescence was detected for both the neat and 1:1 diluted concentration for all strains. The dot blot was used to avoid the membrane transfer and the subsequent degradation gel by directly blotting the extracted peptides onto a nitrocellulose membrane then subsequently treating with both the primary and secondary antibody. The detection in the M1146 strain may be due to background expression of ChpE which *S. coelicolor* uses to reduce the surface tension of the surrounding environment during vegetative growth (Figure 3) [16]. As the culturing of the bacterium was conducted within liquid shake flasks and that *S. coelicolor* does not sporulate in liquid cultures and there is no morphological

differentiation, *S. coelicolor* remains vegetative but extensively dense pellets. M1146 in liquid culture may be constitutively producing ChpE at low level [110].

As the method for purification results in the precipitation of all proteins within the supernatant, purity analysis of the purified proteins was carried out by SDS-PAGE. The samples were subjected to the same preparation and running conditions with the presence of a synthetic peptide control. The gels run however, did give a partial band at the expect size after silver staining (Figure 43) for all extracts, Figure 43, lane 3 had the presence of contaminating bands due to biomass poor pelleting, resulting in proteins extracted from the biomass. The band intensity of Figure 43 lane 4 was slightly higher than the M1146 and M1146-pIJ6902, respectively. The detection of chaplin proteins extracted from *S. griseus* resolved on SDS-PAGE is routinely done by staining with Coomassie blue, but the limit of detection for this stain is higher (30 ng) than that of the silver stain (1 ng). Faint bands were observed on all lanes at the expected size with a prominent band for the synthetic peptide control.

The overexpression of the ChpE protein under the conditions and fractions tested does not suggest that expression cannot be carried out at a larger scale, but purification of the peptide is the likely bottle neck in the process. This could potentially be alleviated by chromatography or filtration-based methods. Stephens et al has been successful in the purification of monomeric amyloid-β proteins using ion exchange chromatography [115]. The use of a tangential flow filtration module could filter out the chaplin proteins after growth and expression. This particular method is where the culture flows parallel to a membrane with specific pore sizes. The process is driven by the pressure within the module. It would be hypothesised that the chaplin proteins and smaller molecules would be filtered out of the culture, but this assumes that the chaplin proteins remain in a monomeric form as it passes through the membrane. The likelihood of chaplins remaining in the monomeric form is unlikely due to the agitation and aeration of the bioreactor causing increases in total area of hydrophilic-hydrophobic interfaces. By having a membrane pore size like the monomeric size of the chaplin protein, the filtrate would contain fewer coextracted molecules. As the pore size is increased more contaminating molecules would be filtered. Pore size can be varied but there is a significant chance that the pores may be become blocked with the chaplin proteins or the hyphal growth. This blockage would have a detrimental effect on the purification efficiency of the module.

Chaplin proteins are amyloidogenic, which means that these peptides have a propensity to form fibril structures in relation to external stimuli [116]. Chaplin fibrils form at the hydrophilic-hydrophobic interface (e.g. water and air) [117] but they can also assemble when in solution in the presence of glycans such as glycosamines and cellulose [28, 118]. Other amyloids such as Curli form assemblies more readily in comparison to chaplin proteins but not all amyloids can interact with glycosamines.

Both these stimuli have the potential to be problematic in the purification as the fibril size can vary depending on the degree of fibrillisation. The aeration process required for growth of any strain secreting chaplin proteins would induce the fibrillisation and unless using a *ClsA* deletion strain, *S. coelicolor* can produce bacterial cellulose-like glycan which can also induce the fibrillisation[30, 112]. It is the later that has been shown to aid in the attachment to surfaces in standing liquid cultures [82]. As the fibrillisation occurs, the length increases and becomes morphologically different from the monomeric form. By increasing the pore size, small fibrils may still pass through, but is likely to congest the pores which would ultimately lead to cake layer formation, which is when the biomass covers across the whole tangential flow filtration membrane and blocks all the pores.

The MALDI-TOF spectra obtained did not yield any relevant peaks for the M1146, M1146-pIJ6902 or the M1146 pIJ1800 *s*train (Figure 45, Figure 46 and Figure 47). The peaks obtained across the three strains' supernatants were similar suggesting that the medium or other co-purified proteins are being ionised and detected. The purity of the samples as per the SDS-PAGE gel, suggested that there would be a certain degree of co-purified proteins in the M1146-pIJ6902 (Figure 43). The *S. coelicolor* synthetic chaplin E ionisation intensity (~$1x10^4$ a.u.) (Figure 44) was higher than the ionisation intensities obtained from the three strains, which were ~$3x10^3$ (Figure 45, Figure 46 and Figure 47). The combination of low intensity and co-purified peptides may be overshadowing any peaks for chaplin E. The spectra obtained for the ChpE expression strain did contain a m/z peak at 7628 which would suggest that the signal peptide has not been cleaved, however, the intensity of the peak was low (~1500 a.u.). This peak was also observed in the M1146 control sample (Figure 44), which would suggest that the peak observed in the ChpE expression spectrum (Figure 47) is likely to be the background expression of ChpE rather than the overexpression caused by the inducible promotor plasmid. Across the spectra recorded for each of the purified samples, the m/z ions that could be present for ChpE with or without the signal peptide can vary depending on the association with either hydrogen, sodium or potassium. These cause an increase in the m/z by 1, 23 and 39 respectively. At these m/z's, no significant distinguishable peaks were evident.

4.5. Conclusions

The plasmid, pIJ1800, comprised of pIJ6902 containing a thiostrepton-inducible promotor (*pTipA)* and the chaplin E gene (*chpE*) was successfully constructed and mobilised into M1146 yielding strain, M1146-pIJ1800. Growth of M1146-pIJ1800 in R2YE followed by induction with thiostrepton led to a detectable increase in both ThT fluorescence and amyloid-specific chemiluminescence in dotblots suggesting ChpE protein was indeed expressed. However, secreted chaplin protein could not be detected in supernatants by SDS-PAGE and MALDI-TOF MS. The peaks identified appear to be co-purified compounds. Further analyses of pellet biomass may indicate the presence of retained chaplins. The research here demonstrates that the plasmid can be successfully conjugated with *S. coelicolor* M1146. The culturing conditions, specifically the medium, is important as not all media facilitated the (over)expression of the chpE protein. Although, expression appears to be occurring, definitive proof of the expression is required before final conclusions can be drawn. The research and data obtained here provides a foundation for future work for the expression using an inducible promotor and purification of chaplin proteins from liquid cultures.

Although significant insight into the over expression of *chpE* using an inducible promotor has been gained, further work is still required to improve and scale up the process. Within in this work, only chaplin E has been included on the plasmid for inclusion into M1146. Investigating the other chaplin proteins may yield different results due to the other chaplin proteins having cysteine residues which can form disulphide bridges. If the cysteine residue containing chaplins are being expressed, the folding of the proteins would be impeded if they remain within the cytoplasm due to the reducing environment unlike the surrounding medium which is generally oxidising, which promotes protein folding. If the chaplin proteins are preferentially folding in the media, this would lead to the formation of amyloid fibrils.

Changing the strain in which the chaplins are expressed in is a worthwhile experiment. The *S. coelicolor* M1146 strain does not contain the antibiotic gene clusters but the mechanisms present that aid in the adhesion to substrates are still present. Mutant strains with disruption of *cslA* and *glxA* chaplin proteins may not be able to interact and may improve the overall concentration of peptide after precipitation and/or purification as they would not be associated with the biomass[112]. This association with the bacterial cellulose-like glycan and subsequently the biomass is hypothesised and would require further experimentation to determine if the chaplin proteins are interacting with the biomass. However, until proven, the optimal expression host could be with a liquid sporulating strain such as *S. lividans*, *S. albus* or *S. venezulae*. These strains have been efficiently used for heterologous

protein expression and may be more accustomed to the expression of chaplin proteins in liquid cultures.

The detection of the chaplin proteins have been based on the use of amyloid specific dyes, SDS-PAGE and modified western blots. Enhancements to the detection could be achieved with the introduction of a fluorescent reporter protein such as the green fluorescence protein (*gfp*) to track the location of the chaplin proteins. As the proteins are expected to be secreted into the medium, alternative signal peptides could be trialled to determine the most efficient for expression of chaplin proteins.

Acetone precipitation was conducted on culture supernatants to concentrate the proteins present. The detection of amyloid proteins by thioflavin T fluorescence assay and immunoblotting was successful, however, detection using SDS-PAGE and MALDI/TOF was unsuccessful. Alternative strategies could be developed to limit the number of contaminating proteins that would be co-extracted from the media. The addition of a histidine tag to the chaplin protein could aid in the purification using immobilized metal affinity chromatography. The Histidine tag has an affinity for metals such an Ni^{2+} and Cu^{2+} which means that the protein of interest is retained within the chromatography column as the other proteins are removed. The bound peptides could then be eluted before removing the histidine tag using proteases. The inherent chaplin adhesion to other substrates rather than the binding to the column would be problematic as yields would be lower and TFA treatment would be required to remove the chaplin proteins.

Thiostrepton has been shown to have effects on the expression levels and mycelial pellet morphology [112]. Because thiostrepton can have an effect on the mycelial pellet, investigating alternative inducible promotor plasmids would be of interest to determine if chaplin expression can be improved. However, the life cycle of *Streptomycetes* are complex and mutant strains with several deletions and insertions may be required to fully facilitate the efficient expression of chaplin proteins into the supernatant.

5. The characterisation and corrosion resistance of a chaplin protein based biocomposite coating

5.1. Introduction

5.1.1. Corrosion Prevention Strategies

Due to the degradation of metallic substrates, various strategies have been employed to combat the prevalence of corrosion and to extend the life cycle of the substrate before repairs must be made. Techniques such as hot dip galvanisation, electro-plating and organic coatings are commonly used. The galvanisation of steel is achieved by submerging into a bath of molten zinc. This zinc layer provides a barrier between the corrosive ions and the steel which also sacrificially corrodes compared to the steel [119]. After corrosion of the zinc layer, a zinc oxide layer is formed and provides additional protection to the underlying substrate. The use of hot dip galvanization is considered to be one of the most effective techniques for the protection of steel. However, this particular technique is an expensive process due to the molten zinc which requires temperatures exceeding 450^{o}C. This elevated temperature carries an increased cost over organic coatings which do not require elevated temperatures for their application. The galvanisation of steel can lead to an increased operational downtime in comparison to organic coatings as galvanised material repair cannot be carried out *in situ*.

Another strategy that cannot be carried out *in situ* is electroplating. This corrosion prevention method is applied by controlled electrolysis to form a metal coating on top of another. This is achieved by submerging both an anode (the metal used for plating) and a cathode (the metal to be coated) which when an electrical current is applied, anions move towards the anode and cations travel to the cathode which then plate out on the surface. Different materials can be electroplated and chosen based on the desired properties required. One such material used in the electroplating process for corrosion resistance is hexavalent chromium. The chromium used is in a +6 oxidative state which is effective for corrosion resistance but is also carcinogenic especially when airborne and inhaled [120]. Use of this compound has now been heavily restricted in its use under REACH (Registration, Evaluation, Authorisation and Restriction of chemicals) legislation except in aerospace applications.

The use of hexavalent chromium has also been used as a surface pre-treatment and in coating formulations for corrosion resistance applications. Hexavalent chromium has been used extensively due to its high corrosion resistance across a range of pH and electrolyte concentration [121, 122]. Figure 48 gives an overview of how chromate interacts in response to its surrounding environment (i.e. defect formation) to protect the underlying substrate.

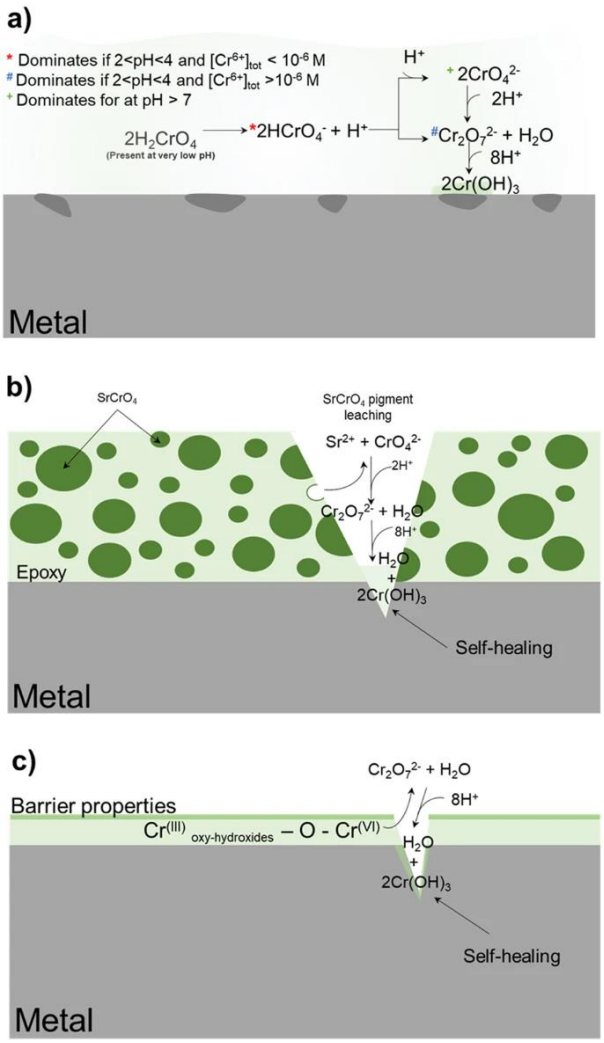

*Figure 48: Adapted from Gharbi et al[123]. illustration of chemical compositional changes for corrosion resistance when in solution(**a**), in the presence of a Sr-Cr-based primer(**b**) and a Cr(VI) conversion coating (**c**).*

Across these different pH's and electrolyte conditions, the hexavalent chromium is effective at both the anode and the cathode by restricting the metal dissolution rate at the anode and reducing the reduction rate at the cathode [121, 124, 125]. The strong corrosion resistance performance and the relatively low cost of hexavalent chromium makes the challenge of finding an effective alternative more difficult.

5.1.2. Biobased Corrosion Inhibition Technologies

The development and/or discovery of biobased corrosion inhibitors has been ongoing since the 1920's with an exponential trend in publications relating to green corrosion inhibitors [126]. Such publications have investigated the development of natural polymers, plant extracts and medicinal products [127-130]. Umeron et al was able to demonstrate the use of pectin extracted from apples as an effective corrosion inhibitor [130]. The inhibition increased as the pectin concentration and

temperature were increased. From the potentiodynamic polarization results obtained, the pectin was deemed to have a predominant effect at the cathode by adsorbing onto the steel surface [130].

The development of superhydrophobic coatings on mild steel is another approach to limiting corrosion. By forming a superhydrophobic substrate, this creates an effective barrier between the aggressive electrolytes and the surface. Research conducted by Cao et al developed a superhydrophobic topcoat composed of polybenzoxazine and amine-modified silica. This topcoat displayed interesting mechanical properties by resisting sandpaper abrasion and corrosion after submerging in a NaCl solution for 90 days [131].

The characterisation of newly developed technologies requires stringent testing to determine the performance capabilities. Coatings in general would be subjected to a series of tests depending on its required function [132]. Previous research has shown that chaplin proteins can exert some corrosion resistance on AZ31 and magnesium alloy [56]. As the proteins are amphiphilic, they have the ability to change the surface wettability of a substrate from hydrophilic to hydrophobic and vice versa. This feature may be the main reason for the observed increase in corrosion resistance as it would be interfering with the corrosion cell. The protein only material lacked the mechanical properties but *in vivo*, *Streptomyces* uses β-glucans and chaplin proteins to adhere to surfaces [28, 56]. With this information, the biocomposite containing chaplin proteins and β-glucan was developed to determine if the mechanical properties can be achieved whilst also being able to provide corrosion resistance.

5.1.3. Coating Analysis

Atomic force microscopy is an effective technique for the characterisation of nano structures and features. As well as measuring mechanical properties, images can be generated which can provide topography of the scanned area. This technique is advantageous over other imaging techniques as it can be used to provide information on conductivity, friction, adhesion and the Young's-modulus. The resolution of AFM can be sub-nanometre depending on the sensitivity of the equipment, relevant cantilever and tip used. The premise for AFM is how the charge of the substrate interferes with the tip and subsequently the cantilever. These nano scale changes are detected by a laser which is shone on the back of the cantilever. As the equipment is very sensitive, the external environment must be free of vibrations so that it does not interfere with the readings. AFM was used to analyse the different properties of the different coatings being deposited. From previous research, fibrils composed of chaplin proteins have been imaged using AFM but no information regarding the size and overall structure of the fibrils has been published when deposited as a biocomposite [36, 133]. It is hypothesised that the glycan addition allows for the formation of the chaplin proteins in solution rather than at the air-solvent interface, but it is unclear if the fibral length is altered by the glycan.

Corrosion is the electrochemical degradation of metals. Various approaches have been taken to reduce corrosion such as hot dip galvanisation, electroplating and coatings. All of which have their advantages and disadvantages. The environmental conditions play a significant factor in the rate in which corrosion occurs. This is due to the high salt and humidity content which accelerates the rate of corrosion.

The formation of amyloid fibres by amyloidogenic proteins, when solubilised in water, occurs at the hydrophilic-hydrophobic interface [36]. With the addition of a glycan, initiation of fibril formation of chaplin proteins into amyloid fibrils can also occur in solution [28, 118].

Cathodic disbondment occurs due to the formation of galvanic couples. Within this galvanic couple, the defect on the steel has a low potential and the steel-coating interface has a more positive potential. These areas of low potential and more positive potential forms the anode and the cathode, respectively. At the cathode, oxygen reduction occurs leading to disbondment of the coating from the substrate. This cathodic area advances away from the defect after the immersion in an aqueous electrolyte. Due to the differences in potential between the anode and the cathode, Scanning Kelvin Probe can be used to quantify the disbondment as the cathode advances under the coating.

5.2. Materials and Methods

5.2.1. β-glucan Selection

For protein and glucan biocomposite testing, two β-glucans were selected, Ethyl Cellulose (Sigma Aldrich) and Hydroxypropyl cellulose (Sigma Aldrich). A series of dilutions were created ranging from 100 µg/ml to 300 µg/ml. These were prepared as double strength to accommodate the dilution when mixed with equal strength chaplin protein extracts or chaplin protein synthetic peptides. For ethyl cellulose, dilutions were achieved using ethanol whereas ethanol and water were used as the diluent for hydroxypropyl cellulose, respectively.

5.2.2. Synthetic Peptide Design

Custom designed peptides, supplied by GeneCust, were based on *Streptomyces griseus* chaplin protein sequences after the cleavage of the signal peptide. The cleavage site was determined using an online signal peptide analyser known as SignalP. The sequences for each peptide after cleavage were synthesised and were provided as 1 mg freeze dried aliquots with varying purities. Table 5 provides the sequences and purity of each synthetic peptide.

Table 7: Designed synthetic peptide sequences with purity

Name	Sequence	Purity (%)
ChpE-Short	HGVATHSPGVASGNLAQVPVAVPVNVVGNTVNVVGLLNPAFGNLGLNH*	86.20
ChpE-+8	TGHSGADA HGVATHSPGVASGNLAQVPVAVPVNVVGNTVNVVGLLNPAFGNLGLNH*	85.04
ChpD	DSGAEAIAAHSPGVLSGNILQVPIHIPVNVCGNTVNVIGALNPAFGNTCVNK*	84.31
ChpG	DAGAQGLAAGSPGVASGNAVQVPVHVPVNLCGNTINVIGLLNPAFGNTCANVDAGHHDNGGYGYGR*	82.75
ChpH	DAGAQGAAIGSPGVLSGNVVQVPVHVPINVCGNTVSVIGLLNPAFGNTCVNA*	89.71

Due to the uncertainty of the cleavage site in Sgris-ChpE, two synthetic peptides were designed, ChpE-short and ChpE+8. These peptides were analysed by MALDI-TOF mass spectrometry to determine their respective m/z prior to the analysis of chaplin peptides extracted from *S. griseus.*

5.2.3. Solubilisation of Synthetic Peptides

To determine the solubility of each synthetic peptide, 500 µl of an appropriate solvent was added to the freeze-dried pellet to determine its suitability. The solvents tested were, ethanol, methanol, dimethyl sulfoxide (DMSO) and distilled water.

5.2.4. Substrate Preparation

For the preparation of non-metallic substrates, firstly the substrates were submerged into 100% acetone for 30 seconds before being removed and wiped with lint free wipes until dry. This was

repeated a total of three times then covered to reduce dust and debris contaminating the surface before deposition of coatings. gives an overview of the substrates tested. Substrate water contact angles were tested prior to deposit to ensure low water contact angles were observed.

Table 8: List of substrates used for the deposition of samples

Substrate
Glass Coverslips (hydrophilic)
Silica Wafer (hydrophobic) (Agar Scientific)
Unpolished Low carbon Steel (College of Engineering, Swansea University)
Polished Low carbon Steel
Titanate Wiped Polished low carbon Steel
PTFE (Hydrophobic)

For the preparation of metallic substrates, firstly coupons were mounted using a series of grinding and polishing was carried out to remove the oxide layer and create a uniform substrate. The initial grinding step (Grind – 1,Table 9) used a course sandpaper (P320) before using finer grades (P500 and P1000). Between the use of the finer grades of sandpaper, the coupon was rinsed for 30 seconds under water to remove any course particulates. After the grinding, the coupons were polished using DiaTwin Polycrystalline water-free diamond suspensions of decreasing size from 6 µm to 0.25 µm. The table provides an overview of the materials required in conjunction with the operating parameters of the automated polishing wheel (Buehler EcoMet250).

Table 9: Grinding and polishing conditions of mild steel

	Grind - 1	**Grind - 2**	**Grind - 3**	**Polish - 1**	**Polish - 2**	**Polish - 3**	**Polish - 4**
Surface	P320	P500	P1200	PT Seda[1]	PT Seda Blue[1]	PT Nap Cloth[1]	PT Nap Cloth[1]
Abrasive				6 micron poly[1]	3 micron poly[1]	1 micron poly[1]	0.25 micron poly[1]
Lubricant	Water	Water	Water	Oil based	Oil based	Oil based	Oil based
Force/specimen	40N	40N	40N	40N	35N	35N	35N
Platen RPM	300	300	300	150	150	150	150
Head RPM	150	150	150	150	150	150	150
Rotation	Comp	Comp	Comp	Comp	Comp	Comp	Contra
Time	0.5 - 1 min	0.5 - 1 min	0.5 - 1 min	3 - 4 mins	3 - 4 mins	1 min	1 min

[1] = Optimal Scientific

5.2.5. Sample Deposition

Deposition of protein only and biocomposite solutions were carried out by drop casting 100µl onto the relevant substrate. The substrate used was dependent on the analysis being carried out. Stock solutions of protein were made up fresh at double the required concentration and either diluted with equal parts of the relevant solvent or with equal parts of double concentrated glycan solution in the relevant solvent. gives an outline on the methodology for depositing the sample onto the substrate.

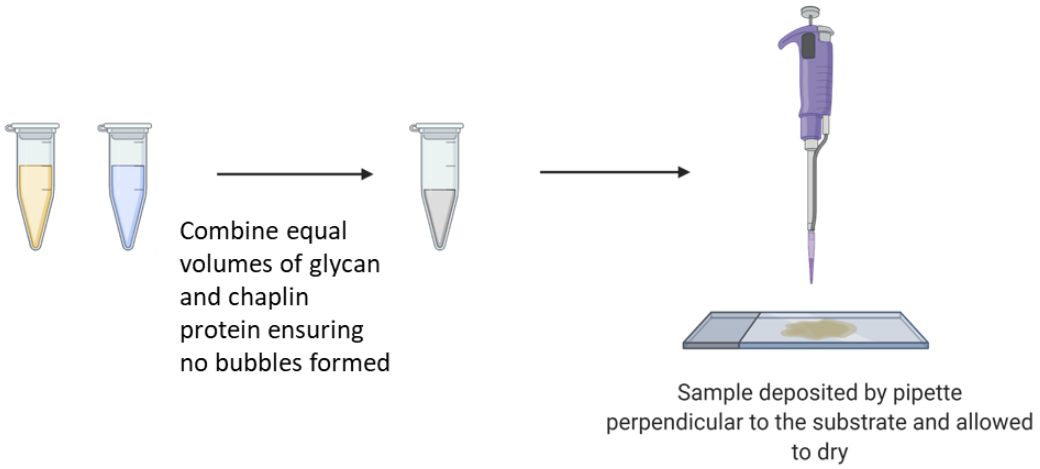

Figure 49: Sample preparation of biocomposite and drop casting method using a micropipette (Created using Biorender.com)

Ethanol based deposits spread naturally across the surface, unlike the water-based deposits. To spread the water-based deposits, a pipette tip was drawn through the deposit and onto areas of bare substrate until the solvent covered the required area.

5.2.6. Goniometer Measurements

Initial water contact angle (WCA) trials were carried out on glass microscope slides using conventionally extracted protein material from *S. griseus* as per previous research into protein only coatings [56]. A 3 µl droplet of de-ionised water was dispensed from the end of a flat needle and the stage was slowly raised, then lowered, to gently remove the water from the end of the syringe ().

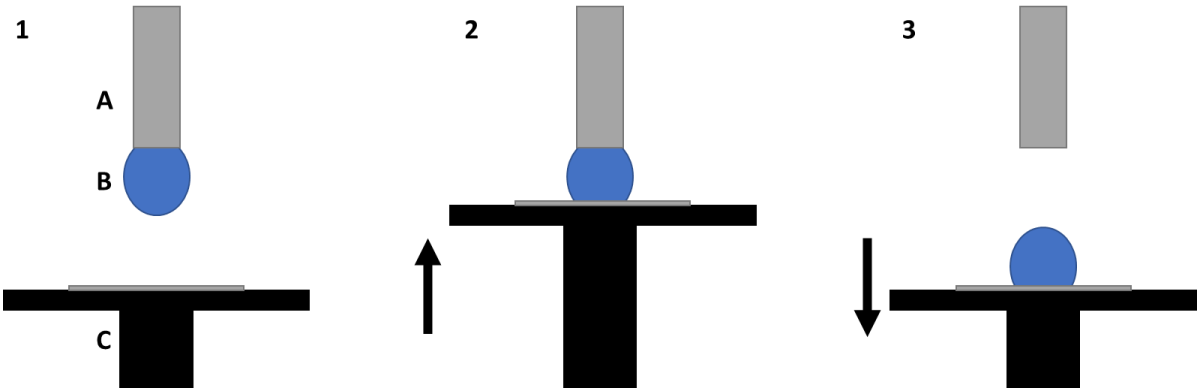

Figure 50: Stage movement for application of water droplet from goniometer needle. Needle (**A**), dispensed water (**B**) and Stage (**C**). Arrows indicate direction of stage movement

Contact angles for each drop were measured with the KRÜSS Drop Shape Analyzer™ software using a linear baseline and a sessile drop (Laplace-Young) curve fit immediately following deposition. A single contact angle for each deposit was determined by averaging the replicate contact angles and taking the standard deviation. Water contact angles for 3 drops were recorded for each deposit.

5.2.7. Atomic Force Microscopy

Deposits of chaplins were at a final concentration of 150 µg/ml and biocomposite deposits were at a final concentration of peptide at 150 µg/ml with a final concentration of HPC at 100 µg/ml (as determined in Figure 56). Atomic force microscopy was used to image and obtain the elastic modulus of synthetic peptide-based deposits and biocomposites on various substrates. Samples were analysed using a BioScope Catalyst (Bruker Instruments, USA), in water, and using Novascan colloidal probes, with a spring constant of 0.03 N/m and a borosilicate spheric probe of 20 µm diameter. 100 force curves equally spaced were acquired in a 100 µm x 100 µm are for each sample, with an applied force of 10 nN and a rate of 1 Hz. The approach part in the contact regime of each force was fitted with the Hertz model using the dedicated function of the Nanoscope Analysis software v 1.50:

Equation 4: Hertz model. E is the elastic modulus, v is the Poisson ratio (0.5), R is the ratio of the indenter, δ is the indentation depth.

$$F = \frac{4E\sqrt{R}\,\delta^{3/2}}{3\,(1-\upsilon^2)}$$

Atomic force microscopy (AFM) was performed using a JPK NanoWizard III instrument to produce nano-scale topographical measurements of the sample surface. Scans were performed in alternating contact (AC) mode over a 5 x 5 µm area at a resolution of 512 x 512 pixels. A gold-coated silicon supersharp cantilever (SHR150 provided by afm-probes.apexprobes.uk) was used to scan the sample

surface in the resonant frequency of 150 KHz with a force constant of 5 N/m. The scanning images were processed using Gwyddion software (Version 2.55) and the false colour maps presented represent the topography of the sample surface.

5.2.8. Scanning Electron Microscopy

Deposited samples were imaged using scanning electron microscopy. Samples were prepared in the same way as mentioned in section 0 on a variety of conductive substrates.

Coated substrates were made by drop casting solutions of chaplin proteins and/or biocomposite onto steel coupons with dimensions of 2 cm by 2 cm and allowed to dry at room temperature for 24 hours before imaging. Voltage of electron beam was set at 10 kV.

5.2.9. Corrosion Testing

Corrosion testing was carried out using qualitative and quantitative methods to determine the level of corrosion resistance. Initial testing was carried out by setting up the coated samples into Stratmann cells similar to Wint et al [134]. Stratmann cells were built by applying low tack scotch™ tape horizontally at the top of the coupon, covering ~15mm from the top of the coupon. This was followed by applying insulating tape (RS components) vertically on both the left and right side of the coupon while exposing roughly a two-centimetre strip of substrate in the middle. A 15.5% (w/v) Poly(vinyl butyral-co-vinyl alcohol-co-vinyl acetate) (PVB) (Sigma Aldrich, #418439) was prepared in 100% ethanol by gentle heating and mixing. PVB powder was slowly added to ensure thorough solubilisation and dispersion. Once in solution, gas bubbles contained within the viscous PVB solution were removed by applying vacuum. The vacuum was released once no visible bubble were being drawn from solution. The PVB solution was then applied to the Stratmann by using a cylindrical glass rod. Once the PVB layer was dry, the low tack tape was carefully peeled until almost removed. A well was made by applying a wall of RS™ non-corrosive silicon rubber (RS494-118) which held the electrolyte in place. gives a representation of the Stratmann cell and how the PVB layer was applied.

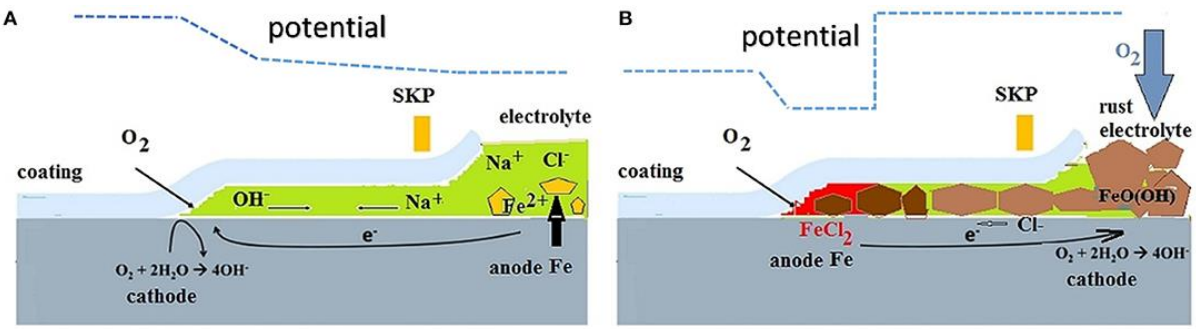

Figure 51: Cathodic delamination (**A**) and anodic undermining (**B**) galvanic cells and potential distributions along the interface[135]

These cells were then placed within a chamber with a controlled relative humidity using reservoirs of 0.86M NaCl solution. 0.86M NaCl was then added to the electrolyte reservoir formed by the non-corrosion silicon rubber and low tack tape and then left at room temperature for 24 hours. The delamination of the PVB was recorded and imaged.

5.2.10. HCl Chamber test

To test the performance of the material against corrosive vapour, a 20% HCl solution contained within an open top container was placed inside of a glass staining chamber then sealed with a lid and malleable plastic tape (Parafilm™). The chambre was equilibrated with the vapour from the solution for 1 hour. Steel coupons with and without coatings were then placed within the chamber and imaged every hour to determine the corrosion resistance.

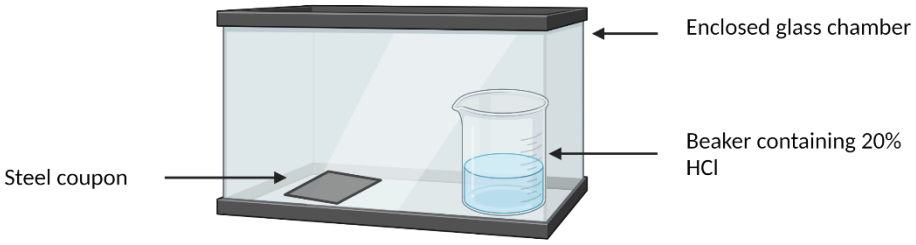

Figure 52: HCl Fuming chamber set up for exposure of coated and uncoated steel coupons (Created using BioRender.com)

5.3. Results

5.3.1. Determining the Solubility of Synthetic Peptides

Ethanol, methanol and DMSO was used to determine the solubility of each of the synthetic peptides. The solubility was visually inspected then deemed soluble or insoluble based on the presence of a pellet. The solubility of each synthetic peptide is summarised in Table 10.

Table 10: Summary of the solubility of each synthetic peptide in a range of solvents. '+' indicates soluble and '-' indicates insoluble.

	ChpD	ChpE-short	ChpE+8	ChpG	ChpH
Distilled water	-	+	+	+	+
Ethanol	-	-	-	-	-
Methanol	-	-	-	-	-
DMSO	+	+	+	+	+

When water was added to the synthetic peptides, ChpD was the only synthetic peptide which did not solubilise. The freeze-dried pellet of the ChpD appeared to go into suspension rather than solubilise. All other synthetic peptides were fully soluble in water. All synthetic chaplins did not solubilise when ethanol or methanol was added. When DMSO was used as the solubilising solvent, all synthetic chaplins solubilised.

5.3.2. Composition, Ratio and Concentration Determined for Protein and Glycan Biocomposite using Synthetic Peptides

The synthetic peptides synthesised by GeneCust were designed to reduce the overall time from growth of *S. griseus* to extraction. Although time was a factor, the synthetic peptides did not contain residual Trifluoroacetic acid, co-extract peptides and cell wall fragments like conventionally extracted chaplin proteins. Eliminating these contaminates meant that a true reflection of chaplin proteins performance could be det

ermined. Firstly, the composition of chaplin proteins within each deposit was investigated to determine where high water contact angle could be achieved. Deposits were composed of either each individual chaplin protein or a mixture containing 2 or 3 chaplin proteins. Synthetic chaplin peptides were dissolved in distilled water and deposited onto glass coverslips with an area of 4 cm^2 at a final concentration of 150 µg/ml as determined from Alex Harolds research[56].

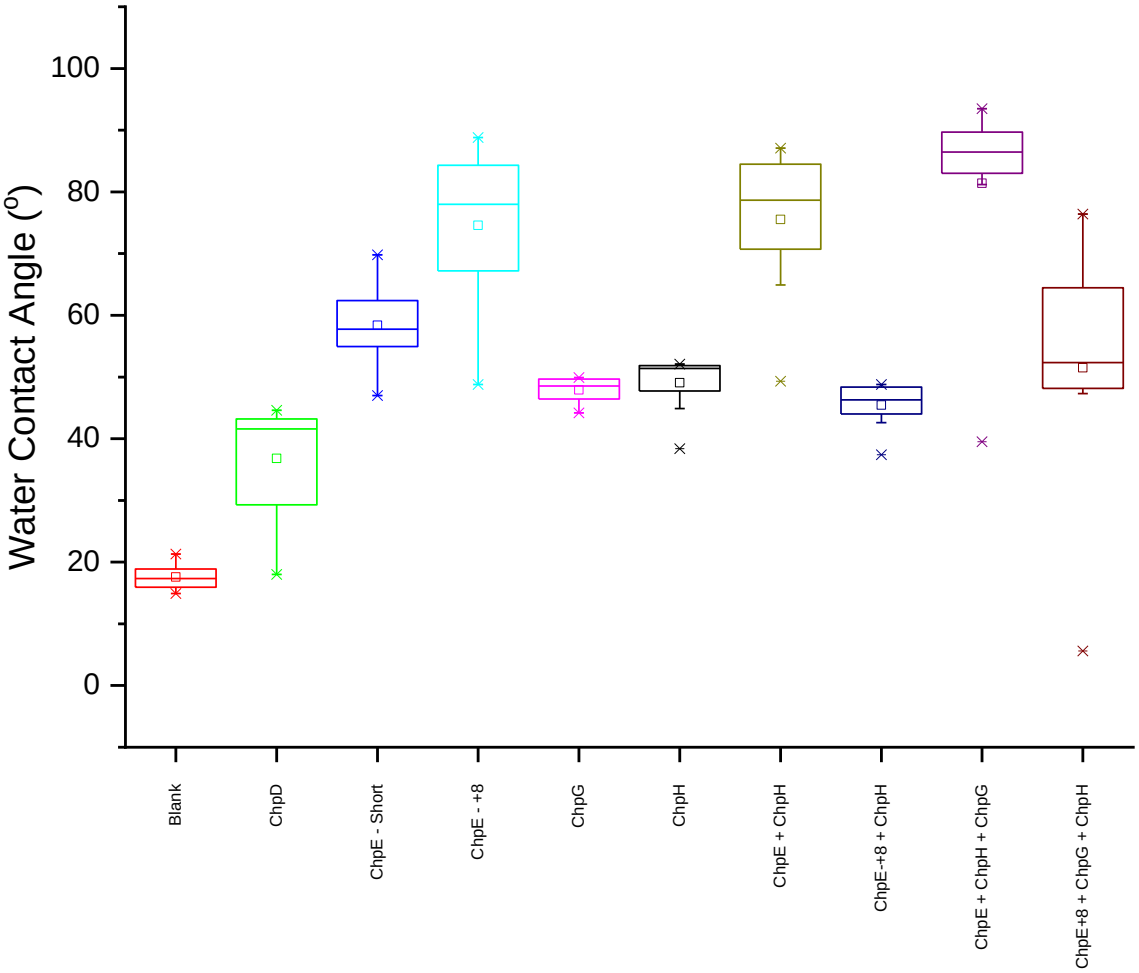

Figure 53: Water contact angle measurements for coatings composed of either 1, 2 or 3 synthetic chaplin proteins with a final concentration of 150 µg/ml (n=9).

Bare substrate was used as a negative control which had an average water contact angle of 17.4° (Figure 53 Blank). When a sample containing one peptide was applied, an increase in the water contact was observed. All samples successfully went into solution in water except for ChpD. The ChpD had the smallest increase over the control with an average increase in water contact angle of 16.0°. The water contact angle observed for ChpE-short showed an increase of 42.2° over the control. The average water contact angle measurement for the ChpE+8 was increased over the control and the ChpE-short, but higher variance was recorded. ChpG and ChpH had a similar water contact angle increase over the control with average increases of 30.5° and 31.7°. ChpE+8 had the greatest increase in water contact angle over the control. The purpose of mixing chaplin proteins together was to determine if water contact angles could be increase in comparison to the individual chaplin protein deposits. ChpH was added in equal parts to both ChpE-short and ChpE+8 to a final concentration of 150 µg/ml after which the mixture was then deposited onto the coverslips. A further increase in the average water contact angle was observed for the protein-only sample composed of both ChpE-short

and ChpH (15.9°) when compared to the ChpE-short individual deposit. A decrease of 29.1° was observed when comparison to the ChpE+8 individual deposit was observed when ChpH was added to ChpE+8. ChpE-short with the addition of ChpG and ChpH provided the highest water contact angles across all the samples tested with an average WCA increase over the control of 64.0°. A water contact angle of 57.7° was observed for the deposit which contained ChpE+8, ChpG and ChpH. The value was a slight increase in comparison to the ChpE+8 with ChpH deposit, but still higher that the negative control. The change in water contact angle from the deposition of multiple layers has been investigated previously, where further increases in water contact angles can be achieved [57]. Therefore, additional layers were added to determine if synthetic *S. griseus* chaplin deposits behaved in a similar manner (Figure 54).

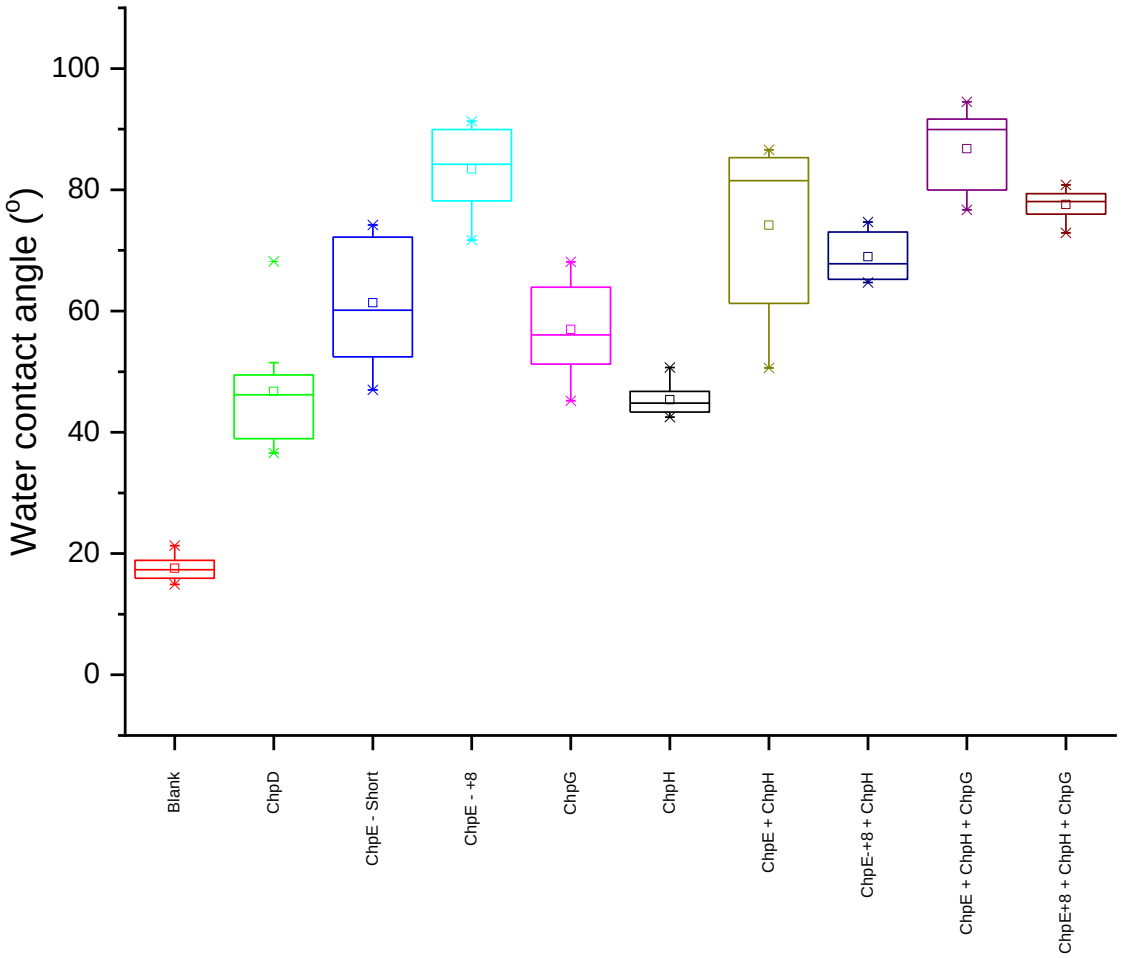

Figure 54: Water contact angle for double deposit for deposits containing either 1, 2 or 3 different chaplin proteins (n=9)

The average water contact angles measured for the double layer of ChpD was 46.8° (Figure 54 ChpD) but with only a slight increase over the single layer (15.5°) (ChpD). ChpE-short water contact angles had an average water contact angle of 61.4° when a second layer was deposited. The double layer of

ChpE+8 had an average water contact angle of 83.4^{O}, which was higher that the single layer average. Importantly, a reduction in variance in observed WCAs was seen. A marginal increase in the water contact angle was observed for the double layer over the single layer deposit for ChpG (52.22^{o}) but an increase in variance was recorded. A double layer of ChpH (Figure 54 ChpH) caused the water contact angle to reduce by 4^{o} in comparison to the ChpH single layer (Figure 53 ChpH).

The results obtained for the double layer (Figure 54) were similar to that of the single layer (Figure 53) except for ChpE+8 with ChpH and ChpE+8 containing both ChpG and ChpH. The ChpE+8 with ChpH double layer had an average water contact angle of 68.9^{o} but the highest average water contact angle observed was the ChpE-short containing ChpG and ChpH with an average of 86.8^{o}.

In summary, the single layer sample of ChpE-short containing ChpG and ChpH provided the highest water contact angle across the single- and double-layer results with low variance in comparison to the other samples measured. This sample mixture was used for subsequent testing.

5.3.3. Biocomposite ratio analysis using synthetic peptide

Due to the inability for the synthetic peptides to be solubilised in ethanol, the use of ethyl cellulose as a counter part was not viable so an alternative glycan was investigated. An alternative glycan that was of interest was hydroxypropylcellulose (HPC). This glycan has the ability to be solubilised in either water or ethanol. The ability to be soluble in both solvents allowed for the glycan to be used in conjunction with extracted material for the material characterisation studies on steel. To determine the optimal ratio of peptide to glycan, a series of coverslips with an area of 4cm^2 were coated with a mixture of the previously identified protein mixture and hydroxypropyl cellulose with a final combined concentration of 150 µg/ml dissolved in distilled water. Water contact angles were then recorded for each sample (Figure 55).

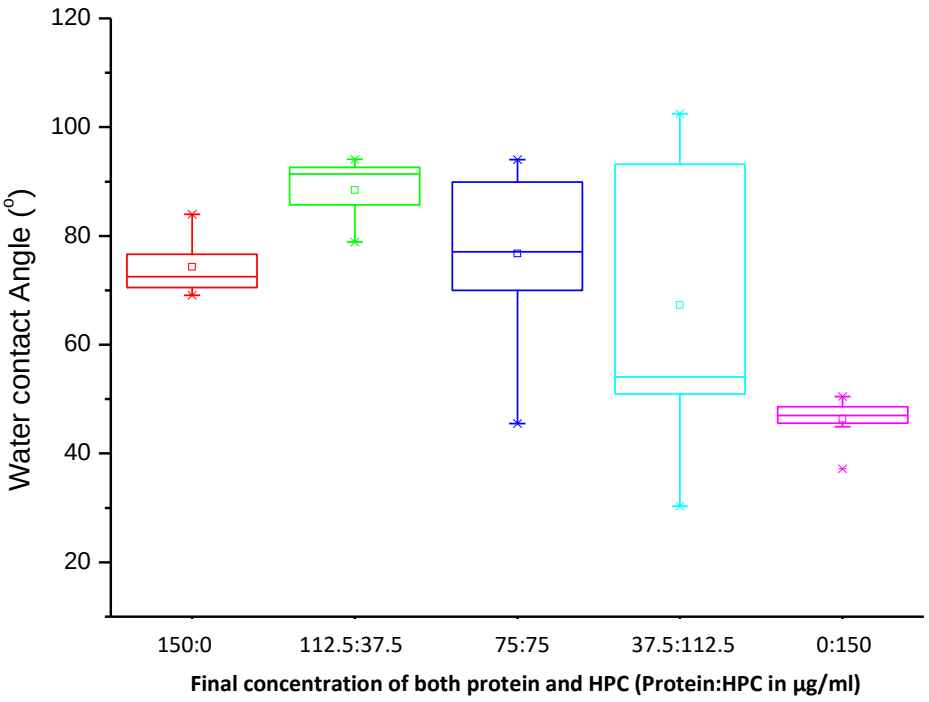

Figure 55: Water contact angle measurements of differing concentrations of both protein and glycan (HPC), where the total concentration remained at 150 µg/ml (n=9)

As a control, the peptide-only sample containing chaplins E, G and H were used, which gave an average water contact angle of 74.05°. The introduction of the glycan at a ratio of 3:1 (Figure 55, 112.5:37.5) had an average water contact angle of 88.4°, which was an increase over the peptide-only control by 14.1°. As the glycan level was increased and the peptide level was decreased, the water contact angle became more variable (Figure 55, 75:75). This was further exaggerated in the 1:3 ratio sample (Figure 55, 37.5:112.5). When the sample contained 100% glycan, the variance was reduced but there was a dramatic decrease in the average water contact angle (Figure 55, 0:150) when compared to the protein only.

Upon visual examination of the coatings after the water droplet used for measuring the water contact angle was blotted and dried, areas where the measurements were taken did not appear to contain any coating.

5.3.4. Glycan Addition to Optimised Peptide Concentration

Previously, the ratio of peptide-to-glycan was investigated (Figure 55). Here an increasing amount of glycan was added to a fixed peptide concentration (Figure 56) to determine if the water contact angle can be increased when compared to a protein only deposit.

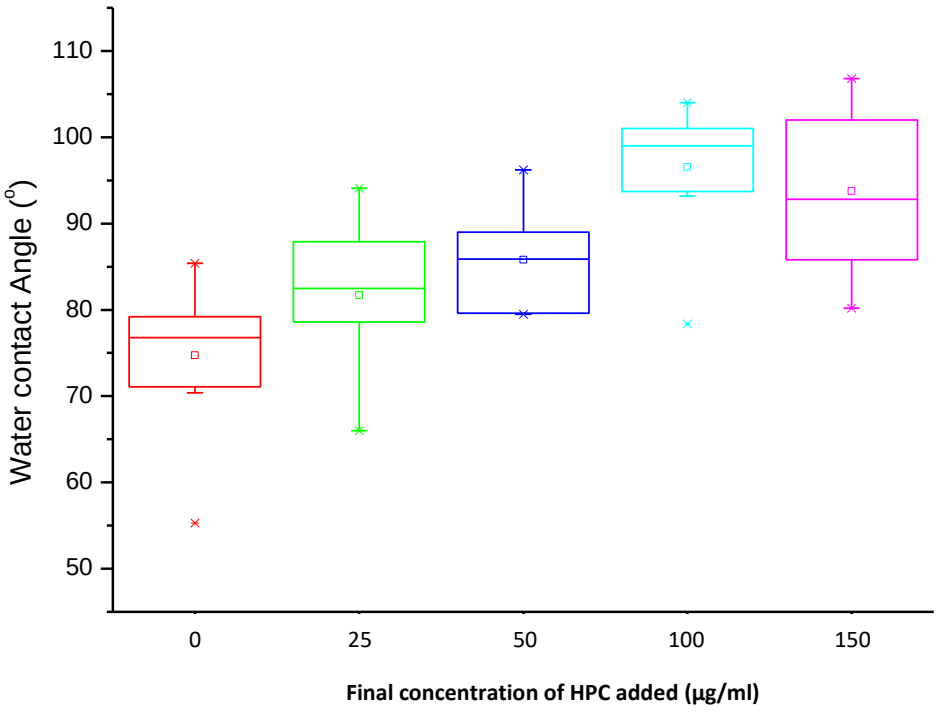

Figure 56: Water contact angle measurements of deposits containing increasing amounts of glycan (HPC) when the chaplin protein (ChpE-short containing ChpG and ChpH) concentration kept at 150 µg/ml

Concentrations of stock solutions for both the glycan and the peptide were prepared at double strength in water and combined at a 1:1 ratio. 100µl of the mixture was deposited and spread onto 4cm^2 glass cover slips. The ChpE containing ChpG and ChpH control had an average water contact angle of 74.3°. A final concentration of 25 µg/ml of HPC with peptide caused an increase in the water contact angle over the protein-only but there was also a large increase in the variance (Figure 56, 25 µg/ml). When the glycan amount was increased to 50 µg/ml, the water contact angle remained similar to the mixture of peptides and 25 µg/ml glycan concentration sample, but the variance was reduced (Figure 56, 50 µg/ml). When the HPC concentration was increased to 100 µg/ml, the average water contact angle was increased to 96.5° (Figure 56, 100 µg/ml). Further increases in the HPC concentration to 150 µg/ml of glycan led to a reduction in the average water contact angle (93.7°) and an increase in the variance.

In summary, the peptide sample composed of ChpE-short containing ChpG and ChpH, at a final concentration of 150 µg/ml with HPC at a final concentration of 100 µg/ml, gave the highest WCA, and was subsequently used for all future biocomposite testing.

5.3.5. Biocomposite Optimisation using *S. griseus* Extracted Chaplins on Glass

The purpose of this experiment was to determine the effects of different β-glucans at different concentration (Ethyl Cellulose or Hydroxypropyl cellulose). Ethylcellulose (EC) or hydroxypropyl cellulose (HPC) was solubilised in ethanol at 100 µg/ml, 200 µg/ml and 300 µg/ml. These β-glucan concentrations were mixed in equal volume with 300 µg/ml of chaplin extract. 100 µl of the mixture was deposited onto 2x2 cm acetone washed glass coverslips. Chaplin only and β-glucan only were mixed in equal volume with ethanol and 100 µl were deposited at a final concentration of 150 µg/ml. Water contact angle measurement were recorded for each.

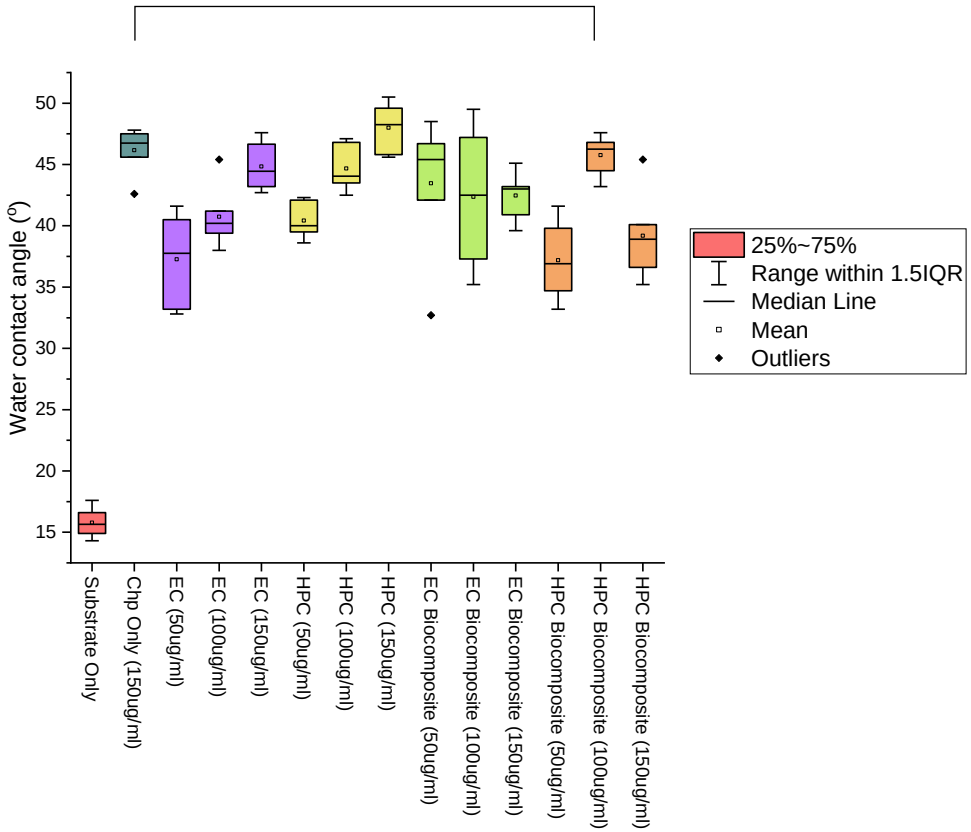

Figure 57: Water contact angle measurements for biocomposite formulation optimisation of chaplin proteins extracted from *S. griseus.* Substrate only (Red), Ethyl cellulose only (EC) (Purple), Hydroxypropyl cellulose only (HPC) (Yellow), Ethyl cellulose biocomposite (Green) and Hydroxypropyl cellulose biocomposite (HPC) (Orange). Mann-Whitney U Test p=0.631.

Figure 57 shows that the average water contact angle for the substrate-only control was 15.7°. Coatings resulting from deposits of the protein-only control at a concentration of 150 µg/ml had an average water contact angle of 46.1°. As the ethyl cellulose (EC) only control concentration was

increased from 50 µg/ml to 150 µg/ml, an increase in the water contact angle was observed. The average water contact angle 150 µg/ml with an average of 44.8° (Figure 57 Purple). Hydroxypropyl cellulose (HPC) followed a similar trend to the EC and increased with the increase in concentration (Figure 57 Yellow). An average water contact angle of 48° was recorded for the 150 µg/ml deposit of HPC. The biocomposite was formulated with chaplin proteins extracted from *S. griseus* and mixed with ethyl cellulose before depositing onto glass cover slips. At 50 µg/ml of EC within the biocomposite formulation, an average of 43.6° was recorded. When the concentration of ethyl cellulose was increased to 100 µg/ml, there was a minor decrease in the average (42.3°) however the variance was substantial (Figure 57 Green). At 150 µg/ml of ethyl cellulose, the average was similar (42.6°) to 100µg/ml but the variance was reduced. For HPC biocomposites (Figure 57, Orange), the addition of the β-glucan at 50 µg/ml, reduced the water contact angle in comparison to the protein only control and HPC only samples. The 100 µg/ml however had a similar average water contact angle to both the protein only and the β-glucan only. A reduction in the water contact angle was observed for samples containing 150 µg/ml of HPC when compared to the protein only sample (Figure 57, Blue).

5.3.6. Synthetic Peptide Performance on Unpolished Low Carbon Steel

The water contact angle of unpolished steel was measured by goniometry with and without the presence of synthetic peptide-based deposits (Figure 58).

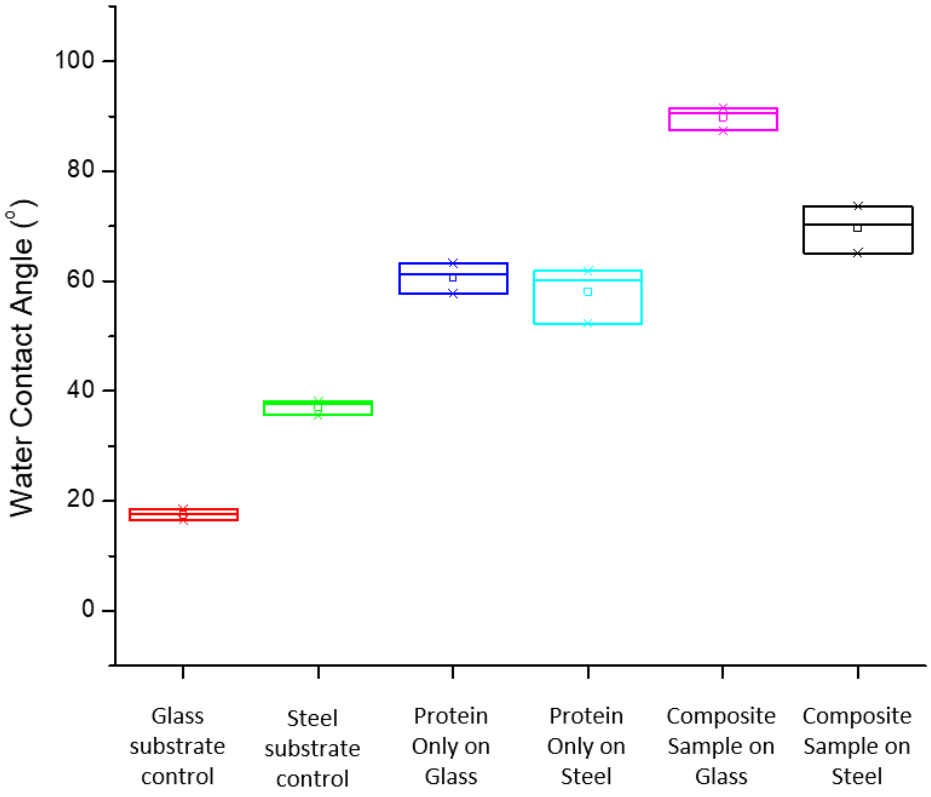

Figure 58: Water contact angle measurements on glass and low carbon steel substrates using synthetic peptide only and synthetic peptide biocomposite deposits.

Water contact angles on the low carbon steel substrate did yield slight improvements after the protein only deposit. The increase in the water contact angle was not as great as the protein only on the glass substrate. The water contact angles from the glass and low carbon steel substrates increased after the introduction of the biocomposite.

5.3.7. Protein and Biocomposite Coating Morphology on Low Carbon Steel

This section investigates the morphology of the ChpE-short containing ChpG and ChpH and biocomposite coatings on steel substrates using a Scanning Electron Microscopy (SEM). The use of SEM as an initial investigative tool was chosen as the coatings could be imaged on a single substrate and would be able to determine how the coating is deposited on the surface unlike transmission electron microscopy which images by transmitting electrons through the specimen. The use of TEM would not give an accurate depiction of how the protein and glycan would behave as a coating. Metal coupons are normally ground and polished to remove the oxide layer before coatings are applied [136]. The removal of the oxide layer also affects a change in water contact angle of the metal substrate.

From the biocomposite optimisation water contact angle measurements (Figure 56), 150 µg/ml of chaplin protein with 100 µg/ml of HPC was deposited onto glass coverslips before carrying out sputter coating. The addition of the platinum layer allows for the sample to become conductive and for features on the substrate to be visualised. From the imaging of the protein only and biocomposite samples, no observable features were found. To alleviate this issue, alternative substrates were used to visualise the deposits.

To visualise and image the morphology of the protein only coating and biocomposite coating, protein only (ChpE-short containing ChpG and ChpH), Glycan only and biocomposite (ChpE-short containing ChpG and ChpH with glycan addition) were deposited onto unpolished low carbon steel as the oxide layer would be able to limit corrosion during the drop casting of the water-solubilised biomaterials. As the substrate was conductive and a contrast was achieved, a sputter coating of a conductive element such as platinum was not required.

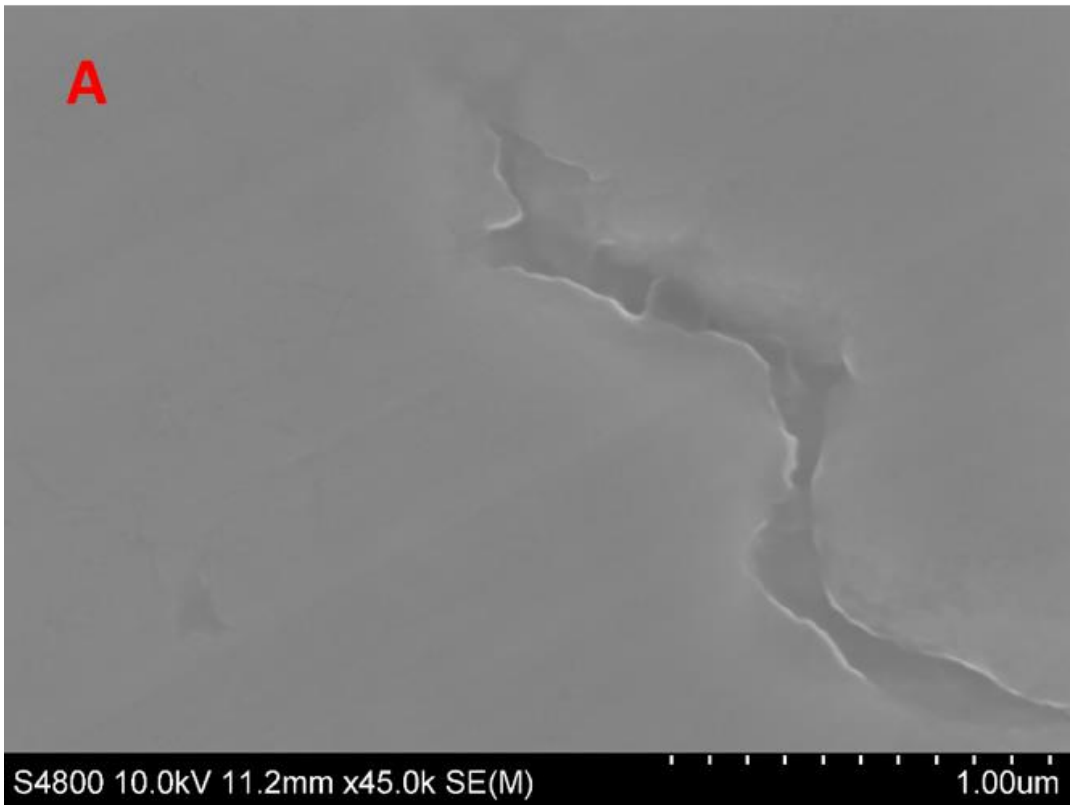

Figure 59: Scanning electron micrograph of low carbon steel showing an almost featureless surface. A defect was observed on the substrate surface. Magnification = 45,000x, Scale bar = 1 µm.

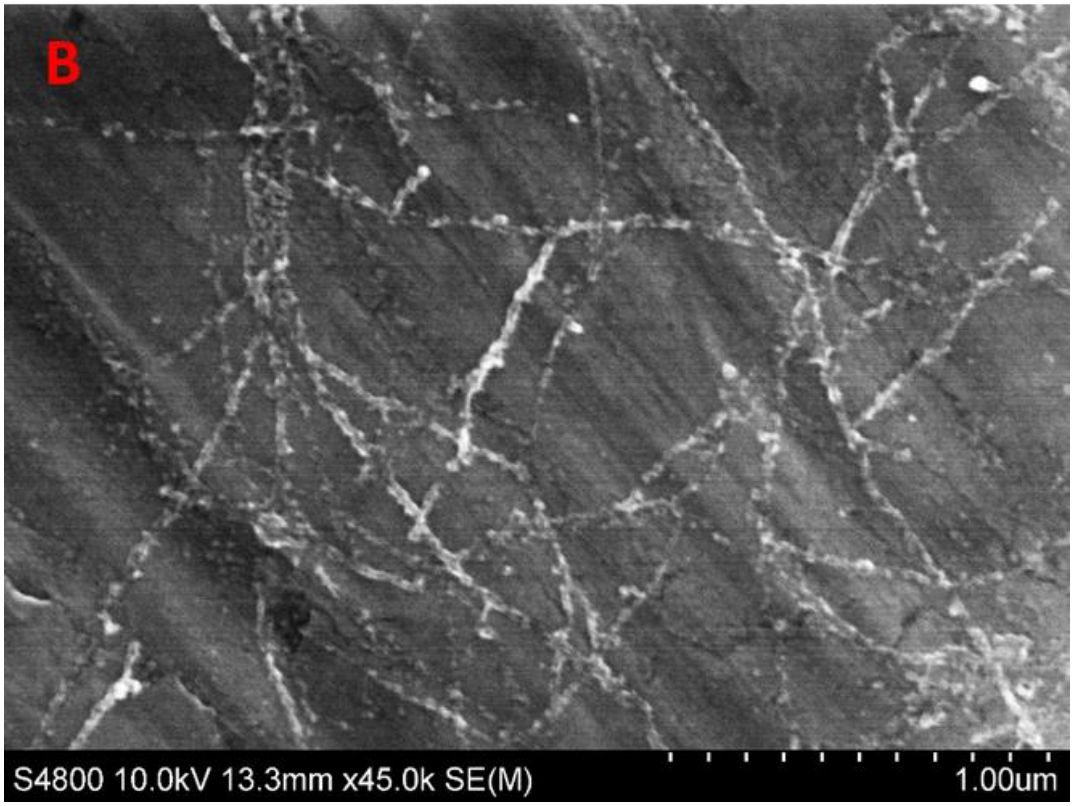

Figure 60: Scanning electron micrograph showing the distinctive amyloid fibrils formed from a protein only deposit. Magnification x45,000. Scale Bar = 1 µm

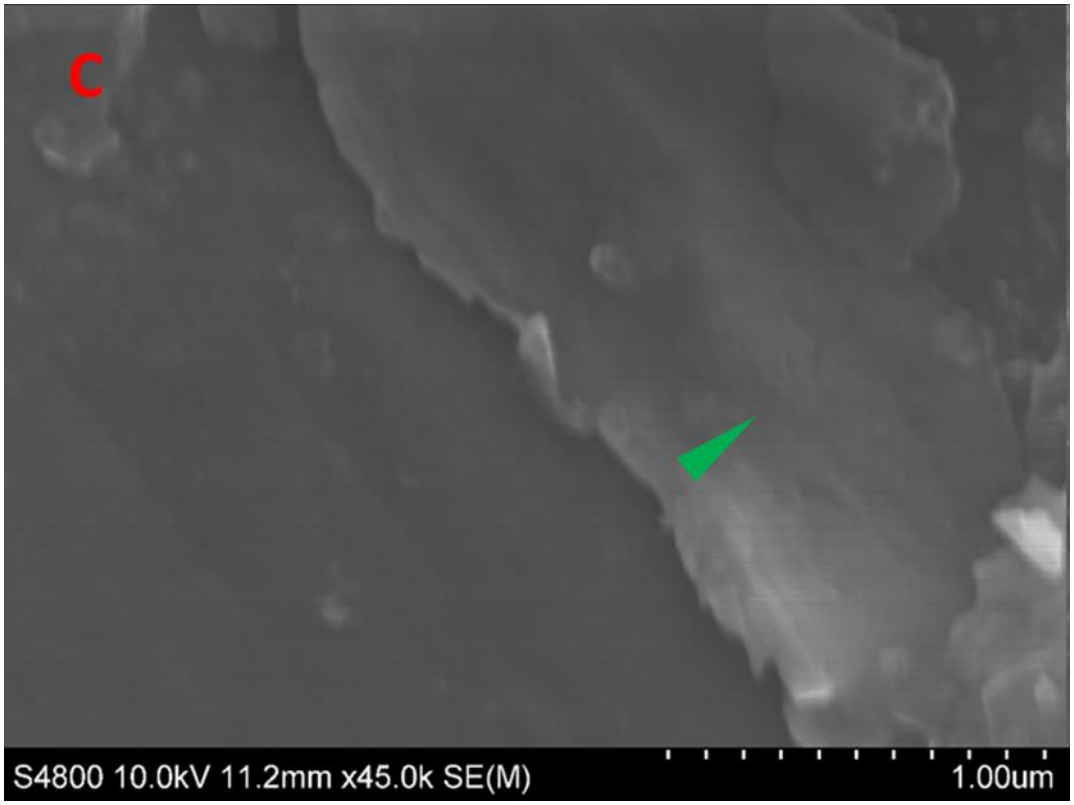

Figure 61: Scanning electron micrograph showing platelet like structures formed by a glycan only coating. Pinpointed by the green arrow. Magnification = 45,000x, Scale = 1 µm.

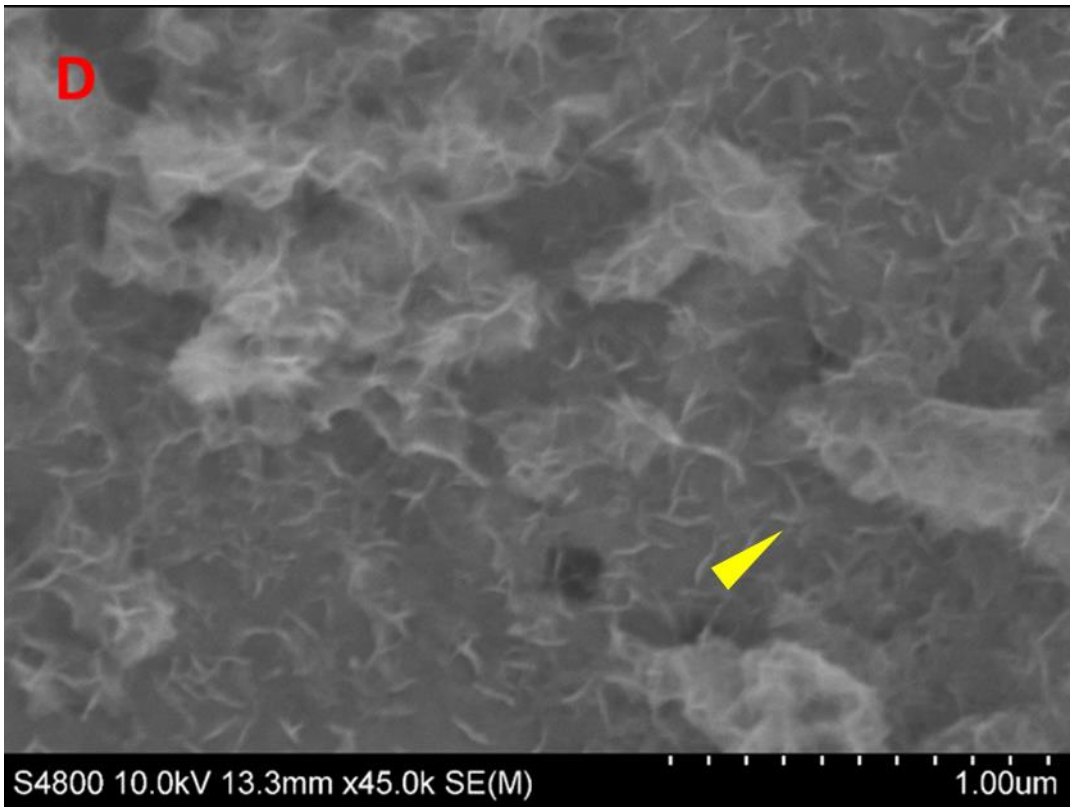

Figure 62: Scanning electron micrograph of metal surface after deposition of biocomposite coating showing numerous small fibre like features highlight by the yellow arrow.. Magnification = 45,000x, Scale = 1 µm

The SEM micrograph of unpolished steel (Figure 59), indicates a mostly smooth surface topography of the protective oxide layer, except for the area with a defect. Figure 60 shows the fibrillar topography of a single deposit of a mixture of three Chp peptides that is typical of amyloid proteins and peptides. On the glycan only (Figure 61) deposit, 'flakes' of material (Green) were observed. On observation of the biocomposite (Figure 62), small fibre like structures were evident (yellow) across the substrate.

As the amyloid fibrils were identified from the combined peptide deposit using synthetic peptides (Figure 60), extracted proteins from *S. griseus* were deposited to determine if the amyloid fibrils could be identified as part of a single, double or triple deposit. The substrate was prepared by manually polishing coupons with a series of increasing grit paper before being viewed at magnifications of x350 and x7,000. Due to conductive nature of the substrate, sputter coating was not carried out.

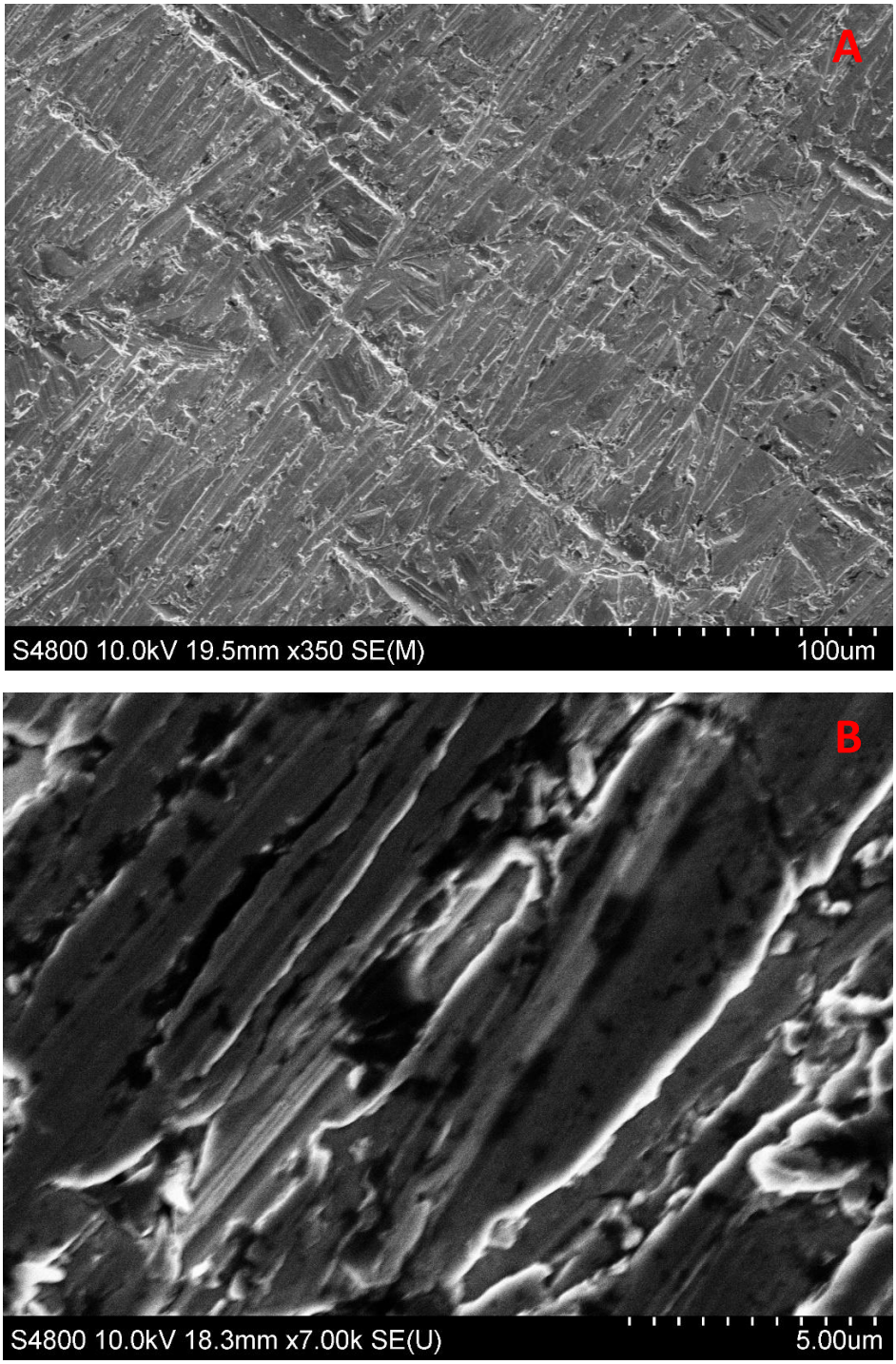

*Figure 63: Scanning Electron Micrograph of polished steel substrate showing striations from the polishing process at magnifications of x350 (**A**, Scale Bar = 100 µm) and x7,000 (**B**, Scale bar = 5 µm).*

Figure 63A and B shows a series of scratch-like defects caused by the polishing process which were observed across both magnifications. Steel coupons used for biomaterial deposits were prepared using the same process.

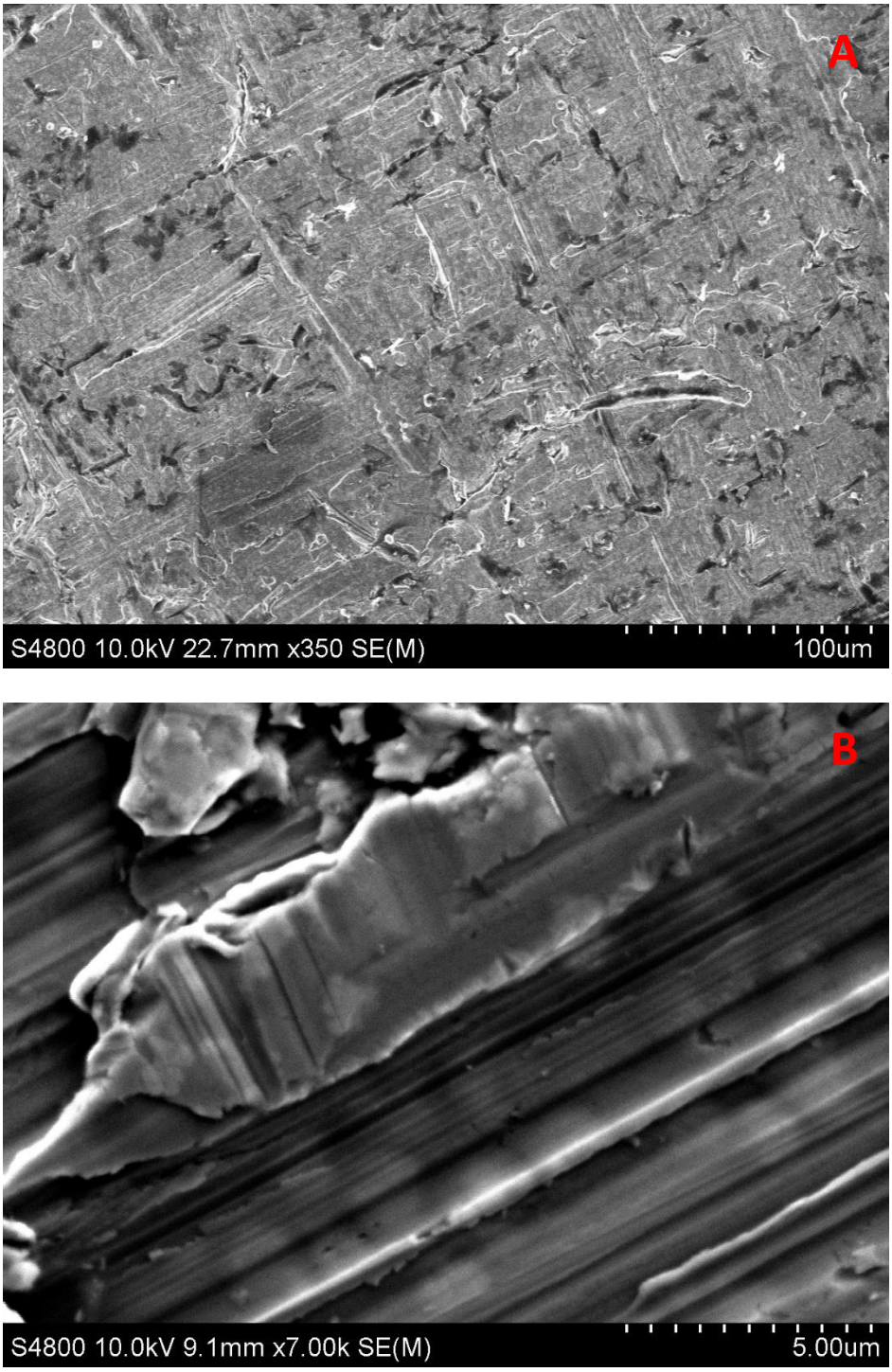

Figure 64: Scanning electron micrograph after a single deposit of HPC at 100 µg/ml. Scratch marks still present not as apparent when compared to Figure 63. Magnifications of x350 (**A**, Scale Bar = 100µm) and x7,000 (**B**, Scale bar = 5 µm).

After a single deposit of HPC, imaging at low magnification (Figure 64A) also identified scratch-like features, however they appeared to be less prominent in comparison to the control (Figure 63A & B). At the higher magnification (Figure 64B), the striations appeared similar to the bare substrate control at the same magnification (Figure 63A). A further deposit of HPC was added and re-imaged.

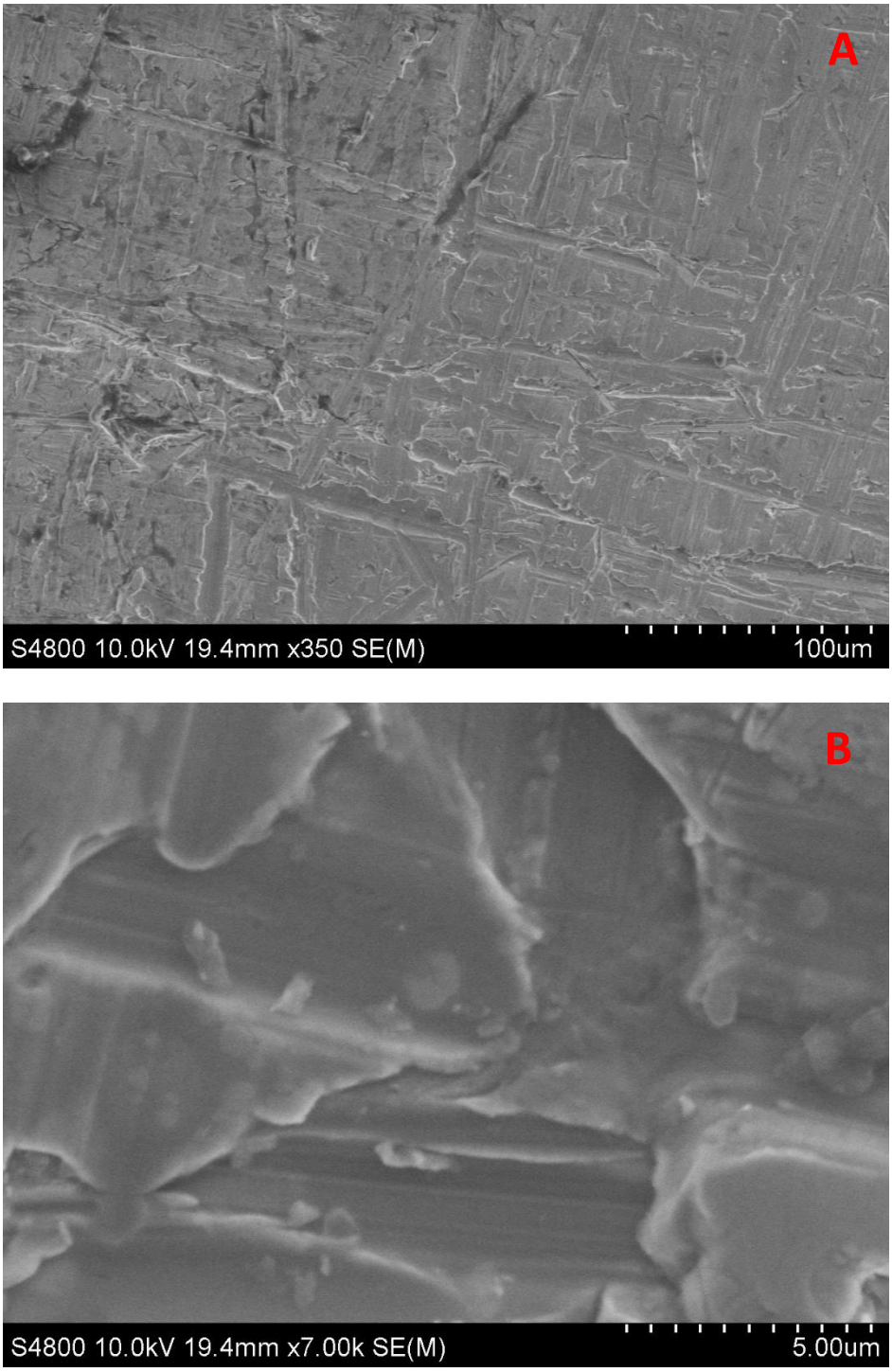

Figure 65: Electron micrographs of polished steel substrate with a double deposit of HPC at 100 µg/ml. Scratches appear less distinctive in comparison to the control. Magnifications of x350 (**A**, Scale Bar = 100µm) and x7,000 (**B**, Scale bar = 5 µm).

The striations, at both magnifications, became less pronounced after a double deposit of HPC (*Figure 65*A & B). A further deposit of HPC was added to the double deposit to determine if a cumulative effect could be achieved.

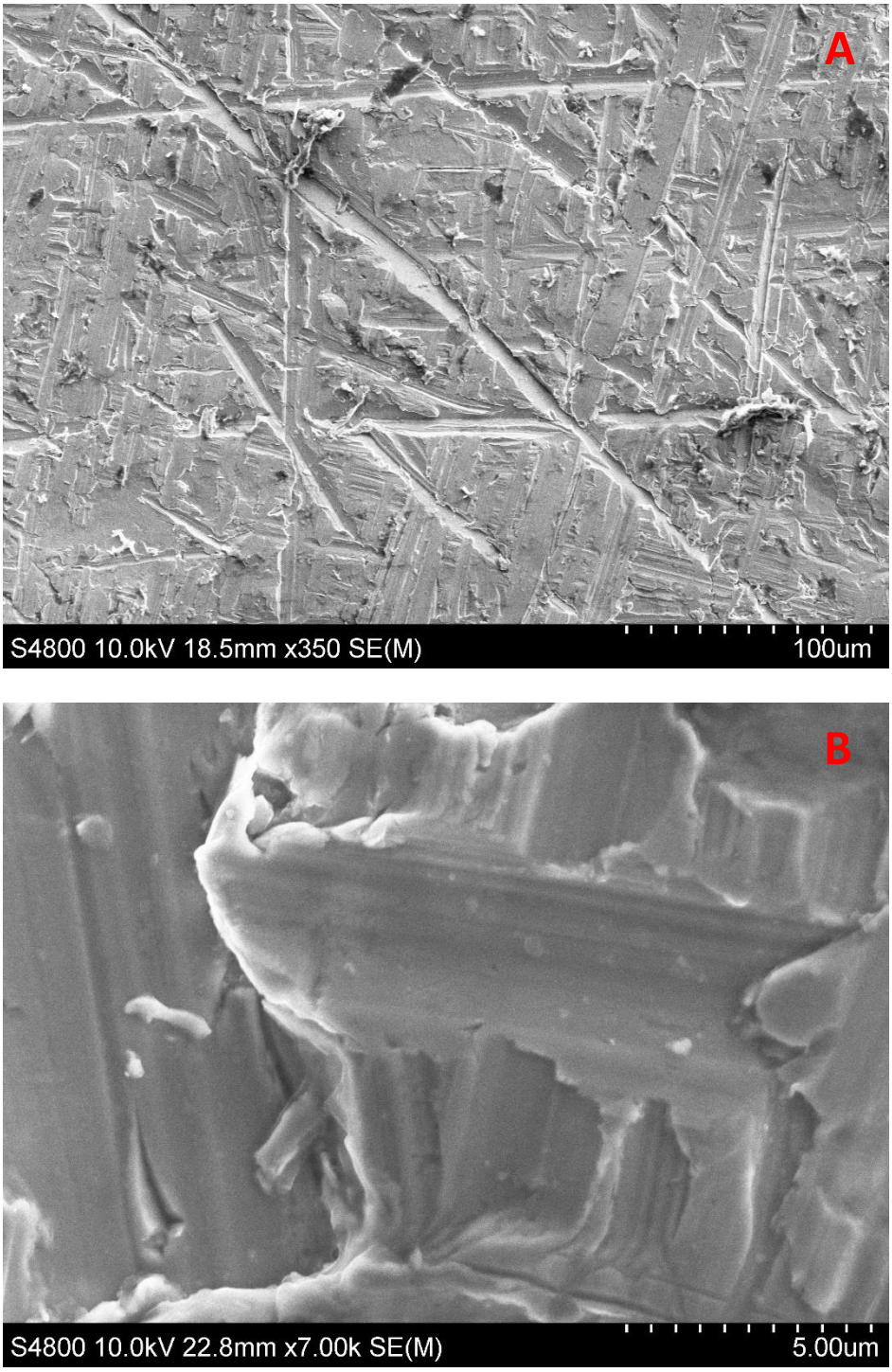

Figure 66: Electron micrographs of polished steel substrate with a triple deposit of HPC at 100 µg/ml. Striations still evident after a third deposit. Magnifications of x350 (**A**, Scale Bar = 100µm) and x7,000 (**B**, Scale bar = 5 µm).

The blanketing of the scratches in the triple deposit at low magnification was not as evident but deeper scratches were present (Figure 66A & B). At higher magnification of the triple HPC deposit (Figure 66), the visibility of scratches were similar to the double deposit (*Figure 65*).

Multiple deposits of *S. griseus* chaplin protein extract were next investigated to determine (changes to) surface topography of polished steel.

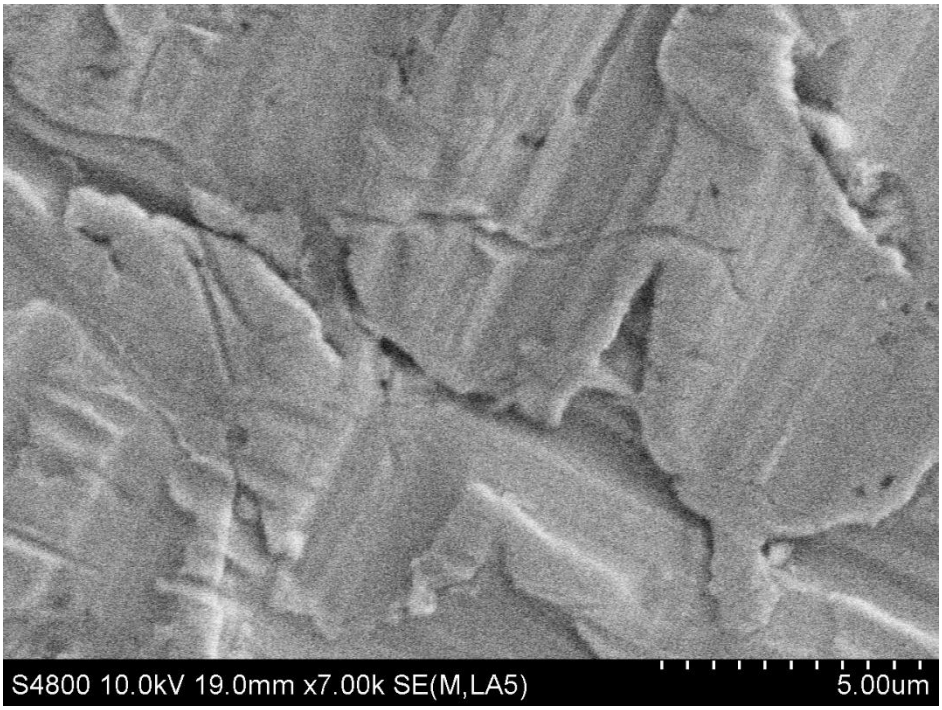

Figure 67: Scanning Electron Micrograph of a single deposit of *S. griseus* chaplin extract at x7,000 magnification with striations evident suggesting poor coverage. Scale Bar = 5 µm.

Imaging of polished steel coupons with a single chaplin protein deposit showed that scratches were still visible (Figure 67). A second deposit was added to determine if coverage could be improved.

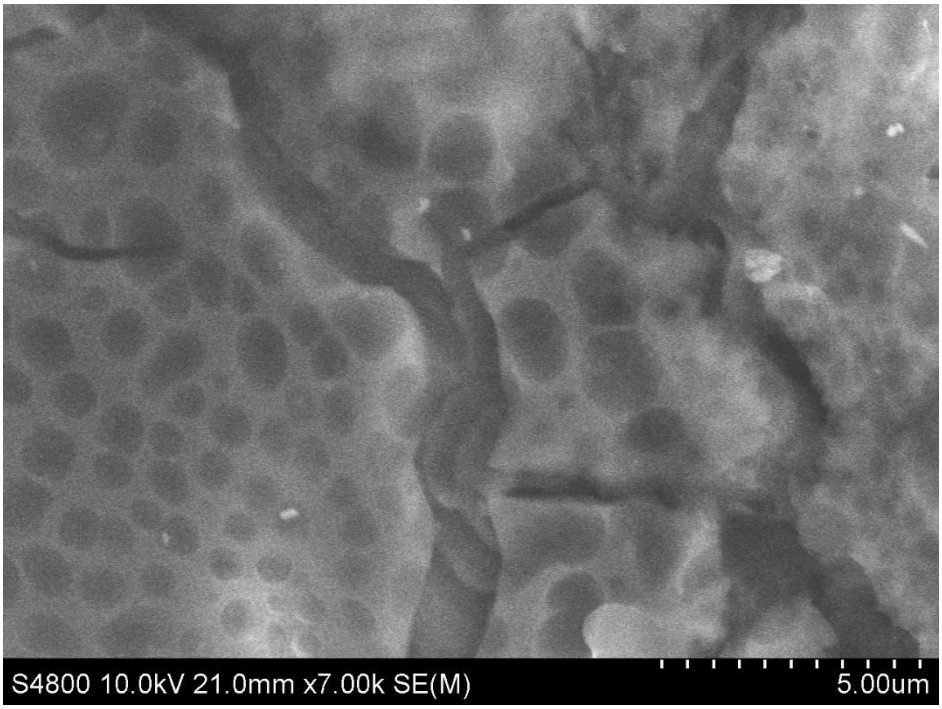

Figure 68: Scanning Electron Micrograph of a double deposit of S. griseus chaplin extract at x7,000 magnification with improved coverage but defects present. Scale Bar = 5 µm.

After an additional deposit (Figure 68), the extracted material was clearly visible, but it did not appear uniform due to the presence of defect breaks between the bulk of the deposited material. These

breaks in the material were mitigated by the addition of another deposit (Figure 69). However, microcracks in the material were observed and as exposure to the electron beam increased, these cracks propagated. The cracks appeared to propagate from weaknesses in the coating in the shape of pin holes.

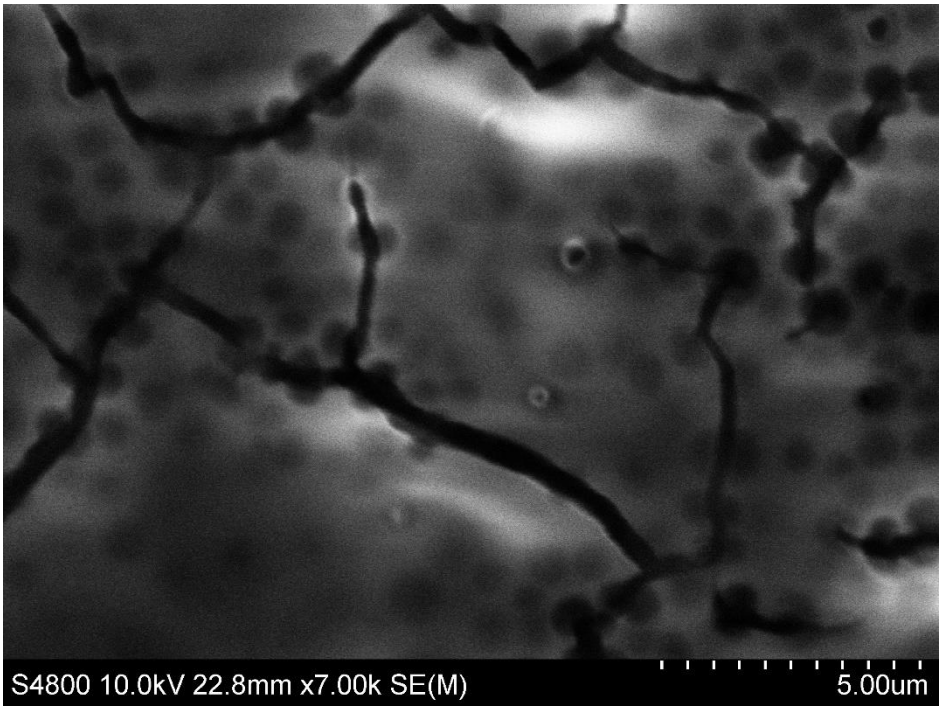

Figure 69: Scanning Electron Micrograph of a double deposit of *S. griseus* chaplin extract at x7,000 magnification with further improved coverage but microcracks originating from areas of poorer coverage. Scale Bar = 5 µm.

Finally, the microstructure of the biocomposite was imaged via SEM: *S. griseus* chaplin extract was deposited in single and multiple layers at a concentration of 150 µg/ml with HPC at 100 µg/ml.

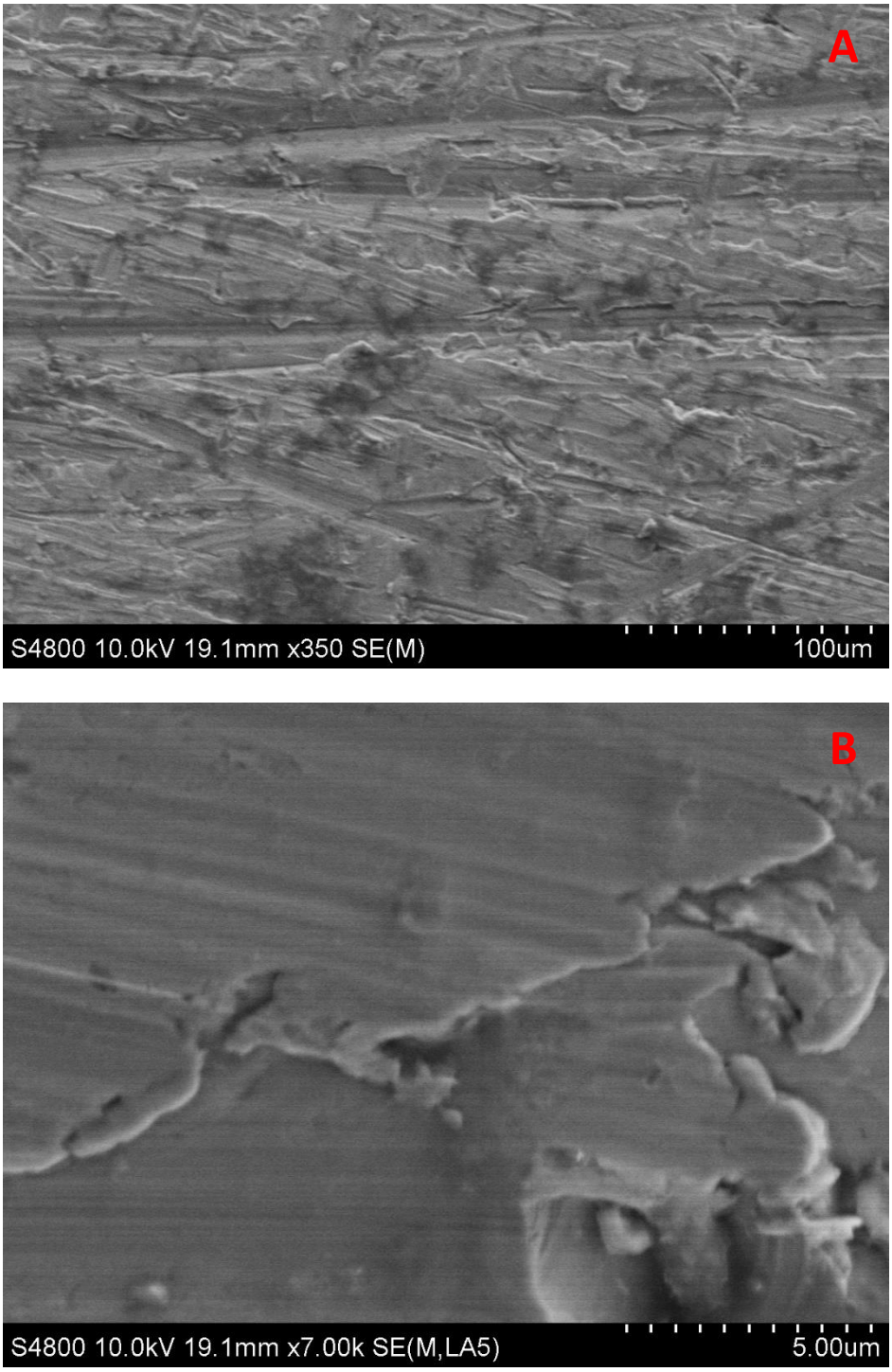

Figure 70: Electron micrograph of a single biocomposite deposit on polished steel. Striations from the polishing process appear less apparent in comparison to the protein only and HPC only controls. Magnifications of x350 (**A**, Scale Bar = 100µm) and x7,000 (**B**, Scale bar = 5 µm).

Figure 70 depicts the microstructure of the biocomposite (chaplin extract and HPC) after a single application. After the single deposit, the biocomposite material did not appear to fully cover the substrate. A second deposit of the biocomposite was added then imaged.

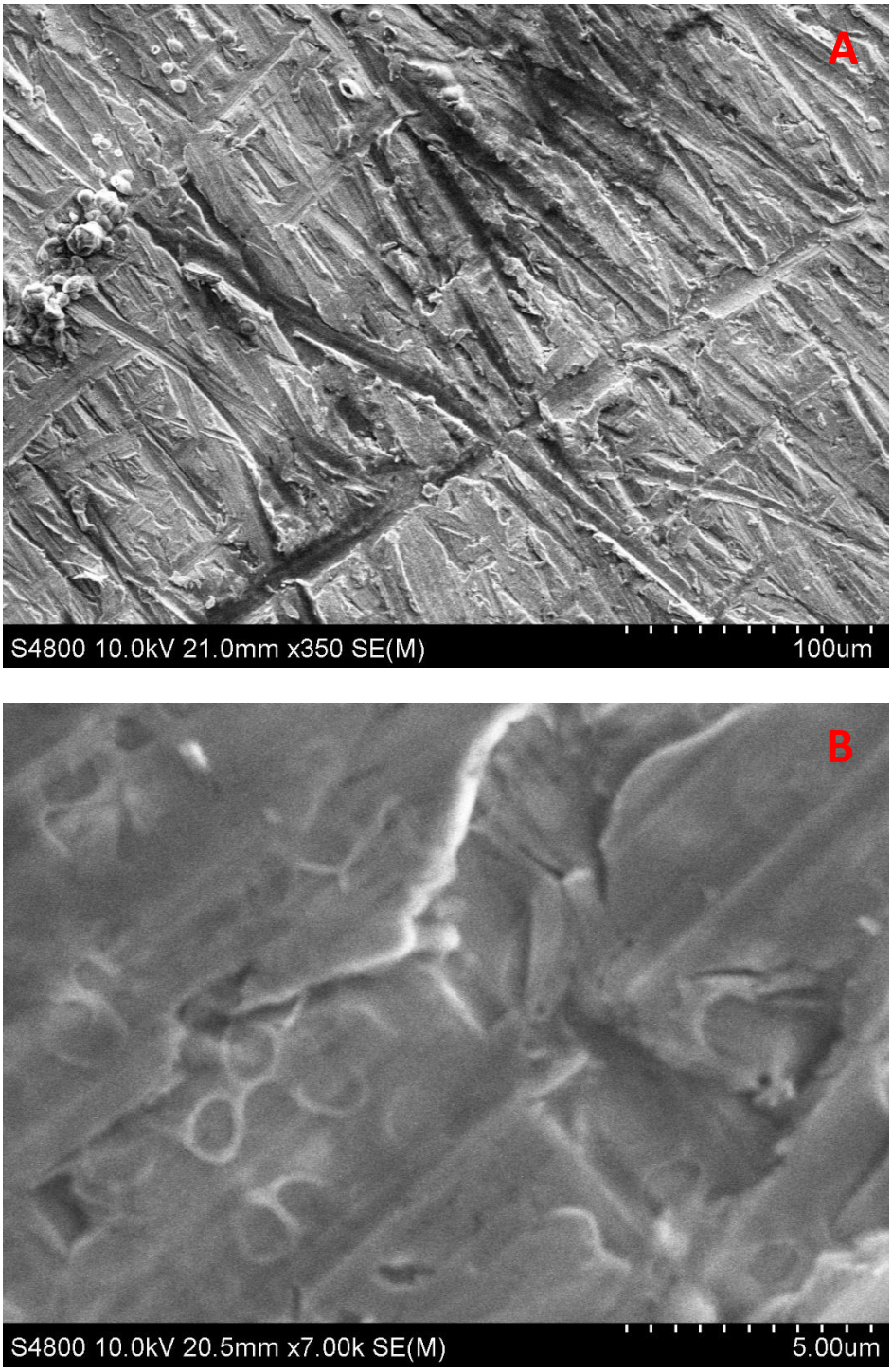

Figure 71: Electron micrograph of a double biocomposite deposit on polished steel. Striations from the polishing process remained evident at low magnification but partially masked at high magnification. Magnifications of x350 (**A**, Scale Bar = 100 µm) and x7,000 (**B**, Scale bar = 5 µm).

After two deposits, at low magnification (Figure 71A), substrate coverage appeared to remain incomplete, however, when the magnification was increased (Figure 71B), the biocomposite appeared to have improved the coverage over the single deposit by partially masking the scratches formed during the grinding process. An additional deposit was visualised.

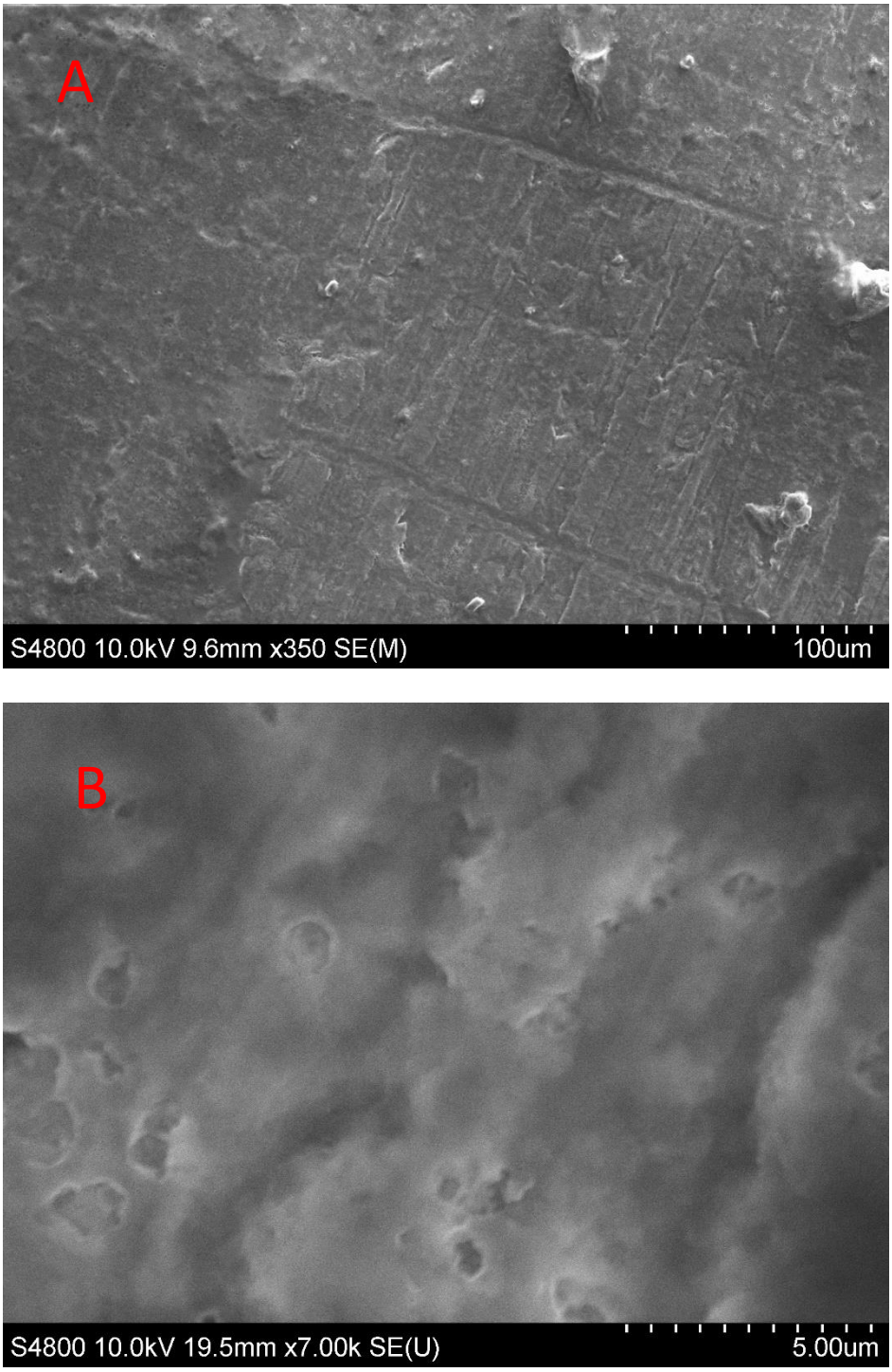

Figure 72: Electron micrograph of a double biocomposite deposit on polished steel. Striations appear smoothed at high and low magnifications suggesting an even coating. Magnifications of x350 (**A**, Scale Bar = 100 µm) and x7,000 (**B**, Scale bar = 5 µm).

The striations present were barely visible at low magnification for the triple deposit (Figure 72A) which was an improvement over the double deposit. This improvement was also observed at higher magnification (Figure 72B), showing that the glycan addition aids in the uniformity of the coating as well as its ability to cover the substrate. This coverage would aid in its ability to reduce electrolyte interacting with the substrate.

5.3.8. Topographical Analysis of Protein & Biocomposite Deposits and the Effects on Surface Roughness

Due to the electron beam in SEM damaging the biocoated materials during image capture, the differences in surface topography between coatings of protein-only samples and protein-glycan biocomposite were also followed with the less destructive high-resolution imaging technique, Atomic Force Microscopy. The scans were carried out using the to determine the topography of the coating across a fixed area using an alternating contact mode. The data obtained was then used to determine the surface roughness.

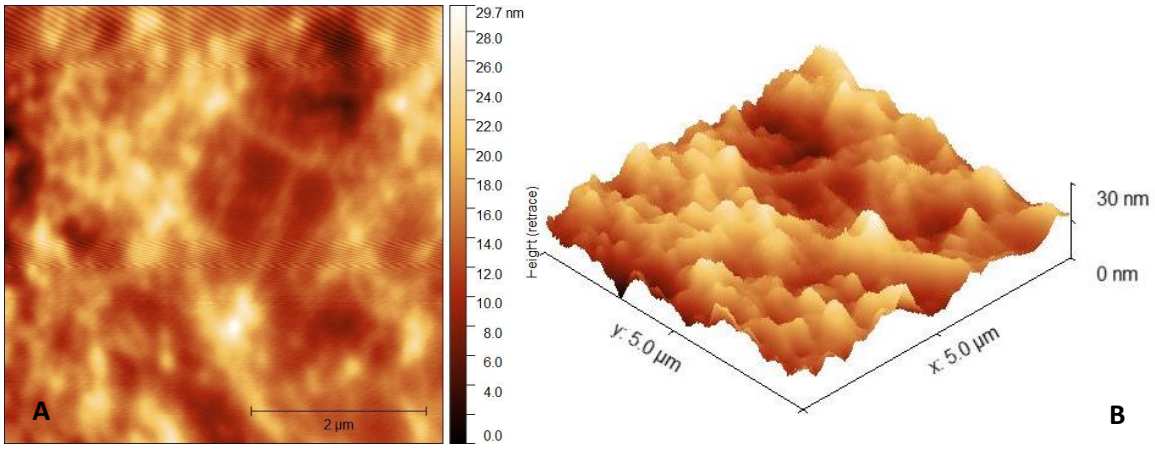

*Figure 73: Two (**A**) and three-dimensional (**B**) topography of chaplin protein deposited at 150 µg/ml on glass substrate. Scale Bar 2µm(**A**) and 5µm. Z-scale = 30nm.*

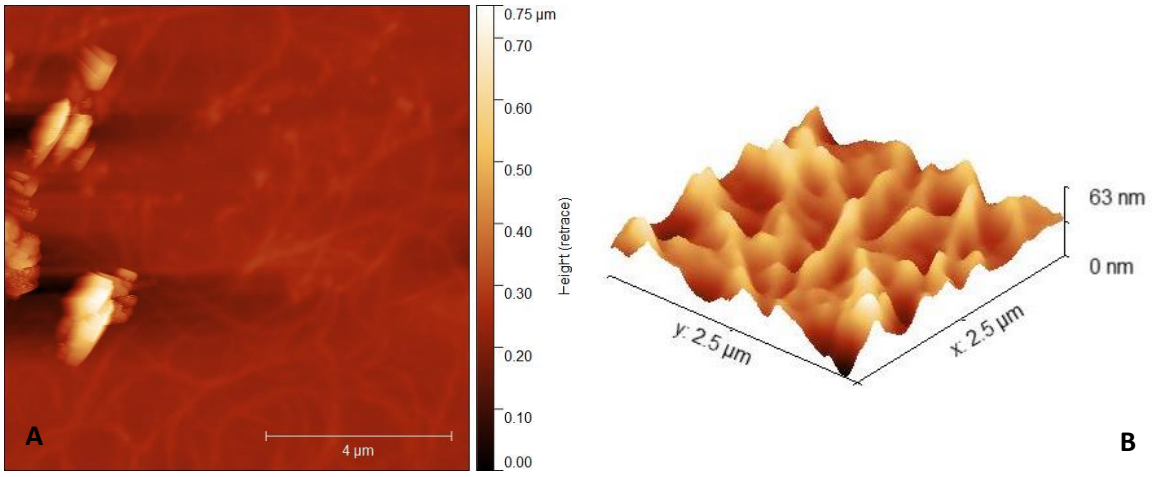

*Figure 74: Two (**A**) and three-dimensional (**B**) topography of biocomposite deposited as 150µg/ml of chaplin protein and 100µg/ml on glass substrate. Scale bar = 4µm(**A**) and 2.5µm(**B**). Z-scale = 63 nm.*

The AFM scans of the protein only coating showed the distinctive amyloid fibral structure throughout, but these were not evenly distributed and appeared to be partially stacked. The AFM topography maps of chaplin-coated glass (Figure 73) indicated that the median coating thickness obtained was 14.78 nm with an average roughness of 3.14 nm. The two-dimensional scan of the biocomposite (Figure 74A) appeared to be relatively uniform except for a few areas of higher peak height, which are

likely to be dust and/or debris. The fibrillar structure can be observed and appear dispersed throughout the scanned area. When a three-dimensional scan was generated, the fibrils can be observed overlapping, which is not as evident in the two-dimensional scan. The biocomposite coating on glass (Figure 74) had a median coating thickness of 32.36 nm with an average roughness of 6.27 nm, but this may be skewed due to the high peaks obtained from the contaminant.

5.3.9. Mechanical Properties as Determined by Atomic Force Microscopy

To determine the elastic modulus of the deposits, glycan only (HPC), Protein only (Synthetic Peptide) and the biocomposite were drop cast onto 2 x 2 cm acetone washed glass cover slips. Samples were dried for a minimum of 24 hours before analysis. Atomic Force Microscopy was used to determine the elastic modulus of each deposit.

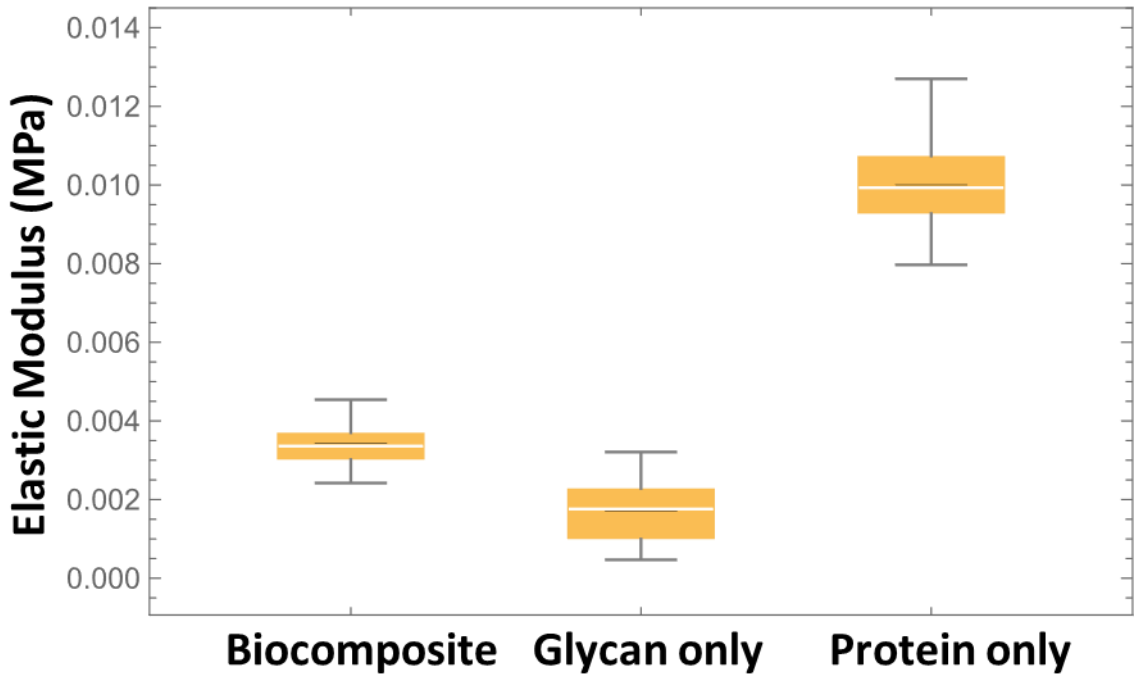

Figure 75: Elastic modulus of the synthetic peptide only, Glycan only and biocomposite. The elastic modulus was calculated used (Equation 4).

The average elastic modulus values obtained for the biocomposite was 0.0034 MPa. For the glycan only, the MPa was smaller than the biocomposite with an average elastic modulus of 0.0019 MPa. The protein only was dramatically high than both the biocomposite and the glycan only with an average elastic modulus of 0.0010 MPa. Nanoscale measurements may not provide a true reflection of the coating due to interference from the substrate.

5.3.10. Cathodic Disbondment of Protein and Biocomposite Coatings on Low Carbon Steel

In order to determine the functional anti-corrosive performance of the biocoatings, Stratmann cells were prepared to follow NaCl electrolyte-enhanced corrosion (Section 2.24). Each cell was created on top of the respective sample and 0.86M sodium chloride electrolyte was added to the well (Figure 76, Green Arrow). Stratmann cells were incubated at room temperature within a humidity chamber at ~95% for 24 hours. After the initial 24 hours exposure, the results of the disbondment were not evident and subsequently were left for 24 hours after removing the NaCl.

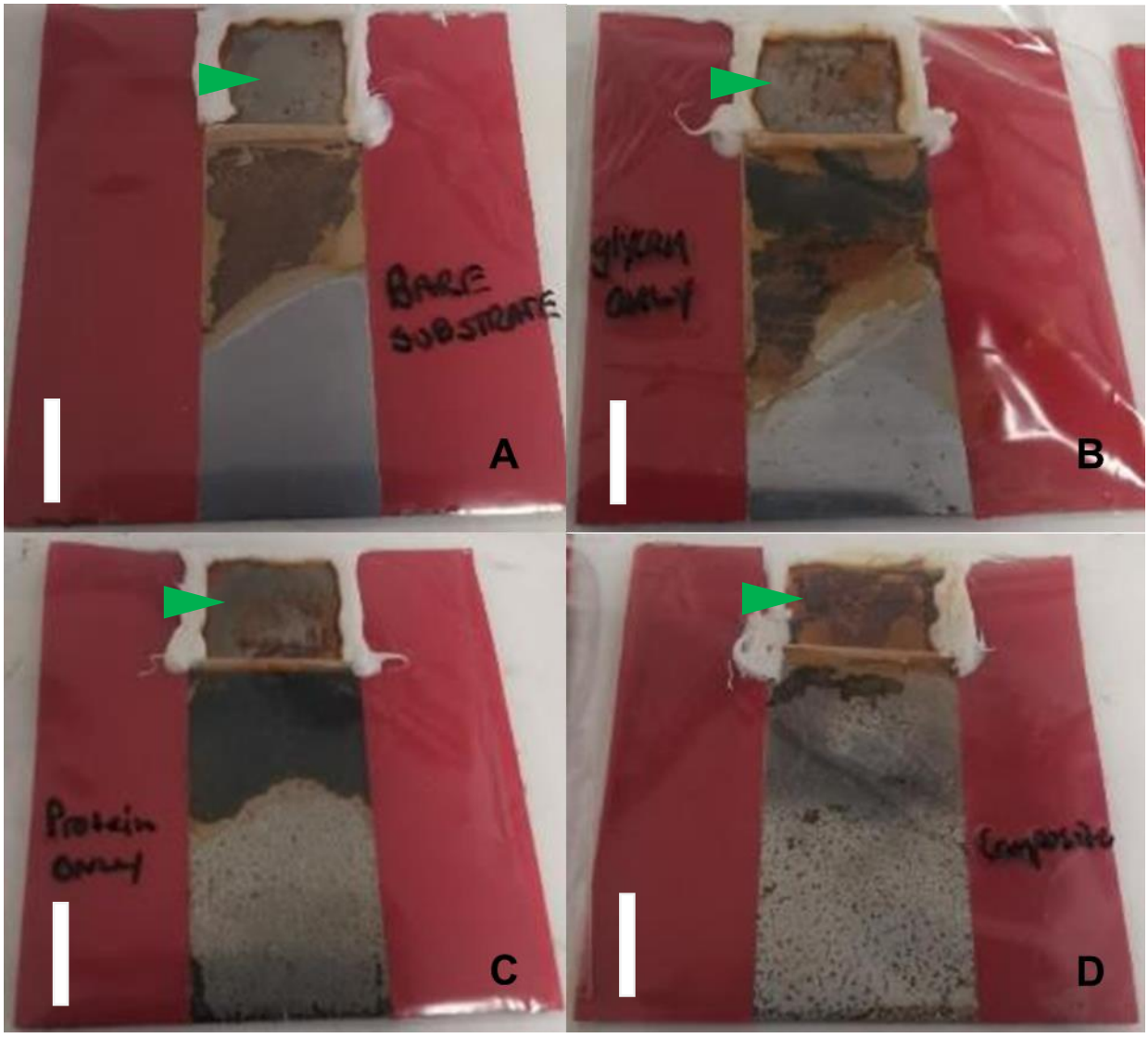

Figure 76: Cathodic disbondment of biomaterial coated low carbon steel coupons (5 x 5 cm) in a Stratmann cell exposed to NaCl electrolyte for 24h before removing and drying for 24hours. Bare substrate control (**A**), Glycan Only (**B**), chaplin protein extract only (**C**) and Biocomposite (**D**). Scale bar = 1 cm.

Figure 76A shows the negative control consisting of 5 x 5 cm bare steel substrate in which the delamination and corrosion under the PVB layer was clear from the typical brown rust development.

The disbondment travelled 21 mm from the electrolyte reservoir. Accelerated cathodic corrosion using a steel coupon with a glycan-only coating (Figure 76B) had slightly more disbondment in comparison to the bare substrate (Figure 76A) with the apparent rust travelling 25 mm. The steel coupon with a protein-only coating (Figure 76C) also displayed a similar disbondment and corrosion to the bare substrate (17mm). However, the area below the disbonded PVB layer had several small areas which appeared to be pitting. The delamination of the biocomposite-coated steel coupon (Figure 76D) was less than all other samples, with a distance travelled of 7mm. However, small, localised areas of corrosion was also evident across the remainder of the coupon. The pitted corrosion was hypothesised to derive from residual TFA present within protein-extracted material upon coating deposition.

In order to avoid pitted corrosion from residual TFA, protein extracts treated via the modified Diethyl ether downstream processing (Section 3.2.2.2) method were investigated as alternative protein source for biocomposite coatings to improve anti-corrosive performance. Stratmann cells were prepared in the same manner as described before with a different coloured tape.

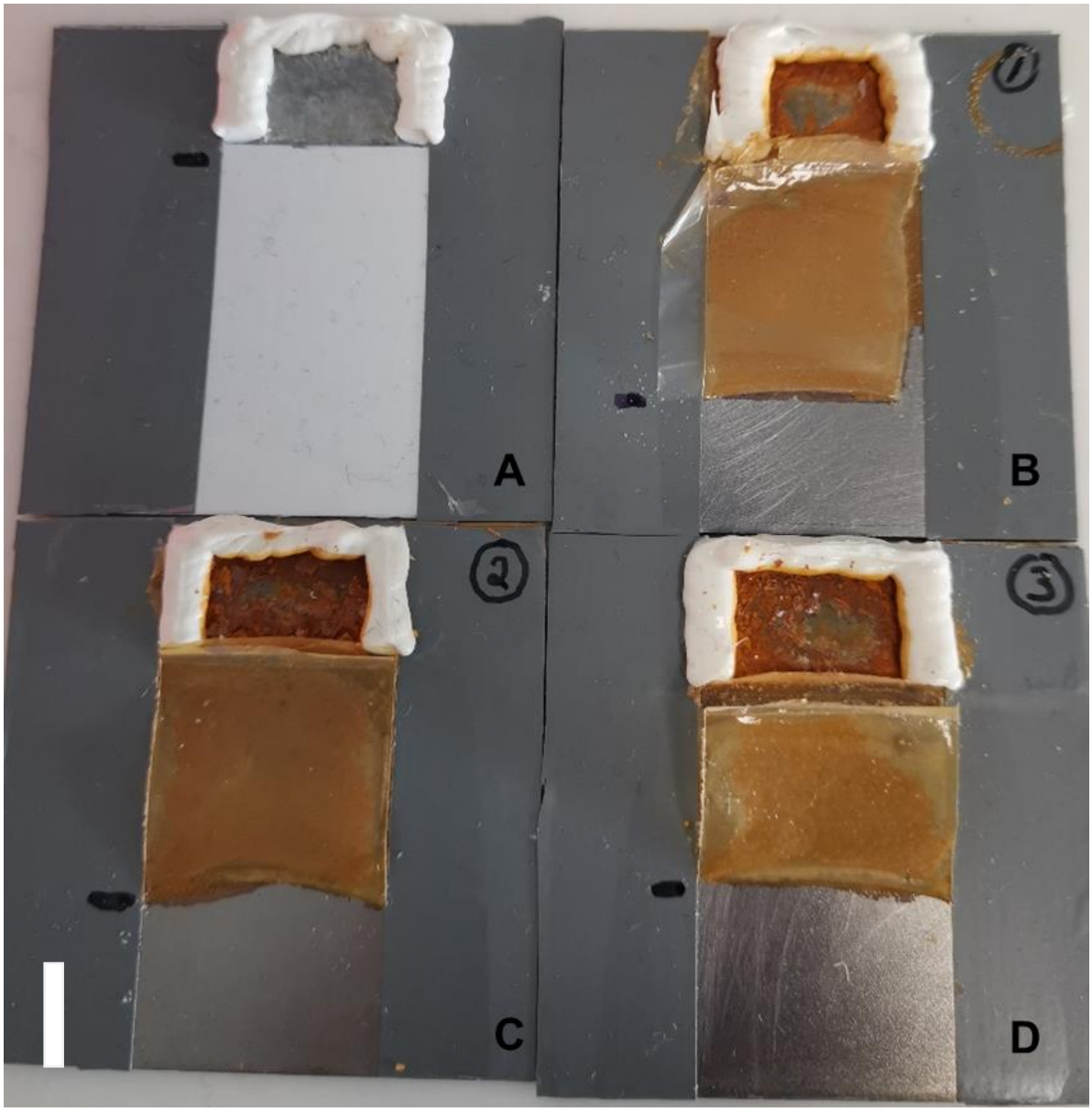

*Figure 77: Cathodic disbondment of biomaterial coated low carbon steel coupons (5 x 5 cm) in a Stratmann cell exposed to NaCl electrolyte for 24 hours, with protein extracted via the alternative diethyl ether method. Positive control anticorrosive polyester coating (**A**), Steel substrate only (**B**), chaplin protein-only (**C**) and Biocomposite (**D**). N=1, Scale bar = 1 cm.*

A 30 µm thick anti-corrosion polyester coating on steel provided by Swansea university college of engineering was used as a positive control (Figure 77A). The anticorrosive organic coating showed very little, if any, disbondment of the PVB layer following accelerated corrosion in an Stratmann cell with NaCl electrolyte. The negative control consisting of bare steel substrate (Figure 77B) was the poorest performing of the tested samples as expected, showing brown-rust formation for 23mm. The coupon with a protein-only coating (Figure 77C) did have clear disbondment of the PVB layer but was slightly improved over the bare substrate (Figure 77B), the disbondment recorded was 20mm from the electrolyte reservoir. The disbondment of the biocomposite coating on steel (Figure 77D) was marginally less than the protein only coated sample, with a disbondment distance of 17 mm.

Interestingly, the zones below the disbonded areas of the coatings that contained diethyl ether treated protein (protein-only (Figure 77C) and biocomposite (Figure 77D)) samples did not have any indication of pitted corrosion as observed for the coupons treated with TFA-extracted protein coatings (Figure 76C &D). Further repeats required to determine the variability of each sample.

The Stratmann cells provided an informative qualitative assessment of corrosion performance. Scanning Kelvin Probe (SKP) experiments were next carried out in order to gain quantitative measurements of the cathodic disbondment, while using the same type of Stratmann cell setup of accelerated corrosion in the presence of NaCl electrolyte. SKP scans were carried out every hour for 11 hours. During each scan, the potential was recorded, as the cathodic disbondment advanced, an increase in the potential was detected.

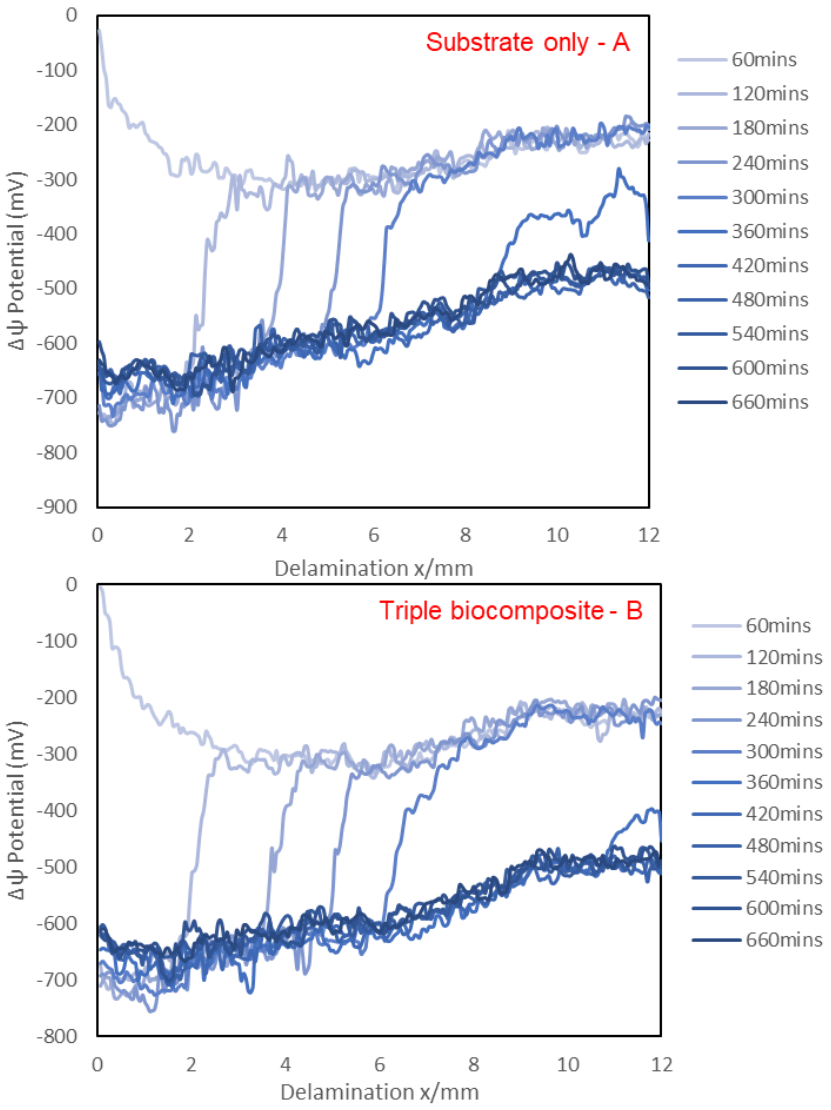

Figure 78: SKP scans of Triple deposit of Biocomposite using TFA extracted material. Bare substrate control (**A**) and triple biocomposite (**B**)

The negative control (Figure 78A) potential after each hour shows that the cathode has advanced 2 mm. After 2 hours there was an increase in the potential from -600 mV to -300 mV. Figure 78A shows the potentials as recorded for the progression of the cathodic disbondment for untreated steel. From the SKP scans in Figure 78, the triple biocomposite sample did not give any significant improvements over the bare substrate over the 6 hours as it appeared to delaminate at a similar rate to the control. Every hour the delamination front advanced ~2 mm in both samples.

5.3.11. Corrosion Testing of Samples HCl Test

To examine the performance of the chaplin protein-only and biocomposite coatings in a corrosive atmosphere, manually polished steel coupons were subjected to hydrogen chloride (HCl) fumes within a sealed container. Deposit layers were increased number to determine if increasing the number of layers would increase the corrosion resistance when exposed to the HCl fumes. Coupons were coated with a single, double and triple layer of protein-only and biocomposite at 150 µg/ml of chaplins and 100 µg/ml glycan and photographed every hour after being subjected to the HCl fume environment.

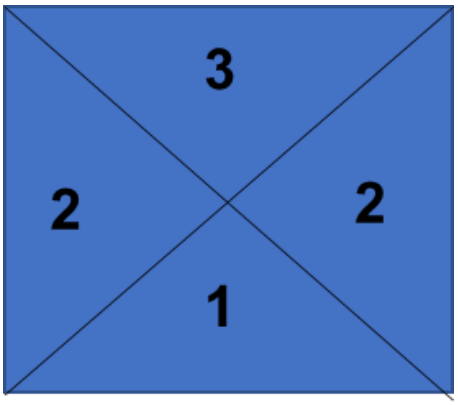

Figure 79: Positioning of single, double, and triple deposits.

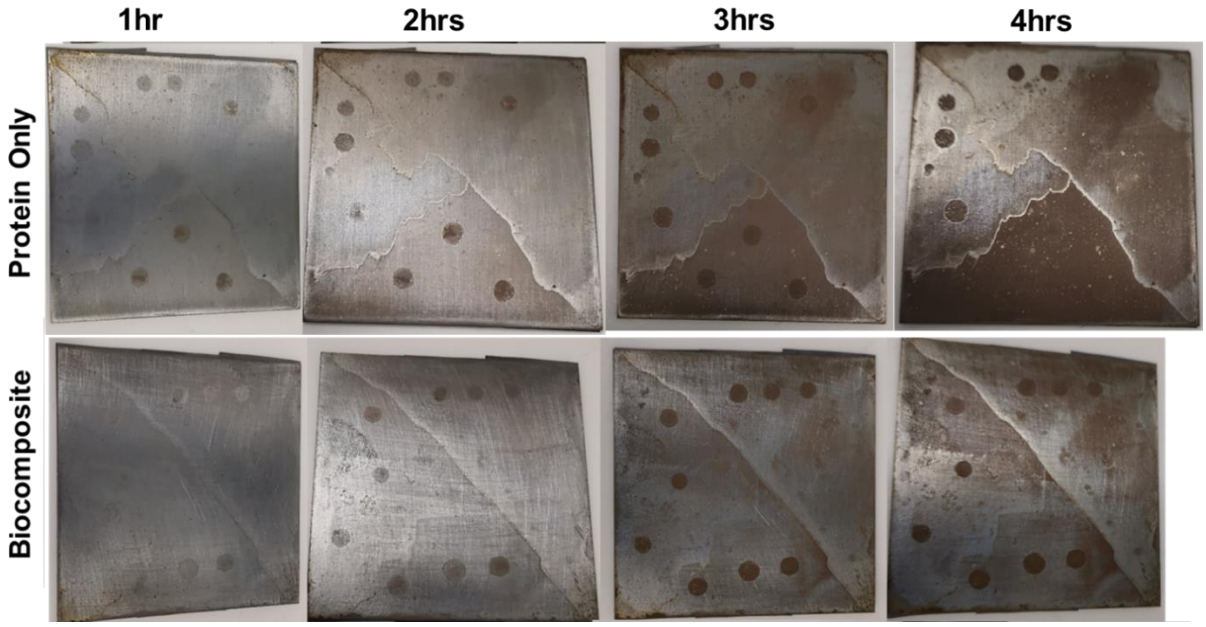

Figure 80: Photographs of single, double and triple deposits of protein-only (top row) and biocomposite (bottom row) coatings on polished steel exposed to HCl fumes over 4 hours.

Figure 79 shows the orientation of the different numbers of layers of coatings on each coupon. For the protein only single coating deposit, there was a steady increase in the degree of corrosion as the exposure time increases as observed by the 'rust'-browning of the bottom triangle (Figure 80). With the addition of a second and third deposit, the degree of corrosion present, as judged by the extent of brown rust formation, was reduced in comparison to the single deposit. For all the layers of the biocomposite coatings, there was a steady increase in the amount of corrosion present as the exposure time increases, but to a lesser extent as the protein-only deposits. There did not appear to be a discernible difference in corrosion between the different number of layers of biocomposite coating. The spots present on all coupons are areas where goniometry measures were taken prior to exposure to the HCl fumes and in the process has subsequently removed part of the coating exposing the substrate to the corrosive environment.

5.4. Discussion

5.4.1. Synthetic Peptide Solubilisation

The synthetic peptides did not solubilise well in any alcohols but were soluble in water and DMSO, respectively. Of the ordered synthetic peptides, only ChpD did not solubilise in water. Generally, most proteins are soluble in water and remain stable. In different polar solvents, the stability and solubility can vary as determined by Pace et al[137]. Amyloidogenic peptides in their monomeric form are soluble however, when these β-sheet proteins form fibrils, they become insoluble [116]. The inability for solubilisation in water of the ChpD peptide may be due to fibril formation of ChpD. For the purpose of carrying out water contact angle measurements on glass, water was used as the solubilisation solvent. The use of water would only be useful on non-metallic substrates due to the initiation of corrosion that would occur if used as the solvent prior to coating untreated metals. Dimethyl Sulfoxide (DMSO) was considered as a deposition solvent and trials were conducted but this particular approach would require the blotting of the solvent or heat to remove due to its high boiling point and would not be a viable process for downstream applications so was not investigated further.

5.4.2. Synthetic Peptide Coating Composition Optimisation

Synthetic peptides designed based on *S. griseus* and glass coverslips of a known area were used to determine the optimal composition of chaplin proteins for a high-water contact angle as determined by goniometry. Initial experiments were conducted using each genome sequence derived minus the signal peptide (ChpD, ChpE-short, ChpE+8, ChpG and ChpH) and a combination of these designed chaplins. To emulate a similar composition of peptides to the *S. griseus* extracted peptides, the synthetic chaplins were mixed in equal proportions to a final concentration of 150µg/ml. The water contacts angles and variance differed for each of the different chaplin protein samples (Figure 53). The samples containing more than one chaplin protein generally increased the water contact angle. These angles were marginally higher with the increase in the number of deposits however variance was increased. It was identified that a combination of ChpE-short, ChpG and ChpH gave the highest increase for both single and double deposits over the control (Figure 54). Di Bernardo *et al.* have already hypothesised that *S. coelicolor* small chaplin proteins that contain cysteine residues (ChpD, ChpF, ChpG and ChpH) lead to improved stabilisation which may be leading to the higher water contact angles [24]. The water contact angles, and variance achieved by chpD were lower than the other chapin protein deposits due to the protein being in suspension rather than in solution causing an uneven distribution across the coverslip. Given the positive results obtained, the mixture of ChpE-short, ChpG and ChpH peptides were used for subsequent biocomposite analyses.

5.4.3. Biocomposite Analysis using Synthetic Peptides

As the chaplin concentration of the deposit had been determined, two questions were raised for the initial biocomposite analysis: Is the final total concentration of the biocomposite material optimal for 150 µg/ml or must the final concentration of the peptide remain at 150 µg/ml after the addition of the glycan?

5.4.3.1. Biocomposite Ratio Optimisation

Peptide and glycan solutions in distilled water were mixed to give decreasing peptide concentrations and increasing glycan concentrations but to a final total biomass concentration of 150 µg/ml. Biocomposite solutions were then coated onto glass and WCAs measured. It was identified that as the concentration of the peptide decreased, the water contact angle also decreased with the only exception of 11.25:3.75 protein-to-glycan (Figure 55) sample which did increase WCA but also introduced more variance. The trend of the decreasing water contact angles was as expected due to the reducing levels of the protein and glycan WCAs being low. The variance and water contact angle observed for the HPC-only deposit was low. HPC is relatively hydrophobic in comparison to other water-soluble cellulose ethers but, it is believed that when the measurements were being taken, the HPC coating was being solubilised [138]. These areas were less visible as the protein concentration increased. This would be expected due to no protein being present and causing the final coating to be a uniform coating of HPC which would solubilise during goniometry measurements.

5.4.3.2. Glycan Addition to Optimum Peptide Concentration

The second question was investigated by adding increasing amounts of glycan to the solution with fixed 150µg/ml of synthetic peptides concentration. As the glycan concentration increased, an increase in the water contact angle was observed (Figure 56). The data displayed in Figure 56 shows that the increase to 150 µg/ml introduces more variance, but the water contact angle measurements were higher than the protein only. This suggests that the HPC in the biocomposite is having a greater effect on the water contact angle in comparison to the chaplin proteins. This increase in the water contact angle may be due to the glycan mediating chaplin protein binding to the hydrophilic substrate, which has been suggested from investigations on a class I hydrophobin (Vmh2) in the presence of a glycan [139]. This mediation would cause the orientation of the hydrophilic domains of the fibrils towards the hydrophilic substrate resulting in the hydrophobic domains being exposed to the hydrophobic environment(air). Alternatively, the addition of the glycan may be leading to a more stable conformation [140]. Due to the increase in water contact angles observed when determining the optimum addition of glycan (Figure 56) the biocomposite mixture used for further analyses had a

final concentration of 150 µg/ml with an equal mix of chaplin peptides (ChpE-short, ChpG and ChpH) with 100 µg/ml HPC.

5.4.4. Barrier Coating Development of Chaplin Protein Extract Based Biocomposite

Research conducted identified that the optimal concentration for *S. griseus* extracted material to provide a hydrophobic coating on glass slides was 150 µg/ml [56]. The concentration of glycan was yet to be investigated. To determine the optimal concentration of ethyl cellulose and hydroxypropyl cellulose for a barrier coating with chaplin protein extract, a range of concentrations of the biopolymer (in ethanol) were combined and deposited onto glass cover slips of a fixed area of 4 cm^2.

Due to ethanol being used, an additional ethanol soluble glycan was investigated, ethyl cellulose. The water contact angles obtained from the protein extract only was as expected and corresponded to previous research where water contact angles of between 45^o and 55^o were obtained [56, 57, 117]. The HPC and EC had similar water contact angles, where an increase was observed as the concentration was increased. The concentrations used in this research for the glycans are considerably lower than that used in film forming experiments which is likely causing the slight differences in the water contact angle measurements for the glycan controls. The water contact angles achieved were lower than that of the synthetic peptides due to the presence of co-extracted peptides and these may be interfering with the glycan-protein interactions during the deposition process. Based on the water contact angles obtained, HPC gives less variance but no significant change in the water contact angle when compared to the protein only.

For the ethyl cellulose, which is not soluble in water, it is unlikely that the coating would solubilise but may go into suspension if no interaction with the substrate was occurring. Water contact angle were similar to the HPC, but it has been recorded in other research to have contact angles of 70^o. This water contact angle measurement was from a coating with a different formulation and preparation used within this research [141]. The difference in formulation is the likely cause of the differences between the results obtained here. The biocomposite formulations containing ethyl cellulose increased the variance. As chaplin proteins can adopt different conformations (exposed hydrophilic residues or exposed hydrophilic residues), the ethyl cellulose may be forming some of the fibrils in the opposite orientation causing the variance in the water contact angles. Chaplin extracts have been shown to cause water contact angle changes on both hydrophilic and hydrophobic substrates [117].

5.4.5. Water Contact Angle Measurements on Low Carbon Steel

Due to the unknown effects the peptide deposit would have on the steel coupon, water contact angle measurements were taken to compare how the peptide only and glycan would affect the

measurements. It was quickly observed that the steel coupons had a higher water contact angle than the glass substrate but also contained a larger amount of variance. This observation led to the hypothesis that the deposits would also contain a high amount of variance as the fibrils would orientate in both hydrophilic and hydrophobic confirmations. It is well established that the steel surface undergoes oxidation and forms an oxide layer which has a certain degree of corrosion resistance but also exerts an increase in water contact angle [142]. With the deposits on the unpolished steel with the water-based samples, it was unclear how the substrate would behave during the drying process. The water contact angle measurements did contain a high amount of variance in both the protein only and the biocomposite deposits. By grinding and polishing the steel prior to deposition, it removes the oxide layer present, and the water contact angle of the substrate was reduced. This should cause the orientation of the chaplin proteins to be hydrophobic at the surface and create a hydrophobic barrier and subsequently reduce the variance when compared to the unpolished substrate.

5.4.6. Amyloid Morphology of Biocomposite Coating

After determining the optimum biocomposite formulation between the two components, the characterisation of the morphology and topography of the coatings was investigated using high-resolution imaging techniques. It was hypothesised that the addition of the glycan would drive fibril formation of the chaplin proteins in solution, in contrast to the formation of fibrils at the hydrophilic-hydrophobic interface i.e., at the water-air interface only [36]. But it was unclear if solution-based fibril formation in the presence of glycans had an effect on the length and width of the fibrils formed [28]. For biological samples, electrons fly through without interaction. Pt or Au/Pd sputter oating delivers a fine layer of heavy nuclei which then enables the visualisation of a biomaterial. Due to the nanoscale of the biocomposite sputter coating was not carried out. The synthetic peptide only and biocomposite were deposited onto unpolished steel coupons then subjected to the SEM. The bare substrate-only coupon appeared amorphous with no distinguishable features which was advantageous for the visualisation of the protein only and biocomposite deposits as the bare substrate would not interfere in capturing images of the amyloid fibrils. The protein-only deposit gave a clear visual of the fibrillar structure (Figure *59*) that would be expected of chaplin proteins [16]. Although fibres were visualized, it was evident that there were gaps between the fibrils, showing bare substrate. This was followed by the analyses of the biocomposite deposit. From this, there were no discernible features found, only what appeared to be corrosion features. Fibrils within the biocomposite may be masked due to these corrosion features, the film forming properties of the HPC and a reduction in the size of the fibrils (Figure 59) [143].

5.4.7. Scanning Electron Microscopy of Extracted Protein-based Coatings

S. griseus extracts were examined for chaplin proteins and their interaction with HPC. Deposits of *S. griseus* chaplin proteins and biocomposite were deposited on polished steel. From a visual examination, there appeared to be no significant corrosion product after drying of the deposits. These deposits were subjected to SEM and no fibrils could be identified in either the protein-only or the biocomposite coated polished steel (Figure 67). The material present is believed to be coextracted proteins and cell wall fragments carried over from the extraction process. Due to these contaminants, the fibrils may be imbedded within this layer.

During the visualisation under SEM, the protein-only extracted material coating disintegrated under the 10kV electron beam. Areas on the surface appeared thinner than others and microcracks became evident before developing into larger cracks (Figure 67). The presence of small pits in the coating were evident under SEM and the cracks propagated through these pits suggesting that they are areas of poor coating cohesion (Figure 67). This cracking phenomenon however was not observed on the biocomposite deposit using bacterial protein extracts (Figure 70). Cohesion of coatings is vital for full coverage and performance which is mainly influenced by the binding agent and the solid material within the formulation. The formulation of a coating is dependent on the function of the coating. The amount of solid material per volume of a coating allows for the prediction of film thickness. The total amount of protein being deposited as a weight per volume percentage was 0.015% compared to that of the biocomposite which has 0.025%. These values would be true for the synthetic peptides, however, for extracted material, these values are the minimum amounts that would be present due to coextracted material that would not necessarily be detected by the Pierce™ total protein assay. The protein used for the protein-only and biocomposite deposits contained the same amount of coextracted material so a fair comparison can be made between the samples. The addition of the glycan may be improving the overall coverage and allowing for coating cohesion to be strengthened but it cannot be ruled out that the absence of cracking on the biocomposite is due to the increased amount of material being deposited.

5.4.8. Surface Topography of Biocomposite Coatings

Synthetic peptide fibrils were identified successfully for protein-only deposits on unpolished steel (Figure 59), however, the surface morphology of the biocomposite coating on glass was still unconfirmed. Atomic Force Microscopy, which has increased sensitivity and spatial resolution in comparison to SEM, was used for further analysis of the surface topography of the synthetic peptide and synthetic peptide based biocomposite. The AFM scans of protein-only deposits on glass determined that the median peak height was 14.78 nm with an average roughness of 3.14 nm (Figure

73). The topography image for the protein-only coating indicated there was no organisation to the fibrillar structures similar to the SEM images obtained on unpolished steel (Figure *59*). The topography of the biocomposite coating (Figure 74) had a higher average roughness of 6.27 nm. The addition of a glycan with amyloid proteins has been shown to increase the surface roughness [144]. The increase in the roughness possibly allowed for the trapping of air underneath the water droplet, which in turn reduced the contact of the water droplet with the substrate. As glass has a high surface energy, it leads to water spreading across the substrate, the biocomposite provided an effective barrier and stopped the spreading across the surface. This supports the roughness data recorded by AFM and other studies [145]. The scans carried out gives strong evidence that the introduction of the glycan can help induce the formation of a hydrophobic layer which exerts a Cassie-Baxter effect [8].

5.4.9. Mechanical Property Testing by Atomic Force Microscopy

From the elastic modulus measurements recorded from the synthetic peptide only, glycan only and biocomposite (Figure 75), the protein only had the highest average MPa whereas the glycan only had the lowest MPa. The forces recorded suggest that the synthetic protein only sample is more rigid in comparison to both the biocomposite and glycan only. The measuring of the elastic modulus of biological samples can be limited due to the lack of homogeneity. This lack of homogeneity plays a factor on the calculation for the elastic modulus when using the Hertz model. The mechanisms involved in the interaction between glycans and proteins is not well understood. The mechanical properties of the biocomposite were only carried out on one glycan as a counterpart to chaplin proteins to improve adhesion, so alternative glycans may provide an increase in performance. Chaplin proteins and glycan linkage has been established for adherence to substrates [28]. With the hypothesis that the glycans orientate along the backbone of the amyloid fibril and subsequently interact with the hydrophilic surface of the substrate, the strength of interaction between the substrate and the glycan appears to be less than that of the protein only. The coatings are nanometre in scale and is important to be critical of the values obtained as the substrate could be interfering with the measurements.

5.4.10. Cathodic Disbondment of Protein and Biocomposite Coatings

Cathodic disbondment was first investigated qualitatively by subjecting coatings on metallic substrates to a high humidity chamber and observing the disbondment of the PVB after 24 hours (Figure 76). The steel coupons containing TFA-treated peptide coatings had observable cathodic disbondment with slight improvements observed for the biocomposite coating (Figure 76D). However, across all samples containing TFA-treated peptide, pitted corrosion was evident. Pitted corrosion was avoided after depositing diethyl ether prepared chaplin protein extract (Figure 76, Figure 77). There was no discernible improvements observed for the biocomposite over the controls. Corrosion resistant

coating are in place to provide protection to the underlying surface and historically, chromium VI has been used for corrosion resistance but has now been severely restricted in its use. Typical coatings are non-aqueous based systems to prevent initiation of corrosion during deposition. The binding agent used typically dictates the mechanical properties, whereas the additives, such as pigments give the coating functionality. These coating when dry have a variety of thicknesses depending on the amount of solid material is present within the formulation. Ultimately, current commercial corrosion resistant coating has film thicknesses in the μm range. The coating being developed here is 10's of nm so the overall performance comparison between the polymer coating and the biocomposite is not a fair one. For quantitative analysis, the use of a Scanning Kelvin Probe (SKP) was used which measures the corrosion potential and can be used for studying the corrosion under very thin electrolytic films [146]. A Stratmann cell was set up on top of polished uncoated and coated steel coupons and then subjected to the SKP (Figure 78). For the triple layer biocomposite using TFA-treated chaplins, the potentials being recorded over the 11 hours indicated the disbondment of 12 mm of PVB within 6 hours. The disbondment for the substrate only control also disbonded 12 millimetres within 6 hours (Figure 78). The extracted material used for the triple deposit biocomposite was from the TFA evaporation method and residual TFA would be present. The presence of residual TFA may be monomerising the biocomposite and/or degrading the substrate, leading to delamination of the coating. The use of additional layers has shown that an improvement in the corrosion resistance can be achieved using extracted chaplin proteins on mild steel and magnesium alloy AZ31 [57]. The potentials observed after each hour suggest that it is cathodic disbondment rather than anodic undermining.

5.4.11. HCl Fuming test

The use of stratmann cells and SKP required the use of relatively high concentrations of sodium chloride directly added to the surface of the coating/substrate to initiate corrosion. A testing method was developed using Hydrochloric acid fumes as a means of accelerated corrosion. Section 2.25 gives a representation of the set up and running conditions. The chaplin protein extract only (Figure 80) corrosion became apparent on the single deposit after 3 hours, after 4 hours the single deposit section of the coupon was completely covered. The double deposit was beginning to show sign of corrosion after 4 hours. The biocomposite had improved corrosion resistance in comparison to the protein only deposit. The reduction in the amount of corrosion present may be due to the integrity of the deposited film remaining intact without the presence of pinholes as identified by SEM. However, Hydroxypropyl cellulose has been shown to be an effective corrosion inhibitor for aluminium [147].

5.5. Conclusion

The development of a biocomposite for corrosion resistance is required to withstand extreme conditions and resisting corrosion of the substrate. The use of peptides extracted from wild type strains require further purification to remove contaminants. The removal of contaminants would likely improve the hydrophobicity of the coating by removing the residual cell wall fragments. Synthetic peptides are useful for applying hypotheses and reducing variables. The synthetic peptide with the hydroxypropyl cellulose appears to give an improved water contact angle in comparison to the protein only and by AFM, the addition of the glycan increases the average roughness of the coating and causes a Cassie-Baxter phenomena. The glycan can be used within ethanol and water which makes it ideal for a range of solvent-based systems. The corrosion-based testing were aggressive tests and due to the gaps identified in the coating, they may not be the most appropriate technique until formulation amendments can be implemented to improve the coating deposition.

6. General Discussion

6.1. Introduction

The investigation and application of biobased solutions is becoming increasingly more important given the (relatively) rapid increase in the global climate. This key driver has led to legislative efforts for multiple industries to reduce their carbon footprint by finding alternative technologies and processes. Not only the impact of global warming, but also the implications of current technologies which can have an impact on health. The development of biobased alternatives to products has advantages over existing technologies but exploiting these natural products and bioinspired phenomena can be challenging. Replicating the biological process *in vitro* to the same performance level *in vivo* is just one challenge faced but also achieving this at a competitive cost in comparison to existing technologies can be a major hurdle. It is the work carried out within this project that falls into this category of developing bioinspired technology for real world applications, specifically, but not limited to, bioprocess development and corrosion resistance. Corrosion is a global issue which has significant financial implications. Materials must withstand harsh environmental conditions to ensure longevity. Current corrosion resistance technologies contain processes and additives that are hazardous to health and the environment, so the development of new technologies is crucial to find alternatives for these processes and additives. Bio-based and bio-inspired technologies is just a couple of approaches which can be used to find alternatives. The overall aim of this research was to optimise production and purification of chaplin proteins to then formulate a biocomposite coating for corrosion resistance.

6.1.1. Media and downstream processing optimisations

The current biotechnological process for the extraction of chaplin proteins is crude and co-extracted pigments and cell wall fragments can remain which can have an impact on application testing. In Chapter 3, it was demonstrated that for the *S. griseus* strain, an alternative medium and buffering agent could be used for the generation of biomass and subsequent submerged sporulation. The complex and laborious R2YE medium normally used for the culturing of liquid sporulating strains of *Streptomyces* contains TES as the buffer which contributed a significant proportion of the cost. The use of the newly developed medium based on MYM can provide a financial saving estimated to be around 75% which is a great achievement. Furthermore, by switching to a potassium bicarbonate buffer, the 'greenability' of the culturing process is improved as recycled carbon dioxide could be used in the fermentation process, possibly also enabling carbon capture/carbon sequestration thereby aiding climate action objectives. Not only has a bicarbonate buffer positive implications for the yield of chaplin proteins, but it may also be efficient for the cultivation of other *Streptomyces* strains for extraction of high value compounds and/or industrial enzymes. The medium was optimised for full morphological differentiation of *S. griseus* and cost savings, the technology developed was able to be

scaled up from 200 ml to 1700 ml in a controlled bioreactor environment with high shear stress, which gives promise for scale up to industrially relevant culture volumes. *Streptomyces* differentiation time can vary between strains based on multiple factors such as the media composition and growth conditions. The submerged differentiation to sporulation of *S. griseus* in the modified MYM medium can be achieved in 5-6 days. After this period, chaplin protein levels would be at their highest as they coat the spores. The time required could be deemed a limitation an efficient heterologous protein expression system could be achieved in a shorter timescale with potential for enhanced yields if nutrients were prioritised towards Chp expression rather than differentiation or growth.

The downstream processing and purification of chaplin proteins requires ultrasonication of spores to achieve cell lysis, boiling in SDS to remove detergent-sensitive proteins, freeze-drying and monomerization in TFA followed by evaporation of TFA. This monomerization step is required to obtain chaplin proteins in the desired confirmation before fibril formation is completed *in situ* as biomaterial. But the presence of residual TFA after the solubilisation of the chaplins has detrimental pitted corrosion effects when applied to metallic substrates such as low carbon steel. Following solid phase synthesis of peptides, the solvent diethyl ether has been typically used in chemistry to precipitate the peptides from the cleavage cocktail which contains TFA. In chapter 3, the research demonstrated that adapting the peptide precipitation process used for synthetic peptides, chaplin proteins can also be precipitated, with concomitant TFA removal. Figure 25 shows the distinct difference between the conventional extraction method in comparison to the diethyl ether precipitation. This precipitation process also improves on the environmental impact as the TFA would not require evaporation into the atmosphere. From the experiments and the findings from chapter 3, it has been shown that the sporulation and subsequent extraction of chaplin proteins from *S. griseus* can be achieved in a more economical and environmentally friendly way in comparison to the traditional method. Although positive detection of the chaplin proteins was achieved with various assays (ThT fluorescence and SDS-PAGE), detection by MALDI/TOF MS remained elusive for several chaplins. This could have been due to the poor ionisation of specific chaplin proteins *per se* while the presence of contaminating pigments or cell wall fragments that have been co-extracted may have caused additional problems as these compounds typically ionise well and may have quenched the chaplin signal.

The precipitation of the proteins using diethyl ether does appear to provide TFA-free material that does not initiate corrosion when applied to metallic substrates. However, this process requires copious amounts of diethyl ether for the precipitation and subsequent washes. Due to the volume required, when scaled-up, this process may be deemed unsuitable and alternative strategies may be required, such as recycling of solvent. Alternatively, ‘green ethers’ could be explored as these solvents

provide preferable environmental, and health and safety characteristics, with further features that may of benefit to biomaterials development.

6.1.1.1. Conclusions

The developments made on the growth of *S. griseus* within a modified Maltose-Yeast Extract- Malt extract medium provides evidence that this strain of *Streptomyces* can complete its lifecycle and lead to spore formation. The growth is facilitated with the use of a potassium bicarbonate buffer, which replaces the TES buffer which carries a high percentage of the mediums cost. The switch to the 'greener' buffering agent led to a 75% in the medium cost, which allows the growth process to be more economically viable.

The sporulation within the modified MYM medium was achieved at both 200ml scale and 1.7L scale, with the latter also giving key real-time information, such as pH and dissolved oxygen. The research has shown that scale up of the growth using a bioreactor can be achieved. This ability to be effectively scaled-up may have positive impact on secondary metabolite project where media costs can be substantial and hinder the ability for certain products to be profitable. Although positive outcomes were achieved from the growth in the modified MYM medium, further research could be made into the growth process. A variety of different approaches could be made, such as: acid and base pH control and alternative carbon sources could provide further developments to the growth profile.

The extraction and purification of chaplin proteins from wild type strains was also investigated and appeared that the use of diethyl ether as a method for removing TFA was successful. The removal of TFA from the chaplin protein extracts has significant influence on the applications of these proteins on metallic substrates. Although not MALDI-TOF confirmed, this process appears to precipitate the chaplin proteins following monomerization. The outlook of this process is positive for both the purification of chaplin proteins and existing processes where TFA is used and can influence the end performance of the extracted material. The function of the chaplin proteins following diethyl ether precipitation is yet to be determined.

6.1.2. Controlled expression of Chaplin E in a homologous host, *Streptomyces coelicolor*

In some industries, the production of high value compounds is achieved by harnessing the power of synthetic biology. Heterologous protein expression can be achieved by taking the gene of interest and incorporating it onto an expression vector which can then subsequently be transformed into a relevant host organism such as *E. coli.* Using *E. coli* as a host for expression can have benefits over the native host as the genetic manipulation of this organism can be easily achieved. The growth of *E. coli* is also considerably quicker than *Streptomyces* but, for chaplin production proved difficult due to the

formation of multiple chaplin species with and without signal peptide sublocalised to different fractions in and outside of the cell. Plasmids can be integrated into the *Streptomyces* chromosome for heterologous expression but is slower growing when compared to *E. coli* or yeasts. In Chapter 4, it has been shown that a plasmid with a *chpE* gene after a thiostrepton inducible promotor can be incorporated onto the *Streptomyces* chromosome and induced to express *chpE*. The results were conflicting as the Thioflavin T amyloid specific fluorescence dye and the Amyloid antibody dot blot tests gave a strong response whereas the protein could not be identified from MALDI-TOF spectra or SDS-PAGE. The overexpression of the ChpE protein from the M1146 superhost strain therefore showed some promise but optimisations would be required to improve the downstream purification. The strain was successfully developed, and the protein appeared to be expressed into the supernatant which was one of the main objectives of this research. The concentrating of the peptides within the supernatant appeared to be successful with the detection by ThT and the amyloid antibody assay using acetone precipitation, but alternative strategies may be required due to the lack of detection by SDS-PAGE and MALDI/TOF. When considering the scale up of acetone precipitation, it may not be a viable process due to the volume and low temperatures required to precipitate the protein. This process also does not purify the chaplin E protein from the supernatant, so the final precipitated pellet contains a mixture of peptides and media components, which is likely to influence the performance of the chaplin proteins.

6.1.2.1. Conclusions

The over expression approach to produce chaplin proteins provides alternative strategies to upscale the production process. Not only does it potentially increase the yield of production, specific individual chaplin proteins could be expressed. The research carried out focussed on the *S. coelicolor* chaplin E expression from an inducible promotor plasmid which had been conjugated with the *S. coelicolor* M1146 chromosome. The expression of the protein was tested in different media and was determined that R2YE provided the strongest evidence for overexpression into the supernatant. Supernatant expression has increased benefits of the existing extraction protocol and the research conducted showed that the precipitation of the chaplin E protein could be achieved using acetone.

The findings may allow for the exploration into expression of different chaplin proteins to determine if overexpression yields could be improved, which would ultimately allow for larger scale biocomposite testing. Although amyloid specific assays provided positive results for the expression, MALDI-TOF confirmation is required to ensure that the overexpression system was successful.

6.1.3. Biocomposite development

The development of a bio-inspired coating using glycans as a co-polymer to the chaplin proteins was investigated to create a hydrophobic barrier coating to limit electrolyte contact with the substrate. Limiting the amount of electrolyte interacting with the substrate, ultimately, limits the degradation of the metal. In Chapter 5.3.2, an optimal concentration was determined for increasing the water contact angles on hydrophilic substrates such as glass using two different glycans: a glycan only soluble in ethanol (ethyl cellulose) and a glycan that is soluble in both ethanol and water (Hydroxypropyl cellulose). From the biocomposite samples tested using these two glycans, it was evident that each has a different effect on the overall water contact angle when combined with the extracted chaplin proteins. The two-part formulation using the chaplin proteins and glycan was developed where the HPC glycan was able to drive the formation of the chaplin protein fibrils and aid in the adhesion to the substrate, which in turn formed a more uniform coating. This uniformity in deposition across the substrate appears to be a key factor in the improvements observed for the water contact angle of the coated surfaces. The partial resemblance to the characteristics of hydrophobins gives chaplin proteins the potential to be used as an alternative and may provide additional benefits. The use of the relatively pure synthetic *S. griseus* peptides gave insight into the effects on water contact angles and elastic modulus when combined with a glycan, whilst eliminating the variability hypothesised to be caused by the coextracted pigments and residual TFA. The research conducted here is only the start of developing a mechanically robust nanoscale chaplin protein biocomposite. Here, only two glycans were tested however there is a wide range of glycans with different chemistries which may result in improved mechanical properties. The quantification of the elastic modulus using AFM did not show any significant improvement for the biocomposite coating but the development of the biocomposite in this research has increased its water contact angle over the chaplin protein-only coating. Mechanical properties for any coating are crucial to ensure longevity of a coating and protection to the underlying substrate. Quantifying the mechanical properties of a nanoscale coating does have its limitations. Organic corrosion coatings are generally microns thick and clearly visible to the naked eye. Techniques and processes have been developed to quantify mechanical properties such as adhesion and wear resistance. The American Society for Testing and Materials (ASTM) has a range of standardised tests, one of which-ASTM D4541-22- quantifies the adhesion of coating by measuring the perpendicular force required to remove a plug from the surface. Another adhesion test (ASTM D3359), known as the cross-hatch test requires the visibility of the coating, as the adhesion is quantified based on a grading scale of the coating that has been removed. No reliable data would be obtained from a nanometre thick biocomposite coating using these methods so nanoscale

measurements using techniques such as AFM are the only viable route for quantifiable data of the mechanical properties of these biocomposite coatings.

The use of AFM for material characterisation of the protein-glycan composite is crucial and can give higher spatial resolution than scanning electron microscopy and does not require samples/ substrates to be conductive. The AFM topography measurements obtained for the synthetic protein only and synthetic biocomposite highlights how the addition of the glycan can provide a more even coverage of the substrate and enhance the surface roughness which subsequently reduces the wettability. Visualising the amyloid fibrils formed from chaplin protein extracts with SEM was unsuccessful in both the protein only and the biocomposite. However, the structural integrity of the biocomposite deposits appear to be enhanced as the degradation of the material when exposed to the electron beam was not evident unlike the protein only. Numerous pin holes and the propagation of cracks was evident on the protein only deposit when viewed with SEM. Limitations on the availability and training for specialist equipment was significant and led to chaplin protein extracts being unable to be scanned under AFM to quantify for the mechanical properties. There is potential that the coextracted material associated with the chaplin extracts could be acting like a natural filler and allowing for full coverage of the substrate unlike the relatively pure synthetic peptides

The functionality of the protein only for corrosion resistance has been investigated with the CDE project and was able to show barrier properties. The subjective testing carried out within this research showed that the biocomposite does appear to improve the corrosion resistance. The CDE project used TFA extracted chaplin proteins which may be hampering the results obtained within that project, but the investigations here using a diethyl ether precipitation method for TFA removal and protein purification may allow for improvements to be gained. The stratmann cells (figure 13) of the diethyl ether precipitation appear to have a clear advantage over the protein only when exposed to HCl fumes. All the deposits carried out resulted in coatings of nanometre scale, which for a corrosion resistance coating, would have limitations. There is scope for the further investigations into higher concentration deposits to increase the overall thickness of the coating.

Amyloid proteins and glycans are linked to adhesion of various microorganisms and the ability to exploit their interactions would have a large biotechnological impact. The DASA project for armoured glass laminates investigated the chaplin-glycan biocomposite for adhesive properties, which resulted in variance of the lap shear testing. The TFA and the nanometre scale was hypothesised as the causes of this variance. The research within this project has positive implications on developing this further by trialling diethyl ether precipitated chaplin extracts.

6.1.3.1. Conclusions

This research has shown that from the glycans tested Hydroxypropyl cellulose was successful in maintaining water contact angles when mixed with chaplin proteins. The addition of the glycan to the chaplin proteins improved the overall coverage of the substrate leading to fewer voids present in the coating. Scanning electron microscopy suggests that the cohesive strength of the coating was improved when the glycan was present. Topographical comparison of protein only and biocomposite coatings showed the change in roughness which may provide a basis to why the water contact angle was maintained. The developments on the overall coverage of the coating may allow for quantitative corrosion-based experiments.

It was identified that residual TFA may be having a substantial effect on the final coating. Diethyl ether precipitation methods for the removal of TFA appear positive and may have a positive impact on the performance of the protein only and biocomposite coatings based on *S. griseus* extracted chaplin proteins. The removal of the TFA was shown to reduce the corrosion reduced during the evaporation of the solvent. The functionality of the precipitated protein has not yet been determined and provides an avenue for future research.

6.1.4. Future Vision

The research conducted has developed key areas on improving the production and purification of chaplin proteins for the use as a biocomposite coating. Confirmatory analysis using MALDI-TOF is required to ensure the production of chaplin proteins has been successful. The precipitation of the *S. griseus* extracts using diethyl ether has the potential to be included in the extraction protocol to allow for efficient removal of TFA which may be hindering further analysis. The development of the biocomposite onto glass substrates was successful and provided a basis for the concentration and ratio required to obtain significant water contact angles. However, the solvent used was water which hindered its application on metallic substrates. Protein only deposits were shown to have voids within the vinal coating which makes the coating susceptible to corrosion when exposed to an electrolyte solution. Upon efficient extraction and purification of the chaplin proteins, further developments could be investigated with the use of hydroxypropyl cellulose to determine if an effective barrier could be achieved.

7. References

1. Linder MB. Hydrophobins: Proteins that self assemble at interfaces. Curr Opin Colloid Interface Sc. 2009;14(5):356-63.

2. Santhiya D, Burghard Z, Greiner C, Jeurgens LPH, Subkowski T, Bill J. Bioinspired Deposition of TiO2 Thin Films Induced by Hydrophobins. Langmuir. 2010;26(9):6494-502.

3. Latthe SS, Terashima C, Nakata K, Fujishima A. Superhydrophobic surfaces developed by mimicking hierarchical surface morphology of lotus leaf. Molecules. 2014;19(4):4256-83.

4. Zhou C, Wu JT. Bioinspired Micro-Nano Fibrous Adhesion Materials. Progress in Chemistry. 2018;30(12):1863-73.

5. Godawat R, Jamadagni SN, Garde S. Characterizing hydrophobicity of interfaces by using cavity formation, solute binding, and water correlations. PNAS 2009;106(36):15119-24.

6. Parvate S, Dixit P, Chattopadhyay S. Superhydrophobic Surfaces: Insights from Theory and Experiment. Journal of Physical Chemistry B. 2020;124(8):1323-60.

7. Wenzel RN. Resistance of solid surfaces to wetting by water Industrial & Engineering Chemistry Research. 1936;28(8):988-94.

8. Cassie ABD, Baxter S. Wettability of Porous Surfaces. Trans Faraday Soc. 1944;40.

9. Park S, Huo J, Shin J, Heo KJ, Kalmoni JJ, Sathasivam S, et al. Production of an EP/PDMS/SA/AlZnO Coated Superhydrophobic Surface through an Aerosol-Assisted Chemical Vapor Deposition Process. Langmuir. 2022.

10. Gu Z, Li SH, Zhang FL, Wang ST. Understanding Surface Adhesion in Nature: A Peeling Model. Advanced Science. 2016;3(7).

11. Federle W, Barnes WJP, Baumgartner W, Drechsler P, Smith JM. Wet but not slippery: boundary friction in tree frog adhesive toe pads. Journal of the Royal Society Interface. 2006;3(10):689-97.

12. Nakajima A. Design of hydrophobic surfaces for liquid droplet control. Npg Asia Materials. 2011;3:49-56.

13. Barka EA, Vatsa P, Sanchez L, Gaveau-Vaillant N, Jacquard C, Klenk HP, et al. CD Taxonomy, Physiology, and Natural Products of Actinobacteria. Microbiol Mol Biol Rev. 2016;80(1):1-43.

14. Yagüe P, López-García MT, Rioseras B, Sánchez J, Manteca Á. Pre-sporulation stages of *Streptomyces* differentiation: state-of-the-art and future perspectives. FEMS Microbiol Lett. 2013;342(2):79-88.

15. McCormick JR, Flardh K. Signals and regulators that govern *Streptomyces* development. Fems Microbiology Reviews. 2012;36(1):206-31.

16. Claessen D, Rink R, de Jong W, Siebring J, de Vreugd P, Boersma FG, et al. A novel class of secreted hydrophobic proteins is involved in aerial hyphae formation in *Streptomyces coelicolor* by forming amyloid-like fibrils. Genes & Development. 2003;17(14):1714-26.

17. Claessen D, Wösten HAB, Keulen Gv, Faber OG, Alves AMCR, Meijer WG, et al. Two novel homologous proteins of *Streptomyces coelicolor* and *Streptomyces lividans* are involved in the formation of the rodlet layer and mediate attachment to a hydrophobic surface. Mol Microbiol. 2002;44(6):1483-92.

18. Elliot MA, Talbot NJ. Building filaments in the air: aerial morphogenesis in bacteria and fungi. Curr Opin Microbiol. 2004;7(6):594-601.

19. Claessen D, De Jong W, Dijkhuizen L, Wösten HA. Regulation of *Streptomyces* development: reach for the sky! Trends Microbiol. 2006;14(7):313-9.

20. Schwedock J, McCormick JR, Angert ER, Nodwell JR, Losick R. Assembly of the cell division protein FtsZ into ladder-like structures in the aerial hyphae of *Streptomyces coelicolor*. Mol Microbiol. 1997;25(5):847-58.

21. Kleinschnitz EM, Heichlinger A, Schirner K, Winkler J, Latus A, Maldener I, et al. Proteins encoded by the mre gene cluster in Streptomyces coelicolor A3(2) cooperate in spore wall synthesis. Mol Microbiol. 2011;79(5):1367-79.

22. Mazza P, Noens Ee Fau - Schirner K, Schirner K Fau - Grantcharova N, Grantcharova N Fau - Mommaas AM, Mommaas Am Fau - Koerten HK, Koerten Hk Fau - Muth G, et al. MreB of *Streptomyces coelicolor* is not essential for vegetative growth but is required for the integrity of aerial hyphae and spores. Mol Microbiol. 2006(0950-382X (Print)).

23. Elliot MA, Karoonuthaisiri N, Huang J, Bibb MJ, Cohen SN, Kao CM, et al. The chaplins: a family of hydrophobic cell-surface proteins involved in aerial mycelium formation in *Streptomyces coelicolor*. Genes & Development. 2003;17(14):1727-40.

24. Di Berardo C, Capstick DS, Bibb MJ, Findlay KC, Buttner MJ, Elliot MA. Function and redundancy of the chaplin cell surface proteins in aerial hypha formation, rodlet assembly, and viability in *Streptomyces coelicolor*. J Bacteriol. 2008;190(17):5879-89.

25. Capstick DS, Willey JM, Buttner MJ, Elliot MA. SapB and the chaplins: connections between morphogenetic proteins in *Streptomyces coelicolor*. Mol Microbiol. 2007;64(3):602-13.

26. Straight PD, Willey JM, Kolter R. Interactions between *Streptomyces coelicolor* and Bacillus subtilis: Role of surfactants in raising aerial structures. J Bacteriol. 2006;188(13):4918-25.

27. Sawyer EB, Claessen D, Haas M, Hurgobin B, Gras SL. The assembly of individual chaplin peptides from *Streptomyces coelicolor* into functional amyloid fibrils. PLoS One. 2011;6(4):e18839.

28. de Jong W, Wösten HA, Dijkhuizen L, Claessen D. Attachment of *Streptomyces coelicolor* is mediated by amyloidal fimbriae that are anchored to the cell surface via cellulose. Mol Microbiol. 2009;73(6):1128-40.

29. Zhong X, Zhang L, van Wezel GP, Vijgenboom E, Claessen D. Role for a Lytic Polysaccharide Monooxygenase in Cell Wall Remodeling in *Streptomyces coelicolor*. mBio. 2022;13(2):e0045622.

30. Xu H, Chater KF, Deng Z, Tao M. A cellulose synthase-like protein involved in hyphal tip growth and morphological differentiation in *streptomyces*. J Bacteriol. 2008;190(14):4971-8.

31. White AP, Gibson DL, Collinson SK, Banser PA, Kay WW. Extracellular polysaccharides associated with thin aggregative fimbriae of *Salmonella enterica* serovar enteritidis. J Bacteriol. 2003;185(18):5398-407.

32. Hektor HJ, Scholtmeijer K. Hydrophobins: proteins with potential. Current Opinion in Biotechnology. 2005;16(4):434-9.

33. Stringer MA, Timberlake WE. Cerato-Ulmin, a Toxin Involved in Dutch Elm Disease, Is a Fungal Hydrophobin. Plant Cell. 1993;5(2):145-6.

34. De Chiffre L, Kunzmann H, Peggs GN, Lucca DA. Surfaces in precision engineering, microengineering and nanotechnology. Cirp Annals-Manufacturing Technology. 2003;52(2):561-77.

35. Otzen D, Riek R. Functional Amyloids. Cold Spring Harb Perspect Biol. 2019;11(12).

36. Bokhove M, Claessen D, de Jong W, Dijkhuizen L, Boekema EJ, Oostergetel GT. Chaplins of *Streptomyces coelicolor* self-assemble into two distinct functional amyloids. J Struct Biol. 2013;184(2):301-9.

37. Spasic J, Mandic M, Djokic L, Nikodinovic-Runic J. *Streptomyces spp.* in the biocatalysis toolbox. Appl Biochem Biotechnol. 2018;102(8):3513-36.

38. Pervaiz I, Ahmad S, Madni MA, Ahmad H, Khaliq FH. Microbial biotransformation: a tool for drug designing (Review). Prikl Biokhim Mikrobiol. 2013;49(5):435-49.

39. Katz L, Baltz RH. Natural product discovery: past, present, and future. J Ind Microbiol Biotechnol. 2016;43(2-3):155-76.

40. Waksman SA, Geiger WB, Reynolds DM. Strain Specificity and Production of Antibiotic Substances: VII. Production of Actinomycin by Different Actinomycetes. PNAS. 1946;32(5):117-20.

41. Jones D, Metzger HJ, Schatz A, Waksman SA. Control of Gram-Negative Bacteria in Experimental Animals by Streptomycin. Science. 1944;100(2588):103-5.

42. Worrall JA, Vijgenboom E. Copper mining in *Streptomyces*: enzymes, natural products and development. Nat Prod Rep. 2010;27(5):742-56.

43. Nielsen J. Production of biopharmaceutical proteins by yeast: advances through metabolic engineering. Bioengineered. 2013;4(4):207-11.

44. Sauer M, Porro D, Mattanovich D, Branduardi P. Microbial production of organic acids: expanding the markets. Trends Biotechnol. 2008;26(2):100-8.

45. Xia JY, Wang G, Fan M, Chen M, Wang ZY, Zhuang YP. Understanding the scale-up of fermentation processes from the viewpoint of the flow field in bioreactors and the physiological response of strains. Chin J Chem Eng. 2021;30:178-84.

46. Marth JD. A unified vision of the building blocks of life. Nat Cell Biol. 2008;10(9):1015-6.

47. Klemm D, Heublein B, Fink HP, Bohn A. Cellulose: fascinating biopolymer and sustainable raw material. Angew Chem Int Ed Engl. 2005;44(22):3358-93.

48. Romeo T. Bacterial biofilms. Preface. Curr Top Microbiol Immunol. 2008;322:v.

49. Nishiyama Y, Langan P, Chanzy H. Crystal structure and hydrogen-bonding system in cellulose Ibeta from synchrotron X-ray and neutron fiber diffraction. J Am Chem Soc. 2002;124(31):9074-82.

50. Nwanonenyi SC, Madufor IC, Uzoma PO, Chukwujike IC. Corrosion Inhibition of Mild Steel in Sulphuric Acid Environment Using Millet Starch and Potassium Iodide. Indian J Pure Appl Chem. 2016;12:1-15.

51. Koch G, Varney J, Thompson N, Moghissi O, Gould M, Payer J. International measures of prevention, application, and economics of corrosion technologies study. NACE international. 2016;216:2-3.

52. Popov BN. Chapter 10 - Atmospheric Corrosion. In: Popov BN, editor. Corrosion Engineering. Amsterdam: Elsevier; 2015. p. 451-80.

53. Liu Y, Wang Z, Ke W. Study on influence of native oxide and corrosion products on atmospheric corrosion of pure Al. Corrosion Science. 2014;80:169-76.

54. Dickie RA, Floyd FL. Polymeric Materials for Corrosion Control - an Overview. Am Chem J. 1986;322:1-16.

55. Siva T, Kamaraj K, Karpakam V, Sathiyanarayanan S. Soft template synthesis of poly(o-phenylenediamine) nanotubes and its application in self healing coatings. Progress in Organic Coatings. 2013;76(4):581-8.

56. Harold A. Incorporation of Microbial Organisms into Organic Steel Coatings. Swansea University: Swansea University; 2019.

57. van Keulen Gw, G. penney, D. Griffin, S. Allen, G. Subramanian, R. Developing a novel protein-based coating technology for anti-corrosion of magnesium light alloy materials. Athena report collection2017. Report No.: CDE100367 - DSTLX1000104111.

58. van Keulen GP, CO. Griffin, S. Clifford, B. Developing a synthetic biology-inspired adhesive technology for transparent defence materials. UK: Ministry of Defence2018. Report No.: ACC101824-DSTLX1000112928.

59. van Keulen GP, CO. Griffin, S. Clifford, B. Gallagher, J. Bryant, D. Morris, M. Guscott, B. Phase II development of a synthetic biology-inspired adhesive technology for transparent defence materials. UK: Ministry of Defence2020. Report No.: ACC500276-DSTL1000125502.

60. Kieser T, Bibb M, Buttner M, Chater K, Hopwood D. Practical streptomyces genetics. Norwich: John Innes Foundation; 2000.

61. Hopwood DA. Streptomyces in nature and medicine: the antibiotic makers: Oxford University Press; 2007.

62. Glazebrook MA, Doull JL, Stuttard C, Vining LC. Sporulation of Streptomyces-Venezuelae in Submerged Cultures. Journal of General Microbiology. 1990;136:581-8.

63. Kuimova TF, Soina VS. A submerged sporulation and ultrastructural changes in the mycelium of Streptomyces chrysomallus. Hindustan Antibiot Bull. 1981;23:1-5.

64. Novella IS, Barbes C, Sanchez J. Sporulation of Streptomyces antibioticus ETHZ 7451 in submerged culture. Can J Microbiol. 1992;38(8):769-73.

65. Rho YT, Lee KJ. Kinetic characterization of sporulation in Streptomyces albidoflavus SMF301 during submerged culture. Microbiology (Reading). 1994;140 (Pt 8):2061-5.

66. Rueda B, Miguelez EM, Hardisson C, Manzanal MB. Mycelial differentiation and spore formation by Streptomyces brasiliensis in submerged culture. Can J Microbiol. 2001;47(11):1042-7.

67. Chater KF. Regulation of sporulation in *Streptomyces coelicolor* A3 (2): a checkpoint multiplex? Curr Opin Microbiol. 2001;4(6):667-73.

68. Kutzner K. The family Streptomycetaceae The prokaryotes, A Handbook on Habitats, Isolation and Identification of Bacteria: Springer-Verlag, New York; 1986.

69. Locci R. Streptomycetes and related genera1989.

70. Daza A, Martin JF, Dominguez A, Gil JA. Sporulation of Several Species of Streptomyces in Submerged Cultures after Nutritional Downshift. Journal of General Microbiology. 1989;135:2483-91.

71. Coin I, Beyermann M, Bienert M. Solid-phase peptide synthesis: from standard procedures to the synthesis of difficult sequences. Nat Protoc. 2007;2(12):3247-56.

72. Kendrick KE, Ensign JC. Sporulation of Streptomyces griseus in submerged culture. J Bacteriol. 1983;155(1):357-66.

73. Kontro M, Lignell U, Hirvonen MR, Nevalainen A. pH effects on 10 Streptomyces spp. growth and sporulation depend on nutrients. Lett Appl Microbiol. 2005;41(1):32-8.

74. Pacios-Michelena S, AGUILAR CN, Alvarez-Perez OB, Rodriguez-Herrera R, Chávez-González ML, Arredondo Valdés R, et al. Application of Streptomyces antimicrobial compounds for the control of phytopathogens. Front Sustainable Food Syst. 2021:310.

75. Aharonowitz Y. Nitrogen metabolite regulation of antibiotic biosynthesis. Annu Rev Microbiol. 1980;34:209-33.

76. Sanchez S, Chavez A, Forero A, Garcia-Huante Y, Romero A, Sanchez M, et al. Carbon source regulation of antibiotic production. J Antibiot (Tokyo). 2010;63(8):442-59.

77. Chouayekh H, Virolle MJ. The polyphosphate kinase plays a negative role in the control of antibiotic production in *Streptomyces lividans*. Mol Microbiol. 2002;43(4):919-30.

78. Noens EE, Mersinias V, Willemse J, Traag BA, Laing E, Chater KF, et al. Loss of the controlled localization of growth stage-specific cell-wall synthesis pleiotropically affects developmental

gene expression in an *ssgA* mutant of *Streptomyces coelicolor*. Mol Microbiol. 2007;64(5):1244-59.

79. Rioseras B, López-García MT, Yagüe P, Sánchez J, Manteca Á. Mycelium differentiation and development of *Streptomyces coelicolor* in lab-scale bioreactors: Programmed cell death, differentiation, and lysis are closely linked to undecylprodigiosin and actinorhodin production. Bioresour Technol. 2014;151:191-8.

80. Schelden M, Lima W, Doerr EW, Wunderlich M, Rehmann L, Buchs J, et al. Online measurement of viscosity for biological systems in stirred tank bioreactors. Biotechnol Bioeng. 2017;114(5):990-7.

81. van der Aart LT, Spijksma GK, Harms A, Vollmer W, Hankemeier T, van Wezel GP. High-Resolution Analysis of the Peptidoglycan Composition in *Streptomyces coelicolor*. J Bacteriol. 2018;200(20).

82. van Keulen G, Jonkers HM, Claessen D, Dijkhuizen L, Wösten HA. Differentiation and anaerobiosis in standing liquid cultures of *Streptomyces coelicolor*. J Bacteriol. 2003;185(4):1455-8.

83. Gamboa-Suasnavart RA, Marin-Palacio LD, Martinez-Sotelo JA, Espitia C, Servin-Gonzalez L, Valdez-Cruz NA, et al. Scale-up from shake flasks to bioreactor, based on power input and *Streptomyces lividans* morphology, for the production of recombinant APA (45/47 kDa protein) from *Mycobacterium tuberculosis*. World J Microbiol Biotechnol. 2013;29(8):1421-9.

84. Ferraiuolo SB, Cammarota M, Schiraldi C, Restaino OF. Streptomycetes as platform for biotechnological production processes of drugs. Appl Biochem Biotechnol 2021;105(2):551-68.

85. Misra R, Li J, Cannon GC, Morgan SE. Nanoscale reduction in surface friction of polymer surfaces modified with Sc3 hydrophobin from *Schizophyllum commune*. Biomacromolecules. 2006;7(5):1463-70.

86. von Vacano B, Xu R, Hirth S, Herzenstiel I, Ruckel M, Subkowski T, et al. Hydrophobin can prevent secondary protein adsorption on hydrophobic substrates without exchange. Anal BioanalChem. 2011;400(7):2031-40.

87. Opwis K, Gutmann JS. Surface modification of textile materials with hydrophobins. Textile Research Journal. 2011;81(15):1594-602.

88. Joudan S, De Silva AO, Young CJ. Insufficient evidence for the existence of natural trifluoroacetic acid. Environ Sci Processes Impacts. 2021;23(11):1641-9.

89. de La Torre BG, Andreu D. On choosing the right ether for peptide precipitation after acid cleavage. J Pept Sci. 2008;14(3):360-3.

90. Osarolube E, Owate IO, Oforka NC. Corrosion behaviour of mild and high carbon steels in various acidic media. Scientific Research and Essays. 2008;3(6):224-8.

91. Wosten H, De Vries O, Wessels J. Interfacial Self-Assembly of a Fungal Hydrophobin into a Hydrophobic Rodlet Layer. Plant Cell. 1993;5(11):1567-74.

92. Ahmed Y, Rebets Y, Estevez MR, Zapp J, Myronovskyi M, Luzhetskyy A. Engineering of *Streptomyces lividans* for heterologous expression of secondary metabolite gene clusters. Microb Cell Fact. 2020;19(1):5.

93. van Dissel D, van Wezel GP. Morphology-driven downscaling of *Streptomyces lividans* to micro-cultivation. Antonie Van Leeuwenhoek. 2018;111(3):457-69.

94. van Dissel D, Claessen D, van Wezel GP. Morphogenesis of *Streptomyces* in submerged cultures. Adv Appl Microbiol. 2014;89:1-45.

95. van Wezel GP, McDowall KJ. The regulation of the secondary metabolism of Streptomyces: new links and experimental advances. Nat Prod Rep. 2011;28(7):1311-33.

96. van Wezel GP, Krabben P, Traag BA, Keijser BJF, Kerste R, Vijgenboom E, et al. Unlocking *Streptomyces spp.* for use as sustainable industrial production platforms by morphological engineering (vol 72, pg 5283, 2006). Appl Environ Microbiol. 2006;72(10):6863-.

97. Dragos A, Kovacs AT, Claessen D. The Role of Functional Amyloids in Multicellular Growth and Development of Gram-Positive Bacteria. Biomolecules. 2017;7(3).

98. Rosano GL, Ceccarelli EA. Recombinant protein expression in Escherichia coli: advances and challenges. Front Microbiol. 2014;5:172.

99. Barnhart MM, Chapman MR. Curli biogenesis and function. Annu Rev Microbiol. 2006;60:131-47.

100. Austin JW, Sanders G, Kay WW, Collinson SK. Thin aggregative fimbriae enhance *Salmonella enteritidis* biofilm formation. FEMS Microbiol Lett. 1998;162(2):295-301.

101. Hammar M, Bian Z, Normark S. Nucleator-dependent intercellular assembly of adhesive curli organelles in *Escherichia coli*. PNAS. 1996;93(13):6562-6.

102. Bai C, Zhang Y, Zhao X, Hu Y, Xiang S, Miao J, et al. Exploiting a precise design of universal synthetic modular regulatory elements to unlock the microbial natural products in *Streptomyces*. Proc Natl Acad Sci U S A. 2015;112(39):12181-6.

103. Remans K, Lebendiker M, Abreu C, Maffei M, Sellathurai S, May MM, et al. Protein purification strategies must consider downstream applications and individual biological characteristics. Microb Cell Fact. 2022;21(1).

104. Wingfield PT. Overview of the purification of recombinant proteins. Curr Protoc Protein Sci. 2015;80:6 1 -6 1 35.

105. Duong-Ly KC, Gabelli SB. Salting out of Proteins Using Ammonium Sulfate Precipitation. Methods Enzymol. 2014;541:85-94.

106. Gomez-Escribano JP, Bibb MJ. Engineering *Streptomyces coelicolor* for heterologous expression of secondary metabolite gene clusters. Microb Biotechnol. 2011;4(2):207-15.

107. Álvarez-Fernández R. Chapter One - Explanatory Chapter: PCR Primer Design. In: Lorsch J, editor. Methods Enzymol: Academic Press; 2013. p. 1-21.

108. Gallardo G, Holtzman DM. Antibody Therapeutics Targeting Abeta and Tau. Cold Spring Harb Perspect Med. 2017;7(10).

109. O'Nuallain B, Wetzel R. Conformational Abs recognizing a generic amyloid fibril epitope. Proc Natl Acad Sci U S A. 2002;99(3):1485-90.

110. Jeong Y, Kim JN, Kim MW, Bucca G, Cho S, Yoon YJ, et al. The dynamic transcriptional and translational landscape of the model antibiotic producer *Streptomyces coelicolor* A3(2). Nat Commun. 2016;7:11605.

111. Thibessard A, Bertrand C, Hiblot J, Piotrowski E, Leblond P. Construction of pDYN6902, a new *Streptomyces* integrative expression vector designed for cloning sequences interfering with *Escherichia coli* viability. Plasmid. 2015;82:43-9.

112. Wang H, Zhao GP, Ding XM. Morphology engineering of *Streptomyces coelicolor* M145 by sub-inhibitory concentrations of antibiotics. Sci Rep. 2017;7.

113. Romero-Rodriguez A, Rocha D, Ruiz-Villafan B, Guzman-Trampe S, Maldonado-Carmona N, Vazquez-Hernandez M, et al. Carbon catabolite regulation in *Streptomyces*: new insights and lessons learned. World J Microbiol Biotechnol. 2017;33(9):162.

114. Arend KI, Bandow JE. Influence of Amino Acid Feeding on Production of Calcimycin and Analogs in *Streptomyces chartreusis*. Int J Environ Res Public Health. 2021;18(16).

115. Stephens AD, Lu M, Fernandez-Villegas A, Kaminski Schierle GS. Fast Purification of Recombinant Monomeric Amyloid-beta from *E. coli* and Amyloid-beta-mCherry Aggregates from Mammalian Cells. ACS Chem Neurosci. 2020;11(20):3204-13.

116. Rambaran RN, Serpell LC. Amyloid fibrils: abnormal protein assembly. Prion. 2008;2(3):112-7.

117. Ekkers DM, Claessen D, Galli F, Stamhuis E. Surface modification using interfacial assembly of the *Streptomyces* chaplin proteins. Appl Biochem Biotechnol. 2014;98(10):4491-501.

118. van Dissel D, Willemse J, Zacchetti B, Claessen D, Pier GB, van Wezel GP. Production of poly-beta-1,6-N-acetylglucosamine by MatAB is required for hyphal aggregation and hydrophilic surface adhesion by *Streptomyces*. Microbial Cell. 2018;5(6):269-79.

119. Maaß P. Corrosion and Corrosion Protection. Handbook of Hot-Dip Galvanization. 2011:1-19.

120. IARC. Arsenic, metals, fibres, and dusts. IARC Monogr Eval Carcinog Risks Hum. 2012;100(Pt C):11-465.

121. Frankel GS, McCreery RL. Inhibition of Al alloy corrosion by chromates. Electrochem Soc Interface. 2001;10(4):34.

122. Kendig MW, Buchheit RG. Corrosion inhibition of aluminum and aluminum alloys by soluble chromates, chromate coatings, and chromate-free coatings. Corrosion. 2003;59(5):379-400.

123. Gharbi O, Thomas S, Smith C, Birbilis N. Chromate replacement: what does the future hold? npj Mater Degrad. 2018;2(1):12.

124. Hurley BL, McCreery RL. Raman spectroscopy of monolayers formed from chromate corrosion inhibitor on copper surfaces. Journal of the Electrochemical Society. 2003;150(8):B367-B73.

125. Baghni IM, Lyon SB, Ding BF. The effect of strontium and chromate ions on the inhibition of zinc. Surf Coat Technol. 2004;185(2-3):194-8.

126. Marzorati S, Verotta L, Trasatti SP. Green Corrosion Inhibitors from Natural Sources and Biomass Wastes. Molecules. 2018;24(1).

127. Fu JJ, Zang HS, Wang Y, Li SN, Chen T, Liu XD. Experimental and Theoretical Study on the Inhibition Performances of Quinoxaline and Its Derivatives for the Corrosion of Mild Steel in Hydrochloric Acid. Industrial & Engineering Chemistry Research. 2012;51(18):6377-86.

128. Umoren SA, Banera MJ, Alonso-Garcia T, Gervasi CA, Mirifico MV. Inhibition of mild steel corrosion in HCl solution using chitosan. Cellulose. 2013;20(5):2529-45.

129. Zadeh ARH, Danaee I, Maddahy MH. Thermodynamic and Adsorption Behaviour of Medicinal Nitramine as a Corrosion Inhibitor for AISI Steel Alloy in HCl Solution. Journal of Materials Science & Technology. 2013;29(9):884-92.

130. Umoren SA, Obot IB, Madhankumar A, Gasem ZM. Performance evaluation of pectin as ecofriendly corrosion inhibitor for X60 pipeline steel in acid medium: Experimental and theoretical approaches. Carbohydr Polym. 2015;124:280-91.

131. Cao YZ, Chen C, Lu X, Xu D, Huang J, Xin Z. Bio-based polybenzoxazine superhydrophobic coating with active corrosion resistance for carbon steel protection. Surf Coat Technol. 2021;405.

132. Amer M, Hayat Q, Janik V, Jennett N, Nottingham J, Bai MW. A Review on In Situ Mechanical Testing of Coatings. Coatings. 2022;12(3).

133. Dokouhaki M, Prime EL, Hung A, Qiao GG, Day L, Gras SL. Structure-Dependent Interfacial Properties of Chaplin F from Streptomyces coelicolor. Biomolecules. 2017;7(3).

134. Wint N, Ansell P, Edy J, Williams G, McMurray HN. A Method for Quantifying the Synergistic Inhibitory Effect of Corrosion Inhibitors When Used in Combination: A 'Chromate Generating Coating'. Journal of the Electrochemical Society. 2019;166(15):C580-C8.

135. Nazarov A, Thierry D. Application of Scanning Kelvin Probe in the Study of Protective Paints. Frontiers in Materials. 2019;6.

136. Warren AD, Martinez-Ubeda AI, Payton OD, Picco L, Scott TB. Preparation of Stainless Steel Surfaces for Scanning Probe Microscopy. Microscopy Today. 2016;24(3):52-5.

137. Pace CN, Trevino S, Prabhakaran E, Scholtz JM. Protein structure, stability and solubility in water and other solvents. Phil Trans R Soc Lond B. 2004;359(1448):1225-34; discussion 34-5.

138. Narang AS, ScienceDirect. Handbook of pharmaceutical wet granulation : theory and practice in a quality by design paradigm. London: Academic Press; 2019.

139. Armenante A, Longobardi S, Rea I, De Stefano L, Giocondo M, Silipo A, et al. The *Pleurotus ostreatus* hydrophobin Vmh2 and its interaction with glucans. Glycobiology. 2010;20(5):594-602.

140. Paul A, Segal D, Zacco E. Glycans to improve efficacy and solubility of protein aggregation inhibitors. Neural Regener Res. 2021;16(11):2215-6.

141. Youshia J, Ali ME, Lamprecht A. Artificial neural network based particle size prediction of polymeric nanoparticles. European Journal of Pharmaceutics and Biopharmaceutics. 2017;119:333-42.

142. Hedberg Y, Karlsson M-E, Blomberg E, Odnevall I, Hedberg J. Correlation between surface physicochemical properties and the release of iron from stainless steel AISI 304 in biological media. Colloids Surf, B. 2014;122:216-22.

143. Correia DM, Lizundia E, Meira RM, Rincon-Iglesias M, Lanceros-Mendez S. Cellulose Nanocrystal and Water-Soluble Cellulose Derivative Based Electromechanical Bending Actuators. Materials. 2020;13(10).

144. Gilbert J, Reynolds NP, Russell SM, Haylock D, McArthur S, Charnley M, et al. Chitosan-coated amyloid fibrils increase adipogenesis of mesenchymal stem cells. Mater Sci Eng C Mater Biol Appl. 2017;79:363-71.

145. Alnoush W, Sayed A, Solling TI, Alyafei N. Impact of calcite surface roughness in wettability assessment: Interferometry and atomic force microscopy analysis. J Pet Sci Technol. 2021;203.

146. Frankel GS, Stratmann M, Rohwerder M, Michalik A, Maier B, Dora J, et al. Potential control under thin aqueous layers using a Kelvin Probe. Corrosion Science. 2007;49(4):2021-36.

147. Nwanonenyi SC, Obasi HC, Eze IO. Hydroxypropyl Cellulose as an Efficient Corrosion Inhibitor for Aluminium in Acidic Environments: Experimental and Theoretical Approach. Chemistry Africa-a Journal of the Tunisian Chemical Society. 2019;2(3):471-82.